PHOSPHODIESTERASE-5 INHIBITORY AND VASODILATOR ACTIONS OF QUINAZOLINE DERIVATIVES

USANA CHATTURONG

A Thesis Submitted to the Graduate School of Naresuan University
in Partial Fulfillment of the Requirements
for the Doctor of Philosophy in Physiology
2023

PHOSPHODIESTERASE-5 INHIBITORY AND VASODILATOR ACTIONS OF QUINAZOLINE DERIVATIVES

USANA CHATTURONG

A Thesis Submitted to the Graduate School of Naresuan University
in Partial Fulfillment of the Requirements
for the Doctor of Philosophy in Physiology
2023

Thesis entitled "Phosphodiesterase-5 inhibitory and vasodilator actions of quinazoline derivatives"

By Usana Chatturong

has been approved by the Graduate School as partial fulfillment of the requirements

for the Doctor of Philosophy in Physiology of Naresuan University

Oral Defense Committee

..... Chair
(Professor Corine Girard, Ph.D.)

..... Advisor
(Associate Professor Krongkarn Chootip, Ph.D.)

..... Co Advisor
(Professor Céline Demougeot, Ph.D.)

..... Co Advisor
(Professor Kornkanok Ingkaninan, Ph.D.)

..... Co Advisor
(Assistant Professor Prapapan Temkitthawon, Ph.D.)

..... Internal Examiner
(Assistant Professor Kroekkiat Chinda, Ph.D.)

..... External Examiner
(Emeritus Professor Chaweewan Jansakul, Ph.D.)

..... External Examiner
(Assistant Professor Boris Manoury, Ph.D.)

Approved

.....
(Associate Professor Krongkarn Chootip, Ph.D.)
Dean of the Graduate School

Title	PHOSPHODIESTERASE-5 INHIBITORY AND VASODILATOR ACTIONS OF QUINAZOLINE DERIVATIVES
Author	Usana Chatturong
Advisor	Associate Professor Krongkarn Chootip, Ph.D.
Co-Advisor	Professor Céline Demougeot, Ph.D. Professor Kornkanok Ingkaninan, Ph.D. Assistant Professor Prapapan Temkitthawon, Ph.D.
Academic Paper	Ph.D. Dissertation in Physiology, Naresuan University, 2023
Keywords	Quinazoline derivatives, PDE5, Vasorelaxation, Rat pulmonary artery, Rat mesenteric artery, Liver toxicity

ABSTRACT

Phosphodiesterase-5 (PDE5) inhibitors are the gold standard treatment for pulmonary arterial hypertension (PAH), but a lack of selectivity for this enzyme can induce systemic side effects. A new series of quinazoline derivatives, N^2,N^4-disubstituted quinazoline 2,4-diamines, was developed, with compounds 4, 5, 8, 9, 10 and 11 showing good selectivity for rat PDE5. The aim of the thesis was to characterize their inhibitory effects on human PDE5, their vasorelaxant effects and related mechanisms on the pulmonary artery (PA) compared with the aorta and mesenteric artery (MA), as well as their vascular smooth muscle cells (VSMC) and hepatic toxicity (viability and induction/inhibition of rat cytochrome P450 (CYP)). Compounds 5 and 11 showed the strongest inhibitory activity of human PDE5, with no cytotoxicity for VSMC. These 2 compounds induced a vasodilatory effect on PA, which was less effective than sildenafil but more selective for PA compared with the aorta. Their vasorelaxant effects in PA were partly endothelium-dependent. They involve potentiation of the nitric oxide (NO)/soluble guanylate cyclase (sGC)/cyclic guanosine monophosphate (cGMP) pathway and inhibition of calcium fluxes (extracellular and intracellular). Their vasodilatory mechanisms were different in MA, where they are K_{Ca} channel activators, calcium channel blockers, and alpha-1 (α_1)-adrenergic antagonists. Compounds 5 and 11 did not reduce hepatocyte viability but

had a weak CYP3A inhibitory effect at 10 µM similar to sildenafil. Unlike these 2 above compounds, compound 8 showed better aortic selectivity than PA, leading to assess its effect on systemic vasculature using nifedipine as a comparator. In MA, the vasorelaxant effect of compound 8 was comparable to that of nifedipine. Mechanistically, the effect of compound 8 is endothelium-independent, based on the potentiation of the sGC/cGMP pathway, opening of the K_{Ca} channel, inhibition of calcium influx, and antagonism of α_1-adrenergic receptors. Intravenous administration of compound 8 (0.05 and 0.1 mg/kg) induced arterial hypotension, similar to nifedipine in lowering diastolic and mean arterial pressure, but its effect on lowering systolic arterial pressure was less than nifedipine. Compound 8 did not affect hepatocyte viability and CYP activities, except at high concentrations (>10 µM) at which a weak inhibitory effect on CYP1A and 3A was observed. In contrast, nifedipine showed a strong inductive effect on CYP1A, 2B, 2C and 3A activities. In conclusion, this thesis enabled to identify 2 compounds (5 and 11) that combine a good inhibitory effect on human PDE5, good selectivity for pulmonary vasculature via endothelium-dependent and independent effects, a low hepatic toxicity and a low risk of drug interaction via CYPs. The present study has also identified a new compound (compound 8) with a potent endothelium-independent vasorelaxant effect on resistance vessels, resulting in a hypotensive effect and associated with a low risk of hepatic toxicity/drug interactions. These results demonstrated that N^2,N^4-disubstituted quinazoline 2,4-diamines can serve as a basis for the development of new drugs for PAH or arterial hypertension. These studies paved the way for future *in vivo* studies to test (*i*) the effects of compounds 5 and 11 on animal models of PAH and (*ii*) the effects of compound 8 on animal models of arterial hypertension.

ACKNOWLEDGEMENTS

I would like to express my heartfelt gratitude to my advisor, Associate Professor Dr. Krongkarn Chootip, for providing me with the opportunity to pursue a doctoral degree and for her constant support during my time in the Graduate School, as well as to Professor Dr. Céline Demougeot, both of whom have provided invaluable advice and encouragement, and I will always remember the unforgettable experience of studying in France, which was also supported by both. Their patience, kindness, and understanding are also deeply appreciated. I also would like to thank my co-advisor, Professor Dr. Kornkanok Ingkaninan and Assistant Professor Dr. Prapapan Temkitthawon for their most worthy comments and suggestions.

I would like to acknowledge both Naresuan University and Bourgogne Franche-Comté University for providing the double doctoral degree program, and especially for the co-supervision provided by both universities. I acknowledge the Royal Golden Jubilee Ph.D. Program (PHD/0228/2561, National Research Council of Thailand), the Franco-Thai Scholarship Program (French Embassy in Thailand) and the French Ministry for Higher Education and Research for the graduate student grant that enabled my studies. Additionally, I also acknowledge the Department of Physiology, Faculty of Medical Science and Center of Excellence for Innovation in Chemistry, Naresuan University and PEPITE EA4267, Bourgogne Franche-Comté University, for the use of facilities and equipment. I wish to acknowledge the staff at the Faculty of Medical Science, the Faculty of Pharmaceutical Sciences, the Center for Animal Research, Naresuan University, and PEPITE EA4267 Bourgogne Franche-Comté University for their kind help. I am also grateful to Associate Professor Dr. Matthew Paul Gleeson for providing quinazoline derivatives.

Finally, I fully appreciate the love and affection and support of my parents and family and their unending understanding and encouragement throughout my life. Special thanks go to those whose names are not mentioned here but who have greatly inspired, supported, and encouraged me.

Usana Chatturong

TABLE OF CONTENTS

Page

LIST OF TABLES

Page

LIST OF FIGURES

Page

ABBREVIATIONS

AA	=	arachidonic acid
AC	=	adenylyl cyclase
ACE	=	angiotensin-converting enzyme
ACh	=	acetylcholine
Ang I	=	angiotensin I
Ang II	=	angiotensin II
ANS	=	autonomic nervous system
ARB	=	angiotensin II type I receptor blockers
AT_1	=	angiotensin II type I receptors
ATP	=	adenosine triphosphate
4-AP	=	4-aminopyridine
BMPR2	=	Bone Morphogenetic Protein Receptor Type 2
bpm	=	beats per minute
BROD	=	benzyloxyresorufin-O-dealkylase
BSA	=	bovine serum albumin
BW	=	body weight
Ca^{2+}	=	calcium ion
$CaCl_2$	=	calcium chloride
$[Ca^{2+}]_i$	=	intracellular Ca^{2+} concentration
CAM	=	calmodulin
cAMP	=	cyclic adenosine monophosphate
CCBs	=	calcium-channel blockers
cGMP	=	cyclic guanosine monophosphate
CO	=	cardiac output
CO_2	=	carbon dioxide
COX	=	cyclooxygenase enzymes
CPI-17	=	protein kinase C-potentiated phosphatase inhibitor protein-17 kDa
CRP	=	C-reactive protein
CVD	=	cardiovascular diseases

CYP	=	cytochrome P450
DAG	=	diacylglycerol
DBP	=	diastolic blood pressure
DM	=	dissociation medium
DMSO	=	dimethyl sulfoxide
DTT	=	dithiothreitol
ED	=	erectile dysfunction
EDHF	=	endothelium-derived hyperpolarizing factor
EDRF	=	endothelium-derived relaxing factors
EDTA	=	ethylenediaminetetraacetic acid
EGTA	=	ethylene glycol-bis (β-aminoethyl ether)-N,N,N,N tetraacetic acid
eNOS	=	endothelial nitric oxide synthase
ERA	=	endothelin receptor antagonist
EROD	=	ethoxyresorufin-O-deethylase
Ery	=	erythromycin
ET_A	=	endothelin receptor type A
ET_B	=	endothelin receptor type B
ET-1	=	endothelin-1
FCS	=	fetal calf serum
FDA	=	Food and Drug Administration
g	=	gram
GC	=	guanylate cyclase
GPCRs	=	G-protein-coupled receptors
GTP	=	guanosine triphosphate
h	=	hour
HEK293	=	human embryonic kidney 293
H_2S	=	hydrogen disulfide
HR	=	heart rate
HPV	=	hypoxic pulmonary vasoconstriction
iNOS	=	inducible nitric oxide synthase
IP_3	=	inositol-1,4,5-trisphosphate

IP_3R	=	inositol trisphosphate receptors
IL	=	interleukin
ISH	=	International Society of Hypertension
i.p.	=	intraperitoneal
K^+	=	potassium ion
K_{ATP}	=	ATP-sensitive potassium channel
K_{Ca}	=	large conductance Ca^{2+}-activated K^+ channels
Keto	=	ketoconazole
kg	=	kilogram
K_{ir}	=	inward-rectifier potassium channels
K_V	=	voltage-gated potassium channel
L	=	liter
L-NAME	=	N^G-nitro-L-arginine methyl ester
M	=	molar
MA	=	mesenteric artery
MAP	=	mean arterial pressure
mg	=	milligram
mL	=	milliliter
MLC	=	myosin light chain
MLCK	=	myosin light chain kinase
MLCP	=	myosin light chain phosphatase
mm	=	millimeter
mmHg	=	millimeter of mercury
mPAP	=	mean pulmonary arterial pressure
MTT	=	methyl thiazolyl tetrazolium
MYPT1	=	myosin phosphatase targeting subunit 1
NAPDH	=	nicotinamide adenine dinucleotide phosphate
NCX	=	Na^+-Ca^{2+} exchanger
NE	=	norepinephrine
nNOS	=	neuronal nitric oxide synthase
NO	=	nitric oxide
NOS	=	nitric oxide synthase

nM	=	nanomolar
ODQ	=	1H-[1,2,4]oxadiazolo[4,3-a]quinoxalin-1-one
O_2	=	oxygen
PA	=	pulmonary artery
PAH	=	pulmonary arterial hypertension
PASMCs	=	pulmonary arterial smooth muscle cells
PBS	=	phosphate-buffered saline
PCWP	=	pulmonary capillary wedge pressure
PDEs	=	phosphodiesterases
PDE5	=	phosphodiesterase type 5
PDE5i	=	phosphodiesterase type 5 inhibitors
PE	=	phenylephrine
PGI_2	=	prostacyclin
PH	=	pulmonary hypertension
PIP_2	=	phosphatidyl inositol 1,4-bisphosphate
PKA	=	protein kinase A
PKC	=	protein kinase C
PKG	=	protein kinase G
PLA_2	=	phospholipase A_2
PLC	=	phospholipase C
PMCA	=	plasma membrane Ca^{2+}-ATPase
pmol	=	picomole
PMSF	=	phenylmethylsulfonyl fluoride
PSNS	=	parasympathetic nervous system
PVR	=	pulmonary vascular resistance
RAAS	=	renin-angiotensin aldosterone system
RhoA	=	Ras homolog family member A
ROCCs	=	receptor-operated Ca^{2+} channels
ROCK	=	Rho-associated protein kinase
ROS	=	reactive oxygen species
rpm	=	revolutions per minute
RyR	=	ryanodine receptor

SAR	=	structure activity relationship
SBP	=	systolic blood pressure
SERCA	=	sarcoplasmic reticulum Ca^{2+}-ATPase
sGC	=	soluble guanylyl cyclase
SHR	=	spontaneously hypertensive rat
SMC	=	smooth muscle cell
SMOCs	=	second messenger-operated Ca^{2+} channels
SOCCs	=	store-operated Ca^{2+} channels
SNP	=	sodium nitroprusside
SNS	=	sympathetic nervous system
SR	=	sarcoplasmic reticulum
STZ	=	streptozotocin
SV	=	stroke volume
SVR	=	systemic vascular resistance
TNF-α	=	tumor necrosis factor- alpha
TPR	=	total peripheral resistance
Tris-HCl	=	Tris hydrochloride
TXA_2	=	thromboxane A_2
VSMC	=	vascular smooth muscle cell
VOCCs	=	voltage-operated Ca^{2+} channels
VSMC	=	vascular smooth muscle cell
WHO	=	World Health Organization
WHO FC	=	World Health Organization Functional Class
w/v	=	weight/volume
α-NF	=	alpha-naphthoflavone
α_1	=	alpha-1
β-NF	=	β-naphthoflavone
μg	=	microgram
μL	=	microliter
μM	=	micromolar

CHAPTER I

INTRODUCTION

Rationale of the study

Pulmonary arterial hypertension (PAH) is associated with pulmonary vascular remodeling which is a rise in mean pulmonary arterial pressure (mPAP) due to elevated pulmonary vascular resistance (PVR). This leads to reduced cardiac output (CO), right ventricular hypertrophy, right heart failure, and ultimately death if the PAH patients remain untreated (Hassoun, 2021; Humbert et al., 2022). The pathogenesis of PAH begins with the structural changes of the small PA from the narrowing or obstruction caused by several factors including hypoxia, genetic susceptibility, enhanced inflammation, vasoconstriction, vascular smooth muscle cells (VSMCs) proliferation, and endothelial dysfunction (Gredic et al., 2021; Humbert et al., 2019; Humbert et al., 2008; Sommer et al., 2021). Among the therapeutic options available, phosphodiesterase-5 (PDE5) inhibitors are the gold standard for PAH treatment (Badlam & Bull, 2017; Gredic et al., 2021; Pesto et al., 2016; Sommer et al., 2021). PDE5 specifically hydrolyzes cyclic guanosine monophosphate (cGMP) into 5′GMP, thus a high level of PDE5 activity can reduce cGMP in the VSMCs, leading to vasoconstriction. Therefore, the higher expression of PDE5 in PAH makes it a strong repressor of cGMP signaling in the disease. Therefore, PDE5 inhibitors are powerful vasorelaxant drugs (Andersson, 2018; Gredic et al., 2021). Among them, sildenafil is a first-line drug for the treatment of PAH, in monotherapy or in association with endothelin receptor antagonists (Andersson, 2018; Cruz-Burgos et al., 2021; Gautam V Ramani & Myung H Park, 2010; Zirak et al., 2021). Most of the side effects of sildenafil are secondary to a loss of selectivity for PDE5 (i.e., visual disturbances) and/or for pulmonary circulation (i.e. systemic hypotension, headache, flushing, nasal congestion) (Bhatia et al., 2003; Galiè et al., 2005; Leal et al., 2020). In addition, even though the hepatic toxicity of sildenafil has been considered rare, some cases of sildenafil-associated hepatotoxicity have been reported in the last decade (Graziano et al., 2017). Moreover, sildenafil was suspected as a weak inhibitor

of cytochrome P450 (CYP) 1A2, 2C9, 2C19, 2D6, 2E1 and 3A4 (IC_{50} > 150 µM) (Sheweita et al., 2016). Altogether, these data encourage identifying new PDE5 inhibitors to improve the management of PAH.

Quinazoline is an aromatic heterocyclic chemical compound with the formula $C_8H_6N_2$ and is also known as benzo-1,3-diazine or 1,3-diazanaphthalene. It is a bicyclic structure comprising two fused six-member simple aromatic rings, one benzene ring and one pyrimidine ring (Alagarsamy et al., 2018). These motifs make quinazolines good templates for the development of molecules of biological and pharmaceutical interest (Horton et al., 2003). Many medicines, agrochemicals, and veterinary treatments use quinazoline frameworks as building blocks to develop various compounds, which were used as marketed drugs for the treatment of arterial hypertension (Prazosin, Alfuzosin, Bunazosin, Quinethazone), yeast infection (Trimetrexate), cancer (Gefitinib, Erlotinib), or used as a dihydrofolate reductase inhibitor for pharmacological studies (Trimetrexate) (Selvam & Kumar, 2015). Consistently, pharmacological studies also demonstrated that quinazoline derivatives exhibited anti-inflammatory (Yoon et al., 2012), anti-cancer (Chen et al., 2016), anti-hyperlipidemia and anti-hyperglycemia (Nie et al., 2016), anti-erectile dysfunction (Kim et al., 2008), anti-hypertension (Zuo et al., 2014b) and PDE5 inhibitory properties (Paracha et al., 2019; Pobsuk et al., 2019)

Objectives of the study

Recently, twenty quinazoline derivatives (N^2,N^4-disubstituted quinazoline 2,4-diamines) have been designed based on their pharmacophore similarity to sildenafil by team of Associate Professor Dr. Matthew Paul Gleeson (Faculty of Engineering King Mongkut's Institute of Technology Ladkrabang, Thailand). On a hunch, 2-3 quinazoline derivatives, which were prepared for a malaria project, were tested against PDE5 based on the analysis of pharmacophoric similarity between the compounds and sildenafil. Incidentally, the compounds most active against PDE5 were inactive against the malaria target using molecular docking and scaffold similarity, as described in Pobsuk et al. (2019). Further compounds were then designed based on their pharmacophore similarity to sildenafil to develop the

compounds as the drug for PAH and a total of 20 compounds were developed and measured PDE5 and PDE6 inhibitory activity and structure activity relationship (SAR) as described in Pobsuk et al. (2019). Based on their PDE5 inhibitory activity, Paracha et al. (2019) collected 13 compounds (compounds **1**-**13**) to investigate their vasorelaxant effect on rat PA. Among them, six compounds (compounds **4**, **5**, **8**, **9**, **10** and **11**) demonstrated promising inhibitory effects on rat PDE5 as well as inducing PA vasorelaxation (Paracha et al., 2019). The potent PDE5 inhibitory activity of the quinazoline derivatives suggests that they could potentially be developed as PDE5 inhibitors for the treatment of PAH. Nevertheless, their vasorelaxant effect and underlying mechanisms have never been reported and it remains a matter to be explored whether or not these could lead to a reduction of either pulmonary or systemic blood pressure. Therefore, to evaluate their potential as future new drugs for PAH treatment, the present study investigated the action of quinazoline derivatives as PDE5 inhibitors to determine their beneficial effects on pulmonary as compared to systemic vasculature.

Compound ID	Core structure	R^1	R^2
1	**Quinazoline** 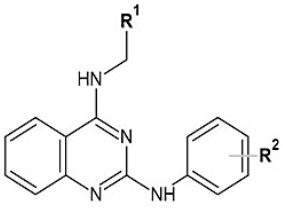	–phenyl	–H
2		–phenyl	–4-morpholino
3		–phenyl	–4-$SO_2N(CH_3)_2$
4		–phenyl	–4-SO_2NH_2
5		–phenyl	–3-SO_2NH_2
6		–2-thiophene	–H
7		–2-thiophene	–4-NHCONHPh
8		–2-thiophene	–4-morpholino
9		–2-thiophene	–4-SO_2NH_2
10		–2-thiophene	–4-$CONH_2$
11		–2-thiophene	–3-SO_2NH_2
12		–2-thiophene	–3-$CONH_2$
13		–furan	–3-SO_2NH_2
14		–3-Methoxybenzylamino	–3-SO_2NH_2
15	**6,7-Dimethoxyquinazoline**	–3-Amino-5-methylpyrazolo	–3-SO_2NH_2
16		–6,7-Dimethoxyquinazoline	–3-SO_2NH_2
17		–3-Methoxybenzylamino	–3-SO_2NH_2
18		–2-Thiophenemethylamino	–3-SO_2NH_2
19		–Furfurylamino	–3-SO_2NH_2
20	**5-Chloropyrimidine**	–Benzylamino	–H

Figure 1 The chemical structure of *N^2,N^4*-diaminoquinazoline based compounds

Source: Pobsuk et al. (2019) (Permission from Elsevier)

Aims of the thesis

Twenty quinazoline derivatives (N^2,N^4-disubstituted quinazoline 2,4-diamines) have been designed based on their pharmacophore similarity to sildenafil, to develop new PDE5 inhibitors for the treatment of PAH (Paracha et al., 2019; Pobsuk et al., 2019). Among them, six compounds (compounds **4**, **5**, **8**, **9**, **10** and **11**) present promising inhibitory effects on rat PDE5 and induced PA vasorelaxation (Paracha et al., 2019). The potent PDE5 inhibitory activity of the quinazoline derivatives suggests that they could potentially be developed as PDE5 inhibitors for the treatment of PAH. However, the effects of the quinazoline derivatives have rarely been reported in studies on rat pulmonary circulation and systemic circulation, thus their mechanisms of actions are still unclear. Therefore, the objective of the present study was to investigate the effect of the quinazoline derivatives on cardiovascular function and its underlying mechanisms in both pulmonary circulation and systemic circulation. Their cytotoxicity on isolated rat hepatocytes and their impact on CYP inhibition and induction were also evaluated. All results obtained from this research project were tested in non-clinical situations, offering scientific evidence or knowledge of the physiological and pharmacological action of quinazoline derivatives which would be needed for animal models or clinical studies. Further development is needed for quinazoline derivatives to be demonstrated as an alternative drug or supplement for patients with PAH or systemic hypertension. The results from this study will provide scientific evidence which will inform the future development of therapies for PAH and hypertension.

Study I: Identification of N^2,N^4-disubstituted quinazoline 2,4-diamines with human PDE5 inhibition, vasorelaxant effects on pulmonary and systemic circulation, cytotoxicity, and CYP activities in comparison to sildenafil.

To address each objective, experiments were carried out as follows:

Scope 1: A two-step radioactive assay was employed to investigate the inhibitory effects against human PDE5 by the quinazoline derivatives. The PDE5 enzymes were extracted from cell cultures of human embryonic kidney 293 (HEK293) cells transfected with human PDE5A1 plasmid.

Scope 2: It was important to identify the selectivity of the quinazoline derivatives on the pulmonary and systemic circulatory system. An *in vitro* study of their vasorelaxation effects was carried out on various types of rat blood vessels including the isolated rat aorta, pulmonary artery (PA) and mesenteric artery (MA).

Scope 3: The vasorelaxant effects of the quinazoline derivatives on isolated rat PA and MA were investigated using the organ bath and myograph techniques. The mechanisms of actions of the quinazoline derivatives on the endothelium, such as the involvement of NO, PGI_2 and EDHF pathways, were examined. The mechanisms of the actions of the quinazoline derivatives on VSMCs, such as the involvement of K^+ channels, Ca^{2+} channels, α_1-adrenergic receptor and sGC/cGMP pathway, were also investigated. Sildenafil was used as a reference comparator.

Scope 4: The structure-activity relationship (SAR) of the quinazoline derivatives were determined based on their tested activities.

Scope 5: The *in vitro* cytotoxicity of the quinazoline derivatives and sildenafil was tested on freshly isolated VSMCs from rat aorta and PA using a methyl thiazolyl tetrazolium (MTT) assay.

Scope 6: The *in vitro* cytotoxicity of the quinazoline derivatives was tested on freshly isolated rat hepatocytes using MTT assay. Sildenafil was used as a reference comparator.

Scope 7: The non-cytotoxic concentrations of the quinazoline derivatives were chosen to treat hepatocytes before testing their effect on CYP activities, including CYP1A, 2B, 2C, and 3A. Sildenafil was used as a reference comparator.

The results from this study were published in Vascular Pharmacology (Chatturong et al., 2022).

Usana Chatturong, Hélène Martin, Perle Totoson, Kornkanok Ingkaninan, Prapapan Temkitthawon, Saharat Sermsenaphorn, Thanachon Somarin, Adchatawut Konsue, M. Paul Gleeson, Céline Demougeot, Krongkarn Chootip. Quinazoline-based human phosphodiesterase 5 inhibitors exhibited a selective vasorelaxant effect on rat isolated pulmonary arteries involving NO-sGC-cGMP pathway and calcium inhibitory effects. *Vascular Pharmacology* (Q1, impact factor 5.738). Volume 147, December 2022, 107111. Doi: 10.1016/j.vph.2022.107111

Study II:. Effects of compound 8 on isolated MA and mechanisms involved, blood pressure, cytotoxicity, and CYP activities in comparison to nifedipine.

To address each objective, experiments were carried out as follows:

Scope 1: The vasorelaxant effects of the compound **8** on isolated rat MA were investigated using myograph techniques. The mechanisms of actions of compound **8** on the endothelium, such as the involvement of NO, PGI_2 and EDHF pathways, were examined. The mechanisms of the actions of the quinazoline derivatives on VSMCs, such as the involvement of K^+ channels, Ca^{2+} channels, α_1-adrenergic receptor, and sGC/cGMP pathway, were also investigated. Nifedipine was used as a reference comparator.

Scope 2: The *in vivo* effect of the intravenous injection of compound **8** on anesthetized rats was determined by measuring systolic blood pressure (SBP), diastolic blood pressure (DBP), mean arterial blood pressure (MAP) and heart rate (HR). Nifedipine was used as a reference comparator.

Scope 3: The SAR of compound **8** was determined based on their tested activities.

Scope 4: The *in vitro* cytotoxicity of compound **8** was tested on freshly isolated rat hepatocytes using MTT assay. Nifedipine was used as a reference comparator.

Scope 5: The non-cytotoxic concentrations of compound **8** were chosen to treat hepatocytes before testing their effect on CYP activities, including CYP1A, 2B, 2C, and 3A. Nifedipine was used as a reference comparator.

The results from this study were published in *European Journal of Pharmacology*.

Usana Chatturong, Krongkarn Chootip, Hélène Martin, Maude Tournier-Nappey, Kornkanok Ingkaninan, Prapapan Temkitthawon, Saharat Sermsenaphorn, Thanachon Somarin, Adchatawut Konsue, M. Paul Gleeson, Perle Totoson and Céline Demougeot. The new quinazoline derivative (N^2-methyl-N^4-[(thiophen-2-yl)methyl] quinazoline-2,4-diamine) vasodilates isolated mesenteric arteries through endothelium-independent mechanisms and has acute hypotensive effects in Wistar rats. *European Journal of Pharmacology* (Q1, impact factor 5.195). Volume 953, 15 August 2023, 175829. Doi: 10.1016/j.ejphar.2023.175829

CHAPTER II

REVIEW OF RELATED LITERATURE AND RESEARCH

Review related to quinazolines

1. Structure of quinazoline

Quinazoline (benzo-1,3-Diazine or 1,3-diazanaphthalene) is an aromatic heterocyclic chemical compound with the formula $C_8H_6N_2$ and molecular weight 130.15 g/mol. It is a bicyclic structure comprising two fused six-member simple aromatic rings, one benzene ring and one pyrimidine ring (Figure 2) (Ajani et al., 2016; Karan et al., 2021). The quinazoline nucleus was first isolated from the Chinese plant aseru (*Dichroa febrifuga* Lour) by chemist Siegmund Gabriel in 1903. Widdege was the first scientist to name this nucleus "quinazoline" based on its appearance (Faisal & Saeed, 2021). The presence of nitrogen-based heterocyclic ring structures in most medicinal chemistry reveals particular specificities in their pharmacological targets (Alsibaee et al., 2023). Thus, these motifs make quinazoline good templates for the development of new derivatives of biological and pharmaceutical interest (Horton et al., 2003). The synthesizing of many medicines, agrochemicals, and veterinary treatments uses quinazoline frameworks as building blocks, mediated by the patterns of substitution on the 1,3-diazine entity of the system (Ajani et al., 2016; Faisal & Saeed, 2021; Horton et al., 2003).

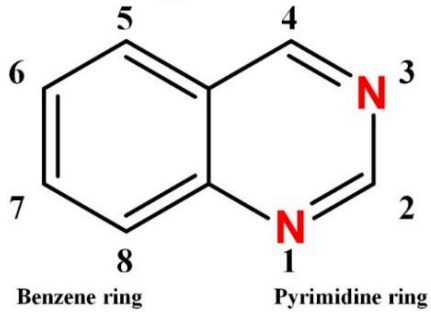

Figure 2 Structure of quinazoline

Source: Made by Usana Chatturong (2023)

Consistently, pharmacological studies also demonstrated that quinazoline derivatives exhibit antioxidant (Almehizia et al., 2019), anti-inflammation (Yoon et al., 2012), anti-bacterial (Misra et al., 2020), anti-cancer (Chen et al., 2016), anti-tubercular (Jadhavar et al., 2020), anti-hyperlipidemia and anti-hyperglycemia (Nie et al., 2016), anti-erectile dysfunction (Kim et al., 2008), anti-hypertension (Zuo et al., 2014b) and PDE5 inhibitory properties (Paracha et al., 2019; Pobsuk et al., 2019).

2. Therapeutic properties of quinazolines

2.1 Antioxidant

Reactive oxygen species (ROS) play a vital role in aging and the pathogenesis of age-related diseases. The basic nuclei of 2-methyl-4H-benzo[d][1,3]oxazin-4-one and 3-amino-2-methylquinazolin-4(*3H*)-one were successfully synthesized as quinazoline derivatives (compound **1**-**6**), as shown in Figure 3. Their antioxidant activities were measured using a 1,1-diphenyl-2-picrylhydrazyl (DPPH) assay and a nitric oxide (NO) radical scavenger assay. The results revealed that compounds **5** and **6** serve as highly resourceful scavengers against DPPH (2,2-diphenyl-1-picryl-hydrazyl-hydrate) and NO and have also shown antioxidant activity higher than the common antioxidant, ascorbic acid (vitamin C) (Al-Azawi, 2016).

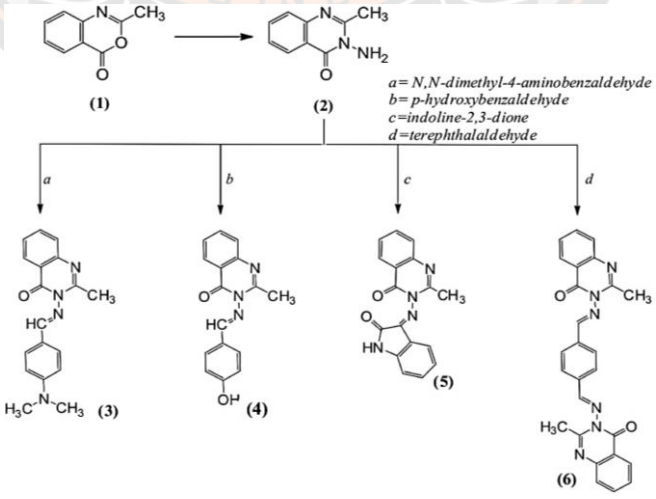

Figure 3 Synthesis of quinazoline derivatives (compound 1-6)

Source: Al-Azawi (2016) (Permission from Scientific Publishers)

2.2 Anti-inflammation

New compounds synthesized from 3-phenyl-2-substituted-*3H*-quinazolin-4-one with different aldehydes and ketones (Figure 4) showed greater anti-inflammatory activity than the reference standard diclofenac sodium. The compounds that moderated the inflammation from carrageenan-induced paw edema in rats are 2-(*N*′-2-butylidene-hydrazino)-3-phenyl-*3H*-quinazolin-4-one (**AS1**), 2-(*N*′-3-pentylidene-hydra zino)-3-phenyl-*3H*-quinazo lin-4-one (**AS2**) and 2-(N′-2-pentylidene-hydrazino)-3-phe nyl-*3H*-quinazolin-4-one (**AS3**). However, **AS3** is the best compound which has a higher percentage analgesic activity than other compounds (Alagarsamy et al., 2007).

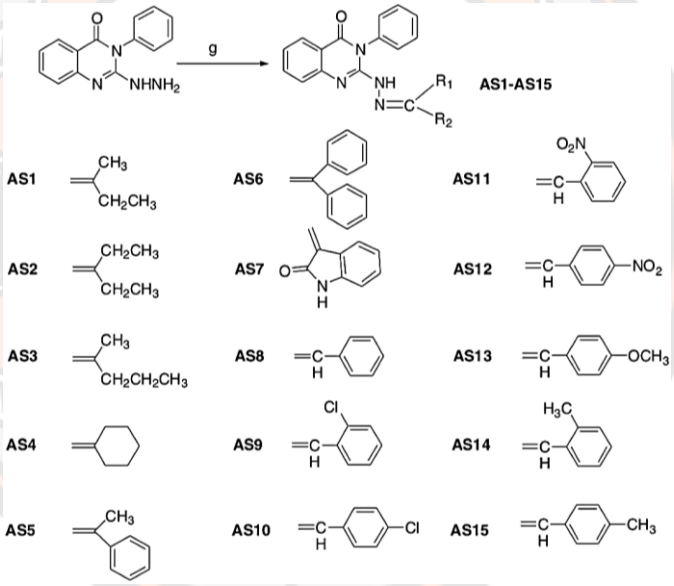

Figure 4 The synthesis of 3-phenyl-2-substituted-*3H*-quinazolin-4-one with different aldehydes and ketones (AS1-15)

Source: Alagarsamy et al. (2007) (Permission from Elsevier)

2.3 Anti-cancer

2-chloro-6-phenyl-8H-quinazolino[4,3-b]quinazolin-8-one is a natural quinazoline derivative isolated from the marine sponge *Hyrtios erectus*. This compound has demonstrated anti-cancer activity by inducing apoptosis of the human

breast carcinoma cell line (De et al., 2019). In addition, quinazoline was used as the core structure in the design of a new series of 6, 7-dialkoxy-4-anilinoquinazolines by substituting different heterocycles on position 6 and a variety of anilines on position 4 (Figure 5). These compounds were evaluated for their cytotoxic effect on the epidermal growth factor receptor overexpressing skin epidermoid carcinoma cell line (A431). This result indicated that 2-butyl-4-chloro-1-[3-[7-methoxy-4-(3-(trifluoro methyl)phenylamino) quinazolin-6-yloxy]-propyl]-*1H*-imidazole-5-carboxaldehyde (**30**), with IC_{50} of 3.5 µM, and 2-butyl-4-chloro-1-(3-[4-(3-iodophenyl amino)-7-methoxyquinazolin-6-yloxy]propyl)-*1H*-imidazole-5-carboxaldehyde (**33**) with IC_{50} of 3 µM, show the highest activity against cell proliferation of A431 (Chandregowda et al., 2009).

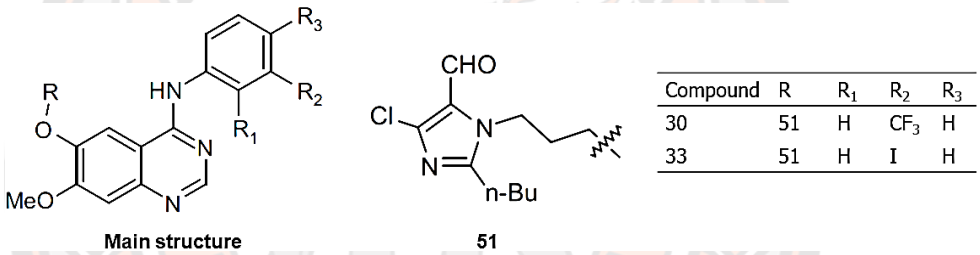

Compound	R	R_1	R_2	R_3
30	51	H	CF_3	H
33	51	H	I	H

Figure 5 Chemical structures of anti-cancer drugs

Source: Chandregowda et al. (2009) (Permission from Elsevier)

2.4 Anti-infectives

Various quinazoline derivatives have been synthesized and screened for their antimicrobial screening against various microbial strains. Constantly increasing antimicrobial resistance requires researchers to synthesize new compounds and test their activities. Vivek Gupta and coworkers synthesized novel 4(3H)-quinazolinone analogues by replacing the styryl moiety and substituted oxadiazole at the second and third position of 4(3H)-quinazolinone. They obtained new compounds called 3-[5-(4-substituted) phenyl-1,3,4-oxadiazole-2-yl]-2-styryl quinazoline-4(3H)-one (**7a**–**o**), as shown in Figure 6. These compounds were screened for their anti-bacterial and anti-fungal activity. Compound **7d**, the most active of the prepared series, inhibited both bacteria; *Staphylococcus aureus*, *Bacillus subtilis*, *Pseudomonas*

aeruginosa, and *Escherichia coli*, and fungi; *Aspergillus niger* and *Fusarium oxysporum* (Gupta et al., 2008).

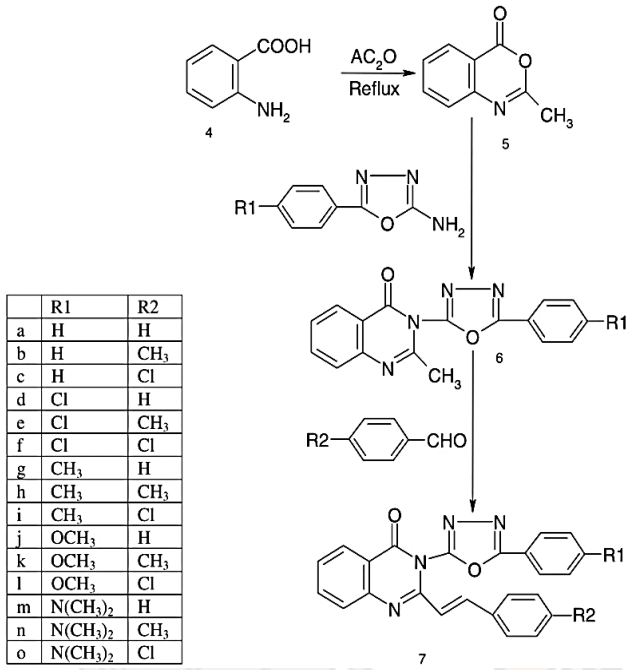

	R1	R2
a	H	H
b	H	CH_3
c	H	Cl
d	Cl	H
e	Cl	CH_3
f	Cl	Cl
g	CH_3	H
h	CH_3	CH_3
i	CH_3	Cl
j	OCH_3	H
k	OCH_3	CH_3
l	OCH_3	Cl
m	$N(CH_3)_2$	H
n	$N(CH_3)_2$	CH_3
o	$N(CH_3)_2$	Cl

Figure 6 Scheme for the synthesis of the 3-[5-(4-substituted) phenyl-1,3,4-oxadia zole-2-yl]-2-styryl quinazoline-4(3H)-one (7a–o)

Source: Gupta et al. (2008) (Permission from Springer Nature)

Rondla Rohini and coworkers developed a new series of indolo[1,2-c]quinazoline derivatives which were prepared through the reaction of 2-(o-aminophenyl)indole **(A)**, the key compound for the building of the indolo[1,2-c]quinazoline, with a variety of arylaldehydes (Figure 7). The new series of indolo[1,2-c] quinazoline derivatives were investigated for their anti-bacterial and anti-fungal activity. The results revealed that the indolo[1,2-c]quinazoline derivatives including compounds **IIa**, **IIf**, **IIh** and **IIi** had the highest activity against all gram-positive bacteria consisting of *Staphylococcus aureus*, *Bacillus subtilis* and *Streptococcus pyogenes* (Rohini et al., 2010).

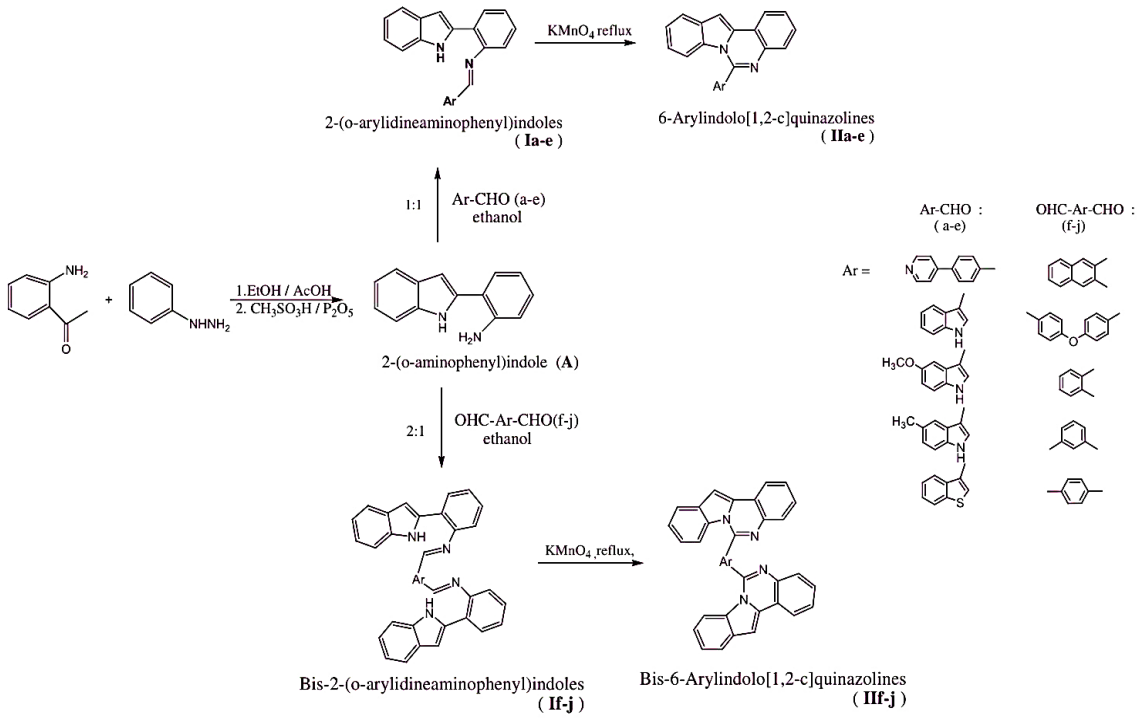

Figure 7 Synthetic route of mono, bis-indolo[1,2-c]quinazolines

Source: Rohini et al. (2010) (Permission from Elsevier)

2.5 Antipsychotics

Mario Alvarado and coworkers synthesized new quinazoline derivatives (compounds **14** and **15**, Figure 7), and their anti-psychotic activity was evaluated using human serotonin subtypes 2A (5-HT_{2A}), 5-HT_{2C} and dopamine D_2 binding site assay. They reported that compound **15** presented the highest affinities to the serotonin 5-HT_{2A} and dopamine D_2 receptors, which are mechanisms of atypical antipsychotics (Alvarado et al., 2006).

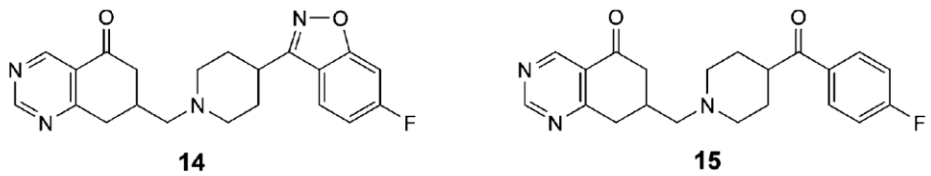

Figure 8 Quinazoline derivative structures for screened anti-psychotics activity.

Source: Alvarado et al. (2006) (Permission from John Wiley and Sons)

2.6 Anti-diabetes and Anti-obesity

Osama Mohamed Ahmed and coworkers designed a novel quinazoline derivative that is 1-thioxo-1,2,7,8,9,10-hexahydro-*3H*-pyrimido[1,6-*a*] quinazolin-3-one. They tested the anti-hyperglycemic and anti-hyperlipidemic properties in neonatal streptozotocin (n-STZ)-induced type 2 diabetic rats. After 14 weeks post-STZ injection, the rats were treated with 1-thioxo-1,2,7,8,9,10-hexahydro-*3H*-pyrimido[1,6-*a*]quinazolin-3-one at the dose of 10 mg/kg body weight (BW) per day by oral administration for 3 weeks. The result showed that this derivative had remarkable potential in STZ-induced type 2 diabetic male and female rats as anti-hyperglycemic and anti-hyperlipidemic agents (Ahmed et al., 2012).

Rutaecarpine or 8,13-dihydroindolo-[2',3':3,4]-pyrido[2,1-*b*]quinazolin -5(*7H*)-one was extracted from the dried fruit of Wu-Chu-Yu (*Evodia rutaecarpa* (Juss) Benth), which is known as the Chinese herb. The anti-diabetic and anti-obesity activities of this compound were studied in male Sprague-Dawley rats fed on a high-fat diet for 8 weeks, followed by STZ injection to induce hyperlipidemia and hyperglycemia. After one week of STZ injection, the rats were orally treated with rutaecarpine at the dose of 25 mg/kg BW/day for 7 weeks. The results showed that the treatment with rutaecarpine significantly decreased obesity, visceral fat accumulation, and serum total cholesterol, triglyceride and low-density lipoprotein cholesterol levels and increased high-density lipoprotein cholesterol levels in fat-fed/STZ rats. In addition, rutaecarpine significantly decreased blood glucose levels at week 16 more than was shown in the fat-fed/STZ-control group. This study suggested that rutaecarpine can attenuate hyperglycemia and enhanced insulin sensitivity (Nie et al., 2016).

2.7 Anti-hypertension

A number of quinazoline alkaloids have been isolated from the dried, unripe fruit of *Evodia rutaecarpa* (Juss.) Benth (Rutaceae, popularly known in China as “Wu-Chu-Yu”), including dehydroevodiamine, evodiamine, rutaecarpine, rutaevine, wuchuyine, and rhetsinine (Chen & Chen, 1933). Wen-Fei Chiou and coworker have evaluated the pharmacological actions of quinazoline alkaloids

isolated from *E. rutaecarpa* including dehydroevodiamine (**1**), evodiamine (**2**), and rutaecarpine (**3**), Figure 9. Their vascular action were evaluated on male Sprague-Dawley rat thoracic aorta using the organ bath technique. All compounds produced cumulative concentration-dependent relaxation (10^{-7}-10^{-4} M) in thoracic aortic rings pre-constricted with phenylephrine (PE, 3×10^{-7} M). These results demonstrated that all compounds elicited concentration-dependent vasodilation in endothelium-intact aortic rings with equal potency, by showing the E_{max} as 100% and IC_{50} as 1.64 µM for **1**, 0.93 µM for compound **2** and 1.05 µM for compound **3**. Compound **3** caused a complete (100%) NO-dependent vasodilatation, while compound **1** produced a 10% endothelium-dependent effect and compound **2** produced a 50% endothelium-dependent effect. At the same time, both compounds **1** and **2** also functioned by other mechanisms such as the probable antagonist effect on the α_1-adrenergic receptor and serotonin receptor (Chiou et al., 1996).

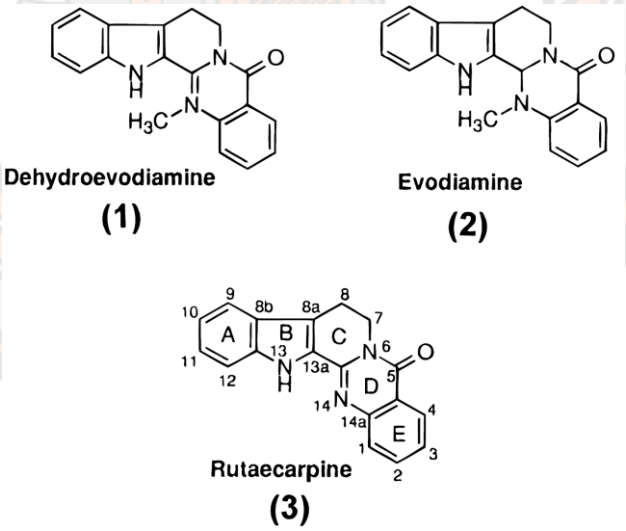

Figure 9 Chemical structure of quinazoline alkaloids isolated from *E. rutaecarpa*, dehydroevodiamine (1), evodiamine (2), and rutaecarpine (3)

Source: Chiou, Liao, & Chen (1996) (Permission from American Chemical Society)

Several quinazolinone-arylpiperazine derivatives (Figure 10) have been tested for their *in vivo* hypotensive activity. The effect of nine selected compounds including **4b**, **9b**, **9e**, **13b**, **13g**, **13i**, **13j**, **13k** and **13l** at the dose of 500 µg/kg BW were investigated for their effect on the blood pressure of normotensive rats using the cannulation technique, of which prazosin was used as a positive control. The results indicated that most of the tested compounds could reduce both systolic blood pressure (SBP) and diastolic blood pressure (DBP). Compound **13j** showed more potent anti-hypertensive activity than prazosin. In addition, compounds **4b**, **9e**, **13i**, and **13j** were found to have potent α_1-adrenoreceptor antagonistic activity, which displayed lower IC_{50} values and higher potency than prazosin in inhibiting norepinephrine-induced contraction in isolated rat aorta (Figure 12) (Abou-Seri et al., 2011).

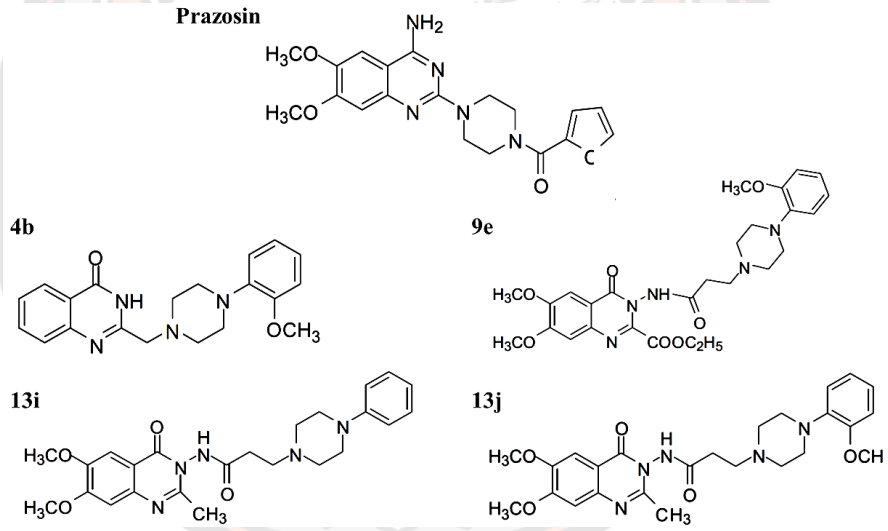

Figure 10 Chemical structure of quinazolinone-arylpiperazine derivatives

Source: Abou-Seri et al. (2011) (Permission from Elsevier)

Other than natural resources, based on diverse pharmacological activities possessed by quinazoline nucleus, scientists have synthesized various analogues such as 3-benzylquinazolin-4(*3H*)-ones. Sai-Jie Zuo and a coworker synthesized a series of 3-benzylquinazolin-4(*3H*)-ones and their vasodilatory effects were evaluated on isolated rat mesenteric arterial rings using a wire myograph. The

results showed that compounds **2a** and **2c** (Figure 11) significantly induced greater vasorelaxation of the isolated rat mesenteric arterial rings than the effect of nitrendipine that was used as a reference drug. In addition, incubation of arterial rings with each compound decreased the vasoconstriction afforded by phenylephrine (PE). The anti-hypertensive effects of compounds **2a** and **2c** were also investigated *in vivo* in hypertensive rat models. The spontaneously hypertensive rats (SHR) were orally administrated with either compounds **2a** and **2c** at the dose of 4 mg/kg BW or with nitrendipine at the dose of 2 mg/kg BW. Systolic blood pressure (SBP) and diastolic blood pressure (DBP) was measured before (0 h) and after (1 h) drug administration. The results indicated that compounds **2a** and **2c** exhibited significant antihypertensive effects in SHR. Compound **2c** was more potent than compound **2a** (Zuo et al., 2014a).

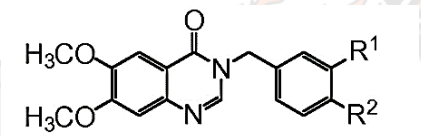

Compd	R^1	R^2
2a	OMe	OBn
2b	OBn	OMe
2c	OMe	OCH_2Ph-4-F
2d	OMe	OCH_2Ph-3-F
2e	OMe	OCH_2Ph-3,4-diOMe
2f	H	OCH_2Ph-4-F
2g	Cl	OCH_2Ph-4-F
2h	F	OCH_2Ph-4-F
2i	OMe	OH
2j	OMe	OCH_2Py-4
2k	OMe	OCH_2Py-3
2l	OMe	OCH_2Ph-2,4-diCl

Figure 11 Chemical structure of 3-benzylquinazolin-4(*3H*)-ones derivatives (2a-2l)

Source: Zuo et al. (2014) (Permission from Elsevier)

2.8 PDE5 inhibitory properties

PDE5 specifically hydrolyses cGMP into 5′GMP, thus a high level of PDE5 can cause a reduction in cGMP that leads to VSMCs contraction and finally vasoconstriction. Therefore, the inhibitors of PDE5 are powerful vasoactive drugs that are widely used to treat ED and PAH (Andersson, 2018; Gredic et al., 2021).

Utilization of sildenafil (PDE5 inhibitor) for ED and PAH treatment comes with shortcomings because of its lack of selectivity. As a result, it is necessary to discover and synthesize more potent compounds capable of inhibiting PDE5 and treating ED and PAH more effectively and with lower side effects.

Rotella et al. (2000) synthesized new quinazoline analogues and investigated their effects on the treatment of ED in a comparative study with sildenafil (as the positive control) on corpus cavernosum tissue strips isolated from adult male white rabbits. The results showed that 1-[3-[1-[(4-Fluorophenyl) methyl]-7,8-dihydro-8-oxo-1*H*-imidazo[4,5-*g*]quinazolin-6-yl]-4-propoxyphenyl] carboxamide (compound **14**,) had higher PDE5 inhibitor activity (IC_{50} as 0.48 nM) than other analogues and had less affinity for PDE6. In a functional assay of erectile function, the compound demonstrated activity similar to sildenafil based on the ability of the compound to induce relaxation of rabbit corpus cavernosum tissue. The search for potent and more selective PDE5 inhibitors is an ongoing process.

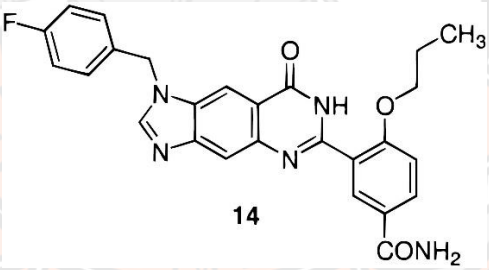

Figure 12 Chemical structure of compound 14

Source: Rotella et al. (2000) (Permission from Journal of Medicinal Chemistry)

Bi et al. (2004) reported that 4-benzylaminoquinoline derivatives were highly potent and selective at the same time with suitable substitutions at **6**,**7** and **8** positions on quinazoline structure (Figure 13). Compounds **6f**, **6h**, **6i** and **6j** demonstrated higher potency for the inhibition of PDE5 than PDE1, PDE6 and PDE11 whose IC_{50} to inhibit PDE5 is around 50 pM.

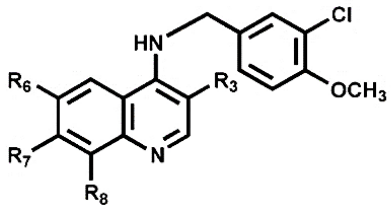

Compd	R_3	R_6	R_7	R_8
6a	COOEt	H	CF_3	H
6b	COOEt	CF_3	H	H
6c	COOEt	CN	H	H
6d	H	CN	H	H
6e	$CONHCH_2$-Py	CN	H	H
6f	CH_2OH	CN	H	H
6g	COOEt	CN	H	H
6h	H	CN	H	H
6i	$CONHCH_2$-Py	CN	H	H
6j	CH_2OH	CN	H	H

Figure 13 Chemical structure of 4-benzylaminoquinoline derivatives

Source: Bi et al. (2004) (Permission from Elsevier)

Kim et al. (2008) studied the effect of new quinazoline derivatives on PDE5 activity with simple substitution at 6-, 7-, or 8-position (Figure 14A), with sildenafil and tadalafil used as positive references. They found that compound **13** (4-(3-chloro-4-methoxy)-benzylamino-7-methoxy quinazoline) with alkyl groups at the 8-position showed higher potency to inhibit PDE5 than other derivatives. Therefore, they are continuing their study by using compound **13** structure as a stereotype for the synthesis second series of new quinazoline derivatives (compounds **23**-**28**, Figure 14B) with various alkyl groups at the 8-position and different functional groups at the R position. Compounds **25** and **28** were the most effective for inhibiting PDE5 at IC_{50} 0.01 µM for compound **25** and 0.001 µM for compound **28**. In addition, compound **28** showed 10-fold more potency to inhibit PDE5 than tadalafil (IC_{50} 0.012) and sildenafil (IC_{50} 0.01 µM). Compounds **25** and **28** were selected for a study on a conscious rabbit model. The rabbits were orally administered with compounds **25** and **28** (3 and 10 mg/kg) and tadalafil (3 mg/kg) for 60 min, followed by a sodium nitroprusside (SNP, 0.1 mg/kg) injection and the length of the penis erection was measured. The results showed that there was no penile erection in the vehicle group, while the erectogenic effect was potentiated by SNP injection which is an NO donor that was used as a sexual stimulant. Both compounds presented a similar dose-dependent erectogenic effect than tadalafil.

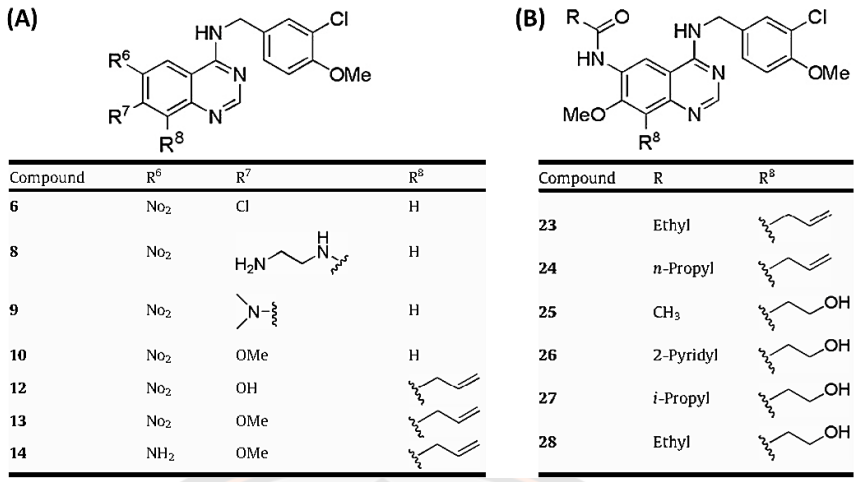

Compound	R^6	R^7	R^8
6	No_2	Cl	H
8	No_2		H
9	No_2		H
10	No_2	OMe	H
12	No_2	OH	
13	No_2	OMe	
14	NH_2	OMe	

Compound	R	R^8
23	Ethyl	
24	*n*-Propyl	
25	CH_3	
26	2-Pyridyl	
27	*i*-Propyl	
28	Ethyl	

Figure 14 Chemical structure of quinazoline derivatives (A) and 4-(3-chloro-4-methoxy)-benzylamino-7-methoxy quinazoline derivatives (B)

Source: Kim et al. (2008) (Permission from Elsevier)

Recently, Associate Professor Dr. Matthew Paul Gleeson and team (Faculty of Engineering King Mongkut's Institute of Technology Ladkrabang, Thailand). synthesized 20 new N^2,N^4-disubstituted quinazoline 2,4-diamines derivatives, as shown in Figure 1. These derivatives were designed based on their pharmacophore similarity to sildenafil and developed as PDE5 inhibitors. The investigation of their PDE5 and PDE6 inhibitory activities revealed that all quinazoline derivatives inhibited the PDE5 enzyme isolated from rat lungs. Specifically, compounds **5** and **11** displayed high potency as PDE5 inhibitors, exhibiting around 4-fold greater selectivity over PDE6 inhibition, while sildenafil demonstrated a 6.5-fold selectivity for PDE5 over PDE6 (Pobsuk et al., 2019). Furthermore, it was found that compound **20**, containing a pyrimidine core, was inactive in inhibiting the PDE5 enzyme, with an IC_{50}>10 μM. This indicates the essential role of a quinazoline ring for PDE5 inhibition. Based on their PDE5 inhibitory activity, Pobsuk et al. (2019) selected 13 compounds (compounds **1-13** with N^2, N^4-disubstituted quinazoline 2,4-diamines core structure) to investigate their cytotoxicity on alveolar basal epithelial cells and their vasorelaxant effect on rat

pulmonary artery (PA). The study revealed cytotoxicity, with an IC_{50} of 3 μM for compound **7** and >11 μM for other compounds. Moreover, compounds **8**, **9**, **10**, **5**, **11**, and **4** were the most active in inducing PA relaxation, respectively. The potent PDE5 inhibitory and vasorelaxant activities of the quinazoline derivatives suggest that they could potentially be developed as PDE5 inhibitors for the treatment of PAH. Nevertheless, their selectivity to induce PA relaxation and the underlying mechanisms have never been reported and it remains a matter to be explored whether or not these could lead to a reduction of either pulmonary or systemic blood pressure.

3. Quinazolines in the markets

Quinazoline is a good template for the development of new derivatives of biological and pharmaceutical interest. There are several approved drugs with a quinazoline structure in the market, as described in the Table 1.

Table 1 Quinazolines in the markets

Drug	Structure	Trade name	Indications	Reference
α_1-adrenergic receptor antagonist				
Alfuzosin	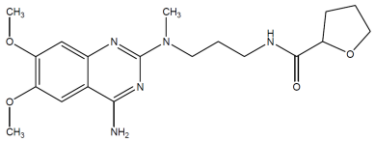	UroXatral Urion Xatral Alfetim	• It is used to treat benign prostatic hyperplasia	(Jardin et al., 1991)
Bunazosin	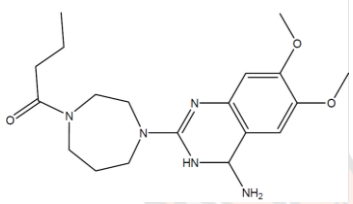	Andante	• It has been clinically used both as a systemic antihypertensive and an ocular hypotensive drug. • It has been approved in Japan in a topical form to treat glaucoma.	(Hara et al., 2005)
Fenquizone	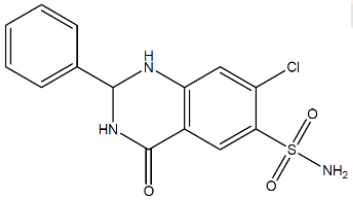	Idrolone	• It is a diuretic drug, which is used primarily in the treatment of edema and hypertension.	(Tiberi & Corinaldesi, 1981)

Drug	Structure	Trade name	Indications	Reference
Prazosin	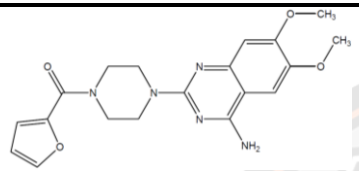	Minipress Vasoflex Pressin	• It has been widely used in treating hypertension and congestive heart failure.	(Stanaszek et al., 1983)
Quinethazone	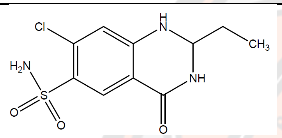	Hydromox	• It is a thiazide diuretic used to treat hypertension.	(Pilewski et al., 1971)
PDE3 inhibitor				
Quazinone	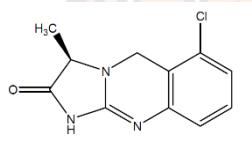	Dozonone Posicor	• It is a cardiotonic and vasodilator drug developed and marketed for treating heart disease.	(Amsallem et al., 2005)
Epidermal growth factor receptor tyrosine kinase inhibitors				
Erlotinib	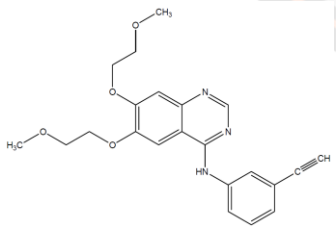	Tarceva	• It is used to treat some types of cancer including non-small cell lung cancer and pancreatic cancer.	(Shi et al., 2014)

Drug	Structure	Trade name	Indications	Reference
Gefitinib	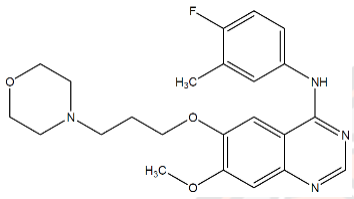	Iressa	• It is the first targeted therapy drugs approved for the treatment of advanced non-small-cell lung cancer.	(Xu et al., 2010)
Raltitrexed	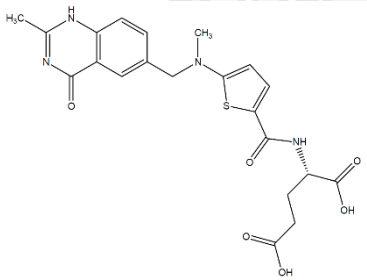	Tomudex	• It is also an inhibitor of thymidylate synthase and dihydrofolate reductase. • It is used as a folate antimetabolite drug for colorectal cancer chemotherapy.	(Ciardiello, 2000; Gunasekara & Faulds, 1998)
Vandetanib	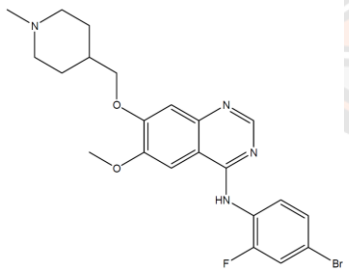	Zactima	• It was developed and marketed for the treatment of certain types of thyroid cancer.	(Brassard et al., 2011)

Drug	Structure	Trade name	Indications	Reference
Medications for myeloproliferative disorders				
Anagrelide	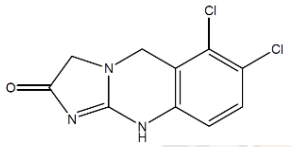	Agrylin Xagrid Shire Anagrelide	• It is a drug used for the treatment of essential thrombocytosis and chronic myeloid leukemia.	(Birgegard, 2006)
Non-steroidal anti-inflammatory agent				
Proquazone	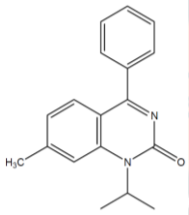	Biarison	• It is used to treat the pain, swelling and redness associated with acute gouty arthritis.	(Clissold & Beresford, 1987)
Dipeptidyl peptidase-4 inhibitor				
Linagliptin	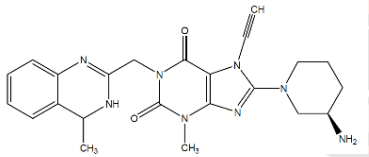	Ondero	• It is used to reduce blood sugar in patients with type 2 diabetes mellitus.	(Forst et al., 2011)

Source: The chemical structure of drugs obtained from PubChem, National Center for Biotechnology Information (https://pubchem.ncbi.nlm.nih.gov).

Review of related cardiovascular physiology and hypertension

1. Vascular structure

Blood vessels transport oxygen (O_2) to critical organs and tissues while also removing metabolic waste from the tissue. Blood vessels include the artery, capillary, and vein that are linked in series. The three types of blood vessels have distinct sizes and histologic characteristics (Figure 15). The wall surrounding the lumen of the artery and vein is made up of three tissue layers, while the capillary is made up of one tissue layer. The innermost layer, the tunica intima, is a single layer of simple squamous endothelial cells lined on the basement membrane that is in direct contact with the blood in the lumen. The middle layer, tunica media, consists of circularly arranged smooth muscle cells (SMCs) and a sheet of elastin, which regulates blood flow and pressure by vasoconstriction or vasorelaxation. The outermost layer, tunica externa or tunica adventitia, is composed of lymphatic, nerve plexus, and fibro-elastic connective tissue that protects the blood vessels and anchors them to the surrounding structures (Pugsley & Tabrizchi, 2000).

Based upon differences in function and histology, arteries can be classified into three distinct types; elastic arteries, muscular arteries, and arterioles (Martini et al., 2011).

1. Elastic (or conducting) arteries are the large blood vessels present near the heart or other organs associated with the movement of a large volume of blood e.g., the aorta, PA, and common carotid artery. The tunica media is composed of many layers of elastic membranes and smooth muscles. These arteries have a good distensibility, which is particularly adapted to accommodate large changes in blood volume, thus helping to maintain relatively constant pressure in the arteries despite the pulsating nature of the blood flow.

2. Muscular (or distributing) arteries are medium-sized arteries, which ensure the rapid and complete distribution of blood from an elastic artery to all organs and tissues. The walls of these arteries contain more smooth muscles than elastic tissues.

3. Arterioles are small diameter blood vessels which have thin muscular walls composed of one or two layers of smooth muscle. The arterioles are the primary site of vascular resistance that extend and branch out from the arteries to the

capillaries. The function of these arterioles is to reduce blood flow from the large arteries. This reduction in flow and pressure is necessary to prevent damage to the capillaries.

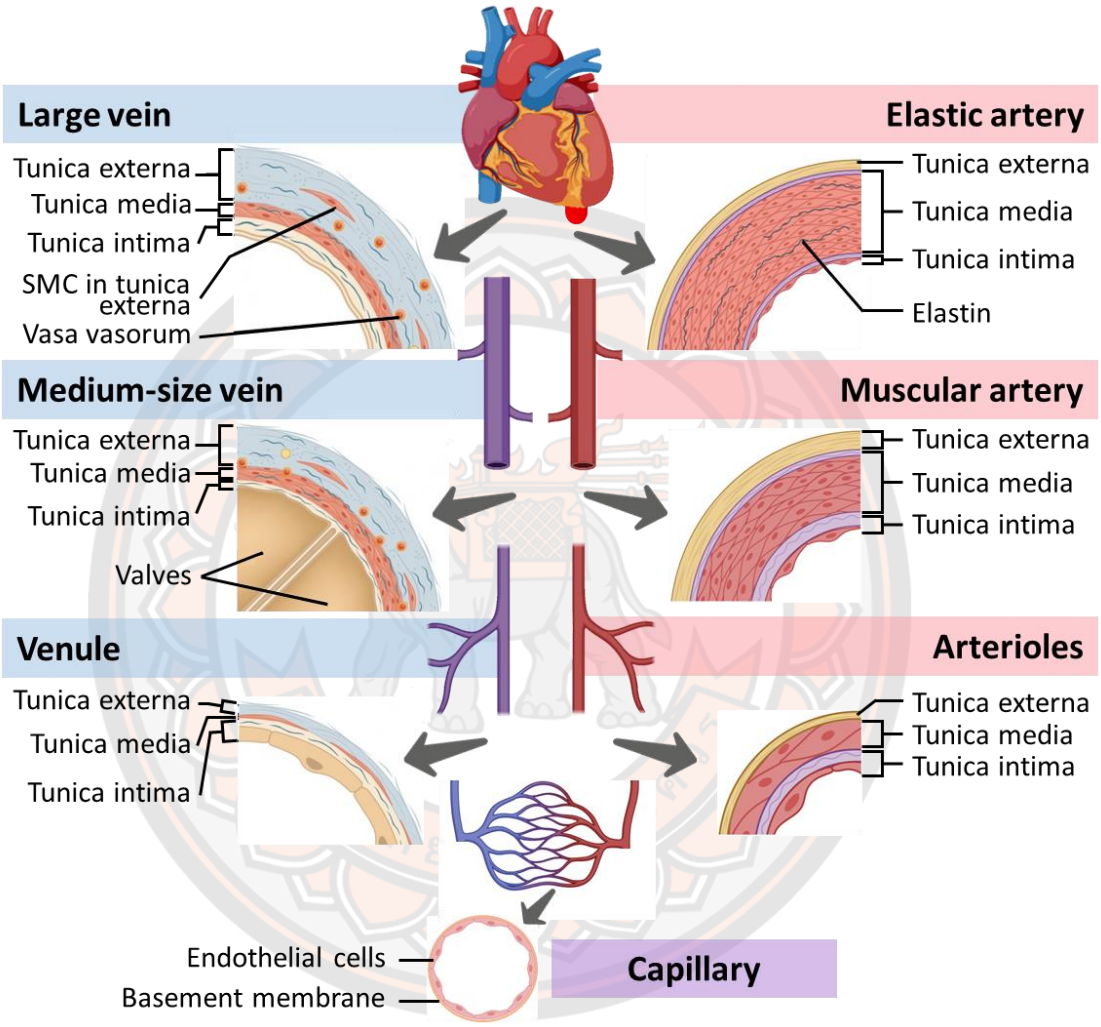

Figure 15 Structure of the artery, capillary, and vein in systemic vasculature

Source: Made by Usana Chatturong (2023)

2. Mechanisms involved in vascular tone regulation.

Vascular tone is regulated by several factors, such as neurotransmitters, hormones, and paracrine mediators. Changes of vascular tone can lead to either vasoconstriction or vasodilation and the mechanisms involved are explained as follows.

2.1 Vasoconstriction

The mechanisms of vasoconstriction involve an increase in intracellular Ca^{2+} concentration ($[Ca^{2+}]_i$) via various signal transduction pathways. The main contractile machinery of VSMCs consists of Ca^{2+}-dependent mechanisms and Ca^{2+}-independent mechanisms.

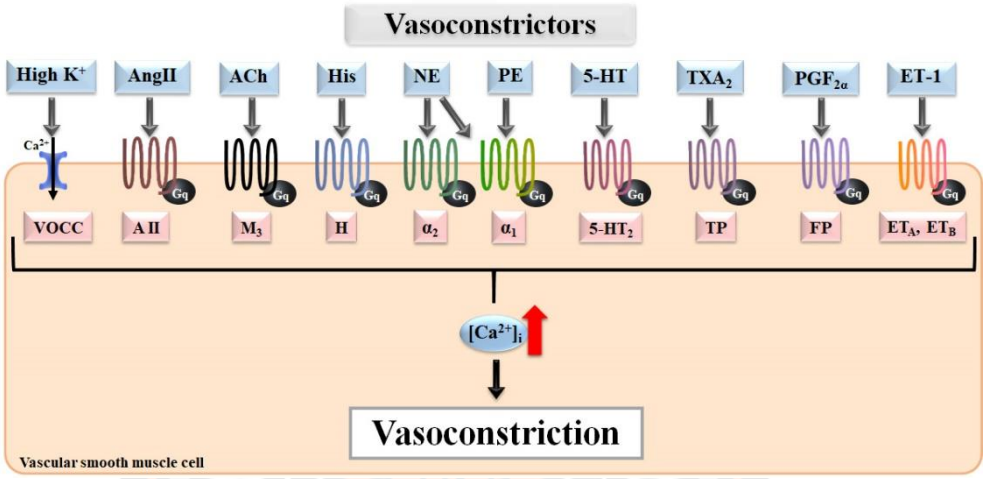

Figure 16 Vasoconstrictive mediators acting on VSMC

Source: Made by Usana Chatturong (2023)

Abbreviations : ACh, acetylcholine; Ang II, angiotensin II; AII, angiotensin II receptors; ET-1, endothelin-1; ET_A, endothelin receptor type A ; ET_B, endothelin receptor type B; His, histamine; H, histamine receptors; NE, norepinephrine, α_1, α_1-adrenergic receptors; α_2, α_2-adrenergic receptors; 5-HT, 5-hydroxytryptamine (serotonin); 5-HT_2, 5-hydroxytryptamine receptors; M_3, muscarinic receptors; PE, phenylephrine; $PGF_{2\alpha}$, Prostaglandin $F_{2\alpha}$; FP, $PGF_{2\alpha}$ receptors; TXA_2, thromboxane A_2; TP, thromboxane-prostanoid receptors; VOCC, voltage-operated Ca^{2+} channels.

2.1.1 VSMC contraction via Ca^{2+}-dependent mechanisms

An increase in $[Ca^{2+}]_i$ in response to drug, humoral, or neural stimuli (Figure 16) is an important role of vascular smooth muscle excitation-contraction coupling (Oguzhan et al., 2013). When a vasoconstrictor, such as phenylephrine (PE, α_1-adrenergic receptor agonist), binds to the G_q-protein-coupled receptors (GPCRs) on the VSMC membrane, the GPCR signaling pathway leads to induce the contraction (Figure 17). PE binds to α_1-adrenergic receptors and then G_q coupling activates phospholipase C (PLC), which promotes the hydrolysis of phosphatidyl inositol-4,5-bisphosphate (PIP_2) into inositol-1,4,5-trisphosphate (IP_3) and diacylglycerol (DAG). IP_3 binds to the inositol trisphosphate receptors (IP_3R) on sarcoplasmic reticulum (SR), which causes Ca^{2+} release from SR. DAG activates receptor-operated Ca^{2+} channels (ROCCs) and protein kinase C (PKC). The activation of PKC leads to the inhibition of the potassium (K^+) channels, which leads to VSMC depolarization and activates Ca^{2+} influx via Ca^{2+} channels such as ROCCs, L-type voltage-operated Ca^{2+} channels (VOCCs), second messenger-operated Ca^{2+} channels (SMOCs), store-operated Ca^{2+} channels (SOCCs), and Na^+-Ca^{2+} exchanger (NCX). PKC also stimulates the activity of the ryanodine receptor (RyR) on SR (Amberg & Navedo, 2013; Liu & Khalil, 2018; Misárková et al., 2016; Touyz et al., 2018). Together, both the extracellular and intracellular sources increase the $[Ca^{2+}]_i$, resulting in VSMC contraction. In addition, PKC inhibits myosin light chain phosphatase (MLCP) activity via phosphorylation of CPI-17, leading to reduced MLCP activity (Liu & Khalil, 2018; Misárková et al., 2016; Touyz et al., 2018).

The elevation of $[Ca^{2+}]_i$ activates the contractile machinery in VSMCs as follows: (1) Ca^{2+} forms a complex with the calcium-binding protein, calmodulin (CAM) to Ca^{2+}-calmodulin complex (Ca^{2+}-CaM). (2) When Ca^{2+}-CaM binds to myosin light chain kinase (MLCK), leading to the phosphorylation of the 20-kDa myosin light chain (MLC20) using adenosine triphosphate (ATP). This phosphorylation event converts the inactive state of myosin light chain (MLC) to an active state, promoting the activation of the myosin ATPase activity. (3) MLCK leads to cross-bridge formation between the myosin heads and the actin filaments, which generates force and shortening and consequent VSMC contraction (see Figure 17) (Cole & Welsh, 2011; Misarkova et al., 2016; Touyz et al., 2018). The regulation of

$[Ca^{2+}]_i$ is very important to maintain vascular tone. This depends on the balance between the extracellular Ca^{2+} influx to the cells via various types of Ca^{2+} channels, mainly L-type and T-type in vessels, or intracellular Ca^{2+} release from the SR via IP_3R and RyR, and the removal of Ca^{2+} either out of the cells via plasma membrane Ca^{2+}-ATPase (PMCA), NCX or back into the SR via SR Ca^{2+}-ATPase (SERCA) (Cole & Welsh, 2011; Misarkova et al., 2016; Touyz et al., 2018).

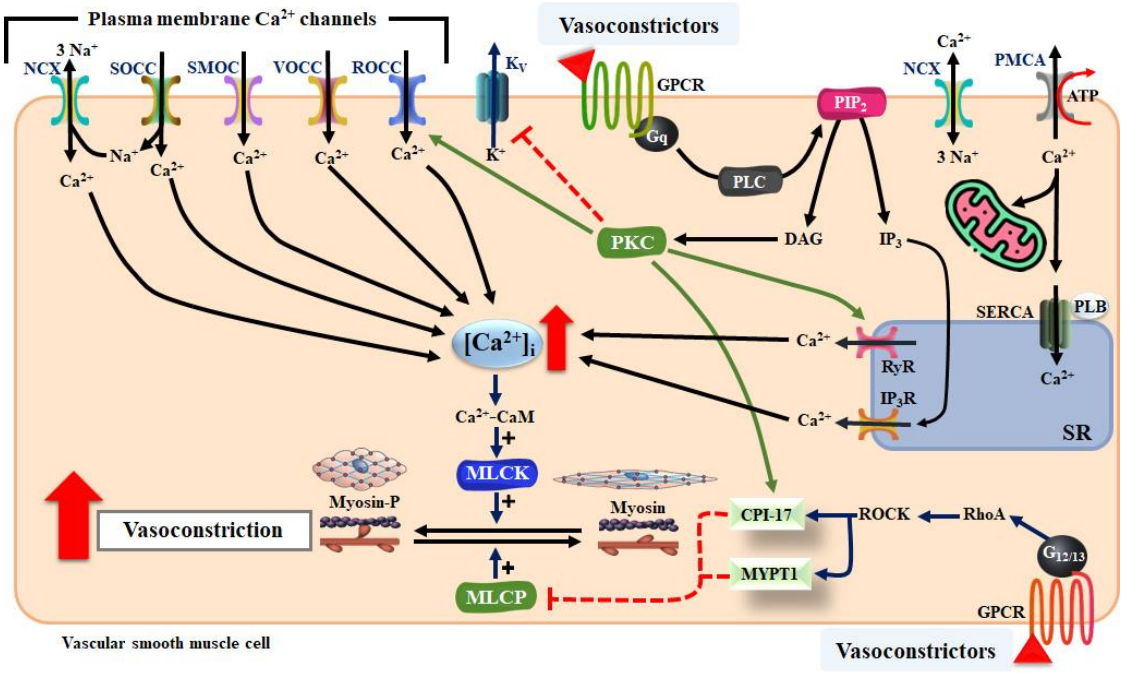

Figure 17 Mechanisms of vasoconstriction

Source: Made by Usana Chatturong (2023)

Abbreviations : ATP, adenosine triphosphate; CaM, calmodulin; CPI-17, protein kinase C-potentiated phosphatase inhibitor protein-17 kDa; DAG, diacylglycerol; GPCR, G-protein-coupled receptor; IP_3, inositol-1,4,5-trisphosphate; IP_3R, inositol trisphosphate receptor; K_v, voltage-gated potassium channel; MLCK, myosin light chain kinase; MLCP, myosin light chain phosphatase; MYPT1, myosin phosphatase targeting subunit 1; NCX, Na^+-Ca^{2+} exchanger; PIP_2, phosphatidyl inositol 1,4-bisphosphate; PKC, protein kinase C; PLC, phospholipase C; PMCA, plasma membrane Ca^{2+}-ATPase; RhoA, Ras homolog family member A; ROCC, receptor-

operated Ca^{2+} channels; ROCK, Rho-associated protein kinase; RyR, ryanodine receptor; SERCA, sarcoplasmic reticulum Ca^{2+}-ATPase; SMOC, second messenger-operated Ca^{2+} channel; SOCC, store-operated Ca^{2+} channel; SR, sarcoplasmic reticulum; VOCC, voltage-operated Ca^{2+} channel.

2.1.2 VSMC contraction via Ca^{2+}-independent mechanisms

Vasoconstriction can result from Ca^{2+} sensitization (Ca^{2+} sensitivity of myofilaments). Myofilament Ca^{2+} sensitization activates the MLCK which is achieved partly by the inhibition of MLCP. There are two basic components in the inhibition of MLCP. These include the phosphorylation of regulatory myosin phosphatase targeting subunit 1 (MYPT1) and the phosphorylation of protein kinase C-potentiated phosphatase inhibitor protein-17 kDa (CPI-17). Both components are phosphorylated by the Ras homolog family member A (RhoA)-Rho-associated protein kinase (ROCK) pathway. The activation of ROCK activates MYPT1 and CPI-17 leading to the inhibition of MLCP activity and vasoconstriction, see Figure 17 (Mahn et al., 2010; Touyz et al., 2018).

2.2 Vasorelaxation

The mechanisms of vasorelaxation involve mainly a decrease in $[Ca^{2+}]_i$ in VSMC. This interferes with contractile machinery by lowering the Ca^{2+}-CaM complex and the cross-bridge formation between actin and myosin. This reduction of the contraction finally induces vasorelaxation. Several signal transduction pathways lead to a decrease in the $[Ca^{2+}]_i$ of VSMCs and vasorelaxation.

2.2.1 Endothelium-dependent mechanisms

The endothelium comprises the major cells of the internal layer and plays a central role in the dynamic regulation of vascular tone by synthesizing and releasing various endothelium-derived relaxing factors (EDRF), see Figure 18. These relaxing factors lead to VSMC relaxation and vasorelaxation. These include the following:

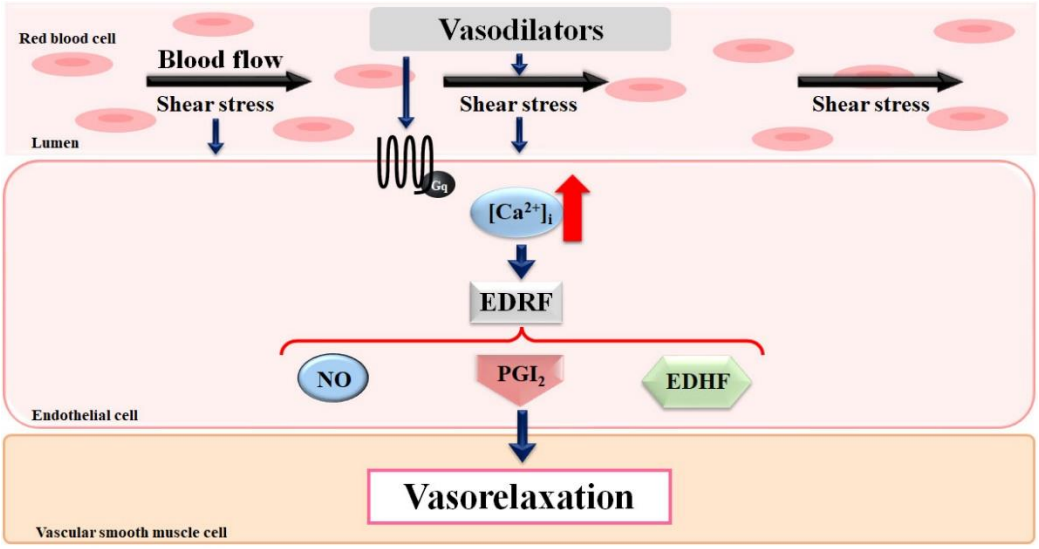

Figure 18 Mechanisms of potential endothelial cell mediated vasorelaxation

Source: Made by Usana Chatturong (2023)

2.2.1.1 Nitric oxide (NO)

NO is an important physiological vasodilator secreted by the endothelial cell. It is produced from the oxidation of L-arginine via the enzymatic action of endothelial NO synthase (eNOS) that produces L-citrulline in the presence of O_2, nicotinamide adenine dinucleotide phosphate (NAPDH), and other essential cofactors such as tetrahydrobiopterin. There are 3 isoforms of NO synthase (NOS); (1) neuronal NOS (nNOS) is predominant in neuronal tissue and found in most normal bodies that can be activated by Ca^{2+}-CaM, (2) Inducible NOS (iNOS) is found in a wide range of cells and tissues that are activated during inflammation. iNOS is Ca^{2+}-CaM independent, therefore the activation does not need Ca^{2+}-CaM, and (3) Endothelial NOS (eNOS) is found in vascular endothelial cells, cardiomyocytes, airway epithelial cells and platelets and is Ca^{2+}-CaM dependent (Alderton et al., 2001). The endothelium-derived NO diffuses into the VSMCs, where it activates soluble guanylyl cyclase (sGC) which converts guanosine triphosphate (GTP) to cGMP. This in turn activates downstream cGMP-dependent protein kinase i.e., protein kinase G (PKG) to relax the VSMC via the increase of Ca^{2+} influx into SR by the activation of SERCA, resulting in the reduction of $[Ca^{2+}]_i$. In addition, PKG

activates the opening of the K^+ channels, which causes membrane hyperpolarization which subsequently inhibits the L-type Ca^{2+} channels on the plasma membrane of the VSMCs and leads to the decrease of $[Ca^{2+}]_i$ (Triggle et al., 2012; Zhao et al., 2015). PKG also inhibits ROCK and MYPT1, thereby increasing MLCP activity and resulting in dephosphorylation of the myosin light chain (Mahavadi et al., 2014; Mahn et al., 2010). These effects ultimately promote vasorelaxation, see Figure 19.

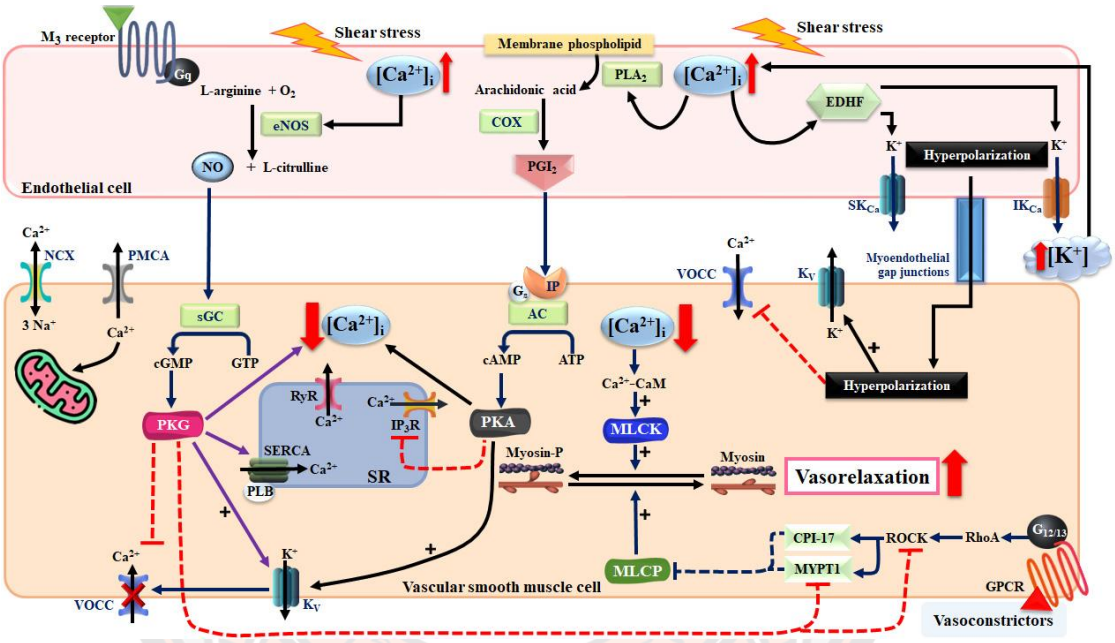

Figure 19 Mechanisms of vasorelaxation

Source: Made by Usana Chatturong (2023)

2.2.1.2 Prostacyclin (PGI_2)

PGI_2 is produced by the endothelium in response to shear stress (it is more for NO than for PGI_2) and also to agonists that increase Ca^{2+} in endothelial cells. The activation of phospholipase A_2 (PLA_2) liberates arachidonic acid (AA) from membrane phospholipids, which is then converted into PGI_2 by the action of cyclooxygenase (COX) and PGI_2 synthase. PGI_2 easily diffuses out of the endothelium to the VSMCs. PGI_2 acts by binding to the IP receptor, a type of cell surface receptor that belongs to the GPCR family (G_S protein). IP receptors are coupled to

adenylyl cyclase (AC) which converts ATP to the cyclic adenosine monophosphate (cAMP) and then activates protein kinase A (PKA). PKA reduces $[Ca^{2+}]_i$ by inhibiting IP_3-dependent Ca^{2+} release and activating the opening of the K^+ channels. The efflux of K^+ causes membrane hyperpolarization, thus inactivate L-type Ca^{2+} channels which leads to the decrease of $[Ca^{2+}]_i$, and finally promotes vasorelaxation (Mitchell & Kirkby, 2019; Pluchart et al., 2017), see Figure 19.

2.2.1.3 Endothelial-derived hyperpolarizing factors (EDHFs)

It is generally defined as a substance produced by the endothelium that causes VSMC hyperpolarization by opening the K^+ channels. EDHFs includes AA metabolites derived from the COX, epoxyeicosatrienoic acids (EETs), lipoxygenases and cytochrome P450 mono-oxygenase pathways, as well as H_2O_2, CO, hydrogen sulfide (H_2S) and various peptides, that can be released by the endothelial cells (Félétou & Vanhoutte, 2009). These responses involve an increase in the $[Ca^{2+}]_i$ of the endothelial cells, followed by the opening of the small and intermediate conductance Ca^{2+}-activated K^+ channels (SK_{Ca} and IK_{Ca}) on the endothelial cells, leading to endothelial cell hyperpolarization. The efflux of K^+ from the endothelial cells not only evokes electrical coupling through the myoendothelial gap junctions but also increases the K^+ ions accumulation in the intercellular space, called the K^+ cloud (Félétou & Vanhoutte, 2006). The K^+ cloud can issue signals that affect the contribution of K^+ ions to EDHF-mediated responses that cause the increase in $[Ca^{2+}]_i$, leading to the activation of SK_{Ca} and IK_{Ca} and resulting in the hyperpolarization of the endothelial cells. These factors activate hyperpolarization, K^+ channels or Na^+/K^+ ATPase on the VSMCs that contribute to the mechanisms leading to their relaxation (Feletou & Vanhoutte, 2006, 2009), see Figure 19.

2.2.2 VSMC-associated mechanisms

2.2.2.1 The opening of the K^+ channels

The activation of different types of K^+ channels on the VSMCs, such as 1) the voltage-gated K^+ channel (K_V), 2) the ATP-sensitive K^+ channel (K_{ATP}), 3) large conductance Ca^{2+}-activated K^+ channels (K_{Ca}), and 4) inward-rectifier potassium channels (K_{ir}), result in the opening of the K^+ channels

which leads to the efflux of K^+ from the VSMCs. These cause hyperpolarization of the VSMCs , which leads to a decrease in $[Ca^{2+}]_i$ and consequently vasorelaxation (Elliott & Ram, 2011).

2.2.2.2 Ca^{2+} removal and Ca^{2+} channel blocker

Ca^{2+} removal is one of the vasorelaxation mechanisms by decreasing $[Ca^{2+}]_i$. There are several processes by which this is achieved: 1) SERCA pumps Ca^{2+} into the SR, 2) Ca^{2+} can be pumped into extracellular space by a high-affinity PMCA and via a high-capacity NCX, and 3) by uptake into the mitochondria (Amberg & Navedo, 2013; Liu & Khalil, 2018; Mahn et al., 2010). In addition, Ca^{2+} channel blockers such as nifedipine, amlodipine, felodipine, nicardipine and verapamil disrupt the movement of Ca^{2+} through the Ca^{2+} channels. A decrease in the $[Ca^{2+}]_i$ of the VSMCs leads to vasorelaxation.

2.2.2.3 Cyclic nucleotide phosphodiesterases (PDEs)

The 3′,5′-cyclic nucleotide PDEs are a class of catalytic enzymes that regulate intracellular signaling by breaking down cAMP and cGMP into their inactive forms, 5’ AMP and 5’ GMP, respectively. cAMP and cGMP are essential intracellular second messengers with widespread roles in cellular signaling. These molecules act as regulators in various systems, including vasculature, exhibiting vasodilating, antiproliferative, and platelet inhibitory properties. cAMP is generated by adenylyl cyclase (AC) upon activation by GPCRs linked to the AC-stimulating G protein G_s, resulting in the activation of PKA. This activation of cAMP then triggers downstream processes by activating PKA and regulating diverse cellular functions. On the other hand, cGMP is produced by sGC, stimulated by NO or particulate guanylyl cyclases activated by natriuretic peptides (NPs). The generated cGMP activates PKG, which subsequently phosphorylates multiple target proteins, mediating various physiological responses (Baillie et al., 2019; Manoury et al., 2020), Figure 20.

Currently, PDEs have been classified into 11 families (PDE1-PDE11) based on their protein sequence, structure, substrate specificity, enzymatic properties, sensitivity to selective inhibitors, and tissue distribution (Baillie et al., 2019; Maurice et al., 2014). Some PDE families are classified based on substrate specificity. These can be divided into 3 groups: cAMP-specific PDEs (PDE4,

7, and 8), cGMP-specific PDEs (PDE5, 6, and 9) and dual-specificity PDEs (PDE1, 2, 3, 10, and 11), see Figure 20. PDEs are found in all tissues, but their distribution and type vary among different tissues, see Table 2. The multiple PDE isoforms within the cells show different enzymatic properties and localization patterns that are critical for determining specific physiological responses (Keravis & Lugnier, 2011; Rorbach et al., 2011; Wood et al., 2015).

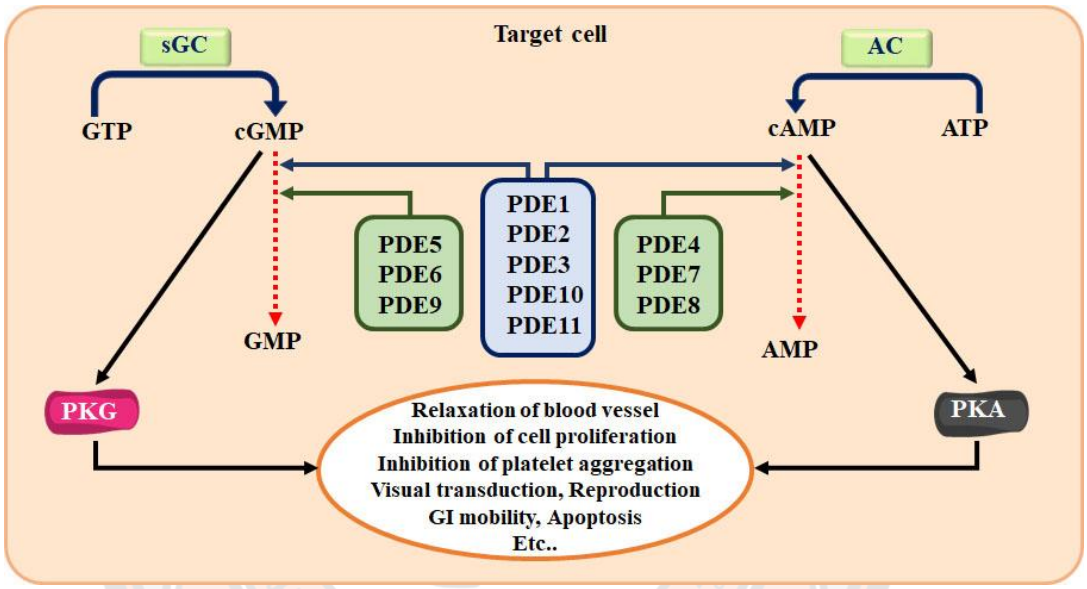

Figure 20 PDEs and their regulation

Source: Made by Usana Chatturong (2023)

The intracellular second messengers, cAMP and cGMP, are important for the regulation of intracellular signal transduction and control many cellular homeostatic processes. Changes in cAMP or cGMP concentrations lead to the activation of many critical physiological processes, including vascular and airway SMC relaxation, inhibition of cell proliferation, inhibition of platelet aggregation, myocardial contractility, gastrointestinal mobility, reproduction, apoptosis, immune/inflammatory responses, visual transduction, secretion, and bone development (Kumar et al., 2015; Omori & Kotera, 2007). PDEs represent the main route for the rapid lowering of cGMP and/or cAMP concentrations inside the cells, which leads to dysregulation of their signaling pathways. This is the cause of the

initiating or modulating pathophysiological pathways related to various diseases, including erectile dysfunction, pulmonary arterial hypertension, acute refractory cardiac failure, intermittent claudication, chronic obstructive pulmonary disease, and psoriasis (Bender & Beavo, 2006; Kumar et al., 2015; Omori & Kotera, 2007; Poulsen et al., 2012; Rahimi et al., 2010).

Table 2 Cyclic nucleotide PDE isozyme families: properties, tissue distribution and reference inhibitors

Family	Specificities	Tissue distribution	Specific inhibitors
PDE1	cGMP>cAMP	Brain, heart, smooth muscle, lung	Vinpocetine, nicardipine, nimodipine
PDE2	cGMP=cAMP	Adrenal gland, lung, heart, platelets, brain, liver, corpus cavernosum, endothelial cells	Erythro-9-(2-hydroxy-3-nonyl) adenine, BAY-60–7750, PDP, IC933, oxindole, ND7001
PDE3	cAMP>cGMP	Heart, liver, lung, platelets, vascular smooth muscle, platelets, adipocytes, immunocytes, corpus cavernosum	Cilostamide, cilostazol, milrinone, enoximone, amrinone, olprinone, Pimobendan, anagrelide
PDE4	cAMP	Lung, mast cells, liver, kidney, brain heart, smooth muscle, endothelial cells	Roflumilast, apremilast, crisaborole, drotaverine
PDE5	cGMP	Lung, corpus cavernosum, vascular, platelets, heart, endothelial cells, brain	Sildenafil, tadalafil, vardenafil, zaprinast, dipyridamole, avanafil, udenafil, mirodenafil

Family	Specificities	Tissue distribution	Specific inhibitors
PDE6	cGMP=cAMP	Retina	Sildenafil, tadalafil, vardenafil, dipyridamole, zaprinast
PDE7	cAMP>cGMP	Skeletal muscle, T-cells, heart, kidney, brain, pancreas	Dipyridamole
PDE8	cAMP	Testes, thyroid, eye, liver, kidney, heart, ovary, skeletal muscle, pancreas, T-cells	Dipyridamole
PDE9	cGMP	Brain, kidney, liver, lung	Zaprinast, BI 409306, PF-04447943
PDE10	cGMP=cAMP	Brain, testes, thyroid	Dipyridamole, papaverine
PDE11	cAMP>cGMP	Prostate, skeletal muscle, kidney, liver, heart, testes, pituitary, salivary glands	Tadalafil, zaprinast, dipyridamole

Source: Kumar et al. (2015); Miller (2015)

3. Vascular tone of the systemic vasculature and arterial blood pressure

Smooth muscle cells (SMCs) are present in the walls of all blood vessels except capillaries. VSMCs are typically organized in circular or spiral patterns. Contraction of VSMCs results in vasoconstriction, while relaxation leads to vasodilation. These alterations in the diameter of blood vessels have a substantial influence on blood flow and blood pressure.

Blood pressure refers to the force that blood applies to the walls of blood vessels. Arterial blood pressure is a basic hemodynamic, but it is the most important physiological parameter and is usually expressed in terms of systolic blood pressure

(SBP), diastolic blood pressure (DBP), and mean arterial blood pressure (MAP), which are measured in millimeters of mercury (mmHg). The SBP is the maximum pressure during ventricular contraction, and the DBP is the minimum pressure during the ventricular relaxation between beats. The MAP is estimated using SBP and DBP measurements, MAP = DBP+1/3(SBP–DBP). The MAP is also determined by cardiac output (CO) and total peripheral resistance (TPR); MAP = CO×TPR. CO is the product of heart rate (HR), which is the number of heart beats per minute (bpm), and stroke volume (SV), which is the volume of blood pumped from the ventricle per beat; CO = HR×SV. TPR is determined by vascular tone, specifically arterioles (Berne et al., 2010; Silverthorn, 2004).

Poiseuille's Law is a fundamental concept in fluid dynamics and is frequently used in physiology and medicine to understand blood flow in the circulatory system. It helps explain how changes in factors such as vessel diameter, length, and blood viscosity can affect the resistance to blood flow in the body's blood vessels, which is crucial for regulating blood pressure and overall circulatory function. The equation is $R = 8\eta L/\pi r^4$, where R represents the resistance to flow, η is the dynamic viscosity of the fluid (blood), L is the length of the tube (blood vessel), r is the radius of the tube, and π is the mathematical constant pi (approximately 3.14). In the context of Poiseuille's equation, TPR is related to the resistance (R) faced by the blood as it flows through the entire network of systemic blood vessels (Secomb, 2016).

TPR is directly associated with the diameter of the blood vessels, especially the resistance arteries (small arteries and arterioles). An increase in the diameter of the blood vessels due to vasorelaxation leads to a decrease in TPR, thereby decreasing blood pressure. Alternatively, a decrease in the diameter of the blood vessels due to vasoconstriction leads to an increase in TPR and ultimately an increase in blood pressure (Joyner et al., 2007). These phenomena are linked to the VSMCs which maintain a constant state of partial contraction, which is termed vascular tone. The contraction of the VSMCs is triggered by the increase in the intracellular Ca^{2+} concentration ($[Ca^{2+}]_i$) causes by either the entry of Ca^{2+} through Ca^{2+} channels on the plasma membrane or the releases of Ca^{2+} from the SR which are the major source of intracellular Ca^{2+}. Vascular tone is regulated by several factors such as neurotransmitters, hormones and paracrine mediators. These factors can be

categorized into vasoconstriction mediators, which lead to vasoconstriction and vasodilation mediators, which lead to vasorelaxation (Tykocki et al., 2017).

Many mechanisms are involved in maintaining normal blood pressure, as follows:

1. Short-term regulation is managed by the baroreceptor mechanism, which consists of afferent nerve endings located in the carotid sinuses and aortic arch walls. These mechanoreceptors detect changes in wall stretching due to pressure fluctuations and adjust their firing frequency accordingly. When MAP decreases, baroreceptor impulse frequency also decreases, resulting in reduced vagal efferent output to the sinoatrial node, leading to an increase in HR (tachycardia). Simultaneously, the sympathetic nervous system (SNS) becomes active, releasing norepinephrine (NE), which influences the heart and most blood vessels, causing enhanced cardiac contractility and narrowing of arteries and veins. NE boosts CO and induces rapid vasoconstriction, effectively elevating blood pressure (Gordan et al., 2015; Joyner et al., 2007). Opposing effects occur when arterial blood pressure rises.

2. Long-term regulation primarily involves the control of extracellular fluid volume through the renin-angiotensin-aldosterone system (RAAS), which plays a crucial role in regulating blood pressure and volume. Renin is synthesized in the kidneys and is released into the bloodstream in response to low blood pressure. In the bloodstream, it acts on angiotensinogen, a protein produced by the liver, to create angiotensin I (Ang I). This inactive peptide is then transformed into the active peptide angiotensin II (Ang II) in the lungs, thanks to the action of angiotensin-converting enzyme (ACE). Ang II, in turn, stimulates Ang II type I (AT1) receptors, leading to vasoconstriction (Martyniak & Tomasik, 2022; Paul et al., 2006). The secretion of aldosterone by the zona glomerulosa in the adrenal cortex helps decrease the loss of fluids and electrolytes through urine. Additionally, it performs other actions that contribute to raising blood pressure by incrementally enhancing venous return, end-diastolic volume, SV, CO and MAP (Lefebvre et al., 2019).

4. Systemic hypertension

Hypertension or high blood pressure is the most common risk factor for premature cardiovascular disease and premature mortality worldwide, accounting for 10.4 million deaths per year (Unger et al., 2020). Hypertension may be primary, which may develop as a result of environmental or genetic causes, or secondary, which has multiple etiologies, including renal, vascular, and endocrine causes. Unhealthy diets (high sodium intake, high saturated and trans fats intake, low potassium intake, and low of fruits and vegetables intake), alcohol consumption, cigarette smoking, lack of physical activity, and being overweight or obese are associated with increased risk of hypertension. The risk is related to the degree of SBP or DBP increase at any age and in either sex (Mills et al., 2020). The recently 2020 International Society of Hypertension (ISH) Global Hypertension Practice Guidelines promotes the change in the definition of hypertension. The blood pressure in adults (>18-year-old) and older is categorized as normal, high, stage 1 or 2 hypertension. Normal blood pressure is defined as SBP<130 and DBP<85 mmHg, high-normal blood pressure is 130-139 and/or <85-89 mmHg, stage 1 hypertension is 140-159 and/or 90-99 mmHg, and stage 2 hypertension is ≥160 and/or ≥100 mmHg (Unger et al., 2020).

Hypertension is not caused by a single dysfunction. It is a slow-progressing disorder that results from an imbalance of numerous contributing factors. At the cellular level, endothelium dysfunction or injury leads to other abnormalities such as vasoconstriction, coagulation abnormalities, and imbalance of vasodilation and vasoconstriction (Münzel et al., 2008). Changes in the structure of the blood vessels lead to vascular remodeling, and increased resistance of the arteries may become evident and develop into thrombosis and inflammation at later stages. The progression of the disease involves irregular and increased growth of endothelial and VSMCs proliferation due to various cytokines and hormonal production (Gallo et al., 2022; Münzel et al., 2008).

4.1 Strategy for hypertension management

There are two standard treatments for hypertension: lifestyle modification and pharmacological treatment (Unger et al., 2020), Figure 21.

4.1.1 Lifestyle modification

While many patients do not adopt lifestyle modifications, they play an important role in blood pressure regulation. Good lifestyle choices may help to delay or even avoid the development of high blood pressure and reduce CVD risk. Thus, lifestyle modification is the first line of treatment because it can also enhance the effects of anti-hypertensive treatments. Lifestyle modifications should include salt reduction, healthy diet and drinks, moderation of alcohol consumption, weight reduction, smoking cessation, regular physical activity, reduced stress, induce mindfulness and reduction in exposure to air pollution and cold temperature (Unger et al., 2020; Verdecchia et al., 2022).

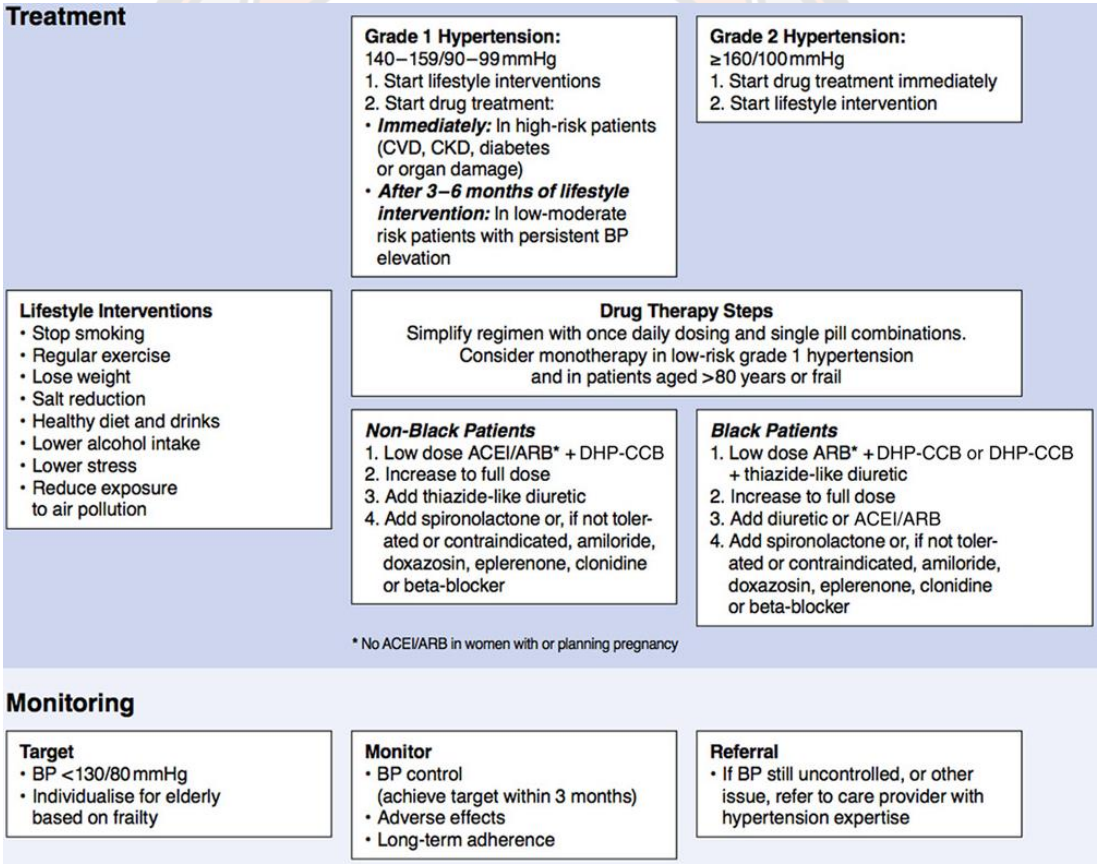

Figure 21 ISH 2020 optimal recommendations for evidence-based standards of hypertension care

Source: Unger et al. (2020) (Permission from Wolters Kluwer Health, Inc.)

4.1.2 Pharmacological treatment

Anti-hypertensive drugs are a class of drugs that are used to treat hypertension. Numerous classes of antihypertensive drugs have widely benefited in clinical applications. The most recommended classes used as first-line treatments for hypertension are thiazide-type diuretics, Ca^{2+} channel blockers, angiotensin-converting enzyme (ACE) inhibitors, Ang II receptor blockers (ARB) (Zisaki et al., 2015) and β-blockers. Only the currently important compounds are described here.

Diuretics: Diuretics can be categorized into four subgroups: K^+-sparing diuretics, loop diuretics, thiazide diuretics, and thiazide-like diuretics. They are crucial for managing hypertension and are often the first choice for hypervolemic hypertension. Diuretics have diverse sites of action within the body, which include the proximal tubule, the Loop of Henle, as well as the distal and collecting tubules. Their treatment effect initially results in a reduction in plasma volume and a decrease in CO (Zisaki et al., 2015).

Ca^{2+} channel blockers (CCBs): CCBs are divided into 2 groups, (i) the dihydropyridine group such as amlodipine, felodipine and nifedipine (ii) non-dihydropyridine groups such as verapamil and benzothiazepine diltiazem. These drugs work by decreasing the concentration of free $[Ca^{2+}]_i$, which leads to decreased vasoconstriction and also inhibit the secretion of aldosterone, a hormone that regulates blood pressure and electrolyte balance (Arnett & Claas, 2009).

RAAS blockers: RAAS blockers play a pivotal role in the treatment of hypertension and are the primary focus of medications like ACE inhibitors and ARBs (Unger et al., 2020). ACE inhibitors, including captopril, enalapril, and lisinopril, work by inhibiting the conversion of Ang I to Ang II in both the bloodstream and tissues, particularly in the blood vessels and kidneys. They also prevent the breakdown of bradykinin, which promotes the production of endothelial-derived relaxing factors, phospholipase A2, and prostaglandins, resulting in vasodilation. Clinically, ACE inhibitors reduce peripheral vascular resistance (Arnett & Claas, 2009). ARBs like losartan and valsartan function by binding to angiotensin II receptors, thereby counteracting the effects of Ang II (Arnett & Claas, 2009; Zisaki et al., 2015).

Beta-adrenergic blockers (β-blockers): β-blockers such as acebutolol, metoprolol, and propranolol, bind to β-adrenergic receptors, thereby antagonizing the binding of endogenous agonists (i.e., norepinephrine and epinephrine), which lower CO, pulmonary vascular resistance (PVR), and also decreases renin release (Arnett & Claas, 2009). These effects lead to a reduction of blood pressure.

According to recent statistics from over 100 countries (Geldsetzer et al., 2019), less than 50% of hypertension patients receive anti-hypertensive drugs, with only a few countries doing well and many performing poorly. In a large meta-analysis project, data from 48 clinical trials of anti-hypertensive drugs were followed up for an average of 4 years, over which time a 5-mmHg reduction in SBP was identified and associated with a 10% reduction in the major CVD risks, including stroke, ischemic heart disease, heart failure, and CVD death, regardless of previous CVD diagnoses and even at normal or high blood pressure values (Rahimi et al., 2021).

5. Systemic vs pulmonary circulation

The cardiovascular system consists of two circulatory paths, systemic circulation and pulmonary circulation, as shown in Figure 22. The major function of systemic circulation involves the blood supply to all body tissues. The structure of the systemic vasculature is well adapted to high blood pressure. The oxygenated blood is pumped from the left ventricle into the aorta, which is the largest artery in the body. The blood from the aorta flows through the arteries, arterioles, and finally the capillaries, which are the sites for gas, nutrient, and metabolic waste exchange with the body tissues. Glucose and O_2 in the blood diffuse from the blood to the cell, while waste and carbon dioxide (CO_2) diffuse out of the cell into the blood. The deoxygenated blood then moves through the capillaries, which merge into venules, then veins, and eventually the vena cava, which drains into the right atrium of the heart before pumping into the right ventricle (DeSaix et al., 2013; Ward & Linden, 2017).

By contrast, the major function of pulmonary circulation involves respiratory gas exchange. The structure of the pulmonary vasculature and pulmonary circulation

are highly adapted to fulfil this role. The deoxygenated blood from the right ventricle flows through the pulmonary artery into the arterioles until it reaches the smallest units, the pulmonary capillaries, which are the site for gas exchange. The walls of the pulmonary capillaries share a membrane with the alveoli, thus allowing O_2 and CO_2 to move freely between the respiratory system and the bloodstream. The air at the alveoli has high O_2 and low CO_2 concentrations, while the blood at the pulmonary capillaries has low O_2 and high CO_2 concentrations. The concentration gradient of this condition results in gas exchange during respiration, in which O_2 moves from the air in the alveoli to the blood while CO_2 moves from the blood to the air in the alveoli. Then the pulmonary vein carries the oxygenated blood from the lungs back to the left atrium before returning to the systemic circulation, completing the cycle of circulation through the body (Kandathil & Chamarthy, 2018; Truog & Kinsella, 2017).

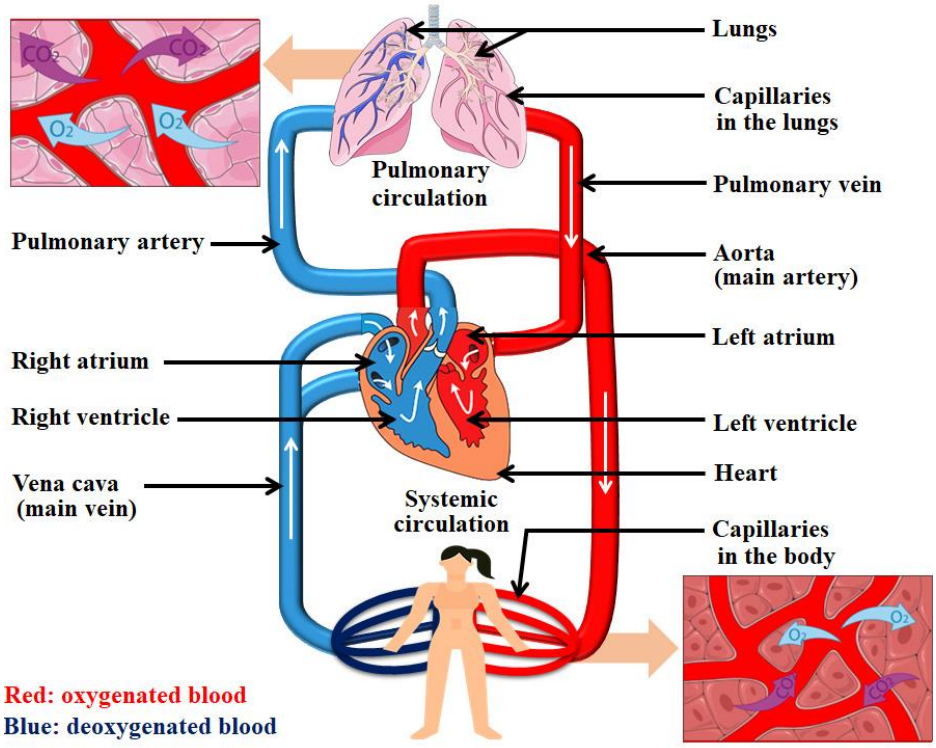

Figure 22 Pulmonary circulation and systemic circulation

Source: Made by Usana Chatturong (2023)

5.1 The differences between systemic and pulmonary circulation

5.1.1 Function: In systemic circulation, the artery carries the oxygenated blood from the left ventricle around the body while the veins carry the deoxygenated blood from the entire body back to the right atrium. In pulmonary circulation, the artery carries the deoxygenated blood from the right ventricle to the lungs for gas exchange and then the vein carries the oxygenated blood from the lungs back to the left atrium (DeSaix et al., 2013; Truog & Kinsella, 2017).

5.1.2 Blood pressure: Systemic arteries have a higher pressure (~90 mmHg) and thicker arterial walls than pulmonary arteries because the systemic circulation must work against the high pressure from the left atrium to pump the blood around the body. The pulmonary circulation has a thin arterial wall, low pressure (~10-15 mmHg), low resistance and high distensibility to obtain a high volume of blood from the right ventricle which is from the entire body (DeSaix et al., 2013; Truog & Kinsella, 2017). In addition, the pulmonary arteries (PAs) exhibit thinner walls, less smooth muscle, and absence of basal tone in contrast to the systemic circulation. This is most likely due to the high endogenous production of vasodilators and the low endogenous production of vasoconstrictors. Consequently, the normal pulmonary vascular resistance is approximately one-tenth that of systemic circulation. While autoregulation is widely known as a unique feature in most systemic vascular beds, this phenomenon is not present in the adult pulmonary circulation (Suresh & Shimoda, 2016).

5.1.3 Role of EDRF: The pulmonary circulation differs from the systemic circulation in that it maintains a low resting tone and is largely dilated under normal condition (Morrell, 2014). As a result, the combination of vasodilators and vasoconstrictors, both circulating and locally produced, influences this resting tone, with vasodilators like EDRF having a predominant role (Pirahanchi et al., 2022). Contrary to the resistance vessels of the systemic vasculature, EDHF is not involved in the ACh-induced vasorelaxation of PA (Norel et al., 2004). The two most important EDRF in the pulmonary circulation are NO and PGI_2, which are produced locally by endothelial cells. Both substances help to relax and widen the blood vessels in the lungs, contributing to the low pulmonary vascular tone (Morrell, 2014). Regarding NO, Rudinsky et al. (1993) studied the effects of inhibiting NOS on vascular tone in

the different circulations in piglets. They found that infusion of a NOS inhibitor caused significant vasoconstriction in the systemic (aorta) and pulmonary (PA) circulations leading to increased systemic vascular resistance (SVR) and PVR. The magnitude of vasoconstriction induced by this inhibitor was similar in the systemic and pulmonary circulations. This suggested an equal contribution of NOS to the basal tone of systemic and pulmonary circulations. The contribution of PGI_2 to the basal tone in PA seems of particular importance. Indeed, inhibiting COX decreased ACh-induced relaxations in isolated human PA, while inhibiting NOS modified only the relaxations induced by the highest concentrations of ACh (Norel et al., 2004).

5.1.4 Role of ET-1: ET-1 was originally identified as a potent vasoconstrictive peptide that was involved in the regulation of blood flow and blood pressure. It is expressed in aortic endothelial cells (Yanagisawa et al., 1988) and also expressed in pulmonary epithelium, SMCs, cardiac myocytes, glomerular renal cells, mesangial cells, leukocytes, macrophages and fibroblasts (Santos-Gomes et al., 2022). ET-1 has been widely studied as potential risk markers for CVD (Jankowich & Choudhary, 2020). The study in an animal model found that rats exposed to hypoxia had increased circulating ET-1 and also increased ET-1 mRNA levels in their lungs and right atrium, but not in their organs perfused by the systemic vascular bed. This study suggested that the pulmonary circulation was the main site of ET-1 production (Elton et al., 1992b). Of note, vasoconstriction is mediated by ET_A receptors in larger elastic PA, but by the ET_B receptor subtype in rat pulmonary resistance arteries of rat (Veyssier-Belot & Cacoub, 1999).

5.1.5 Nervous control: The blood circulatory system is regulated by local and central mechanisms to maintain arterial blood pressure and distribute CO according to metabolic needs. The autonomic nervous system (ANS), including parasympathetic nervous system (PSNS) and sympathetic nervous system (SNS), controls involuntary functions of the heart and blood vessels through cholinergic preganglionic fibers that synapse on postganglionic fibers. In the peripheral circulation, the SNS plays a more important role in regulating blood pressure and blood flow than the PSNS (Thomas, 2011). Indeed, while the heart is innervated by both SNS and PSNS fibers, arteries from the systemic circulation (except coronary and cerebral arteries) are not innervated by PSNS (Sheng & Zhu, 2018). On the

contrary, PA do have PSNS innervation (Kummer, 2011). However, in contrast to the systemic vasculature, the pulmonary circulation seems to have minimal neuronal control with respect to basal vascular caliber (Shimoda, 2006). SNS stimulation leads to increased PVR mediated by α-adrenoreceptors. Baroreceptors in the PA and the initial airway sections trigger the activation of noradrenergic nerve fibers. When arterial O_2 levels drop, chemoreceptors kick in to boost sympathetic nerve activity, ensuring a balance between blood flow and air exchange. Furthermore, vagal stimulation leads to parasympathetic activation, causing the PA to relax through cholinergic mechanisms (Vaillancourt et al., 2017). However, the PA contains fewer parasympathetic than sympathetic nerve fibers (Shimoda, 2006). Despite a low physiological role in the control of pulmonary vascular tone (Morrell, 2014), ANS dysregulation is involved in the development of PAH, which is associated with increased activation of the SNS (Vaillancourt et al., 2017).

5.1.6 Role of adrenergic receptors: Adrenergic receptors are GPCRs found on the surface of cells that respond to the hormone adrenaline and related molecules. While α_1-adrenergic receptors are found in smooth muscle cells of all arteries from the systemic vasculature where they mediate SMC contraction and vasoconstriction (Akinaga et al., 2019), in the PA, the α_1-adrenergic receptors are found only on the small and medium-sized arteries (Salvi, 1999). However, the density of α_1-adrenergic receptors is lower in PA compared to large systemic arteries (Shaul et al., 1990). Their activation by agonists induces a vasoconstrictive response which regulates vascular tone and maintains a suitable ventilation/perfusion matching in the lungs under normal conditions. However, when these receptors are overstimulated by factors such as low O_2 levels, changes in vessel wall pressure, or increases in the levels of its agonists, this can cause not only SMC contraction but also vascular proliferation and remodeling, which leads to the development of PAH (Salvi, 1999). For β-adrenergic receptors, three subtypes have been identified through molecular cloning, namely β_1-, β_2-, and β_3-adrenergic receptors (Bylund et al., 1994). Like vessels from the systemic vasculature, PA arteries expressed mostly β_2-adrenergic receptor (but also β_1- adrenergic receptor), which mediate vasorelaxation (Barnes & Liu, 1995). The study of Priest et al. (1997) reported that β-adrenergic receptors-mediated vasodilation in the large PA was largely NO-dependent whereas it

was NO-independent in the small arteries. Although β_3-adrenergic receptor is expressed in some blood vessels, the role of β_3-adrenergic receptor in mediating vasodilatation in PA remains controversial (Davel et al., 2015). Recently, a β_3-agonist produced a significant reduction in pulmonary vascular resistance in an animal model of PAH (García-Álvarez et al., 2016). Therefore, the positive effect of β-agonists on the one hand, combined with the presence of increased SNS activation in PAH on the other hand, raises the question of the positive or deleterious effects of β-blockers in PAH. In recent European PH guidelines, β-blockers were not recommended for patients with PAH unless required by comorbidities (high blood pressure, coronary artery disease, or left heart failure). However, Perros et al. (2015) investigated the effects of nebivolol (a third generation of β-adrenergic blocker that acts as an antagonist of β_1-adrenergic receptors and an agonist of $\beta_{2,3}$-adrenergic receptors) on a rat model of PAH. They found that nebivolol altered the hyperproliferative phenotype and reduced the overexpression of growth and proinflammatory mediators. Nebivolol induced endothelium-dependent on PA and improved right heart function and pulmonary vascular remodeling.

5.1.7 The mechanism of compensation in hypoxia: In case of hypoventilation, also known as alveolar hypoxia (the condition of low O_2 concentration levels in alveolar), this could induce vasoconstriction of the pulmonary vasculature, which is a phenomenon called hypoxic pulmonary vasoconstriction (HPV). The compensatory vasoconstriction response induced by alveolar hypoxia is to redirect pulmonary blood flow from poorly ventilated lung areas to well-ventilated lung areas to improve gas exchange. As a result, HPV is an important mechanism for maintaining normal blood oxygen levels before it flows back into the left atrium and circulates to the systemic circulation. In contrast, the response to tissue hypoxia in the systemic circulation system is vasorelaxation to expand the blood flow to the tissue and allow greater perfusion (DeSaix et al., 2013; Waypa & Schumacker, 2010).

Therefore, understanding these research findings may help researchers develop new treatments to block their activity and potentially find a cure for pulmonary arterial hypertension.

6. Pulmonary arterial hypertension (PAH)

PAH is a pathological state of pulmonary circulation that develops as a result of constriction or remodeling of the pulmonary vasculature. The combination of endothelial dysfunction, increased contractility of PA, the proliferation and remodeling of endothelium and VSMCs, leads to progressive narrowing of the lumen of the blood vessels. This results in a progressive resistance to blood flow manifested as an increase in both pulmonary vascular resistance (PVR) and mean pulmonary arterial pressure (mPAP). The increase in mPAP is greater than 20 mmHg at rest or greater than 30 mmHg during exercise, along with pulmonary capillary wedge pressure (PCWP) less than 15 mmHg. Pulmonary vascular remodeling and elevation of PVR are greater than 3 wood units when clinically presented in PAH. In the later stages, complex arterial lesions lead to right ventricular heart failure preceding death (Humbert et al., 2022).

6.1 Clinical classification of PAH

The World Health Organization (WHO) defined the classifications of pulmonary hypertension (PH) based on the original cause, histology, and pathophysiology of the disease. The 6th World Symposium on PH (WSPH) held in 2018 in Nice, France, classified PH into 5 groups, as shown in Table 3 (Galiè et al., 2019; Simonneau et al., 2019; Sysol & Machado, 2018). PAH includes idiopathic PAH (the cause of the pulmonary artery hypertension is unknown), heritable PAH, drug and toxin-induced PAH and familial PAH, PAH long-term responders to calcium channel blockers, PAH with overt features of venous or capillaries, as well as PAH associated with other medical conditions such as connective tissue disease, HIV infection, portal hypertension (liver disease), congenital heart disease or schistosomiasis (Firth et al., 2010; Lai et al., 2014; Vallerie V McLaughlin et al., 2015). The incidence of PAH is rare, but it can occur at any age, and approximately 60-70% of all PAH patients are female (Memon & Park, 2017; Thenappan et al., 2012). Idiopathic PAH, one of the 5 categories, is the most common form of the disease, affecting 40-50% of PH patients (Houtchens et al., 2011a). The estimated incidence of idiopathic PAH is around 15 cases per million of the population (Peacock et al., 2007).

Table 3 Current classification of PH and PAH.

1 PAH
1.1 Idiopathic PAH
1.2 Heritable PAH
1.3 Drug- and toxin-induced PAH
1.4 PAH associated with:
1.4.1 Connective tissue disease
1.4.2 HIV infection
1.4.3 Portal hypertension
1.4.4 Congenital heart disease
1.4.5 Schistosomiasis
1.5 PAH long-term responders to calcium channel blockers
1.6 PAH with overt features of venous/capillaries
1.7 Persistent PH of the newborn syndrome
2 PH due to left heart disease
2.1 PH due to heart failure with preserved left ventricular ejection fraction
2.2 PH due to heart failure with reduced left ventricular ejection fraction
2.3 Valvular heart disease
2.4 Congenital/acquired cardiovascular conditions leading
3 PH due to lung diseases and/or hypoxia
3.1 Obstructive lung disease
3.2 Restrictive lung disease
3.3 Other lung diseases with mixed restrictive/obstructive pattern
3.4 Hypoxia without lung disease
3.5 Developmental lung disorders
4 PH due to pulmonary artery obstructions
4.1 Chronic thromboembolic PH
4.2 Other pulmonary artery obstructions
5 PH with unclear and/or multifactorial mechanisms
5.1 Haematological disorders

5.2 Systemic and metabolic disorders
5.3 Others
5.4 Complex congenital heart disease

Source: Simonneau et al. (2019). (This article is open access and distributed under the terms of the Creative Commons Attribution Non-Commercial Licence 4.0.)

6.2 Diagnosis of PAH

A variety of clinical assessment tools have been used for diagnosis of PAH. These require the following progressive steps i.e., a thorough history and physical examination, echocardiogram, right catheterization and vasoreactivity testing. Signs and symptoms needed following up in PAH patients include chest pain, angina, dyspnea, syncope, non-productive cough, fatigue, increased shortness of breath, heart palpitations, dizziness and fainting spell, lips and fingers turning blues, peripheral edema or other signs of right ventricular dysfunction. These symptoms are non-specific of the disease; so that many patients remain undiagnosed up to 2 years, lead to delayed diagnosis and directly correlated with high mortality (Gidwani & Nair, 2014; McLaughlin & McGoon, 2006; Vallerie V. McLaughlin et al., 2015; Vaidya & Gupta, 2015).

6.3 Clinical presentation of PAH

Identifying PAH in its early stages can be tricky due to mild and non-specific symptoms. However, early diagnosis is crucial to begin treatment before right heart failure occurs. Accordingly, a patient presenting even with early stages is classified as belonging to World Health Organization functional class (WHO FC) (Houtchens et al., 2011b).

WHO FC I: Patients with PAH that cause no limitations on physical activities. Routine physical activity does not cause increased dyspnea, chest pain, fatigue, or presyncope.

WHO FC II: Patients with PAH that cause mild limitations on physical activities. Patients are comfortable at rest but routine physical activity results in increased dyspnea, chest pain, fatigue, or syncope.

WHO FC III: Patients with PAH that have marked limitations on physical activities. Patients are comfortable at rest, but less than routine physical activity results in dyspnea, chest pain, fatigue, or palpitations.

WHO FC IV: Patient with PAH that results in the inability to perform any physical activity without symptoms. These patients may have signs of right heart failure. Dyspnea with or without fatigue may be present at rest, and symptoms are increased by any physical activity.

6.4 Pathophysiology of PAH

The pathogenesis of PAH is complex, but usually primarily affects small PAs. PAH is a slowly progressive disorder, which is provoked by an imbalance of multiple responsible factors. It has been evidenced that PAH may occur due to various genetic, environmental or acquired reasons rendering it a complicated vascular disorder (Morrell et al., 2009).

6.4.1 Endothelial dysfunction

At the cellular level, endothelial dysfunction or injury leads to other abnormalities such as coagulation abnormalities, increased contractility of small PAs, and proliferation and remodeling of the endothelium and VSMCs. The primary cause of the development of PAH is an imbalance of vasodilators, such as NO, PGI_2 and vasoconstrictors such as endothelin-1 (ET-1) and thromboxane A_2 (TXA_2) (Lang & Gaine, 2015). This condition precedes the development of cellular proliferation and subsequently leads to pathological changes in pulmonary arterial VSMCs, resulting in the progressive narrowing or obstruction of the blood vessels as well as increasing PVR and mPAP in the PA (Humbert, 2010; Lourenço et al., 2012; Morrell et al., 2009; Santos-Ribeiro et al., 2016).

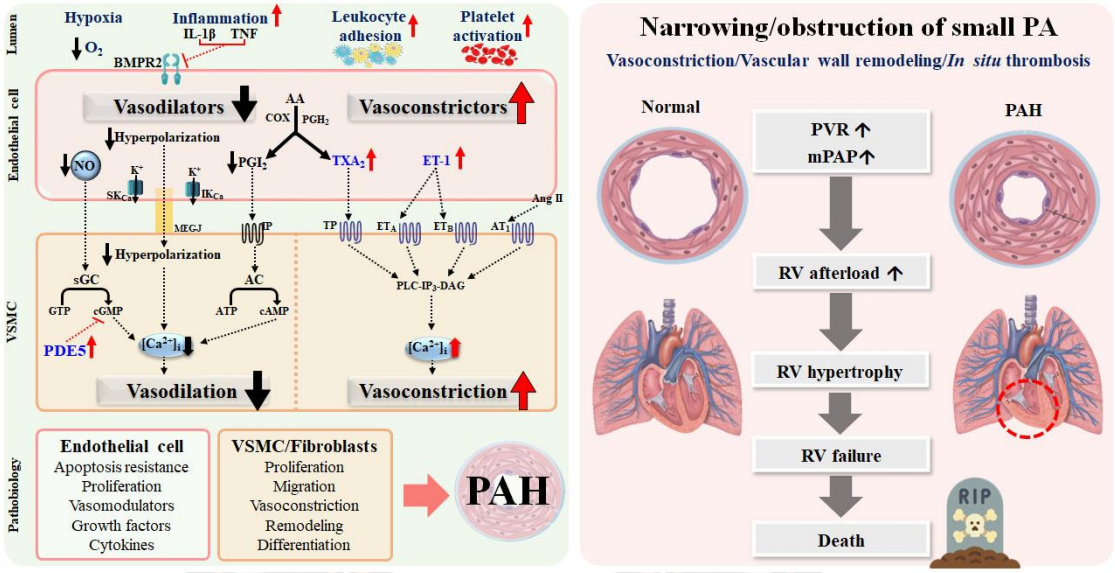

Figure 23 Pathophysiology of PAH

Source: Made by Usana Chatturong (2023)

The changes in the structure of the PAs lead to increased resistance, and increased mPAP and may subsequently lead to the development of thrombosis and inflammation at later stages, see Figure 23. The progression of the disease involves irregular and increased growth of the endothelium and proliferation of the VSMCs due to various hormonal and inflammatory cytokines production (Lourenço et al., 2012; Siques et al., 2018). Specifically, inflammatory cytokines such as IL-1β or transforming growth factor (TNF) have been shown to induce endothelial dysfunction in PA (Liu et al., 2022). PAH is also influenced by numerous genetic risk factors, with mutations in the Bone Morphogenetic Protein Receptor Type 2 (BMPR2) gene being the most prevalent. BMPR2 is a receptor involved in the BMP signaling pathway, which plays a crucial role in regulating cell growth and proliferation in the PAs. Mutations in BMPR2 disrupt this pathway, leading to abnormal cellular responses and remodeling of the pulmonary vasculature. Additionally, BMPR2 downregulation, especially in response to the inflammatory factor TNF, can promote endothelial cell essentialization, potentially contributing to the development of pulmonary vascular calcification (Devendran et al., 2022; Liu et al., 2022). In addition, various stimuli can contribute to the pathogenesis of PAH,

including shear stress from increased pulmonary blood flow, pulsatile stretch, pulmonary ischemia, alveolar hypoxia, cytokines, growth factors, adhesion molecules, and thrombin. These stimuli can lead to endothelial injury, circulating endothelial cells, and endothelial dysfunction (Budhiraja et al., 2004). Consequently, endothelial dysfunction plays a critical role in initiating and developing vascular pathology in PAH by promoting the release of more vasoconstrictors to PASMCs than vasodilators, leading to an imbalance in pulmonary vascular tone (Chemla et al., 2015). The main signaling pathways that involve the pathogenesis of PAH are NO, PGI_2 and ET-1 pathways, where the major source of their mediators are the endothelial cells (Lang & Gaine, 2015). ET-1 is not only a powerful vasoconstrictor, but it also promotes vascular proliferation that is involved in vascular remodeling. The ET-1 receptors (endothelin receptor type A (ET_A) and type B (ET_B)) are located on both the endothelium and the VSMCs. When ET-1 binds to ET_B receptors on the endothelial cells this leads to the production of NO and PGI_2, which induces vasorelaxation. However, binding of ET-1 to the ET_A and ET_B receptors on the VSMC leads to vasoconstriction and proliferation (Shao et al., 2011). Studies using animal models found that exposure to hypoxia caused increased levels of ET-1 mRNA in rat lungs (Elton et al., 1992a) and an upregulation of ET_A and ET_B receptor mRNA in the tunica media of the pulmonary vasculature (Soma et al., 1999). Similar to pre-clinical study, all patients with PH have increased plasma ET-1 levels and the expression of ET-1 in the pulmonary vasculature (Stewart DJ et al., 1991). Therefore, ET-1 has been linked to increased vascular tone and vascular remodeling in PAH.

6.4.2 Role of PDE5 in PAH

PDE5 is a well-studied PDE that was first discovered by Francis and Corbin in 1980. PDE5 is more abundant in the lung and penile corpus cavernosum than other PDEs (Francis et al., 1980; Gopal et al., 2001). PDE5 is a homodimer composed of two identical subunits, including regulatory and catalytic domains (Figure 24). The regulatory domain comprises two allosteric (GAF-A and GAF-B) cGMP-binding sites and a phosphorylation site. The binding of cGMP to both allosteric sites cause a conformational change in the enzyme, resulting in the exposure of N-terminal PKG phosphorylation sites. The catalytic domain is the

specific target of PDE5 inhibitors (Ahmed et al., 2021; Jiann, 2016). PDE5 is identified as 3 isoforms; PDE5 A1, A2, and A3, which are present in virtually all cell types, tissues, and organs. They differ only in the 5'-end of the mRNA, but their cGMP-catalytic activities are similar (Corinaldesi et al., 2015; Guazzi, 2008).

PDE5 is widely expressed in human tissues, but it is particularly abundant in the lung and pulmonary VSMC (Cesarini et al., 2020). PDE5 selectively targets cGMP, which is generally produced by NO-mediated activation of the sGC. It selectively hydrolyses cGMP into 5′GMP, thus a high level of PDE5 can cause a reduction in cGMP which leads to VSMCs contraction (Keravis & Lugnier, 2012). Long-term conditions with low cGMP levels in the VSMC lead to decreased activity of PKG, which causes an increase in $[Ca^{2+}]_i$ in the VSMC, resulting in VSMC contraction and ultimately leading to diseases such as ED and PAH (Corinaldesi et al., 2016; Hatzimouratidis et al., 2016; Lai et al., 2014). In experimental models of PAH, the PDE5 enzyme is shown to be abundantly expressed in the lungs of humans, rodents, and canines (Hemnes & Champion, 2006) which indicates an excessive degree of degradation of cGMP in the pathology of PAH.

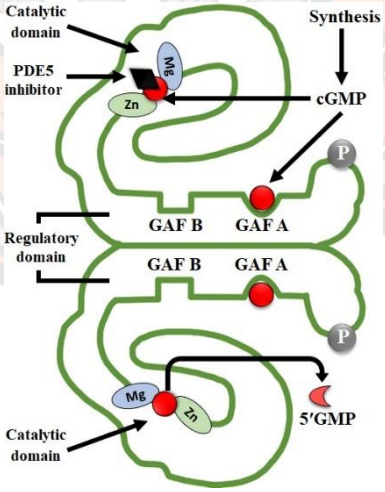

Figure 24 PDE5 structure

Source: Made by Usana Chatturong (2023)

6.4.3 Remodeling

Pulmonary vascular remodeling represents a key step in the progression of PAH that involves changes in all layers of the small PA wall, which pathologically increases PVR (Tuder, 2017). Since the VSMCs control the blood pressure of the pulmonary circulation through vasodilation and vasoconstriction, therefore, the dysfunction of the endothelial cells leads to decreased vasodilator production (NO and PGI_2) and increased vasoconstrictor production (ET-1), resulting in increased and sustained vasoconstriction via VSMC contraction as a result mPAP increases (Lang & Gaine, 2015). In addition, increased expression of PDE5 in VSMCs under PAH also causes an excessive degree of degradation of cGMP. Overproduction of PDE5 could mediate hypoxic pulmonary vasoconstriction (Hemnes & Champion, 2006). Chronic hypoxic exposure is the cause of changes in the structure of PA, as well as in the biochemical and functional phenotypes of each cell type that comprises the artery (Satoh et al., 2010). Hypoxia influences the release of vasoconstrictors, growth factors, and adhesion molecules in endothelial cells and also promotes growth factors in VSMCs that relate to ROS and proinflammatory cytokines production. These events lead to VSMC inflammation, proliferation, migration, and remodeling (Stenmark et al., 2006). PAH, therefore, affects all three layers of the PA wall, and typical arterial lesions include intima formation and fibrosis, medial hyperplasia of the pulmonary VSMC, and adventitial fibrosis. These lesions are accompanied by a variable level of perivascular inflammation, resulting in the progressive narrowing or obstruction of the blood vessels as well as increasing PVR and mPAP (Stenmark et al., 2006; Tuder, 2017). As a result of these symptoms, the RV must work hard to pump blood to the PA, which has high blood pressure (>25 mmHg), leading to RV hypertrophy and finally to RV failure and death (Simon & Pinsky, 2011).

6.5 Treatment options for PAH

Treatment for PAH depends on an accurate diagnosis where all other causes have been ruled out (Figure 25). Appropriate diagnosis and assessment allow suitable therapeutic management for each particular category. Proper management may lead to an increase in the survival rate of PAH patients from 2 years to 4 years.

Even though there exists incomplete awareness regarding the pathogenesis of PAH, the focused medical treatments may prove beneficial towards the reversal of pulmonary remodeling (Fuso et al., 2011).

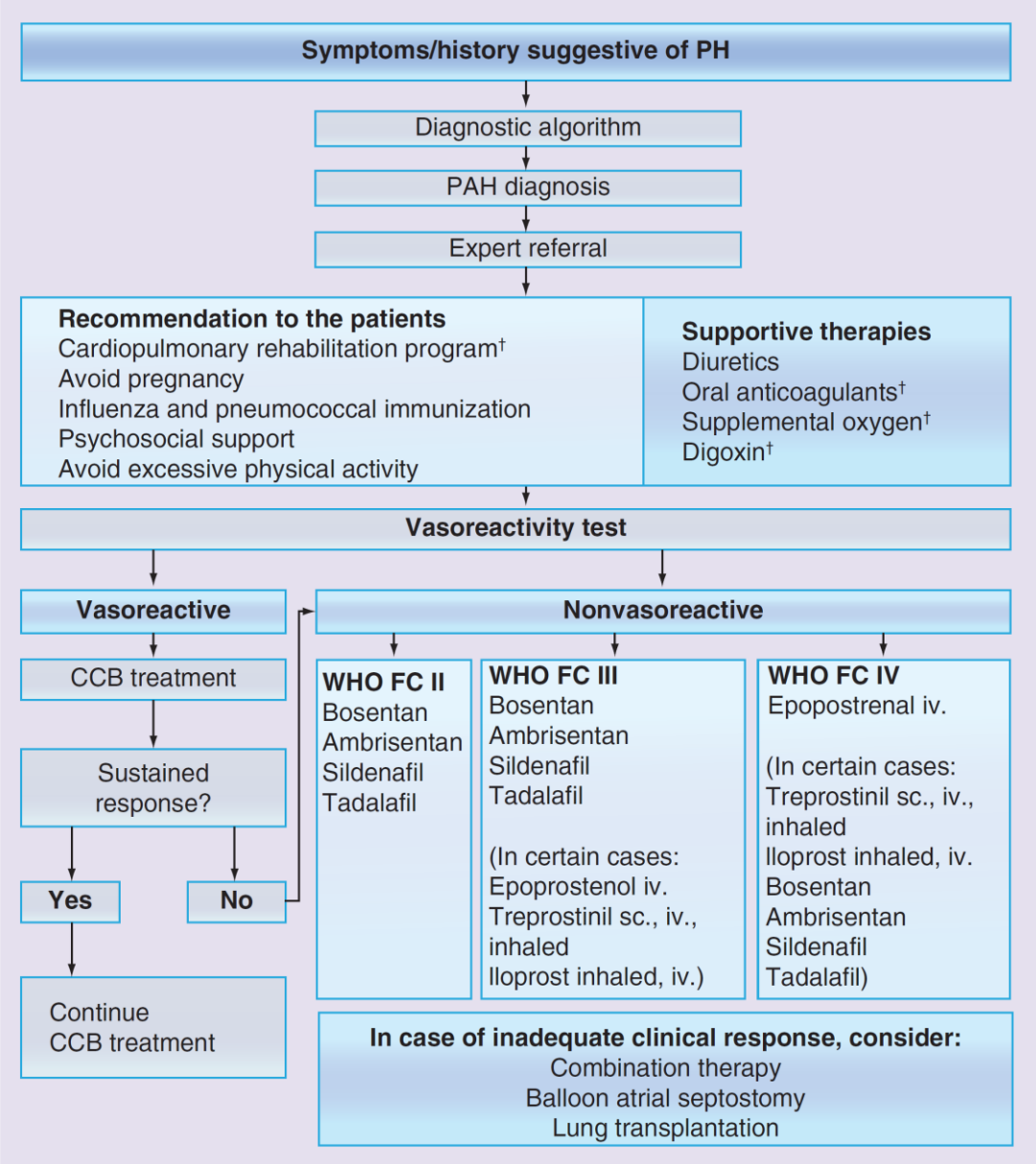

Figure 25 Therapeutic approach for PAH

Source: Malenfant et al. (2013) (Permission from Taylor & Francis)

The therapeutics for PAH are divided into 2 groups; supportive therapy and specific therapy, as described below.

6.5.1 Supportive therapies

Supportive therapies should be considered for all PAH patients, including oxygen supplementation, anticoagulants (warfarin), anti-proliferative agents, vasodilators, diuretics, digoxin, etc. (Grünig et al., 2018; Maron et al., 2021). Each therapy is responsible for the provision of symptomatic treatment.

6.5.1.1 Oxygen supplements: Restoring oxygen levels is fundamental importance in all patients with arterial hypoxemia, and it should be considered for all patients with PAH plus hypoxemia at rest or during exercise. The use of long-term oxygen supply is not yet known, however, the use of low-flow oxygen supply contributing to an improvement in patient condition (hypoxia) has been reported (Fuso et al., 2011).

6.5.1.2 Anti-coagulants: Anticoagulant drugs have been accepted for oral administration for patients with PAH who have a high prevalence of intrapulmonary thrombosis and thromboembolism (Galiè et al., 2010).

6.5.1.3 Inotropic drugs: These drugs are given to improve cardiac output in the failing right ventricle in PAH patients. The use of ionotropic agents (digoxin) requires close monitoring and is specifically meant for the treatment of supraventricular tachycardias. It is also utilized in heart failure conditions for cardiac output improvement (Rich et al., 1998).

6.5.1.4 Diuretics: Drugs used to treat fluid retention from decompensated right heart failure and raised central venous pressure (Maron et al., 2021).

6.5.1.5 Calcium channel blockers (CCBs): Based on positive acute vasoreactivity tests, CCBs have shown effectiveness in reducing PVR (Galiè et al., 2004). Unfortunately, not all patients are responsive to CCBs, with less than 8% of PAH patients showing a positive response to CCBs, which have no effect on cardiac output with a 10 mmHg decrease in PAP (Humbert et al., 2004).

6.5.2 Specific therapies

Specific therapies include those targeting the pathobiological abnormalities of PAH, and are divided into PGI_2 agonists (or prostanoid agonists), endothelin-1 receptor antagonists (ERAs), sGC stimulators and PDE5 inhibitors (PDE5i) or a combination depending upon the responsiveness and patient condition (Fuso et al., 2011; Tettey et al., 2021), Figure 26.

6.5.2.1 PGI_2 agonists: PAH is assessed to have dysregulation in the metabolic pathways of PGI_2 (Galiè et al., 2004). Therapeutic treatment with PGI_2 analogs shows both cytoprotection and anti-proliferative effects, and anti-inflammatory and endothelial regenerating properties (Clapp & Gurung, 2015). PGI_2 analogs used in the treatment of PAH include epoprostenol, treprostinil and selexipag (Figure 26). The different PGI_2 analogs are administered in various ways, with variable degrees of efficacy. Epoprostenol is the only medicine that has been proven to improve mortality and is the treatment of choice in severe situations (Tettey et al., 2021). Stable salt of prostacyclin analogue; epoprostenol via continuous intravenous administration, has been efficacious due to its vasodilation and platelet aggregation inhibitory effects (Rubin et al., 1990). In randomized clinical trials, epoprostenol proved to improve the symptoms but also increased the patients' exercise capacity (Barst et al., 1996). Notwithstanding these benefits, it is not an ideal treatment option due to high cost, complicated intravenous use, and common dose-related side effects (Table 4) such as abdominal pain, anxiety, arrhythmias, arthralgia, chest discomfort, nausea, and diarrhea (Tettey et al., 2021).

6.5.2.2 Endothelin-1 receptor antagonists (ERAs): ERAs have been investigated for their role in PAH. Increased levels of ET-1 are evident in PAH-stimulated VSMC proliferation and direct vasoconstriction effects (Rubin et al., 2002). ERAs used in the treatment of PAH include bosentan, ambrisentan, macitentan and sitaxsentan (Figure 26) and their use has demonstrated for this purpose. However, along with its positive outcomes such as enhanced durability and improved exercise capacity, it is associated with increased liver aminotransferases levels in approximately 10% of subjects (Barst et al., 2003). Therefore, liver function tests are required on regular basis during the use of ERAs. Bosentan; an orally active ERA, acts via both ET_A and ET_B, which prevent ET-1 from binding to its receptors (Tettey

et al., 2021). Sitaxsentan and ambrisentan are selective ET_A receptor blockers that have demonstrated their effectiveness in the improvement of symptoms, recovered hemodynamics and enhanced exercise capacity. However, there is the possibility of negative drug interactions with ERAs (Galiè et al., 2010) and common dose-related side effects (Table 4) such as anemia, diarrhea, flushing, gastroesophageal reflux disease, headache, and nasal congestion (Tettey et al., 2021).

6.5.2.3 sGC stimulator: sGC stimulators directly activate sGC in VSMC to enhance cGMP production. Riociguat is the only approved sGC stimulator for the treatment of PAH (Figure 26). It is a powerful sGC stimulator and increases blood flow in PA by inducing VSMC relaxation (Mihalek et al., 2022). In PAH patients completing 24 weeks of treatment, riociguat reduced mPAP by 9 mmHg and also increased the 6-min walking distance by 31 m as compared to placebo (Hoeper et al., 2017). However, because riociguat possesses a very short half-life, it must be administered three times a day at a dose of 2.5 mg (Mihalek et al., 2022). It also has side effects (Table 4) such as anaemia, constipation, diarrhoea, dizziness, dysphagia, gastroenteritis, gastrointestinal discomfort (Tettey et al., 2021).(Ausó et al., 2021; Humbert et al., 2004; Malenfant et al., 2013; Tettey et al., 2021)

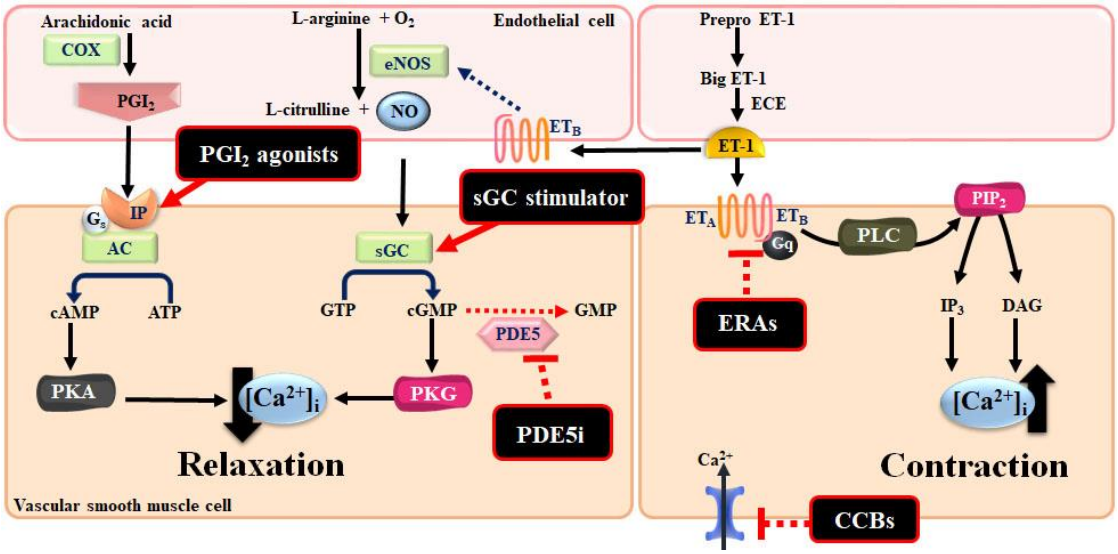

Figure 26 Targets for existing therapies in PAH

Source: Made by Usana Chatturong (2023)

6.5.2.4 PDE5i: In experimental models of PAH, the PDE5 enzyme is shown to be abundantly expressed in the lungs of humans, rodents, and canines (Hemnes & Champion, 2006) which indicates an excessive degree of degradation of cGMP in the pathology of PAH, whereas PDE5i increases cGMP levels in response to stimuli that activate sGC by blocking the catalytic activity of PDE5, see Figure 26. The mechanism of action of PDE5i is to control the hydrolysis of cGMP, which mediates the mediator NO and natriuretic peptide activity. Hence, increased levels of cGMP due to the inhibition of the PDE5 metabolism, produce pulmonary vasodilation and also have anti-proliferative effects (Francis et al., 2008; Ghofrani et al., 2006). PDE5i, such as sildenafil, tadalafil and vardenafil, are powerful vasoactive drugs. The use of PDE5i is not only restricted for penile erection but is also used in pulmonary hypoxia and primary arterial hypertension (Andersson, 2018; Cruz-Burgos et al., 2021; Gautam V Ramani & Myung H Park, 2010; Zirak et al., 2021). Sildenafil (Revatio® or Viagra®) was the first drug in this class. It was approved for ED treatment in 1998 and approved for PAH in 2005 (Gautam V. Ramani & Myung H. Park, 2010). More recently, the Food and Drug Administration (FDA) approved other PDE5i, tadalafil (Cialis®) and vardenafil (Levitra®) for PAH treatment. The highlight of sildenafil is that it is highly selective for the cGMP hydrolyzing isoform PDE (Hemnes & Champion, 2006). Sildenafil, when administered via intravenous route during right heart catheterization, showed a dose dependent decrease in PVR (Wilkens et al., 2001). However, there still exists a gap for improvement since the observed side effects (vision loss, tachycardia, etc.) are relevant to non-specificity and non-selectivity (Guazzi, 2008). It was found that together with PDE5, sildenafil can show cross reactivity towards other isoforms of the PDE enzyme, especially PDE6 and PDE1 (Wallis, 1999). Sildenafil has an IC_{50} of PDE5 inhibitory activity at a concentration of 3.5 nM, followed by IC_{50} values of 34-38 nM for PDE6 (Raja et al., 2006). Side effects due to the inhibition of PDE6 usually results in blurred vision or vision impairment due to its association with the control of the rods and cones in the eye (Ausó et al., 2021). Dose-dependent adverse effects of sildenafil including visual disturbances, headache, nausea, flushing, dyspepsia, diarrhea, back pain, limb pain, insomnia, influenza, nasal congestion, shortness of breath, facial edema, and systemic hypotension, have also been reported (Bhatia et al.,

2003; Galiè et al., 2005). In addition, there are few studies on the hepatotoxicity associated with sildenafil consumption (Graziano et al., 2017). As previously described, sildenafil is extensively and rapidly metabolized in the liver via the cytochrome P450 (CYP) pathway, primarily by CYP3A4 and to a lesser extent by CYP2C9 (Ku et al., 2008). As suggested in Sheweita et al. (2016), sildenafil was thought to be a weak CYP inhibitor. After male rats were administered orally with either low or high doses of sildenafil (1.43 and 7.15 mg/kg BW) for 3 weeks, sildenafil decreased the activity and protein expression of cytochrome c reductase as well as weakly inhibited the protein expression of various CYP isozymes, including CYP1A2, 2B1, 2C9, 2E1, and 3A4 (Sheweita et al., 2016). The high cost and other side effects of sildenafil encourage the identification of new PDE5i to improve the management of PAH. Therefore, to reduce side effects, a good selectivity for PDE5 associated with a greater vasorelaxant effect on pulmonary arteries compared to the effect on the systemic vasculature is required. In addition, low interaction with CYP would also be preferrable so that the new PDE5i is safe and produced less drug interaction.

Table 4 Classification of drugs used in treating PAH.

Generic name	Routes	Side-effects
Prostacyclin analogs		
Epoprostenol	Continuous infusion	Abdominal pain, anxiety, arrhythmias, arthralgia, chest discomfort, diarrhea
Treprostinil	Continuous intravenous or subcutaneous, oral, inhalation	Infusion site reaction, pain, headache, nausea, diarrhea, vasodilation, jaw pain, rash
Iloprost	Inhalation	Chest discomfort, cough, diarrhea, dizziness, dyspnea, hemorrhage, headache, hypotension, nausea

Generic name	Routes	Side-effects
Prostacyclin IP receptor agonist		
Selexipag	Oral	Abdominal pain, anemia, appetite decreased, arthralgia, diarrhea, flushing, headache
ERAs		
Bosentan	Oral	Anemia, diarrhea, flushing, gastroesophageal reflux disease, headache, nasal congestion, palpitations
Ambrisentan	Oral	Abdominal pain, anemia, asthenia, constipation, dizziness, epistaxis, flushing, headaches, hearing impairment
Macitentan	Oral	Anaemia, headache, increased risk of infection, nasal congestion
PDE5i		
Sildenafil	Oral, intravenous	Dry mouth, flushing, gastrointestinal discomfort, hemorrhage, myalgia, headache
Tadalafil	Oral	Flushing, gastrointestinal discomfort, headaches, myalgia, nasal congestion, pain
sGC stimulator		
Riociguat	Oral	Anaemia, constipation, diarrhoea, dizziness, dysphagia, gastroenteritis, gastrointestinal discomfort

Source: Ausó et al., 2021; Humbert et al. (2004); Malenfant et al. (2013); Tettey et al. (2021)

CHAPTER III

RESEARCH METHODOLOGY

Preparation of quinazoline derivatives

Six quinazoline derivatives (N^2,N^4-diphenylquinazoline-2,4-diamines) including compounds **4**, **5**, **8**, **9**, **10** and **11** were synthesized and provided by Associate Professor Dr. Matthew Paul Gleeson, Faculty of Engineering, King Mongkut's Institute of Technology Ladkrabang, Bangkok, Thailand. All compounds were purified to >95%, as reported elsewhere (Pobsuk et al., 2019). The synthesized quinazoline derivatives having various substitutions R^1 and R^2 (Figure 27) have been shown along with the molecular weights in Table 5.

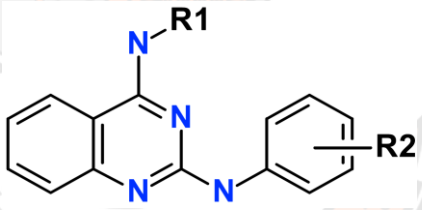

Figure 27 Basic quinazoline nucleus

Source: Made by Usana Chatturong (2023)

Table 5 The name, structure, and molecular weight (MW) of quinazoline derivatives

ID	Code	Chemical name	MW	Structure
4	PG135	4-{[4-(benzylamino) quinazolin-2-yl]amino}benzene-1-sulfonamide	405.5	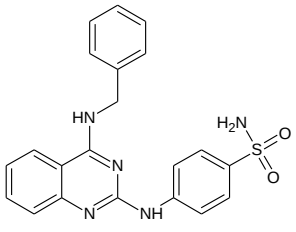

ID	Code	Chemical name	MW	Structure
5	PG170	3-{[4-(benzylamino) quinazolin-2-yl]amino} benzene-1-sulfonamide	405.5	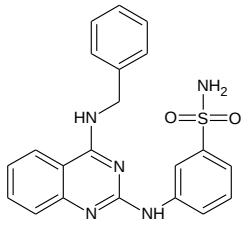
8	PG033	N^2-methyl-N^4-[(thiophen-2-yl)methyl]quinazoline-2,4-diamine	417.5	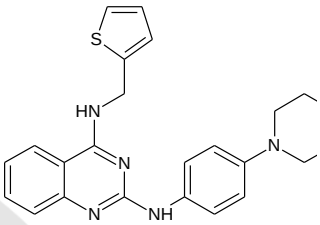
9	PG084	4-[(4-{[(thiophen-2-yl)methyl]amino}quinazolin-2-yl)amino]benzene-1-sulfonamide	411.5	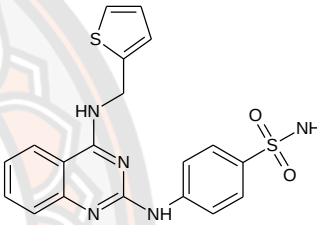
10	PG035	4-[(4-{[(thiophen-2-yl)methyl]amino}quinazolin-2-yl)amino]benzamide	375.5	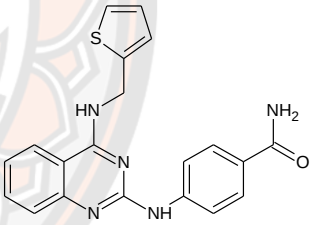
11	PG023	3-[(4-{[(thiophen-2-yl)methyl]amino}quinazolin-2-yl)amino]benzene-1-sulfonamide	411.5	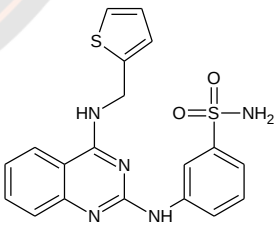

Source: Made by Usana Chatturong (2023)

Animals

Male Wistar rats (200–250 g, 8 weeks old) were purchased from Nomura Siam International Co., Ltd. (Bangkok, Thailand) for vascular reactivity experiments in the pulmonary artery (PA) and aorta, and from Janvier (Le Genest Saint Isle, France) for vascular reactivity experiments in the mesenteric artery (MA), acute hypotensive effect, hepatotoxicity and CYP activities. Animals were kept under a 12-12 h light-dark cycle, at 22±1°C and allowed free access to standard food and water. Experimental protocols were approved by the local committees for ethics in animal experimentation of Naresuan University Animal Care and Use Committee (NUACUC), Naresuan University, Phitsanulok, Thailand (Animal Ethics Approval Number: NU-AE620304 and NU-AE640202) and Franche-Comté University, Besançon, France (No. 2019-003-PT-5PR).

Human PDE5 inhibitory activity

Human PDE5 enzyme preparation and inhibition assay were modified from Bhandari *et al.*, 2019 (Bhandari et al., 2019). PDE5 enzyme was extracted from human embryonic kidney 293 (HEK293) cells transfected with human PDE5A1 plasmids. These transfected cells were lysed by sonication in 1 mL Tris buffer (containing: 50 mM Tris hydrochloride (Tris-HCl) pH 7.5, 2 mM ethylenediaminetetraacetic acid (EDTA), 1 mM dithiothreitol (DTT), and 1:100 of 100 mM phenylmethylsulfonyl fluoride (PMSF)). The homogenate was then centrifuged at 14,000 rpm for 20 min at 4°C and the supernatant was collected as a source of PDE5 enzyme.

All tested compounds (quinazoline derivatives and sildenafil, 10^{-12} - 10^{-4} M) were dissolved in 100% DMSO and diluted serially with distilled water to obtain final test concentrations, which 1% DMSO was used as the negative control.

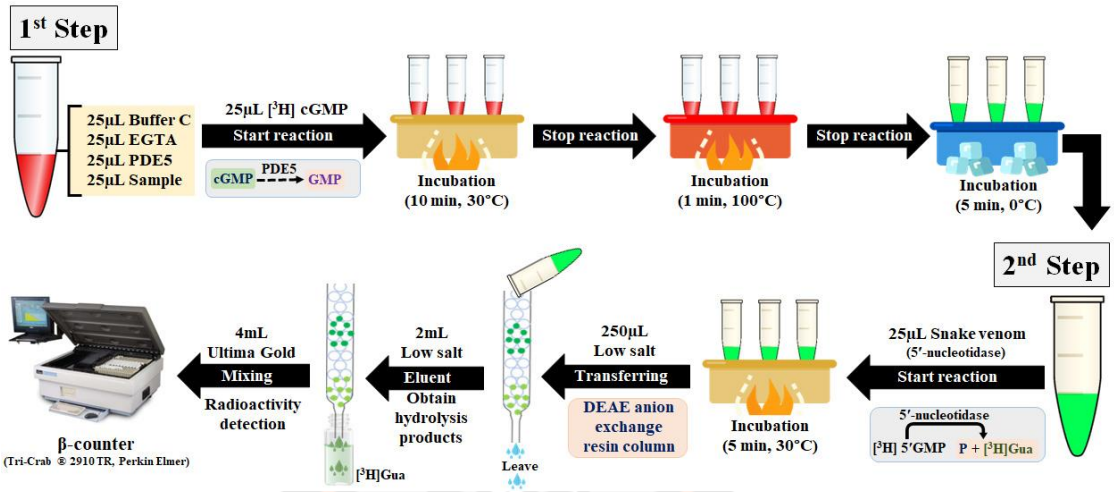

Figure 28 PDE5 radioassay method

Source: Made by Usana Chatturong (2023)

To measure the human PDE5 inhibition assay, in the first step the reaction mixture comprised 25 µL of Buffer C (containing:100 mM Tris-HCl pH 7.5, 100 mM imidazole, 15 mM $MgCl_2$ and 1 mg/mL bovine serum albumin (BSA)), 25 µL of 10 mM ethylene glycol-bis (β-aminoethyl ether)-N,N,N′,N′-tetra acetic acid (EGTA), 25 µL of PDE5 solution, and 25 µL of the test sample (quinazoline derivatives), positive control (sildenafil), or only solvent (1% DMSO) as a blank. The reaction was started by adding 25 µL of 5 µM [^{3}H] cGMP and incubated at 30°C for 10 min. Then, the reaction was terminated by placing the sample tubes in hot boiling water (100°C) for 1 min and then immediately placing them in ice-cold water for 5 min, as shown in Figure 28.

The second step was initiated by adding 25 µL of 2.5 mg/mL snake venom (5′-nucleotidase) and incubating at 30°C for 5 min. The assay was diluted with 250 µL 20 mM Tris-HCl (low salt buffer, pH 6.8) and transferred to a diethylaminoethyl sephadex (DEAE-Sephadex) anion-ion exchange resin column, the reaction mixture sample was passed through the resin column. Uncharged [^{3}H] guanosine was eluted from the resin with 1 mL of low salt buffer twice, and the eluates were collected in a scintillation vial. Finally, 4 mL Ultima Gold (scintillating cocktail) was added to the vial and mixed completely, and then the radioactivity was measured using the β-

counter (Tri-Crab ® 2910 TR, Perkin Elmer). The higher count of uncharged guanosine represented lower PDE5 inhibitory activity and vice versa. The PDE5 activity in the study was standardized to possess hydrolysis activity around 20-30% of the total substrate count. The calculation of hydrolysis of the sample and control is shown in equations (1) and (2), and the PDE5 inhibitory activity is calculated from equation (3).

$$\%\ \text{Hydrolysis}_{\text{sample}} = \left[\frac{\left(\text{CPM}_{\text{sample}} - \text{CPM}_{\text{background}}\right)}{\left(\text{CPM}_{\text{total count}} - \text{CPM}_{\text{background}}\right)}\right] \times 100 \quad (1)$$

$$\%\ \text{Hydrolysis}_{\text{control}} = \left[\frac{\left(\text{CPM}_{\text{control}} - \text{CPM}_{\text{background}}\right)}{\left(\text{CPM}_{\text{total count}} - \text{CPM}_{\text{background}}\right)}\right] \times 100 \quad (2)$$

$$\%\ \text{PDE5 inhibition} = \left[\frac{\left(\%\ \text{Hydrolysis}_{\text{sample}}\right)}{\left(\%\ \text{Hydrolysis}_{\text{control}}\right)}\right] \times 100 \quad (3)$$

Where CPM_{sample} is the radioactive count rate of the assay with the PDE5 enzyme, CPM_{blank} is the same but without the PDE5 enzyme, $CPM_{total\ count}$ is the count rate of 25 µL of substrate plus 2 mL of low salt buffer, and $CPM_{control}$ is the radioactive count rate of the assay with the PDE5 enzyme but without any sample. All experiments were performed in triplicate.

Vascular reactivity study

Preparation of isolated intrapulmonary artery (PA) and thoracic aorta

Rats were anesthetized with sodium thiopental (60 mg/kg, *i.p.*) and the thoracic aorta and the PA were isolated and placed in cold-Krebs solution composed of (mM): NaCl 122, KCl 5, N-[2-Hydroxyethyl] piperazine-N'-[2-ethane-sulfonic acid] (HEPES) 10, KH_2PO_4 0.5, NaH_2PO_4 0.5, $MgCl_2$ 1, $CaCl_2$ 1.8 and glucose 11, pH 7.4, cleaned and cut into ~2-3 mm lengths (To-on et al., 2022; Wisutthathum, Demougeot, et al., 2018). Rings were mounted in organ bath chambers via a pair of intraluminal wires and suspended at a resting tension of 1 g in 15 mL Krebs solution (37ºC) and continuously bubbled with air. One of the wires was fixed, and the other

was connected to a force transducer to record isometric force tension via a Mac Lab A/D converter and Chart^{TM} version 7 (A.D. Instruments, Castle Hill, Australia), see Figure 29. After an initial equilibration period of 1 h, the viability of the rings was checked with a 80 mM high K^+ solution for 10 min and then returned to normal Krebs solution (Wisutthathum, Demougeot, et al., 2018).

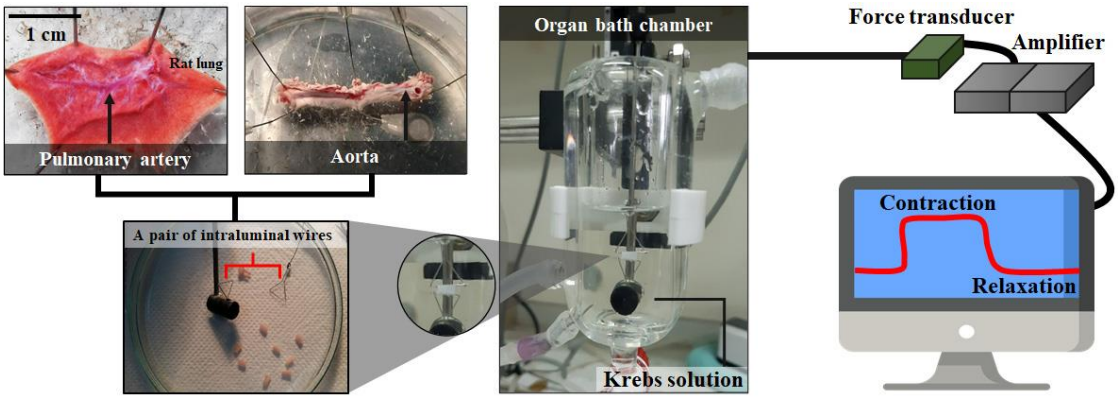

Figure 29 Rat pulmonary artery, thoracic aorta, and organ bath system

Source: Made by Usana Chatturong (2023)

Preparation of isolated second-order mesenteric artery (MA)

Rats were anesthetized with sodium pentobarbital (60 mg/kg, *i.p.*), and rat small intestine were collected and placed in cold-Krebs solution composed of (mM): NaCl 118, KCl 4.7, KH_2PO_4 1.2, $MgSO_4$ 1.2, $CaCl_2$ 2.5, $NaHCO_3$ 25, and glucose 12, pH 7.4. The second-order branches of MA were isolated, cleaned, cut into rings (2 mm in length) and mounted in organ chambers (containing 6 mL of Krebs solution bubbled with 95% O_2, 5% CO_2 and maintained at pH 7.4, 37ºC) via two 40-mm diameter stainless steel wires in myograph (Wisutthathum, Chootip, et al., 2018b), see Figure 30. To measure isometric force, a wire was connected to a Multi Myograph System (Model 610M v.2.2, DMT A/S, Denmark). Data were recorded using Chart^{TM} Ver.7 (ADInstruments, France). For active tension development, the mesenteric rings were stretched to their optimal lumen diameter. The internal circumference/wall tension ratio of the segments was adjusted to 90% of what the vessels would have if they were exposed to a passive tension equivalent to that produced by a transmural

pressure of 100 mmHg to find the optimal lumen diameter which was determined using specific software for normalization of resistance arteries (DMT Normalization Module; ADInstruments). After an initial equilibration period of 30 min, the viability of the rings was checked with a 100 mM high K^+ solution for 10 min and then returned to normal Krebs solution (Wisutthathum, Chootip, et al., 2018a).

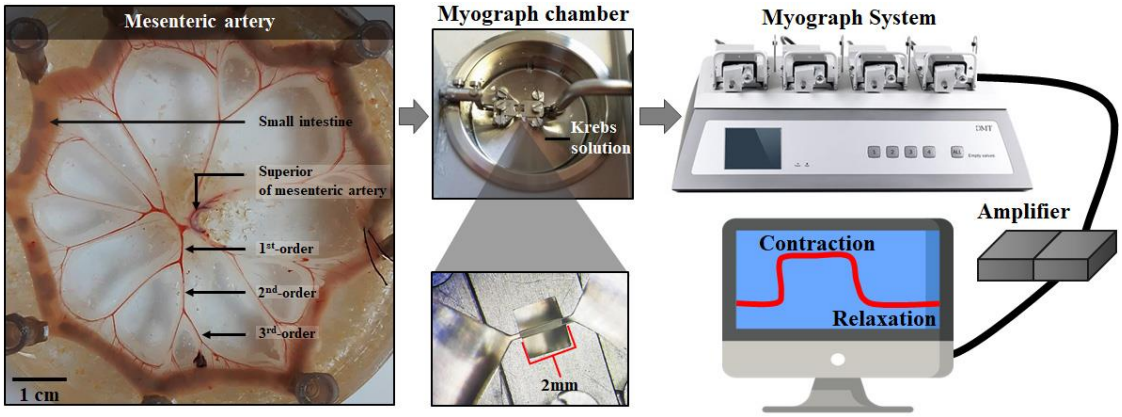

Figure 30 Rat mesenteric artery and multi myograph system

Source: Made by Usana Chatturong (2023)

The presence of functional endothelium was confirmed by a relaxation to 10^{-5} M acetylcholine (ACh) ≥70% in vessels precontracted with 10^{-5} M PE. In some rings, the endothelium was mechanically removed by gently rubbing inside the lumen of the vessel with a small wire. Relaxation ≤10% to 10^{-5} M ACh is considered a successful endothelium removal. The arteries were again allowed to equilibrate for 30 min before the start of the experiments.

Experimental protocols

1. Vasorelaxant effect of quinazoline derivatives, sildenafil and nifedipine

To compare the vasorelaxant effects of six quinazoline derivatives and sildenafil on pulmonary circulation *vs* systemic circulation, a first screening was made on an isolated PA and aorta (endothelium-intact rings). Then, the contribution of the endothelium was studied by comparing the vasodilator effects of the compounds in

endothelium-intact and endothelium-denuded rings. In addition, to investigate if the most relaxant compounds on the PA (compounds **5** and **11**) might induce side effects secondary to vasorelaxation of the systemic vasculature, their effects were studied on a resistance vessel, MA (a type of vessel that determines arterial blood pressure level), by comparing the effect with sildenafil. The most relaxant compound on the aorta (compound **8**) was also studied on MA by comparing the effect with nifedipine.

The rings were precontracted with 10^{-5} M PE. When the contractions reached a stable plateau, quinazoline derivative (10^{-10} – 3×10^{-5} M), sildenafil (10^{-11} – 10^{-5} M for the PA and 10^{-10} – 3×10^{-5} M for MA) or nifedipine (10^{-10} – 3×10^{-5} M) was added cumulatively to the rings to obtain a concentration-response curve. All test compounds were dissolved in 100% DMSO and diluted serially with distilled water to obtain the final test concentrations. The same amount of solvent, DMSO (0.13% at maximum), was used as the negative control (vehicle). The relaxation effect was calculated as the percentage of the contraction in response to PE.

2. Role of endothelium-dependent pathways

To investigate the role of eNOS, COX and EDHFs, endothelium-intact PA or MA rings were pretreated with N^G-nitro-L-arginine methyl ester (L-NAME, a NOS inhibitor, 10^{-4} M), indomethacin (a COX inhibitor, 10^{-5} M), or apamin (a small-conductance Ca^{2+}-activated K^+ channel blocker, 10^{-7} M) plus charybdotoxin (a large-conductance Ca^{2+}-activated K^+ channel blocker, 10^{-7} M), for 30 min before precontraction with 10^{-5} M PE and the rings were then exposed to cumulative concentrations of the tested compounds (Wisutthathum, Chootip, et al., 2018b; Wisutthathum, Demougeot, et al., 2018).

3. Role of endothelium-independent pathways

3.1 Role of vascular smooth muscle K^+ channels

To investigate the contribution of K^+ channels to the relaxant effect of the tested compounds, endothelium-denuded PA or MA rings were incubated with 4-aminopyridine (4-AP, voltage-gated K^+ channel (K_V) blocker, 10^{-3} M), glibenclamide (ATP-sensitive K^+ channel (K_{ATP}) blocker, 10^{-5} M), and iberiotoxin (large conductance Ca^{2+}-activated K^+ channels (K_{Ca}) blocker, 3×10^{-7} M in the PA or 10^{-7} M

in the MA) for 30 min before contraction with 10^{-5} M PE and the rings were then exposed to cumulative concentrations of the tested compounds (Wisutthathum, Chootip, et al., 2018b; Wisutthathum, Demougeot, et al., 2018).

3.2 Role of the sGC/cGMP pathway

As compounds **5**, **8** and **11** pertain to a series of quinazolines developed for their potential as PDE5 inhibitors (Paracha et al., 2019; Pobsuk et al., 2019), the role of the sGC/cGMP pathway was investigated. First, to evaluate whether the vasorelaxant effect of the tested compounds might be dependent on PDE5 inhibition, by determining if the tested compounds might increase the relaxant effect of sodium nitroprusside (SNP), a NO donor, that activates sGC in VSMC and increase the cGMP-induced vasorelaxation. Endothelium-denuded PA or MA rings were incubated with the tested compounds at their EC_{50} (compound **5**, 3×10^{-6} M in the PA or 5×10^{-6} M in MA; compound **11**, 5×10^{-6} M in the PA or 3×10^{-6} M in MA; compound **8**, 6×10^{-7} M in MA; sildenafil, 5×10^{-7} M in the PA) or vehicle (0.02% DMSO) for 10 min before precontraction with 10^{-5} M PE. Then, cumulative concentrations of SNP (10^{-11} – 10^{-4} M) were added to activate the sGC and to enhance cGMP production in the vascular smooth muscles (Wisutthathum, Chootip, et al., 2018b; Wisutthathum, Demougeot, et al., 2018). Second, to determine if the tested compounds directly activated sGC, endothelium-denuded PA or MA rings were preincubated with 1H-[1,2,4]oxadiazolo[4,3-a]quinoxaline-1-one (ODQ, a selective sGC inhibitor, 10^{-5} M) for 30 min before adding 10^{-5} M PE and subsequent cumulative concentrations of the tested compounds (Wisutthathum, Chootip, et al., 2018b; Wisutthathum, Demougeot, et al., 2018).

3.3 Role of extracellular Ca^{2+} influx

To study the role of receptor-operated Ca^{2+} channel (ROCC) or voltage-operated Ca^{2+} channel (VOCC) in the vasorelaxant effect, endothelium-denuded PA or MA rings were incubated in Ca^{2+}-free Krebs solution containing methylene glycol-bis (2-aminoethylether)-N,N,N’,N’-tetraacetic acid (EGTA, 2 mM) for 40 min. Then, 10^{-5} M PE was added to deplete the intracellular Ca^{2+} store of SR. After washing with Ca^{2+}-free Krebs solution 4 times at 10 min intervals, the rings were incubated with the tested compounds at their EC_{50} (compound **5**, 3×10^{-6} M in the PA or 5×10^{-6} M in MA; compound **11**, 5×10^{-6} M in the PA or 3×10^{-6} M in MA;

compound **8**, 6×10^{-7} M in MA; sildenafil, 5×10^{-7} M in the PA), or vehicle (0.02% DMSO), for 10 min in Ca^{2+}-free Krebs solution with 10^{-5} M PE to open the ROCC or with 80 mM high K^+ solution to open the VOCC. Then, cumulative concentrations of $CaCl_2$ (10^{-5} – 10^{-2} M) were added to evoke a contractile response. The %contraction of $CaCl_2$ was normalized with a maximum contraction of 10^{-5} M PE in the normal Krebs solution condition (Wisutthathum, Chootip, et al., 2018b; Wisutthathum, Demougeot, et al., 2018).

3.4 Role of intracellular Ca^{2+} release

For the PA, endothelium-denuded rings were precontracted with 80 mM high K^+ solution for 5 min to stimulate the initial Ca^{2+} loading into SR Ca^{2+} stores. Then, the baths were replaced with Ca^{2+}-free Krebs solution for 15 min and 10^{-5} M PE was added to release Ca^{2+} from SR, thereby eliciting a transient contraction. The same protocol was repeated after incubation for 10 min with vehicle (0.02% DMSO) or the tested compounds at their EC_{50} (3×10^{-6} M compound **5**, 5×10^{-6} M compound **11** or 5×10^{-7} M sildenafil) before adding 10^{-5} M PE (Kamkaew et al., 2019). For MA, the endothelial-denuded rings were incubated with L-type voltage-dependent Ca^{2+} channel inhibitor (verapamil, 10^{-7} M) for 30 min. Then, the tested compounds at their EC_{50} (5×10^{-6} M compound **5**, compound **8**, 6×10^{-7} M, or 3×10^{-6} M compound **11**), or vehicle (0.02% DMSO), were incubated for 10 min before adding 10^{-5} M PE to stimulate intracellular Ca^{2+} release through the opening of IP_3 receptors from SR (Wisutthathum, Chootip, et al., 2018b).

3.5 Role of α_1-adrenergic receptors

Endothelium-denuded PA or MA rings were preincubated with the tested compounds at their EC_{50} (compound **5**, 3×10^{-6} M in the PA or 5×10^{-6} M in MA; compound **11**, 5×10^{-6} M in the PA or 3×10^{-6} M in MA; compound **8**, 6×10^{-7} M in MA; sildenafil, 5×10^{-7} M in the PA), or vehicle (0.02% DMSO), for 15 min. Then accumulating concentrations of PE (α_1-adrenergic receptors, 10^{-10} – 10^{-4}M) were added (Paracha et al., 2019).

Cytotoxicity of the compounds on VSMCs isolated from the rat PA and aorta

VSMCs isolation and cytotoxicity study

Fresh PA and aorta were dissected out from healthy male Wistar rats (250-300 g), cleaned, opened longitudinally, and cut into small strips (3 mm in length). The strips were placed in a dissociation medium (DM) containing (mM): NaCl 110, KCl 5, HEPES 10, $KH2PO_4$ 0.5, NaH_2PO_4 0.5, $NaHCO_3$ 10, taurine 10, EDTA 0.5, $MgCl_2$ 2, $CaCl_2$ 0.16 and glucose 10, and maintained at pH 7, then incubated overnight at 4°C in DM containing 1 mg/mL papain, 0.04% BSA and 0.4 mM DTT and further incubated at 37°C for 15 min. Subsequently, the tissues were digested by adding 1 mg/mL collagenase and then further incubated for 5 min at 37°C. The tissues were transferred into fresh DM and scattered by gentle trituration with a glass pasteur pipette until isolated VSMCs appeared in the bathing solution (To-on et al., 2022). The isolated VSMCs were counted with a hemocytometer using 0.4% trypan blue penetration (Gibco^{TM}, Thermo Scientific, USA) and seeded on 96-well plates at 5×10^5 cells/well then incubated overnight at 4°C for cells attachment. The acute toxicity of quinazoline derivatives and sildenafil on the VSMCs were investigated by determining cell viability by using 3-(4,5-dimethylthiazol-2-yl)-2,5-diphenyltetrazolium bromide (MTT) assay. The VSMCs were treated with 100 µL of the tested compounds (10^{-7} – 10^{-4} M) or 0.1% DMSO for 1h at 37ºC with 5% CO_2 and further cells were incubated with 100 µL MTT solution (0.5 mg/mL) at 37ºC with 5% CO_2 for 4 h. The supernatant was then discarded and 100 µL DMSO was added and shaken in the dark for 30 min to dissolve any formazan crystals. The absorbance was measured at a wavelength of 595 nm by spectrophotometry. The viability of the VSMCs was calculated as a percentage of absorbance, compared with the control in which the viability of control cells (no treatment) was considered as 100%.

Acute hypotensive effect of compound 8 and nifedipine

To investigate whether the direct *ex vivo* vascular effect of compound 8 on resistance vessels translates into an *in vivo* effect, the acute hypotensive effect of compound 8 was compared with nifedipine in anesthetized rats. Male Wistar rats were anesthetized with sodium pentobarbital (60 mg/kg, *i.p.*) and supplemented as needed to maintain deep anesthesia. The left carotid artery and penile vein were cannulated

with a polyethylene tube (PE50, 0.58 mm i.d. × 0.96 mm o.d.) filled with heparinized saline solution (heparin 50 units/mL of 0.9% sodium chloride solution). The arterial catheter was connected to a pressure recorder system (Gould-EasyGraf chart-recorder, USA) (See Figure 31) under rectal temperature control (Verhoeven et al., 2017).

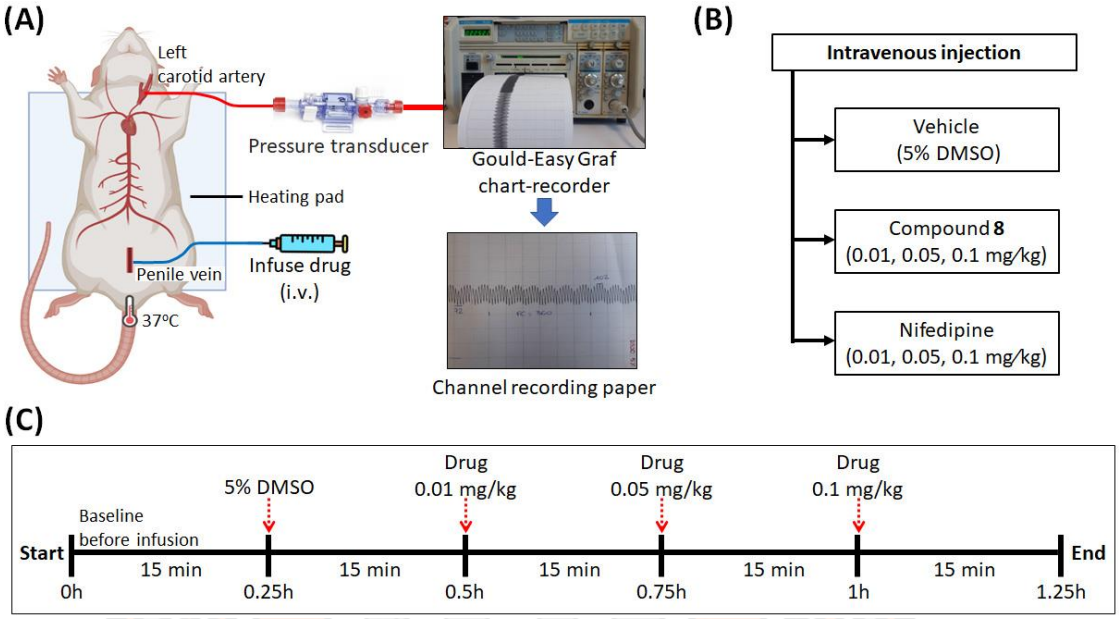

Figure 31 Flow chart and schematic diagram of the acute hypotensive effect study. (A) Schematic diagram illustrating rat cannulation for testing the acute hypotensive effect of the tested compound. The rats were anesthetized, and blood pressure was measured after cannulation of the left carotid artery and connection of the catheter to a pressure recorder system (Gould-EasyGraf chart-recorder, USA) under rectal temperature control. The intravenous infusion (i.v.) of vehicle, nifedipine, or compound 8 were made into the penile vein. (B) The experimental group of the vehicle, nifedipine, and compound 8 infusion. (C) Graphical visualization of the time course of the experiments.

Source: Made by Usana Chatturong (2023)

After a 15 min stabilization period, systolic arterial blood pressure (SBP), diastolic blood pressure (DBP), and heart rate (HR) were recorded before and during intravenous infusion (at 1 mL/min) of a vehicle (0.9% sodium chloride solution containing 5% DMSO), compound **8** or nifedipine (0.01, 0.05, or 0.1 mg/kg BW) (Paulis et al., 2007). The tested compounds were dissolved in 100% DMSO and diluted with 0.9% sodium chloride solution to obtain the final test dose. Successive infusions were separated for sufficient time (>15 min) to allow full recovery of the cardiovascular parameters.

Cytochrome P450 (CYP) induction and inhibition

Drug metabolism is the process of the chemical modification of drugs once they reach the body. In general, the therapeutic effects of drugs are reduced once drug metabolism occurs. As shown in Figure 32, the general pathways of drug metabolism can be divided into 2 reactions, phase I and phase II reactions (Bachmann, 2009). Phase I, the biotransformation reactions, involve the oxidation, reduction, and hydrolysis of the drug to increase its polarity. Phase II, conjugation reactions, generally function as a detoxifying stage in drug metabolism (Bachmann, 2009; Zhao et al., 2021). The liver is a large organ that metabolizes several drugs during both Phase I and II reactions that include complex processes involving CYP enzyme activities (Vaja & Rana, 2020).

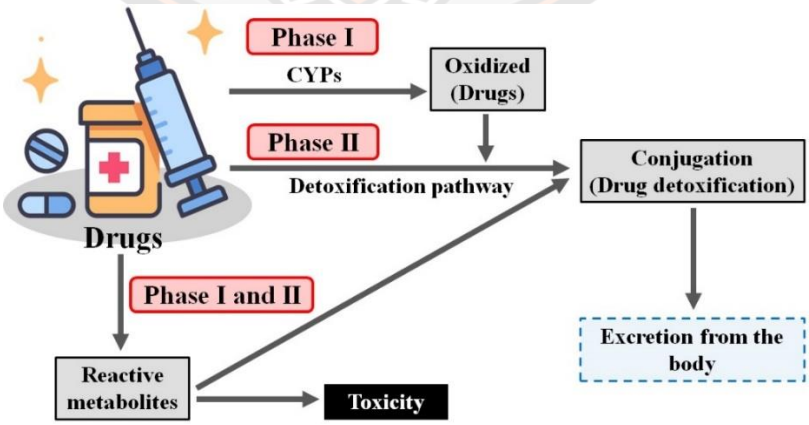

Figure 32 General pathways of drug metabolism

Source: Made by Usana Chatturong (2023)

CYP is the drug-metabolizing enzyme, mainly expressed in the liver, which plays an important role in the metabolism, conjugation, and detoxification of drugs. CYPs are categorized by similar gene sequences. They are allocated a family number (such as CYP1, CYP2, CYP3) and a subfamily letter (such as CYP1A, CYP2B, CYP3A), and the last is differentiated by a number for the isoform or individual enzyme (such as CYP1A2, CYP2B1, CYP3A9) (McDonnell & Dang, 2013). Among the 57 functioning CYPs, three families, CYP1, 2, and 3, are mainly responsible for clinical drug metabolism. The most important CYP enzymes for drug-metabolizing are CYP3A4 (30.2%) and CYP2D6 (20%), followed by, CYP2C9 (12.8%), CYP1A2 (8.9%), CYP2B6 (7.2%), CYP2C19 (6.8%), CYP2C8 (4.7%), CYP2A6 (3.4%), and CYP2E1 (3%) (Zhao et al., 2021). Since 1997, every drug authorized by the United States Food and Drug Administration (FDA) has required a study of, and reporting of, CYP metabolism and its potential for inhibition or induction (Lynch & Price, 2007). Primary hepatocyte cultures that were isolated from human or rat livers were commonly used in the *in vitro* experimental model for the evaluation of hepatotoxicity and CYP induction and inhibition activities (Li, 1997; Soldatow et al., 2013). These models can help predict *in vivo* hepatotoxicity, metabolism, clearance, and potential drug-drug interactions of the new drugs or new compounds.

The parameters that must be known before studying CYP activities are CYP substrate, CYP inducer, and CYP inhibitor.

1) CYP substrates are drugs or other substances that are metabolized by CYP, such as luciferin used as a CYP3A4 and 2C9 substrate in many studies (Cornu et al., 2018; Li, 2009).

2) CYP inducers are substances that can increase the CYP enzyme. Consequently, this increases drug metabolism in the body, which may lead to a decrease in therapeutic concentration and cause treatment failure. Phenobarbital (PB) is an example of a CYP inducer for CYP3A4 and β–naphthoflavone (β–NF) is similar for CYP1A2 (Cornu et al., 2018; McDonnell & Dang, 2013).

3) CYP inhibitors are substances that can inhibit or reduce the CYP enzyme. Consequently, this decreases drug metabolism in the body, which may lead to decreased total clearance and increase the effect or the potential for toxicity. Ketoconazole (Keto) is an example of a CYP inhibitor for CYP3A4, and α-

naphthoflavone (α-NF) for CYP1A2, with erythromycin (Ery) an example of a CYP inducer for CYP2B1 (Cornu et al., 2018; McDonnell & Dang, 2013).

Hepatocytes viability and CYP assays

To determine the potential of quinazoline derivatives (Compounds **5**, **8** and **11**) for drug interactions, their toxicity on rat-isolated hepatocytes and their impact on CYP inhibition and induction were investigated. Sildenafil and nifedipine were used as reference comparators. Healthy male Wistar rats (200-250 g) were anesthetized with sodium pentobarbital (60 mg/kg, *i.p.*). The rat hepatocytes were isolated by a two-step collagenase perfusion via the hepatic portal vein (Cornu et al., 2018). First, the livers were perfused with Ca^{2+}-free HEPES buffer (containing (mM): NaCl 137, KCl 2.7, Na_2HPO_4 0.8, HEPES 25, EGTA 0.5, maintained at pH 7.35, 37°C) for 10 min using a flow rate of 25 mL/min. The livers were then perfused with HEPES buffer containing 0.03% collagenase and 5 mM $CaCl_2$ for 6 min and the digested livers were crushed in phosphate-buffered saline (PBS) and filtered to remove undigested aggregates and washed by PBS at low-speed centrifugation (70 g, 4°C, 3 min). The living cells were then collected by adding hepatocytes on PBS:Percoll (2:1) and centrifuged for 10 min (70 g, 4°C). The resultant pellets were resuspended in PBS and washed once by low-speed centrifugation. Cell viability was estimated by trypan blue exclusion. The living cells and dead cells were counted and calculated as a percentage of living cells to cell death (which should be more than 70%). Then, isolated hepatocytes were resuspended in William's E culture medium supplemented with 10% fetal calf serum (FCS), 4 µg/mL insulin, 10 µM hydrocortisone, 100U/mL penicillin and 100 µg/mL streptomycin. The hepatocytes (7×10^5 cells/well) were seeded in collagen I coated 96-well plates and incubated at 37°C in a humidified chamber with 95%air/5%CO_2 for cell attachment.

For hepatocytes viability assay, fresh William's E culture medium (without FCS) containing 10^{-8} – 10^{-4} M of compounds, was added to the cultures and renewed daily. All the tested compounds were dissolved in 100% DMSO and diluted serially with fresh William's E culture medium (without FCS) to obtain the final test concentrations. 1% DMSO was used as the negative control (vehicle). Evaluation of cell viability after 24 h, 48 h and 72 h of exposure were determined by adding 100 µL

MTT (0.5 mg/mL) and incubating at 37°C in a humidified chamber with 95%air/5%CO_2 for 3 h. Then, MTT was removed and 100 µL DMSO was added to dissolve any formazan crystals before measuring the absorbance at 570 nm using a microplate reader. Cell viability was calculated as the percentage of cell viability in comparison to 0.1%DMSO.

For CYP induction/inhibition evaluation, rat hepatocytes were treated with the tested compounds (10^{-7} – 10^{-5} M) or 0.1% DMSO for 24 h, 48 h and 72 h. β–naphthoflavone (β–NF, 5×10^{-5} M for CYP1A) and phenobarbital (PB, 10^{-3} M for CYP2B or 2×10^{-3} M for CYP2C and 3A) were used for 24 h, 48 h and 72 h of treatment as reference CYP inducers. α–naphthoflavone (α–NF, 10^{-5} M for CYP1A), erythromycin (Ery, 10^{-5} M for CYP2B) and ketoconazole (Keto, 2.5×10^{-5} M for CYP2C and 3A) were added for 2 h (α-NF) or 24 h (Ery and Keto) in the culture as reference CYP inhibitors.

CYP1A and CYP2B activities were evaluated by measuring ethoxyresorufin-O-deethylase (EROD) or benzyloxyresorufin-O-dealkylase (BROD) activity, respectively. These experiments followed the protocol of Cornu *et al.*, 2018 (Cornu et al., 2018). Briefly, cell cultures were washed with PBS for 5 min and incubated for 1 h at 37°C in a culture medium supplemented with 1 mM salicylamide and 10 µM ethoxyresorufin (for CYP1A) or 4.1 µM benzyloxyresorufin (for CYP2B). The content from each well was then removed to 96-well black microplates. The quantity of the fluorescent metabolite resorufin produced was determined at $\lambda_{excitation}$ 530 nm and $\lambda_{emission}$ 580 nm. The activities of CYP1A and 2B were expressed as pmol resorufin formed/min/mg cellular protein.

CYP2C and 3A activities were measured using the P450-Glo™ CYP2C9 (Luciferin-H) or P450-Glo™ CYP3A4 (Luciferin-IPA) assay kit (Promega, Charbonnières-les-Bains, France) according to the manufacturer's instructions. Briefly, cell cultures were washed with PBS for 5 min and incubated with 35 µL luciferin substrate for 4 h (CYP2C) or 1 h (CYP3A) at 37°C. The content from each well was then transferred to 96-well white microplates, and 35 µL of luciferin detection reagent was added before incubating in the dark for 20 min at room temperature. The level of luminescence was then read. The activities of CYP2C and 3A were expressed as relative luminescent units (RLU)/min/mg cellular protein.

Protein content was determined using the bicinchoninic acid protein determination kit (Sigma) and bovine serum albumin (BSA) as a standard. CYP activities were expressed as fold change *vs* 0.1% DMSO, which was set at 1.

Drugs and chemicals

Crude snake venom, Tris-HCL, $MgCl_2$, PMSF, EDTA, DTT, imidazole, BSA, EGTA, DEAE-Sephadex, DMSO, sildenafil citrate salt (purity ≥98%), nifedipine, PE, ACh, nifedipine, 4–AP, ODQ, glibenclamide, verapamil, SNP, β–NF, PB, α–NF, Ery, Keto, BSA, MTT, and collagenase type IV were purchased from Sigma Chemical (St. Louis, MO, USA). [^{3}H] cGMP and Ultima Gold^{TM} were purchased from Perkin Elmer (Boston, MA, USA). Tris-hydroxymethyl-methylamine ($NH_2C(CH_2OH)_3$) were purchased from Univar, Australia. Iberiotoxin was purchased from Smartox Biotechnology (France). William's E culture medium, FCS, insulin, and penicillin/streptomycin were obtained from Invitrogen Corporation (France). ODQ, glybenclamide, 4-AP, β–NF, PB, α–NF, Ery and Keto were dissolved in 100% DMSO. Indomethacin was dissolved in 0.5% w/v Na_2CO_3 and adjusted pH to 7.4 with 1 M NaOH. Other substances were dissolved in distilled water.

Statistical analysis

Data were expressed as mean ± standard error of mean (SEM). Vasorelaxant responses were expressed as the percentage of inhibition of the contractile response to 10^{-5} M PE. Values were analyzed using GraphPad Prism software (version 5.0, San Diego, USA). EC_{50} (half maximal effective concentration) E_{max} (values of maximal relaxation) and IC_{50} (half maximal inhibitory concentration) were calculated by fitting the original dose-response curves. Concentration-response curves were compared by two-way analysis of variance (ANOVA) for repeated measures. According to the OECD Guidelines for the testing of chemicals (Cornu et al., 2018), statistical analysis was performed only when fold change was <1 for CYP inhibition and ≥2 for CYP induction. Comparison between two values was assessed by the unpaired Student's *t*-test. $p < 0.05$ was considered statistically significant.

CHAPTER IV

RESULTS AND DISCUSSION

STUDY I: Identification of N^2,N^4-disubstituted quinazoline 2,4-diamines with human PDE5 inhibition, vasorelaxant effects on pulmonary and systemic circulation, cytotoxicity, and CYP activities in comparison to sildenafil.

Results of study I

1. Human PDE5 inhibition by quinazoline derivatives and sildenafil

As shown in

Figure **33** and Table 6, all quinazoline derivatives inhibited human PDE5 activity, ranging from 0.005 μM for compounds **5** and **11** to 0.062 μM for compound **8**. According to their IC_{50} values, the order of inhibitory activity was compounds **5** = **11** > **4** > **9** > **10** > **8**. For comparison, sildenafil displayed, at an IC_{50} of 0.002 μM, only 2.5-fold more potent than compounds **5** and **11** (p<0.05), while it was ~9 to ~35-fold (p<0.001) more potent than compounds **4**, **8**, **9**, and **10**.

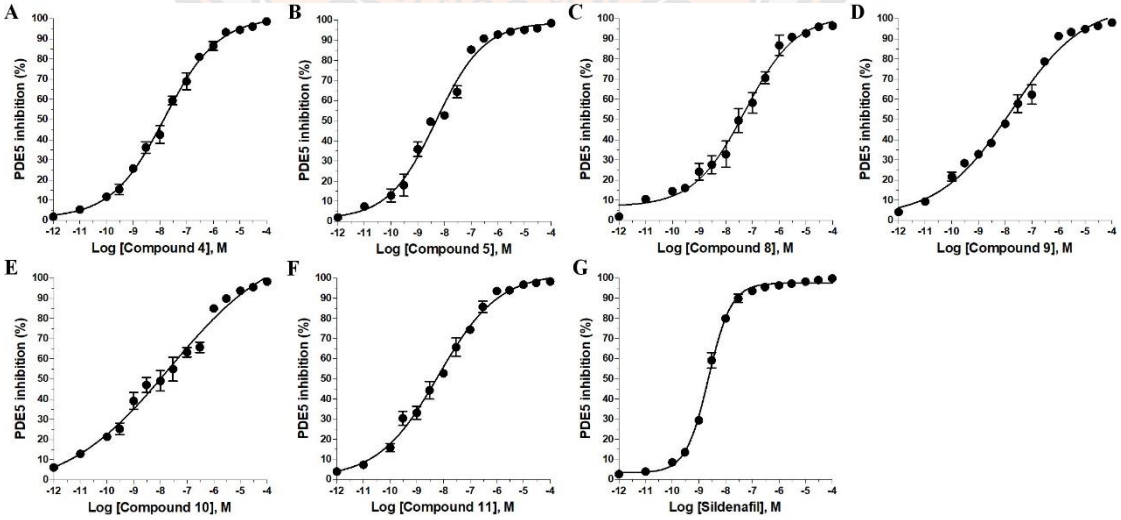

Figure 33 Human PDE5 inhibition by quinazoline derivatives and sildenafil. Representative concentration-response curves of quinazoline

derivatives, (A) Compound 4 (B) Compound 5 (C) Compound 8 (D) Compound 9 (E) Compound 10 (F) Compound 11, and (G) sildenafil against human PDE5 inhibition using the radioactive assay. Values were expressed as means±SEM (*n* = 3 individual experiments)

Table 6 IC_{50} values of test compounds against human PDE5 enzymes

Compound ID	Human PDE5 inhibition activity IC_{50} (µM)
4	$0.015 \pm 0.002^{***}$
5	$0.005 \pm 0.001^{*}$
8	$0.062 \pm 0.007^{***}$
9	$0.019 \pm 0.008^{***}$
10	$0.045 \pm 0.021^{***}$
11	$0.005 \pm 0.001^{*}$
Sildenafil	0.002 ± 0.0004

IC_{50} values were calculated from concentration-response curves of human PDE5 inhibition. Values were expressed as means±SEM (*n* = 3 individual experiments). $^{*}p<0.05$, $^{***}p<0.001$ *vs* sildenafil.

2. Cytotoxicity of quinazoline derivatives and sildenafil on the cultured aorta VSMCs and the PASMCs

The cytotoxicity of quinazoline derivatives and sildenafil towards isolated VSMCs of the rat aorta (Figure 34) and the PA (Figure 35) was assessed by the MTT assay. Treatment with quinazoline derivatives (0.1-100 µM), sildenafil (0.1-100 µM), and the solvent (vehicle, 0.1% DMSO) for 1 h did not influence the viability of either aorta VSMCs or the PASMCs, whereas the highest concentration of sildenafil (at 100 µM) reduced the PASMCs viability from 107.29±3.74 to 79.32±4.81% (Figure 35F, $p<0.05$ *vs* vehicle).

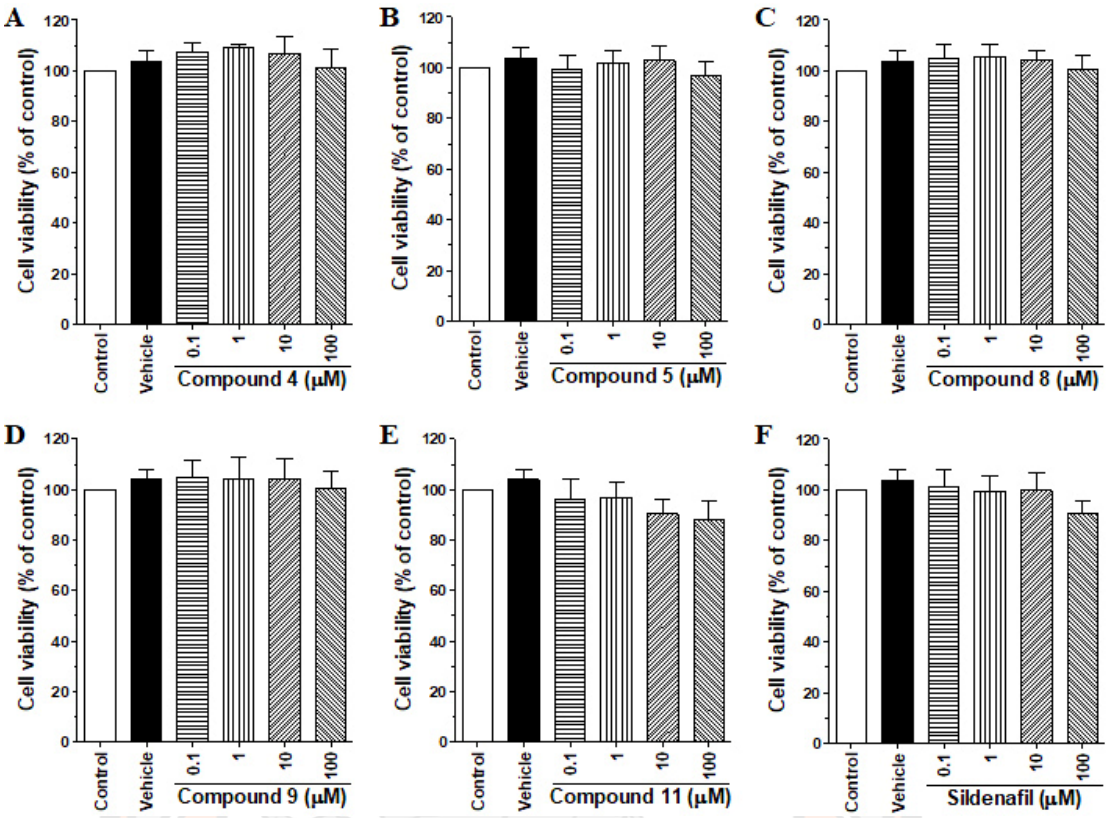

Figure 34 Cytotoxicity of quinazoline derivatives and sildenafil on cultured aorta VSMCs. Cytotoxicity testing of (A) compound 4 (B) compound 5 (C) compound 8 (D) compound 9 (E) compound 11, and (F) sildenafil at concentrations of 0.1-100 μM for 1 h on rat aorta VSMCs. Values were expressed as means±SEM from a triplicate of 3 independent cultures. The absorbance was normalized by the control value (as 100%).

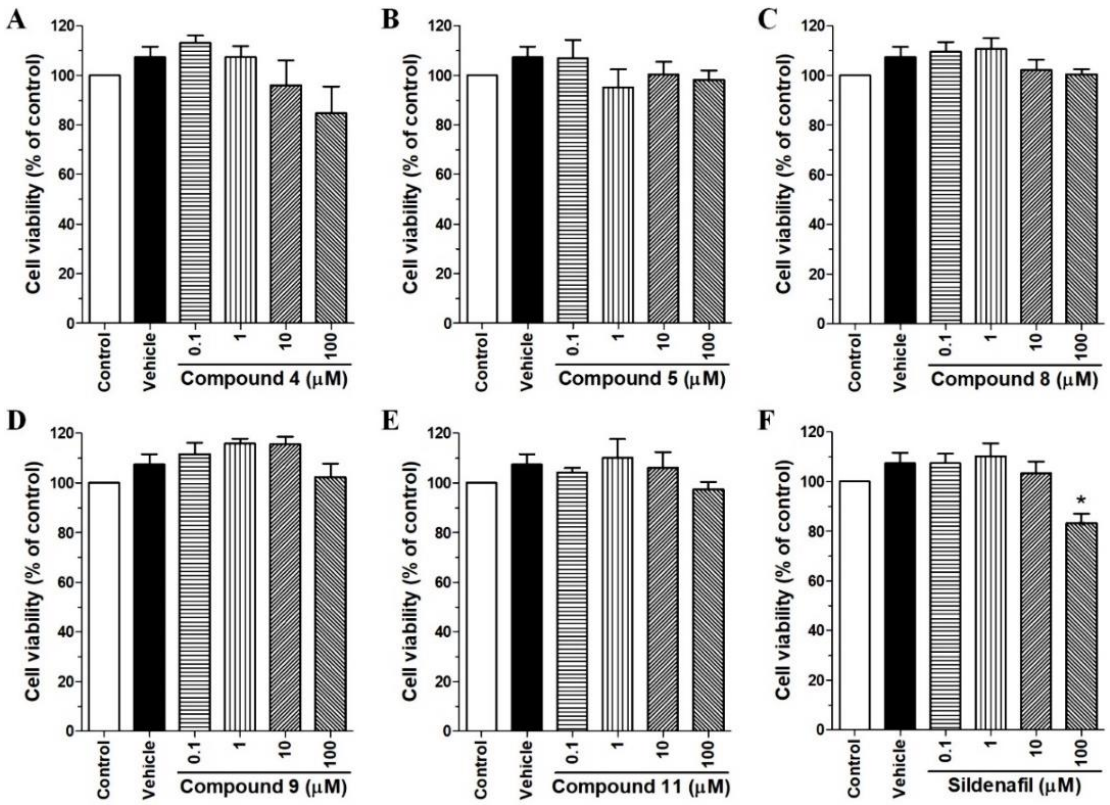

Figure 35 Cytotoxicity of quinazoline derivatives and sildenafil on cultured PASMCs. Cytotoxicity testing of (A) compound 4 (B) compound 5 (C) compound 8 (D) compound 9 (E) compound 11, and (F) sildenafil at concentrations of 0.1-100 μM for 1 h on rat PASMCs. Values were expressed as means±SEM from a triplicate of 3 independent cultures. The absorbance was normalized by the control value (100%). *p<0.05 *vs* cell viability of vehicle.

3. Identification of N^2,N^4-disubstituted quinazoline 2,4-diamines with vasorelaxant effects on pulmonary circulation and systemic circulation in comparison to sildenafil.

3.1 Compounds 5 and 11 induced a stronger vasorelaxant effect on the PA as compared to aorta.

To determine the capacity of quinazoline derivatives to selectively vasodilate the PA, the relaxant effect of the compounds was studied on both the PA and aorta (Figure 36). While all compounds vasodilated both the rat PA and aorta, only two compounds (**5** and **11**) induced a greater relaxation in the PA than in the aorta (Figure 36B and Figure 36F). Conversely, the relaxant effect of compound **8** in the aorta was superior to that in the PA (Figure 36C). Importantly, sildenafil induced a similar vasorelaxant effect in both the PA and aorta (Figure 36G). Table 7 shows the pharmacological parameters of compounds **5** and **11** as compared to sildenafil. Regarding the relaxant effect on the PA, while the potency (EC_{50}) of compounds **5** and **11** was lower than sildenafil (0.94±0.30 and 1.03±0.23 *vs* 0.05±0.02 µM, respectively, $p<0.01$), the maximal relaxation (E_{max}) was not different (87.9±5.03, 96.1±1.30 and 98.0±1.63%, respectively).

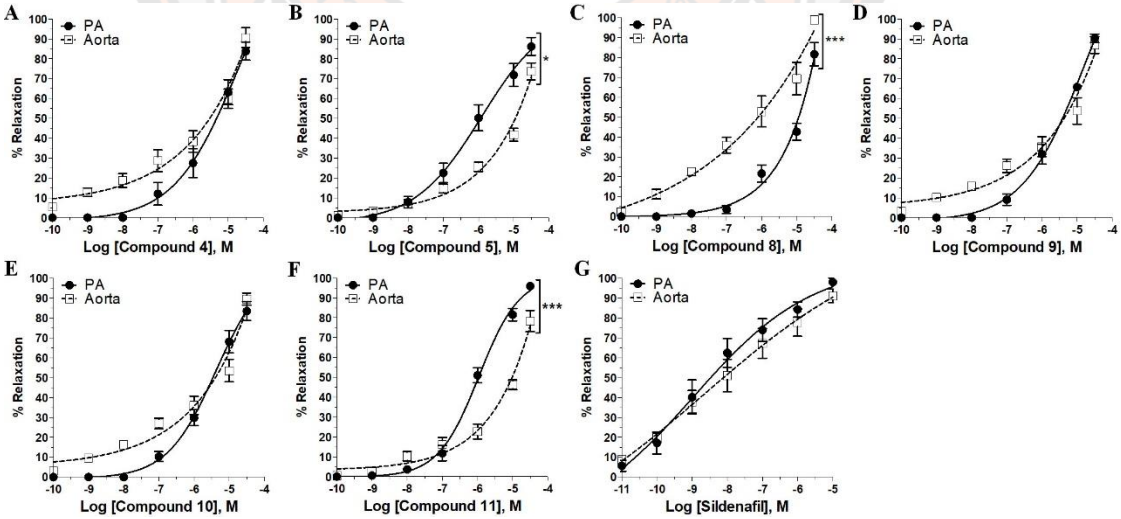

Figure 36 Comparison of the vasorelaxant effect of quinazoline compounds and sildenafil on the PA *vs* aorta. The vasorelaxant effect of six quinazoline derivatives and sildenafil was studied in endothelium-

intact PA and aortic rings preconstricted with 10^{-5} M PE. Values were expressed as means±SEM (*n* = 5-6). $^{*}p<0.05$, $^{***}p<0.001$ *vs* the PA.

Table 7 Pharmacological parameters of quinazoline compounds and sildenafil

Compound	Vasorelaxation EC_{50} (μM)		SI of vasorelaxation
	PA	Aorta	
4	$3.92\pm1.15^{***}$	$3.73\pm0.81^{**}$	1.0
5	$0.94\pm0.30^{**}$	$7.36\pm1.44^{***,\#\#}$	7.8
8	$6.16\pm1.30^{***}$	$1.26\pm0.33^{*,\#\#}$	0.2
9	$3.72\pm0.62^{***}$	$3.84\pm1.68^{**}$	1.0
10	$3.55\pm1.10^{***}$	$2.41\pm0.55^{**}$	0.7
11	$1.03\pm0.23^{**}$	$6.49\pm1.18^{***,\#\#}$	6.3
Sildenafil	0.05±0.02	0.11±0.07	2.1

EC_{50} was calculated from concentration-response curves of vasorelaxation on endothelium-intact isolated the PA and aorta. The selectivity index (SI) is the ratio of (EC_{50} aorta)/(EC_{50} the PA) that reflects the selectivity of each compound for the PA *vs* aorta. Values were expressed as means±SEM (*n* = 5-6 rats). $^{*}p<0.05$, $^{**}p<0.01$, $^{***}p<0.001$ *vs* sildenafil; $^{\#\#}p<0.01$ *vs* the PA.

Even though compounds **5** and **11** had a lower relaxant effect on the PA than sildenafil (Table 7), the calculation of the SI values that reflects the capacity of relaxation of the PA over the aorta showed that SI was greater for compounds **5** (7.8) and **11** (6.3) than sildenafil (2.7). As the aorta is a conductance vessel, the relaxant effect of these compounds was also evaluated in a resistance vessel, the mesenteric artery (MA). As shown in Figure 37, the relaxation induced by both compounds was lower than sildenafil. Consistently, EC_{50} values of compounds **5** and **11** were significantly higher than sildenafil (0.76±0.29 and 0.54±0.13 *vs* 0.03±0.01 μM, respectively, $p<0.05$), while the maximal relaxation (E_{max}) was not different

(95.7±1.00, 93.2±1.93 and 99.0±1.02, respectively), which is consistent with a lesser relaxant effect of compounds **5** and **11** than sildenafil on the systemic vasculature.

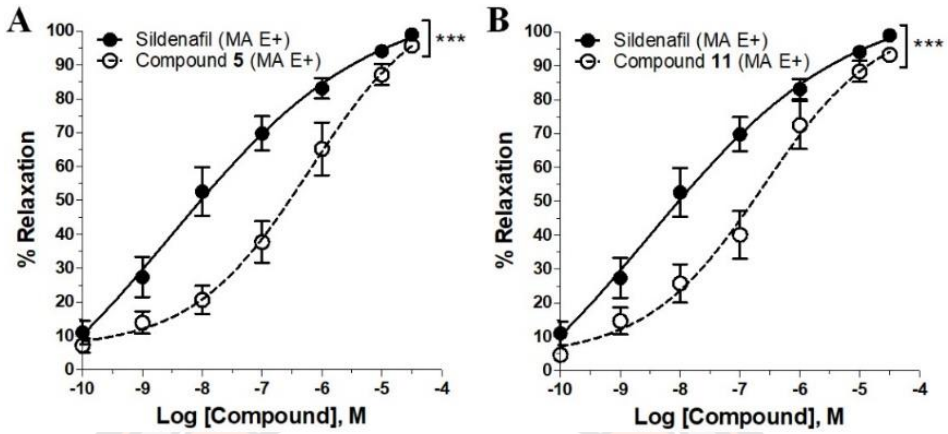

Figure 37 Comparison of the vasorelaxant effect on MA of compounds 5 and 11 *vs* sildenafil. The vasorelaxant effect of the compounds was studied in endothelium-intact MA rings precontracted with 10^{-5} M PE. Values were expressed as means±SEM (*n* = 7-8). ****p*<0.001 *vs* sildenafil.

4. Comparison of the mechanisms of vasorelaxation induced by compounds 5 and 11, and sildenafil on PA

4.1 The vasorelaxant effect of compounds 5, 11 and sildenafil is endothelium- and NO-dependent.

A more detailed investigation of the pharmacological mechanisms involved in the vasorelaxant effect of compounds **5** and **11** in the PA was subsequently undertaken, with a comparison to sildenafil. First, the role of endothelium was investigated. As shown in Figure 38, the removal of the endothelium significantly decreased the relaxation effect of all compounds (Figure 38A-C, Table 8). The solvent used, DMSO at a final concentration of 0.13%, had no effect (Figure 38D, Table 8).

To study the mechanisms involved, endothelium-intact PA rings were first incubated with specific blockers of endothelial signaling pathways (L-NAME, indomethacin, or apamin plus charybdotoxin that inhibit NOS, COX or EDHF, respectively). Among them, only inhibition of NOS by L-NAME reduced the

relaxation induced by compounds **5**, **11** and sildenafil (Figure 39A-C, Table 8), whereas blockade of COX or inhibition of EDHF did not change their effects (Figure 39A-C).

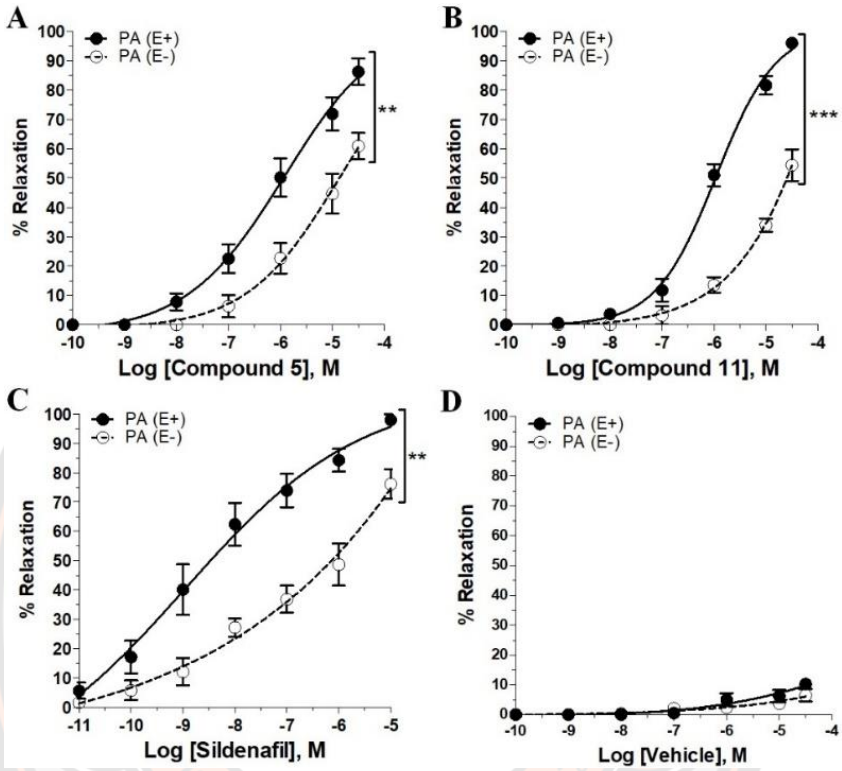

Figure 38 Contribution of the endothelium to the vasorelaxant effects of compounds 5, 11 and sildenafil in the PA. Concentration-response curves of compound 5 (A), compound 11 (B), sildenafil (C) or vehicle (D) in the PA with (E+) or without (E–) endothelium precontracted with 10^{-5} M PE. Values were expressed as means±SEM (*n* = 5-6 rats). $^{**}p<0.01$, $^{***}p<0.001$ *vs* the PA (E+).

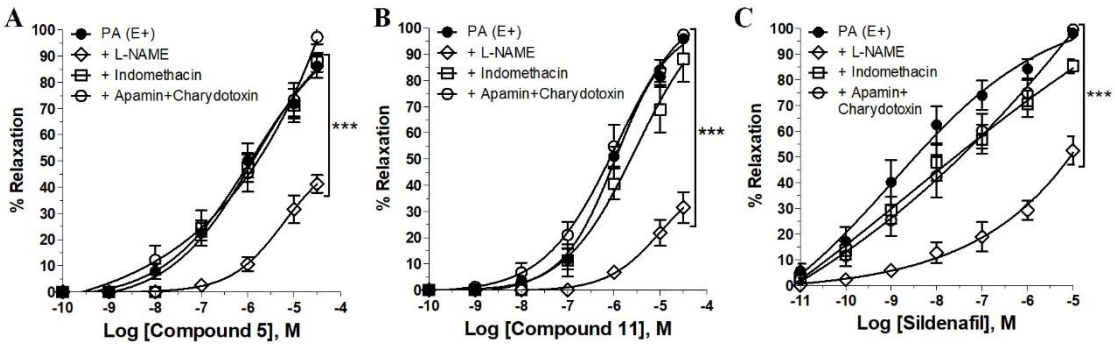

Figure 39 Contribution of the endothelial signaling pathways to the vasorelaxant effects of compounds 5, 11 and sildenafil in the PA. Concentration-response curves of compound 5 (A), compound 11 (B) and sildenafil (C) in endothelium-intact (E+) PA rings precontracted with PE and pretreated with inhibitors of endothelial signaling pathways including L-NAME (NOS blocker), indomethacin (COX blocker), or apamin plus charybdotoxin (EDHF blocker). Values were expressed as means±SEM (*n* = 5–6). ****p*<0.001 *vs* the PA (E+).

Table 8 EC_{50} and E_{max} values for the vasorelaxant response of compounds 5, 11 and sildenafil

Compounds	5	11	Sildenafil
Endothelium-intact (E+)			
Compound (E+)			
EC_{50} (μM)	0.94±0.30*	1.03±0.23**	0.05±0.02
E_{max} (%)	87.9±5.03	96.1±1.30	98.0±1.63
+ L-NAME			
EC_{50} (μM)	5.17±1.41$^{\#}$	5.81±1.18$^{\#\#}$	4.26±0.69$^{\#\#\#}$
E_{max} (%)	41.3±3.3$^{\#\#\#}$	31.48±5.93$^{*,\#\#\#}$	52.42±5.54$^{\#\#\#}$
+ Indomethacin			
EC_{50} (μM)	0.82±0.41	4.09±1.15***	0.48±0.08$^{\#\#\#}$
E_{max} (%)	87.67±3.66	91.85±7.26	81.25±2.72

Compounds	5	11	Sildenafil
+ Apamin + Charybdotoxin			
EC_{50} (μM)	0.79±0.31	1.86±0.21*	0.40±0.11$^{\#}$
E_{max} (%)	97.3±2.73	97.5±1.63	99.5±0.49
Endothelium-denuded (E-)			
Compound (E–)			
EC_{50} (μM)	3.17±0.51$^{*,\#\#}$	5.32±0.87$^{**,\#\#}$	0.53±0.11$^{\#\#}$
E_{max} (%)	60.9±4.43$^{*,\#\#}$	54.4±5.39$^{*,\#\#\#}$	79.3±5.06$^{\#}$
+ ODQ			
EC_{50} (μM)	10.54±1.15$^{\#\#}$	12.34±1.77$^{\#\#}$	9.06 ± 0.69$^{\#\#\#}$
E_{max} (%)	30.0±5.94$^{\#\#}$	33.0±4.17$^{\#}$	46.7±6.32$^{\#\#\#}$
+ 4-AP			
EC_{50} (μM)	5.91±1.56**	7.80±2.14**	2.55±0.36
E_{max} (%)	52.8±1.73*	55.1±5.15	70.9±4.90
+ Glibenclamide			
EC_{50} (μM)	3.15±0.86*	5.76±0.86**	1.87±0.62
E_{max} (%)	62.3±3.24	52.2±2.09*	73.6±6.59
+ Iberiotoxin			
EC_{50} (μM)	2.89±1.42	5.83±1.52**	2.01±0.69
E_{max} (%)	63.2±4.34	52.0±3.18*	75.2±6.97

Experiments were made on endothelium-intact (E+) and endothelium-denuded (E-) PA rings with and without inhibitors. Values were expressed as means±SEM (n = 5-6). $^{*}p<0.05$, $^{**}p<0.01$, $^{***}p<0.001$ *vs* sildenafil in the same condition; $^{\#}p<0.05$, $^{\#\#}p<0.01$, $^{\#\#\#}p<0.001$ *vs* endothelium-intact (E+) or endothelium-denuded (E-) rings without inhibitors.

4.2 Potentiation of sGC/cGMP pathway is involved in relaxation to compounds 5, 11 and sildenafil.

To determine if the PDE5 inhibitory effects of the quinazoline derivatives may be involved in their relaxant effect, their capacity to potentiate the relaxant effect of SNP, a NO donor, that activates sGC and increases cGMP synthesis was investigated. Consistent with a contribution of PDE5 inhibition, compounds **5**, **11** and sildenafil increased SNP-induced relaxation in endothelium-denuded PA rings compared to the vehicle (Figure 40A-C). The EC_{50} values of SNP decreased from 7.1±1.0 nM (vehicle) to 3.6±0.8 nM (compounds **5**), 3.4±0.9 nM (compounds **11**) and 2.4±0.7 nM (sildenafil) (p<0.05) but there was not change in the E_{max} values of SNP (98.7±0.4% (compound **5**), 99.3±0.3% (compound **11**) and 97.9±0.4% (sildenafil) *vs* 99.8±0.1% (vehicle)). To determine if a direct activation of sGC might be also involved, the effect of ODQ was studied. Figure 40D-F and Table 8 showed that the vasorelaxation induced by compounds **5**, **11** and sildenafil was significantly reduced by the sGC inhibitor.

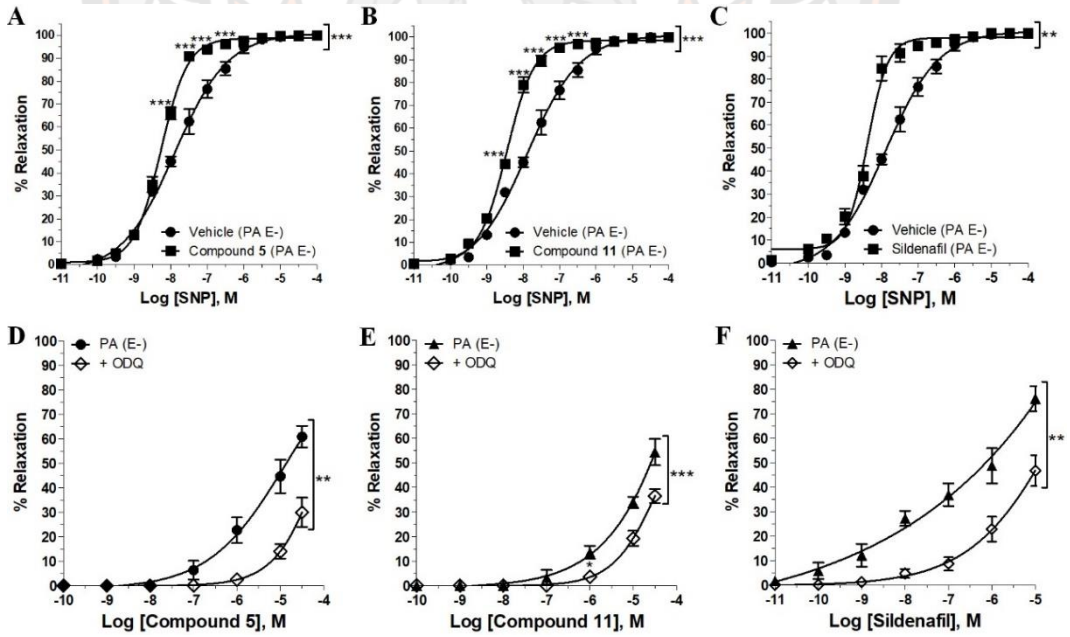

Figure 40 Contribution of the sGC/cGMP pathway to vasorelaxant effects of compounds 5, 11 and sildenafil in the PA. Concentration-response curves of SNP (NO donor) after incubation with compound 5 (A),

compound 11 (B) and sildenafil (C) or vehicle in endothelium-denuded PA (E–) rings. Concentration-response curves of compound 5 (D), compound 11 (E) and sildenafil (F) after incubation with ODQ in endothelium-denuded PA (E–) rings. Values were expressed as means±SEM (*n* = 5-6). ***p*<0.01, ****p*<0.001 *vs* the PA or vehicle.

4.3 The vasorelaxant effect of compounds 5 and 11 relies on ROCC inhibition but not activation of K^+ channels

The effect of various K^+ channel blockers (4-AP, glibenclamide, and iberiotoxin that inhibit K_V, K_{ATP}, and K_{Ca}, respectively) was evaluated on endothelium-denuded PA rings. As shown in Figure 41, K^+ channel blockers did not change the vasorelaxation of compounds **5**, **11** and sildenafil (Figure 41A-C). Then, the impact of the compounds on Ca^{2+} fluxes was studied. Compounds **5**, **11** and sildenafil significantly attenuated the contraction induced by extracellular Ca^{2+} influx in PE-exposed rings (opening of ROCC, Figure 41D, $p<0.001$) whereas no change was observed after 80 mM high K^+ solution (opening of VOCC, Figure 41E). Regarding intracellular Ca^{2+} fluxes, data reported that compounds **5** and **11** and sildenafil significantly reduced PE-induced Ca^{2+} release from SR (Figure 41F, $p<0.01$).

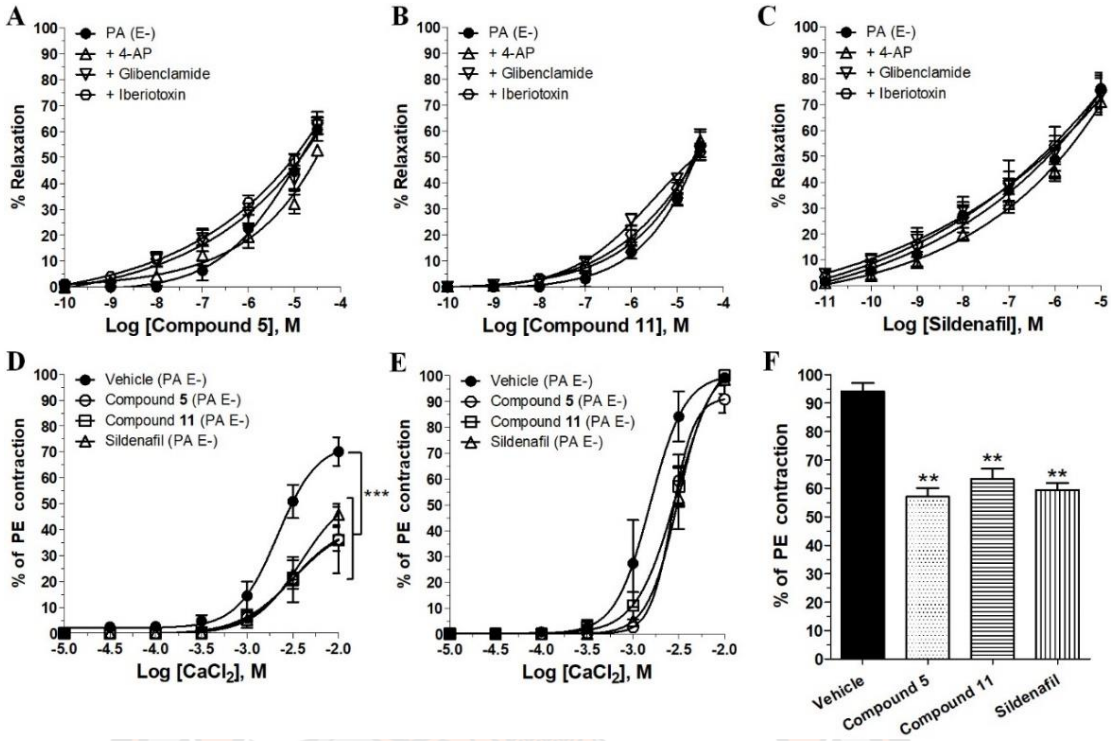

Figure 41 Contribution of K^+ and Ca^{2+} channels to vasorelaxant effects of the compounds in the PA. Concentration-response curves of compound 5 (A), compound 11 (B) and sildenafil (C) in endothelium-denuded pa(E–) rings precontracted with PE and pretreated with various K^+ channel inhibitors: 4-AP (K_V blocker), glibenclamide (K_{ATP} blocker) or iberiotoxin (K_{Ca} blocker). Concentration-response curves of $CaCl_2$ after incubation of the endothelium-denuded PA (E–) rings with compounds or vehicle and exposure to PE (D, ROCC opening) or 80 mM high K^+ solution (E, VOCC opening) in a Ca^{2+}-free Krebs solution. (F) Effect of compounds on Ca^{2+} release from SR. Values were expressed as means±SEM (n = 5-6 rats). $^{**}p<0.01$, $^{***}p<0.001$ *vs* vehicle.

4.4 Compounds 5, 11 and sildenafil do not affect α_1-adrenergic receptors

To determine if the blockade of α_1-adrenergic receptors might be involved, the effect of compounds **5**, **11**, sildenafil or vehicle on PE-induced contraction was studied. As compared to the vehicle, all compounds slightly decreased PE-induced contraction but not significantly (Figure 42). The E_{max} values of compounds **5**, **11**, sildenafil and the vehicle are 48.5±2.8, 53.2±5.4, 51.1±9.9 and 62.9±6.4%, respectively, and the EC_{50} values are 0.5±0.1, 0.6±0.1, 0.5±0.2 and 0.2±0.1 μM, respectively.

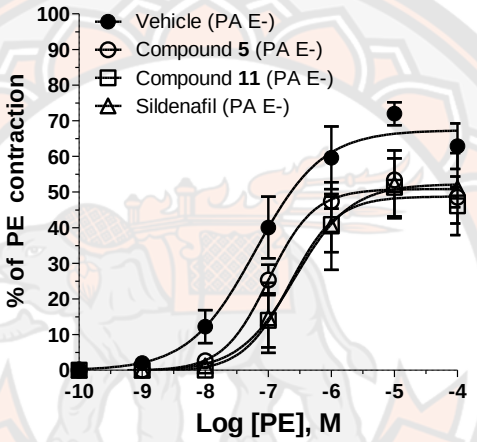

Figure 42 Contribution of α_1-adrenergic receptors to vasorelaxant effects of compounds 5, 11, sildenafil or vehicle in the PA. Concentration-response curves for PE-induced contraction after incubation with compounds 5, 11, sildenafil or vehicle in endothelium-denuded PA (E–) rings. Values were expressed as means±SEM (*n* = 5).

5. Endothelium-independent mechanisms of compounds 5 and 11 are different in the systemic vasculature.

To determine if the mechanisms of vasorelaxation of compounds **5** and **11** differ according to the vascular beds, a mechanistic study was also conducted in MA. As shown in Figure 43 and Table 9, the mechanisms involved in the effects of compounds **5** and **11** are similar in the MA and PA regarding endothelium-dependent mechanisms, potentiation of SNP, and effects on Ca^{2+} fluxes, but differ as regards K^+

channels, sGC activation, and inhibition of α_1-adrenergic receptors, as more details are explained below.

5.1 The vasorelaxant effect of compounds 5 and 11 was endothelium- and NO-dependent in MA.

The removal of the endothelium significantly decreased the relaxation effect of all compounds (Figure 43A-B and Table 9). Inhibition of NOS by L-NAME reduced the relaxation induced by compounds **5** and **11**, whereas blockade of COX or inhibition of EDHF did not change their effect (Figure 43C-D and Table 9).

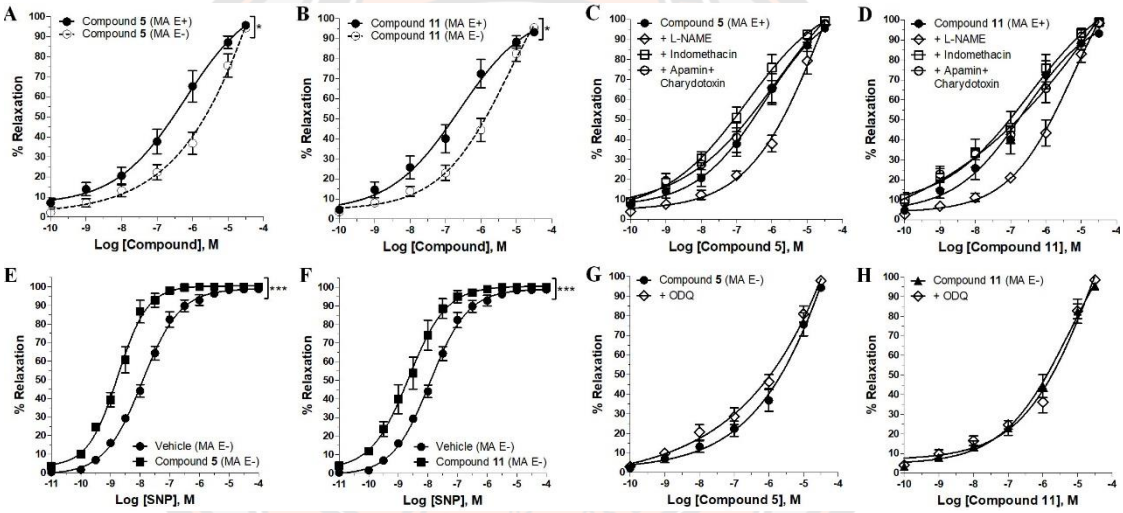

Figure 43 Contribution of the endothelium and NO/sGC/cGMP pathway to the vasorelaxant effects of compounds 5 and 11 in MA. (A-B) Concentration-response curves of compounds in MA with (E+) and without (E–) endothelium. (C-D) the vasorelaxant effect of the compounds after incubation with L-NAME (NOS blocker), indomethacin (COX blocker), or apamin plus charybdotoxin (EDHF blocker) in endothelium-intact MA (E+) rings or (G-H) with ODQ (sGC blocker) in endothelium-denuded MA (E–) rings. (E-F) the vasorelaxant effect of SNP after incubation with the compounds at their EC_{50}. Values were expressed as means±SEM (n=6). $^{*}p\leq0.05$, $^{***}p\leq0.001$ *vs* MA or vehicle.

Table 9 EC_{50} and E_{max} values of compounds 5 and 11 induced relaxations in endothelium-intact (E+) and -denuded (E–) MA rings in the absence or presence of various inhibitors

Compounds	**5**	**11**
Endothelium-intact (E+)		
Compound (E+)		
EC_{50} (μM)	0.76±0.29	0.54±0.13
E_{max} (%)	95.7±1.00	93.2±1.93
+ L-NAME		
EC_{50} (μM)	3.79±1.22**	2.86±1.11**
E_{max} (%)	97.4±0.96	98.4±0.36
+ Indomethacin		
EC_{50} (μM)	0.36±0.18	0.32±0.22
E_{max} (%)	99.2±0.42	98.8±0.52
+ Apamin + Charybdotoxin		
EC_{50} (μM)	0.53±0.12	0.31±0.09
E_{max} (%)	97.9±0.57	98.8±0.63
Endothelium-denuded (E-)		
Compound (E–)		
EC_{50} (μM)	5.24±0.98***	3.12±0.87***
E_{max} (%)	94.3±1.28	95.5±0.51
+ ODQ		
EC_{50} (μM)	2.31±0.50	3.82±0.98
E_{max} (%)	97.9±0.57	98.5±0.58
+ 4-AP		
EC_{50} (μM)	2.28±0.49	2.82±1.06
E_{max} (%)	98.2±0.25	98.0±0.61
+ Glibenclamide		
EC_{50} (μM)	1.59±0.54*	5.21±1.33
E_{max} (%)	82.5±3.92	97.3±0.77

Compounds	5	11
+ Iberiotoxin		
EC_{50} (μM)	18.65±3.07***	14.95±3.8***
E_{max} (%)	93.3±3.13	97.6±0.50

Values were expressed as means±SEM (n = 6-8). EC_{50} is the concentration of the compound giving half-maximal relaxation. E_{max} is the maximum response of MA expressed as a relaxation percentage of the contraction induced by PE. $^{*}p<0.05$, $^{**}p<0.01$, $^{***}p<0.001$ *vs* endothelium-intact (E+) or endothelium-denuded (E–) MA without inhibitors of each compound.

5.2 The relaxant effect of compounds 5 and 11 relied on the potentiation of the sGC/cGMP pathway, activation of K_{Ca} channels and inhibition of α_1-adrenergic receptors and ROCC.

The possible role of compounds **5** and **11** as a potentiator of the sGC/cGMP pathway was studied in endothelium-denuded MA rings. As shown in Figure 44E-F, consistent with a PDE5 inhibitory effect, all compounds slightly but significantly enhanced the relaxant effect of SNP. Consistently, EC_{50} of SNP was reduced by the incubation with the compounds (EC_{50}=16.8±4.5 nM (vehicle) *vs* 3.0±1.3 nM (compound **5**) and 5.96±3.5 nM (compound **11**), $p<0.05$). To determine if a direct activation of the sGC might be also involved, the effect of ODQ (an sGC inhibitor) was studied. Figure 44G-H and Table 7 show that the sGC inhibitor did not change the relaxant effect of the compounds in the MA.

The effect of various K^+ channel blockers (4-AP, glibenclamide, and iberiotoxin that inhibit K_V, K_{ATP}, and K_{Ca}, respectively) was then evaluated on endothelium-denuded MA rings. Among them, only iberiotoxin significantly reduced their relaxant effect (Figure 44A-B and Table 9) as a reflection of the activation of K_{Ca} channels by compounds **5** and **11**.

To determine if the blockade of α_1-adrenergic receptors might be involved, the effect of compounds **5** and **11** on PE-induced contraction was then studied. Both compounds slightly but significantly decreased PE-induced contraction, which was

lower than the contraction demonstrated by the vehicle. (Figure 44C-D). Compounds **5** and **11** enhanced the EC_{50} of PE from 1.9±0.3 µM (vehicle) to 8.5±2.6 µM (compound **8**) and 6.1±1.9 µM (compound **11**) ($p<0.05$) but did not change the E_{max} value (107.5±2.7% (vehicle) *vs* 103.3±2.1% (compound **5**) and 107.2±3.7% (compound **11**).

Finally, the contribution of extracellular or intracellular Ca^{2+} fluxes was evaluated. Both compounds reduced the contraction elicited by extracellular Ca^{2+} influx in PE-exposed rings (opening of ROCC, Figure 44E). However, compounds **5** and **11** changed neither the extracellular Ca^{2+} influx in 80 mM high K^+ solution-exposed rings (opening of VOCC, Figure 44F) nor the intracellular Ca^{2+} release from SR (Figure 44G).

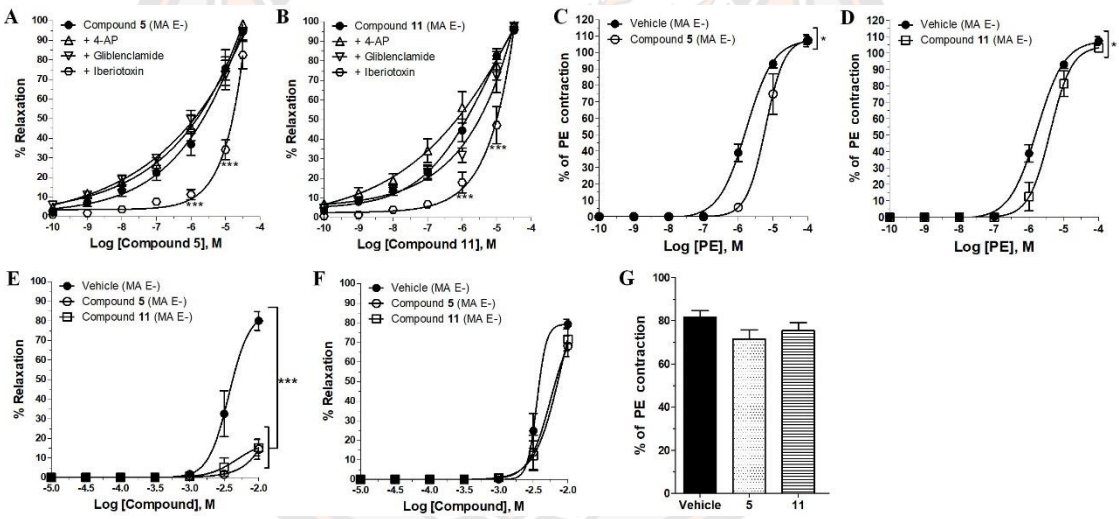

Figure 44 Contribution of K^+ channels, α_1-adrenergic receptors and Ca^{2+} channels to vasorelaxant effects of compounds 5 and 11 in the MA. (A-B) The vasorelaxant effect of compounds after incubation with various K^+ channel inhibitors: 4-AP (K_V blocker), glibenclamide (K_{ATP} blocker) or iberiotoxin (K_{Ca} blocker). (C-D) Concentration-response curves for PE-induced contraction after incubation with compounds or vehicle in endothelium-denuded MA (E–). Concentration-response curves of $CaCl_2$ after incubation of endothelium-denuded MA (E–) rings with compounds or vehicle and exposure to PE (E, ROCC opening) or 80 mM high K^+ solution (F, VOCC opening) in a Ca^{2+}-free

Krebs solution. (G) Effect of compounds on Ca^{2+} released from SR. Values were expressed as means±SEM (*n* = 5-6 rats). **p*<0.05, ****p*<0.001 *vs* vehicle.

6. Cytotoxicity of compounds 5, 11 and sildenafil on cultured hepatocytes

Rat hepatocytes in primary cultures were exposed to compounds **5**, **11,** sildenafil and the vehicle (0.1% DMSO) for 24 h, 48 h and 72 h before the MTT assay. As shown in Figure 45A-C, viability remained >80% with all compounds at concentrations up to 10^{-5} M. At higher concentrations (10^{-5} to 10^{-4} M), compounds **5** and **11** led to a time-dependent and concentration-dependent decrease in cell viability. IC_{50} values for compound **5** at 24 h, 48 h and 72 h of exposure were (µM) 73±12, 43±6 and 18±0.1, respectively, and for compound **11** were (µM) 61±10, 23±1 and 19±0.3, respectively. Sildenafil was less toxic with viability >80% whatever the time or concentration.

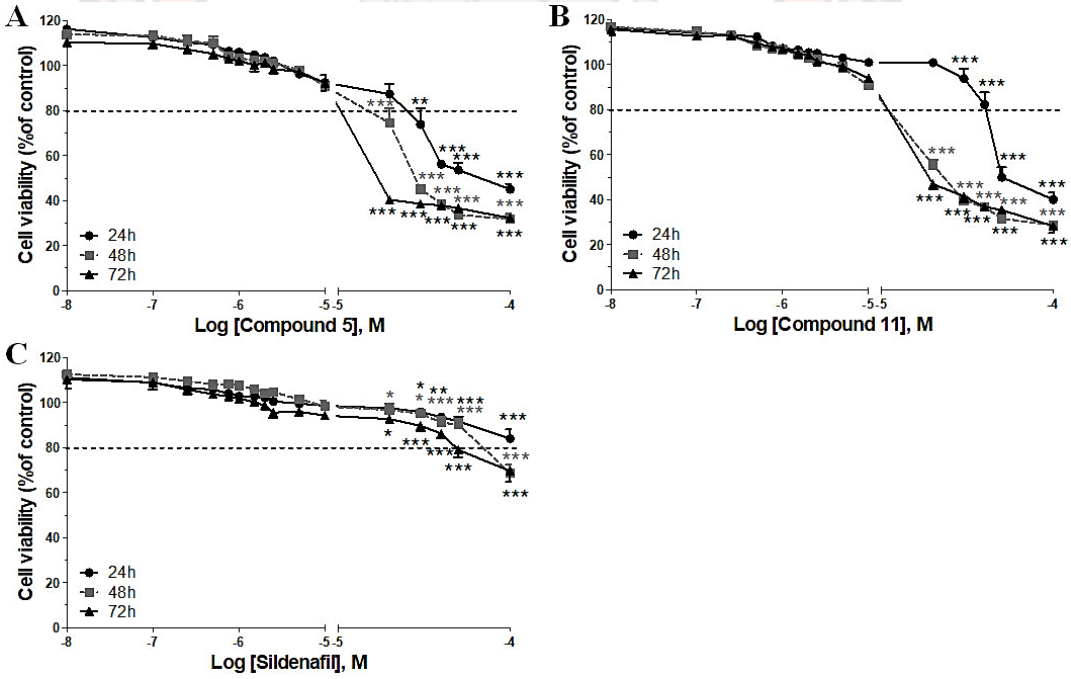

Figure 45 Effects of compounds 5, 11 and sildenafil on cell viability in primary rat hepatocyte cultures. Cell viability was studied in rat hepatocyte cultures after 24h (●), 48h (■) or 72h (▲) exposure with compound 5

(A), compound 11 (B), sildenafil (C) or control (0.1% DMSO) and expressed as a percentage of the control (0.1% DMSO). Values were expressed as means±SEM from a triplicate of 3 independent cultures. $^{*}p<0.05$, $^{**}p<0.01$, $^{***}p<0.001$ *vs* cell viability of control (0.1% DMSO) for each time of culture.

7. Effects of compounds 5, 11 and sildenafil on CYP activities in isolated hepatocytes

CYP1A, 2B, 2C and 3A activities were measured in rat hepatocytes after 24 h, 48 h and 72 h of exposure to compounds **5**, **11**, sildenafil, control (0.1% DMSO), reference inducers or reference inhibitors. Non-cytotoxic concentrations of compounds **5**, **11**, and sildenafil (0.1-10 µM) were chosen.

As shown in Figure 46-47, β-NF was used as a reference inducer for CYP1A activity and PB for CYP2B, 2C and 3A activities, whereas α-NF was used as a reference inhibitor for CYP1A activity, Ery for CYP2B activity, and Keto for CYP2C and 3A activities. As expected, β-NF caused a significant induction (4-, 6- and 17-fold increases at 24 h, 48 h and 72 h, respectively) of CYP1A activity, while PB significantly increased CYP2B (2-, 4- and 8-fold increases at 24 h, 48 h and 72 h, respectively), CYP2C (2-, 3- and 4-fold increases at 24 h, 48 h and 72 h, respectively) and CYP3A activities (3-, 20- and 59-fold increases at 24 h, 48 h and 72 h, respectively), whereas α-NF Ery or Keto had the opposite effect.

Compound **5** (Figure 46) did not change CYP1A and 2B activities but inhibited CYP2C (only at 5 and 10 µM) and CYP3A (only at 10 µM) at all exposure times. Compound **11** (Figure 47) slightly increased CYP1A activity in a concentration-independent manner (0.1-2.5 µM) after 72 h of treatment and inhibited CYP3A activity only at the highest concentration (10 µM), at all exposure times. Sildenafil (Figure 48) led to a concentration-dependent increase in CYP1A activity, up to 6-fold and inhibited CYP3A, only at the two highest concentrations (5 and 10 µM).

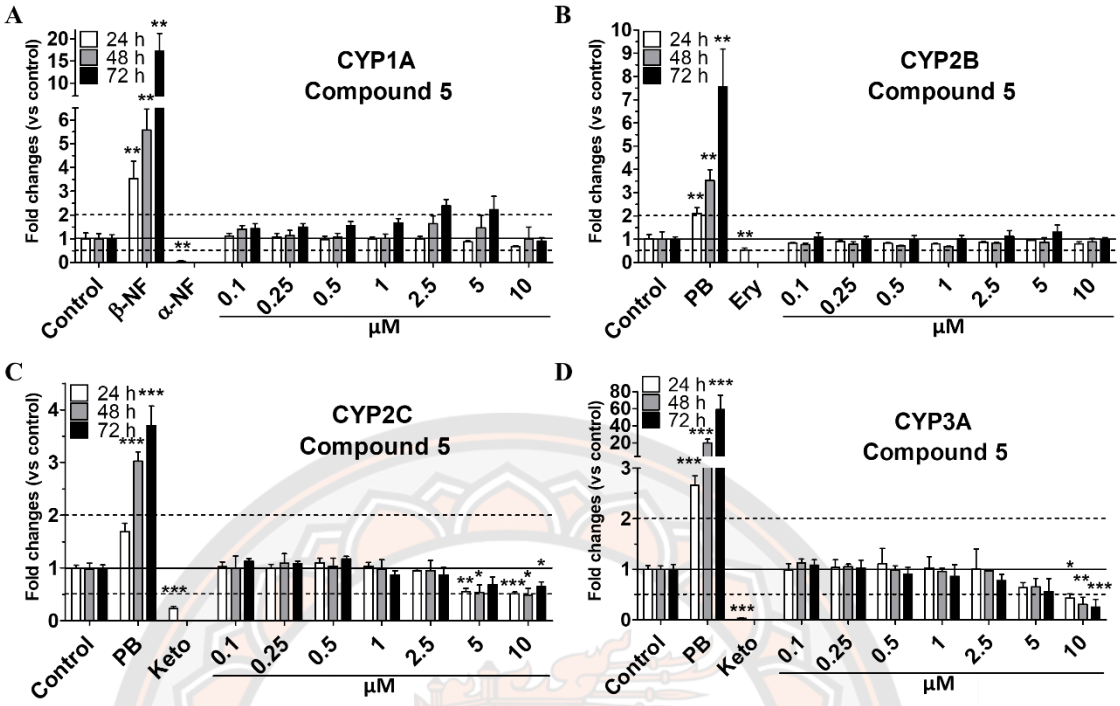

Figure 46 Effects of compound 5 on CYP activity in isolated rat hepatocytes. CYP1A (A), CYP2B (B), CYP2C (C) and CYP3A (D) activities were measured in primary rat hepatocyte cultures after 24 h, 48 h and 72 h of exposure with compound 5 or control (0.1% DMSO). β-NF (50 µM for CYP1A) and PB (1 mM for CYP2B or 2 mM for CYP2C and 3A) were used for 24 h, 48 h and 72 h of treatment as reference CYP inducers. α-NF (10 µM for CYP1A), Ery (10 µM for CYP2B) and Keto (25 µM for CYP2C and 3A) were added for 2 h (α-NF) or 24 h (Ery and Keto) in culture as reference CYP inhibitors. Results are expressed as fold-change *vs* control (0.1% DMSO, set at 1). Statistical analysis was processed only when the fold change was <1 for CYP inhibition and ≥2 for CYP induction. Values were expressed as means±SEM from a triplicate of 3 independent cultures. $^{*}p<0.05$, $^{**}p<0.01$, $^{***}p<0.001$ *vs* control (0.1% DMSO) for each time of culture.

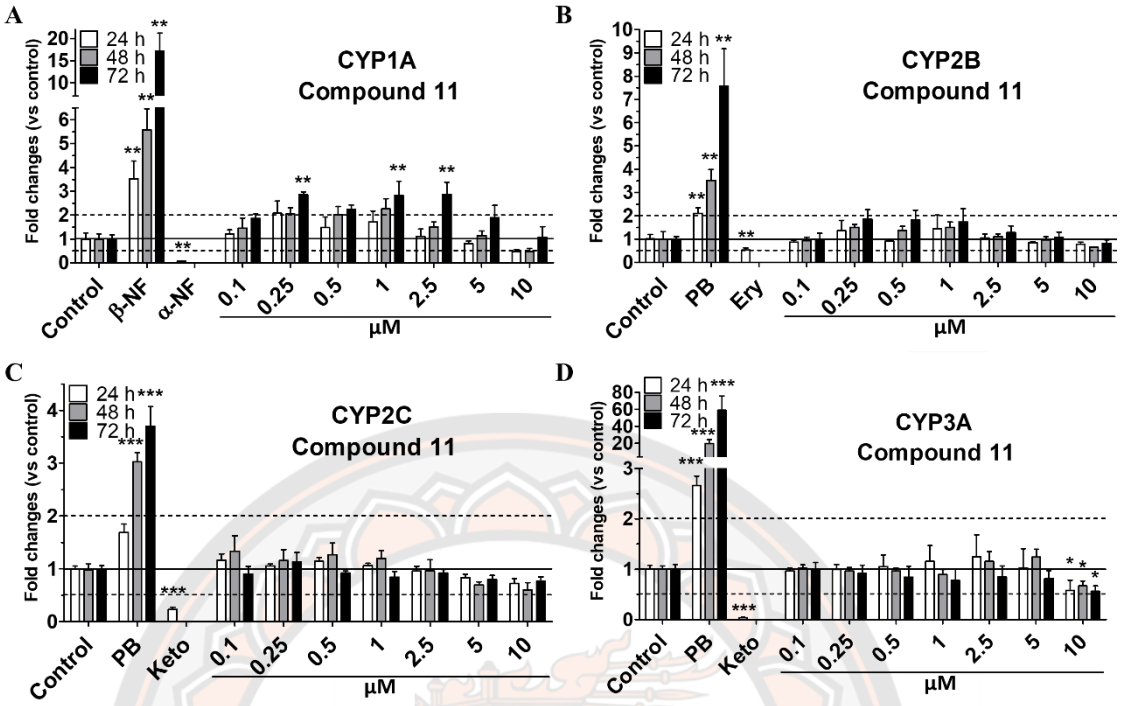

Figure 47 Effects of compound 11 on CYP activity in isolated rat hepatocytes. CYP1A (A), CYP2B (B), CYP2C (C) and CYP3A (D) activities were measured in primary rat hepatocyte cultures after 24 h, 48 h and 72 h of exposure with compound 11 or control (0.1% DMSO). β-NF (50 µM for CYP1A) and PB (1 mM for CYP2B or 2 mM for CYP2C and 3A) were used for 24 h, 48 h and 72 h of treatment as reference CYP inducers. α-NF (10 µM for CYP1A), Ery (10 µM for CYP2B) and Keto (25 µM for CYP2C and 3A) were added for 2 h (α-NF) or 24 h (Ery and Keto) in culture as reference CYP inhibitors. Results are expressed as fold-change *vs* control (0.1% DMSO, set at 1). Statistical analysis was processed only when the fold change was <1 for CYP inhibition and ≥2 for CYP induction. Values were expressed as means±SEM from a triplicate of 3 independent cultures. $^{*}p<0.05$, $^{**}p<0.01$, $^{***}p<0.001$ *vs* control (0.1% DMSO) for each time of culture.

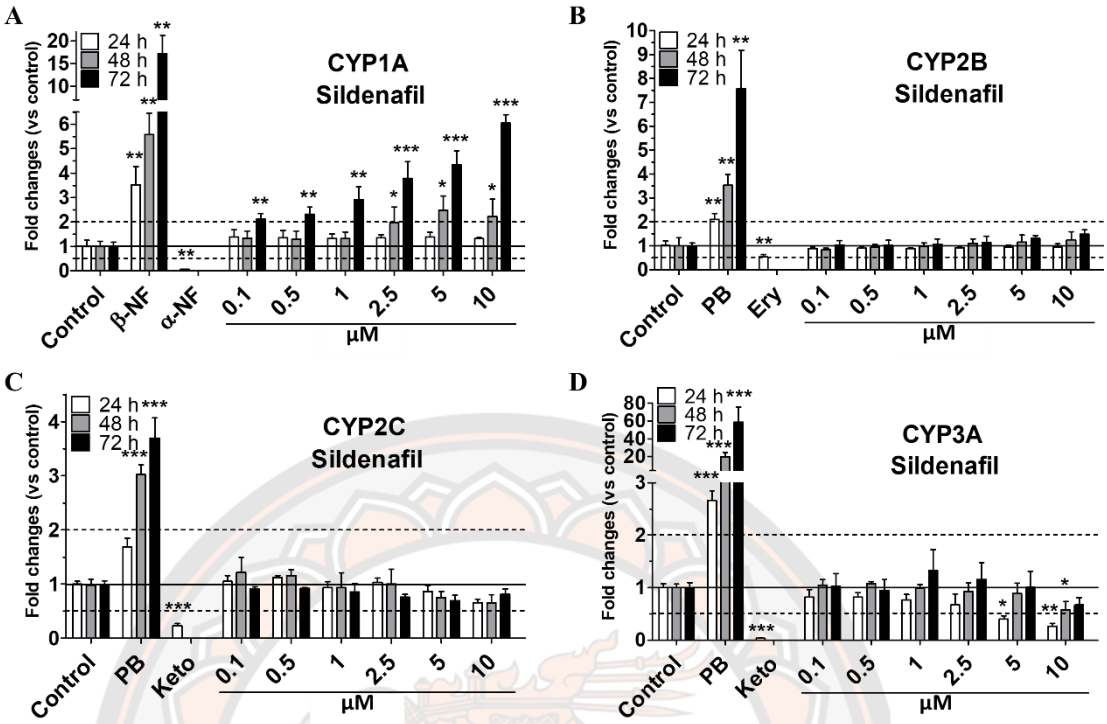

Figure 48 Effects of sildenafil on CYP activity in isolated rat hepatocytes. CYP1A (A), CYP2B (B), CYP2C (C) and CYP3A (D) activities were measured in primary rat hepatocyte cultures after 24 h, 48 h and 72 h of exposure with sildenafil or control (0.1% DMSO). β-NF (50 μM for CYP1A) and PB (1 mM for CYP2B or 2 mM for CYP2C and 3A) were used for 24 h, 48 h and 72 h of treatment as reference CYP inducers. α-NF (10 μM for CYP1A), Ery (10 μM for CYP2B) and Keto (25 μM for CYP2C and 3A) were added for 2 h (α-NF) or 24 h (Ery and Keto) in culture as reference CYP inhibitors. Results are expressed as fold-change *vs* control (0.1% DMSO, set at 1). Statistical analysis was processed only when the fold change was <1 for CYP inhibition and ≥2 for CYP induction. Values were expressed as means±SEM from a triplicate of 3 independent cultures. $^{*}p<0.05$, $^{**}p<0.01$, $^{***}p<0.001$ *vs* control (0.1% DMSO) for each time of culture.

Discussion of study I

The present study has provided new pharmacological and development information on a series of quinazoline-based PDE5 inhibitors. It was found that (*i*) two quinazolines compounds, compounds **5** and **11**, had *in vitro* inhibitory properties on human PDE5 and potent vasorelaxant effect on isolated rat pulmonary arteries, (*ii*) their effect relied on both endothelium-dependent and endothelium-independent mechanisms, (*iii*) they had greater selectivity for pulmonary *vs* systemic circulation than sildenafil, (*iv*) they exhibited weak VSMC and hepatocyte toxicity as well as a weak inhibitory effect on CYP3A ($>10^{-5}$ M).

Pulmonary vasculature regulation via the sGC/cGMP pathway is a critical target for PAH treatment. Degradation of cGMP in the pulmonary VSMCs is primarily regulated by PDE5, and the inhibition of this enzyme leads to an increase in cGMP and vasorelaxation, thus alleviating PAH. The present study evaluated six quinazoline derivatives (N^2,N^4-disubstituted quinazoline 2,4-diamines) which exhibited human PDE5 inhibitory activity. Among them, compounds **5** and **11** had the greatest *in vitro* potency, comparable to that of the drug, sildenafil. The results indicated that 3-sulphonamide (–3-SO_2NH_2) in the compounds **5** and **11** is important for this activity, while the effect of thiophene substitution by a phenyl ring at the R^1 has a smaller, but more favorable, impact on the activity. This configuration appears to maximize the H-bond interactions as well as pi-stacking interactions within the PDE5 active site, as observed for other quinazoline derivatives (Pobsuk et al., 2019).

Consistent with their effects on PDE5 and the role of PDE5 in pulmonary vasculature, compounds **5** and **11** were also the most efficient to induce vasodilation in isolated PA. As a confirmation that their vasorelaxant effects were indeed secondary to PDE5 inhibition, our data showed that they enhanced the vasorelaxant effect of a NO-donor (SNP) on endothelium-denuded PA rings, indicating that cGMP levels in VSMCs have been increased by the 2 quinazolines. Of interest, the selective sGC inhibitor ODQ was able to reduce the vasorelaxant effect of compounds **5** and **11** in endothelium-denuded arteries, thus indicating that direct activation of sGC is also involved. The present study did not identify whether the compounds act as GC stimulators (as Riociguat) requiring heme-containing sGC or as sGC activators (as cinaciguat) activating heme-free sGC. However, this dual action on the sGC/cGMP

pathway is of particular interest as both expressions of PDE5 and sGC are upregulated in PAH (Schermuly et al., 2008). Growing evidence indicates that endothelial dysfunction of the PA is a pivotal mechanism involved in the pathogenesis of PAH. Endothelial dysfunction results in increased vascular resistance through an imbalance between the production of contracting and relaxing factors but also in the uncontrolled proliferation of endothelial cells and smooth muscle cells, fibroblasts, thus leading to vascular remodeling in PAH (Kurakula et al., 2021). The present study demonstrated that the removal of the endothelium significantly impaired the relaxant effect of compounds **5** and **11**. By using selective inhibitors of the main endothelium pathways, we demonstrated that these quinazolines potentiate the NO-cGMP pathways. Combined with their effect on the sGC/cGMP pathway in VSMCs, this indicates that these compounds can enhance the entire NO/sGC/cGMP pathway in PA, similarly to sildenafil.

Hypoxia was reported to selectively inhibit the function and expression of voltage-gated K^+ (K_V) channels in PASMCs, thus contributing to the development of PAH (Le Ribeuz et al., 2020; Mandegar & Yuan, 2002). Here, we tested how these channels are involved in the response to compounds **5** or **11**. Our findings indicate that neither of the tested compounds exhibited significant effects on K_V, K_{ATP}, or K_{Ca} channels in endothelium-denuded PA rings. Thus, we investigated whether the 2 quinazolines may hamper intracellular or extracellular Ca^{2+} fluxes in the VSMC. Indeed in PAH, hypoxia upregulates transient receptor potential channels leading to enhanced Ca^{2+} entry through receptor-operated and store-operated Ca^{2+} channels thereby inducing pulmonary vasoconstriction (Murray et al., 2006). Our data indicated that the vasorelaxant effect compounds **5** and **11** did not involve the inhibition of α_1-adrenergic receptors, whereas they inhibited intracellular Ca^{2+} release from the SR as well as extracellular Ca^{2+} influx via ROCC. We found the same results as the effect of sildenafil on K^+ channels, α_1-adrenergic receptors and Ca^{2+} homeostasis. Although the lack of the VOCC inhibitory effect of sildenafil was reported in isolated rabbit PA (Toque et al., 2008), the present study provided new information that it inhibited ROCC and Ca^{2+} release and a mechanistic study was also conducted on the MA, to determine if the mechanisms of vasorelaxation of compounds **5** and **11** differ according to the vascular beds. The mechanisms involved in the effect of compounds **5** and **11** are similar in both the MA and PA regarding

endothelium-dependent mechanisms, potentiation of SNP, and effects on Ca^{2+} fluxes but differ as regards K^+ channels and sGC activation. Indeed, iberiotoxin reduced the relaxant effect of compounds **5** and **11** whereas the sGC inhibitor did not change the relaxant effect of the compounds in the MA. In an isolated tissue bath, the rings were incubated with the compounds for approximately 1 hr, thus cell viability was tested. To test the cytotoxicity of the quinazoline derivatives on VSMCs, incubation of the freshly isolated rat aorta and PASMCs, with either quinazolines derivatives or sildenafil, for 1hr, did not affect %cell viability of either VSMCs, except for the highest concentration of sildenafil (100 µM) that reduced %cell viability of the PASMCs. In addition, the viability of the rings was tested for their vasoconstriction effects in a high K^+ solution at the end of the experiment. The rings still showed contraction which indicated that the VSMCs remained functional. These data support the direct vasorelaxant effect on the vessels caused by the action of the compounds. Toxicity was not a relevant factor in these actions.

The successful development of a series of quinazoline derivatives is dependent on having negligible on or off-target toxicity. Side effects, rather than unsatisfactory pharmacological efficacy, have been estimated to be responsible for the attrition of approximately one-third of drug candidates and are a major contributor to the high cost of drug development, particularly when not recognized until late in clinical trials or post-marketing (Guengerich, 2011). This has led to the evaluation of toxicity and side effects of new drug candidates necessarily being done in parallel with the optimization of their efficacy at early discovery phases. In the present study, the toxicity of compounds **5** and **11** were evaluated in cultured rat hepatocytes. Our results showed that incubation of rat hepatocytes with compounds **5** and **11** at concentrations greater than 10^{-5} M reduced cell viability in a concentration-dependent and time-dependent manner, whereas toxicity of sildenafil was not observed. However, IC_{50} of compounds **5** and **11** on hepatocytes for 72 hr was ~18 µM whereas their EC_{50} for PA vasodilation was ~1 µM. This indicates that it is unlikely that such hepatotoxicity may occur at pharmacological concentrations. Further studies are needed to better characterize these effects on the liver. In PAH treatments, PDE5 inhibitors are often used in combination with the endothelin-1 antagonists (e.g. bosentan), which are strongly metabolized by CYP3A4 and 2C9 (Srinivas, 2016).

Therefore, we also investigated the drug-drug interaction potential of compounds **5** and **11**. Our results showed that the main effect on CYP was a weak CYP3A inhibition for both compounds, and a weak CYP2C inhibition for compound **5** only. These effects on liver toxicity are only evident for concentrations ~10^{-5} M, so it is unlikely that they would be observed at pharmacological doses. Our study revealed that both quinazoline compounds exhibited a greater inhibitory effect on CYP3A than sildenafil, which was previously shown to have a weak inhibitory effect (Sheweita et al., 2016). Additionally, **5** and **11** did not increase CYP1A activity in a concentration- and time-dependent manner, in contrast to sildenafil. These findings suggest that the quinazoline compounds have the potential for further development.

The most common adverse drug reactions of marketed PDE5 inhibitors include headache, flushing, nasal congestion, nasopharyngitis (linked to a systemic vasodilatory effect), and dyspepsia. Visual disturbances have been reported with PDE5 inhibitors, due to their lack of PDE5 selectivity and their capacity to inhibit retinal PDE6 (Huang & Lie, 2013). Previous data on rat PDE5 and PDE6 showed that compounds **5** and **11** were ~4.6 times more selective for PDE5, which is similar to sildenafil (~6.5 times) (Pobsuk et al., 2019). However, the results obtained in the current study show that the selectivity of compounds **5** and **11** for the PA *vs* the aorta was about 3-times greater than sildenafil suggesting that these compounds are more selective for pulmonary circulation than for systemic circulation than sildenafil.

In conclusion, this study identified 2 quinazoline derivatives with potent human PDE5 inhibitory activity and vasorelaxant effects on the rat pulmonary artery. Despite a lower activity on PDE5 than sildenafil, they have a greater selectivity for pulmonary artery *vs* systemic vasculature. Their vasorelaxant effects involved not only PDE5 inhibition but also other relevant mechanisms in the context of PAH: including direct activation of sGC, blockade of Ca^{2+} channels and activation of NO-dependent endothelial function. Further studies are needed to confirm these positive effects *in vivo*, in animal model of PAH. This work demonstrates the pharmacological effects of this series of quinazolines and give us confidence in their overall developability, particularly when related to liver toxicity, CYP inhibition, and induction effects. This has spurred further efforts to develop additional analogs with a view to improving their PDE5 selectivity and maximizing their vasorelaxant effects.

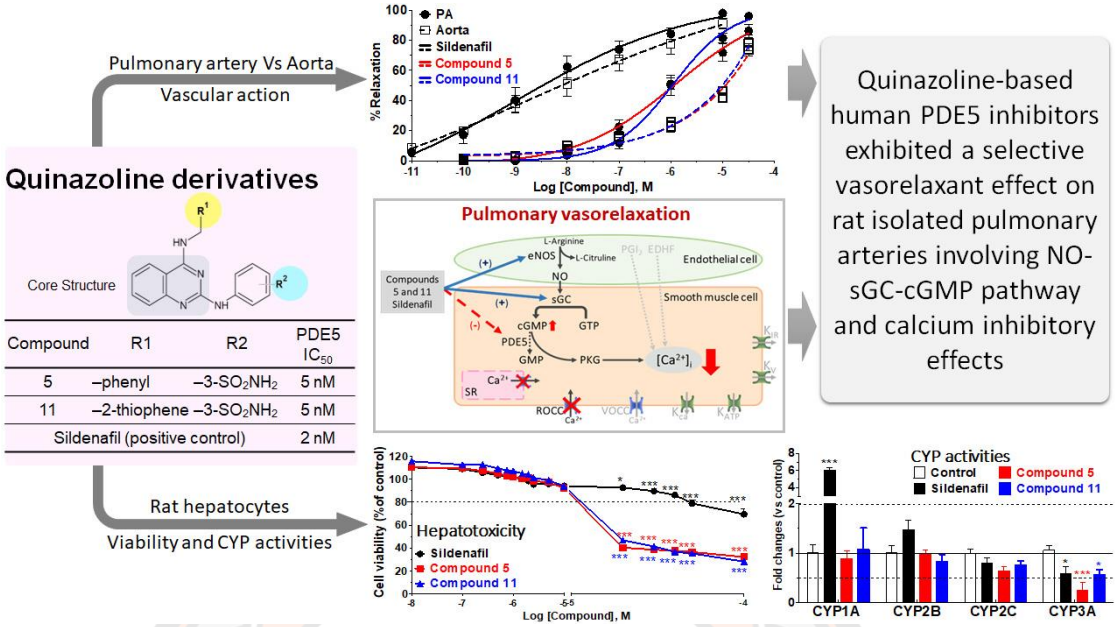

Figure 49 Summary of the mechanisms of action of compounds 5 and 11 compared with sildenafil

STUDY II: **Effects of compound 8 on isolated MA and mechanisms involved, blood pressure, cytotoxicity, and CYP activities in comparison to nifedipine**

Results of study II

As depicted in Figure 36, the comparison of the vasorelaxant effect of six quinazoline derivatives on the PA versus the aorta revealed that only compound **8** displayed better aortic selectivity than PA. This observation led us to investigate its impact on systemic vasculature, using nifedipine as a comparator.

1. Vasorelaxant compound 8 and its underlying mechanism

1.1 Compound 8 induced a robust endothelium-independent vasorelaxant effect.

As presented in Figure 50 and Table 10, compound **8** induced a potent vasodilator effect on MA (EC_{50}=0.56±0.17 µM, E_{max}=98.8±0.5%). This effect was not significantly different in the denuded MA rings (E–, EC_{50}=0.64±0.12 µM, E_{max}=99.2±0.2%, Figure 50A) and was equivalent to that of nifedipine (EC_{50}=0.41±0.09 µM, E_{max}=98.7±0.4%, Figure 50B). The solvent used, DMSO at a final concentration of 0.13% had no effect (Figure 50A, Table 10). Thus, the mechanisms involved in the relaxant effect of compound **8** are endothelium-independent.

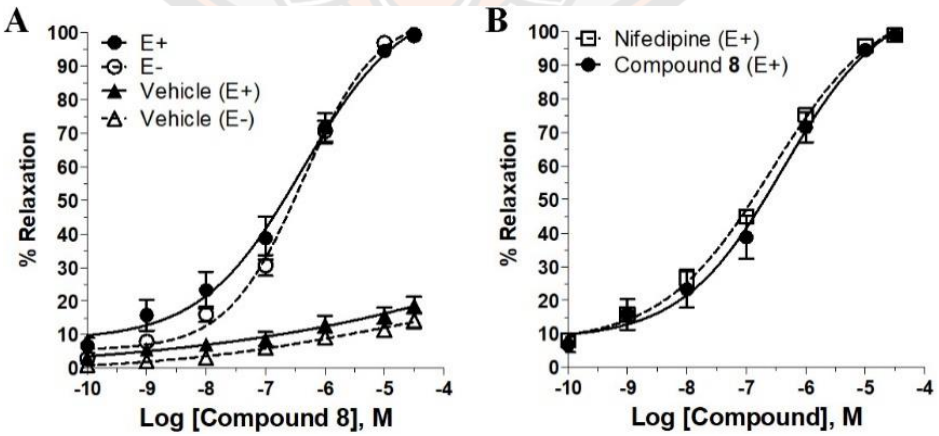

Figure 50 Vasorelaxant effect of compound 8 and nifedipine on rat MA. (A) Concentration-response curves of compound 8 or the vehicle in the

MA with (E+) or without (E–) endothelium precontracted with 10^{-5} M PE. (B) Comparison of the vasorelaxant effect of compound 8 and nifedipine in MA (E+). Values were expressed as means±SEM (*n* = 6-12 rats).

Table 10 EC_{50} and E_{max} values of compound 8 induced relaxation in endothelium-intact (E+) and -denuded (E–) MA rings in the absence or presence of various inhibitors

	EC_{50} (μM)	E_{max} (%)	*n*
Endothelium-intact arteries (E+)			
Compound **8**	0.56±0.17	98.8 ± 0.5	8
Nifedipine	0.41±0.09	98.7 ± 0.4	6
Vehicle	-	18.9 ± 2.4	6
Endothelium-denuded arteries (E–)			
Compound **8**	0.64±0.12	99.2 ± 0.2	12
+ 4-AP	0.35±0.19	99.3 ± 0.4	7
+ Glibenclamide	1.30±0.42	99.1 ± 0.4	7
+ Iberiotoxin	6.05±2.27**	99.1 ± 0.2	7
+ ODQ	4.79±1.48**	97.4 ± 1.1*	6
Vehicle	-	14.1 ± 2.2	7

The values are the means±SEM of the number *n* of rats. EC_{50} is the concentration of the compound giving half-maximal relaxation. E_{max} is the maximum response of MA expressed as a relaxation percentage of the contraction induced by PE. *$p<0.05$, **$p<0.01$ *vs* compound **8**.

1.2 The relaxant effect of compound 8 relied on activation of K_{Ca} channel and ROCC inhibition.

To study the mechanisms involved, endothelium-denuded MA rings were first incubated with various K^+ channels blockers, 4-AP (K_V blocker, 10^{-3} M), glibenclamide (K_{ATP}, 10^{-5} M) or iberiotoxin (K_{Ca}, 10^{-7} M). Among them, only iberiotoxin significantly reduced its relaxant effect as a reflection of the activation of the K_{Ca} channels by compound **8** (Figure 51, Table 10). The contribution of extracellular or intracellular Ca^{2+} fluxes was then evaluated. As compared to the vehicle, compound **8** reduced the contraction elicited by extracellular Ca^{2+} influx in PE-exposed rings (opening of ROCC, Figure 52A) whereas it changed neither the extracellular Ca^{2+} influx in 80 mM high K^+ solution-exposed the rings (opening of VOCC, Figure 52B) nor the intracellular Ca^{2+} release from SR (Figure 52C).

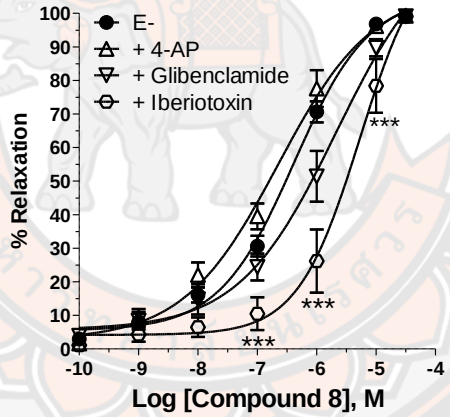

Figure 51 Contribution of K^+ channels to vasorelaxant effects of compound 8 in the MA. Concentration-response curves of compound 8 in endothelium-denuded (E–) MA rings precontracted with PE and pretreated with various K^+ channel inhibitors: 4-AP (K_V blocker), glibenclamide (K_{ATP} blocker) or iberiotoxin (K_{Ca} blocker). Values were expressed as means±SEM (*n* = 6-12 rats). ***$p<0.001$ *vs* E–.

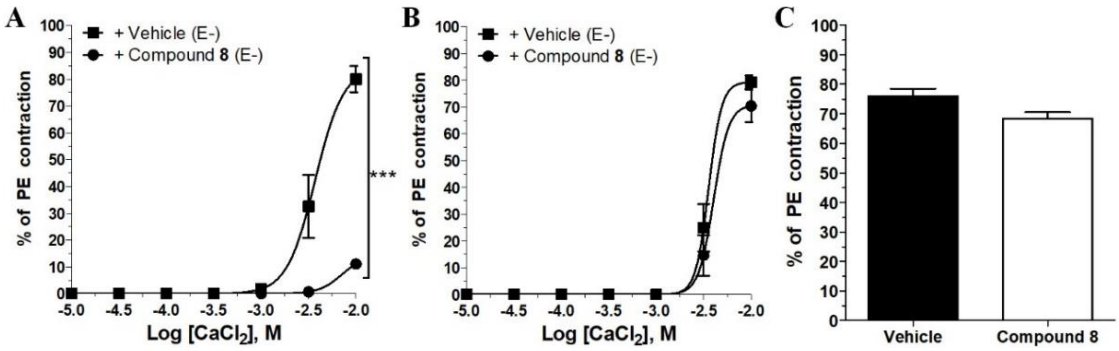

Figure 52 Contribution of Ca^{2+} channels to vasorelaxant effects of compound 8 in MA. Concentration-response curves of $CaCl_2$ after incubation of the rings with compound 8 or the vehicle and exposure to PE (A, ROCC opening) or 80 mM high K^+ solution (B, VOCC opening) in a Ca^{2+}-free Krebs solution. (C) Effect of compound 8 on Ca^{2+} release from SR: after incubation with verapamil (VOCC inhibitor), the rings were exposed to PE to open the Ca^{2+} receptors of SR, in a Ca^{2+}-free solution containing compound 8 or the vehicle. Values were expressed as means±SEM (*n* = 6-7 rats). ***$p<0.001$ *vs* vehicle.

1.3 Effect of compound 8 on sGC/cGMP pathway and α_1-adrenergic receptors

As its chemical structure was inspired by that of the PDE5 inhibitor sildenafil, the possible role of compound **8** as a potentiator of the sGC/cGMP pathway was studied. As shown in Figure 53A, consistent with a PDE5 inhibitory effect, compound **8** slightly but significantly enhanced the relaxant effect of SNP. Consistently, EC_{50} of SNP was reduced by compound **8** incubation (0.008±0.001 µM (compound **8**, n = 7) *vs* EC_{50}=0.0017±0.005 µM (vehicle, n = 9) , $p<0.05$). To determine if a direct activation of the sGC might be also involved, the effect of ODQ (an sGC inhibitor) was studied. Figure 53B and Table 8 show that ODQ markedly decreased the relaxation induced by compound **8**.

Finally, to determine if the blockade of α_1-adrenergic receptors might be involved, the effect of compound **8** on PE-induced contraction was studied. As compared to the vehicle, compound **8** slightly but significantly decreased PE-induced

contraction (Figure 53C). Compound **8** enhanced the EC_{50} of PE (4.3±1.0 µM (compound **8**, n = 6) *vs* 1.9±0.3 µM (vehicle, n = 6, p<0.05) but did not change the E_{max} value (106.6±1.7% (compound **8**) *vs* 107.5±2.7% (vehicle)).

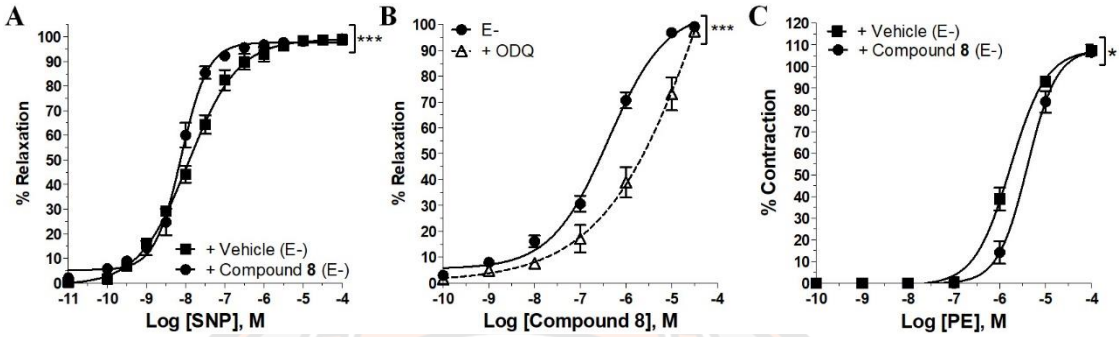

Figure 53 Contribution of sGC/cGMP pathway and α_1-adrenergic receptors to vasorelaxant effects of compound 8 in MA. (A) Concentration-response curves of SNP (NO donor) after incubation with compound 8 or the vehicle. (B) Concentration-response curves of compound 8 after incubation with ODQ. (C) Concentration-response curves for PE-induced contraction after incubation with compound 8 or the vehicle. Values are means±SEM (n = 5–12 rats). *p<0.05 ***p<0.001 *vs* E– or the vehicle.

2. Acute effect of compound 8 and nifedipine on blood pressure

Figure 54 and Table 11 presents the effects of intravenous injection of the vehicle, compound **8** and nifedipine on blood pressure and HR. The values for the baseline (before infusion) were: SBP=139±9 mmHg, DBP=103±8mmHg, MAP=115±9 mmHg, HR=439±18 beats per minute (BPM). After infusion of the vehicle (5% DMSO), the values were SBP= 132±10 mmHg, DBP=97±9 mmHg, MAP=108±9 mmHg, HR=430±20 BPM (not significant *vs* the baseline). As compared to the vehicle, infusion of compound **8** or nifedipine at doses of 0.05 and 0.1 mg/kg resulted in a larger and significant dose-dependent reduction in SBP, DBP and MAP (Figure 54A-C). Conversely, HR was unchanged whatever the dose of compound **8** or nifedipine (Figure 54D). The effect of compound **8** was lower than

that of nifedipine for the effect on SBP (Figure 54A) but not different for the effect on DBP, MAP and HR (Figure 54B-D).

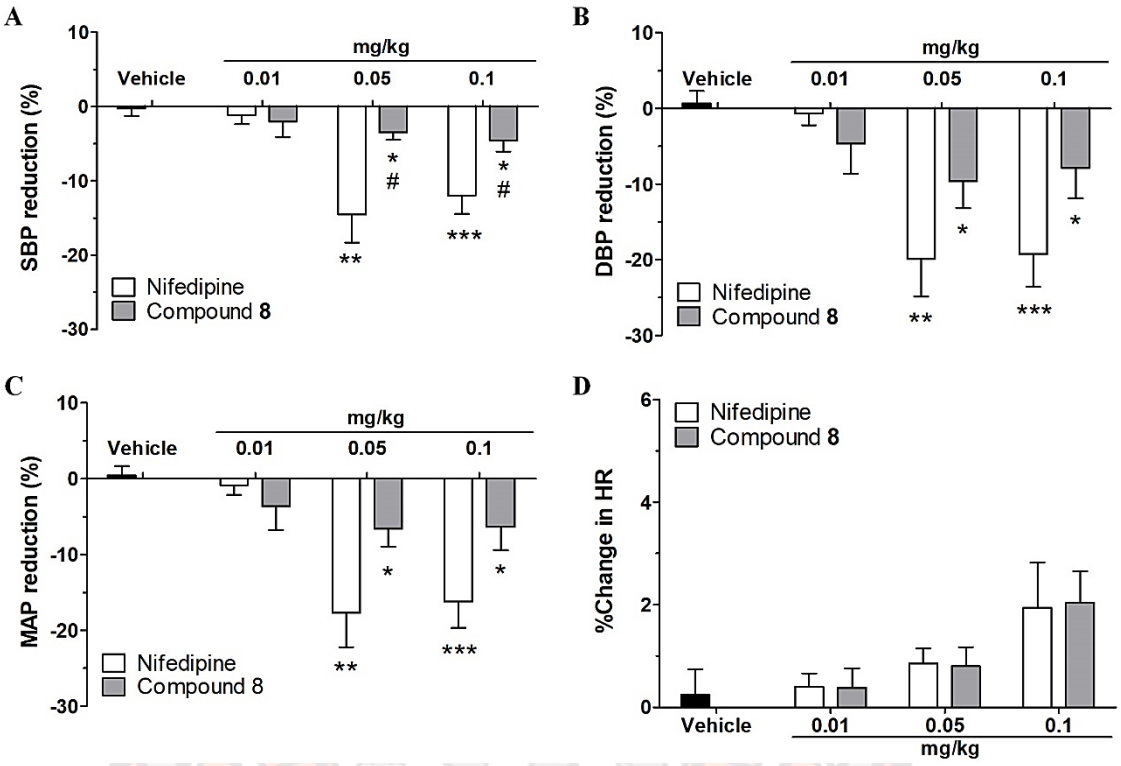

Figure 54 Acute effect of compound 8 and nifedipine on blood pressure in anesthetized rats. The bars show the percentage reduction in (A) SBP, (B) DBP, (C) MAP and (D) the percentage change in HR, calculated from the values measured at the peak effect after intravenous infusion of the vehicle (5% DMSO), compound 8 or nifedipine (0.01, 0.05 and 0.1mg/kg BW), as compared to the baseline value before each infusion. Values were expressed as means±SEM (n = 5 rats per group). ⁎p<0.05, ⁎⁎p<0.01, ⁎⁎⁎p<0.001 vs the vehicle. #p<0.05 vs nifedipine at the same dose.

Table 11 Acute effect of compound 8 and nifedipine on blood pressure in anesthetized rats.

Groups	SBP (mmHg)	DBP (mmHg)	MAP (mmHg)	HR (bpm)	% change from baseline at each dose				
					SBP (%)	DBP (%)	MAP (%)	HR (%)	*n*
Baseline (first)	139±9	103±8	115±9	439±18					8
Vehicle (5% DMSO)	132±10	97±9	108±9	430±20	-0.6±0.9	0.7±1.5	0.3±1.1	0.3±0.5	8
Nifedipine									
Baseline	112±11	80±11	90±11	415±17					5
0.01 mg/kg	110±11	79±10	89±10	415±16	-1.4±1.06	-0.7±1.31	-0.8±1.1	0.4±0.2	5
Baseline	119±10	87±10	97±10	432±14					5
0.05 mg/kg	102±9	69±8	80±8	434±15	-14.5±3.4**	-19.9±4.4**	-17.7±4.0**	0.9±0.3	5
Baseline	111±9	81±9	91±9	434±14					5
0.1 mg/kg	97±6	64±5	75±5	442±14	-12.0±2.2***	-19.2±3.9***	-16.2±3.1***	1.9±0.8	5
Compound **8**									
Baseline	145±10	100±10	115±10	454±24					5
0.01 mg/kg	141±9	94±7	110±7	456±26	-2.0±1.86	-4.7±3.5	-3.6±2.83	0.4±0.3	5
Baseline	145±8	95±7	112±7	437±23					5
0.05 mg/kg	141±7	85±6	104±6	441±24	-2.6±1.2$^{*, \#}$	-9.6±3.2*	-6.6±2.09*	0.8±0.3	5
Baseline	146±7	94±7	112±7	412±25					5
0.1 mg/kg	140±5	87±7	104±6	420±24	-4.5±1.6$^{*, \#}$	-7.9±3.6*	-6.4±2.73*	2.0±0.6	5

The systolic blood pressure (SBP), diastolic blood pressure (DBP), mean arterial blood pressure (MAP), and heart rate (HR) were measured during the peak effect of single intravenous injections of vehicle, nifedipine, and compound **8** at the doses indicated. bpm: beats per minute, *i.v.*: intravenous infusion. All data are expressed as means±SEM of *n* animals. $^{*}p<0.05$, $^{**}p<0.01$, $^{***}p<0.001$*vs* vehicle. $^{\#}p<0.05$ *vs* nifedipine at the same dose.

3. Cytotoxicity of compounds 8 and nifedipine on cultured hepatocytes

Rat hepatocytes in the primary cultures were exposed to compounds **8**, nifedipine and the vehicle (0.1% DMSO) for 24 h, 48 h and 72 h before the MTT assay. As shown in Figure 55A-B, viability remained >80% with compound **8** at concentrations up to 10^{-5} M. At higher concentrations (10^{-5} to 10^{-4} M), compound **8** led to a time- and concentration-dependent decrease in cell viability. IC_{50} values for compound **8** at 24 h, 48 h and 72 h of exposure were (µM) 56±2, 28±4 and 19±2, respectively. Nifedipine was less toxic with viability >80% whatever the time or concentration, except that the concentration of 10^{-4} M at 72 h of exposure reduced cell viability to 65%.

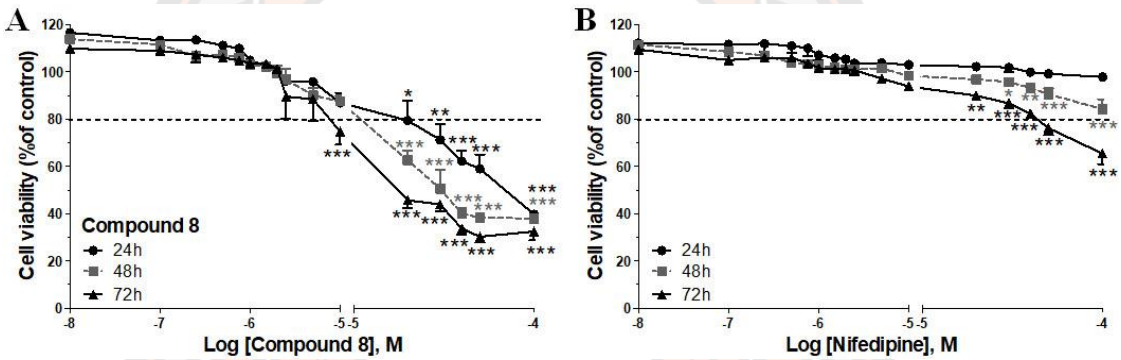

Figure 55 Effects of compound 8 and nifedipine on cell viability in the primary rat hepatocyte cultures. Cell viability was studied in the rat hepatocyte cultures after 24 h (●), 48 h (■) or 72 h (▲) exposure with compound 8 (A), nifedipine (B), or the control (0.1% DMSO) and expressed as the percentage of the control (0.1% DMSO). Values were expressed as means±SEM from a triplicate of 3 independent cultures. $^{*}p<0.05$, $^{**}p<0.01$, $^{***}p<0.001$ *vs* cell viability of control (0.1% DMSO) for each time of culture.

4. Effects of compounds 8 and nifedipine on CYP activities in isolated hepatocytes

CYP1A, 2B, 2C and 3A activities were measured in rat hepatocytes after 24 h, 48 h and 72 h of exposure with compound **8**, nifedipine, control (0.1% DMSO), reference inducers or reference inhibitors. Non-cytotoxic concentrations of compound **8** and nifedipine (0.1 to 10 μM) were chosen.

As shown in Figure 56A-B, BNF was used as a reference inducer for CYP1A activity and PB for CYP2B, 2C and 3A activities, whereas α-NF was used as a reference inhibitor for CYP1A activity, Ery for CYP2B activity, and Keto for CYP2C and 3A activities. As expected, BNF caused a significant induction (4-, 6- and 17-fold increases at 24 h, 48 h and 72 h, respectively) of CYP1A activity, while PB significantly increased CYP2B (2-, 4- and 8-fold increases at 24 h, 48 h and 72 h, respectively), CYP2C (2-, 3- and 4-fold increases at 24 h, 48 h and 72 h, respectively) and CYP3A activities (3-, 20- and 59-fold increases at 24 h, 48 h and 72 h, respectively), whereas α-NF Ery or Keto had the opposite effect.

Compound **8** (Figure 56A) did not change CYP2B and 2C activities but inhibited CYP1A and 3A activities only at the highest concentrations (10 μM). Nifedipine (Figure 56B) strongly increased CYP1A, 2B, and 3A activity in a concentration-dependent manner after 72 h of the treatment, which increased the activity up to 6-fold for CYP1A, 4-fold for CYP2B, and 12-fold for CYP3A. For CYP2C activity, nifedipine increased activity up to 3-fold only at the highest concentrations (10 μM) after 72 h of treatment.

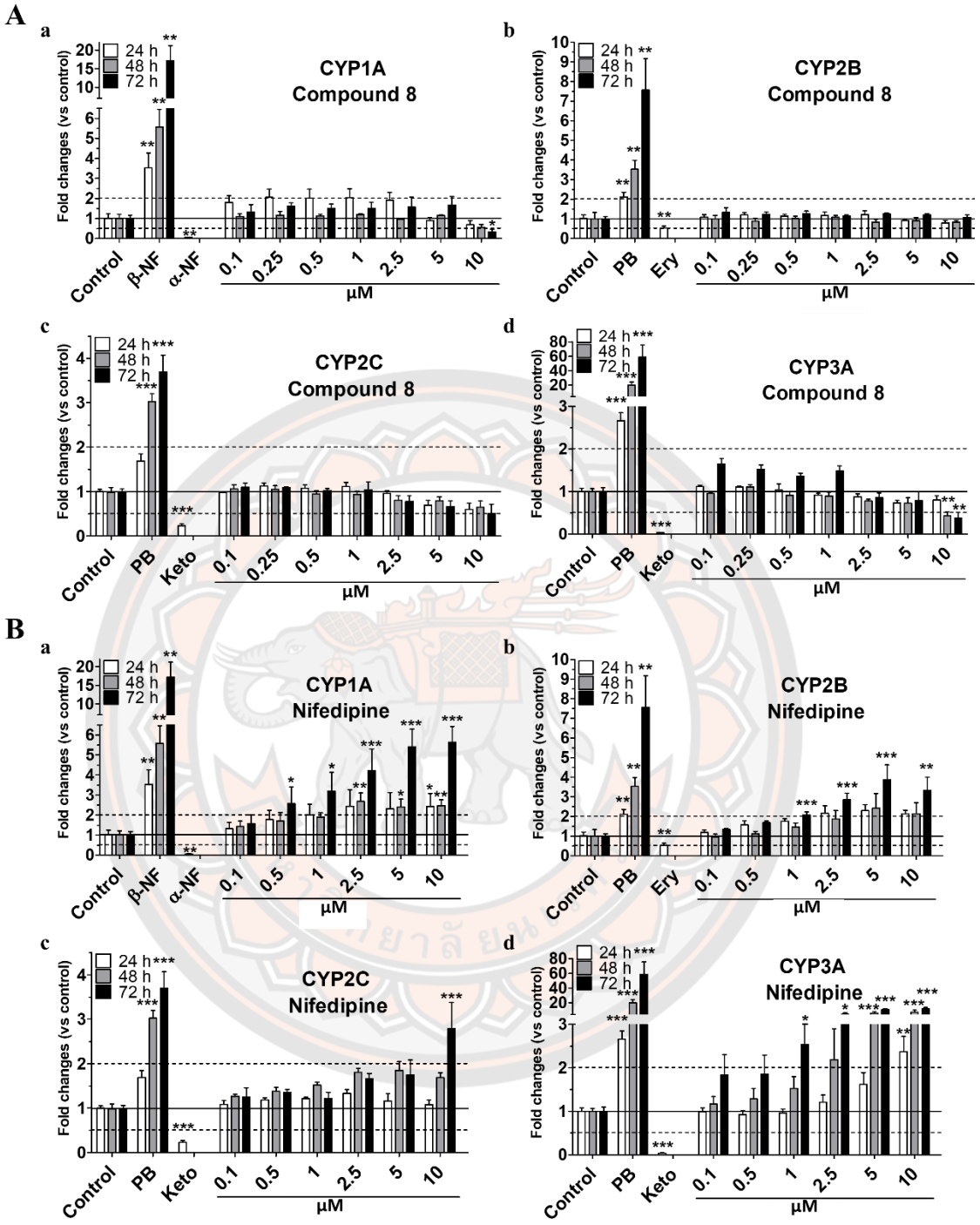

Figure 56 Effects of compounds 8 and nifedipine on CYP activity in isolated rat hepatocytes. CYP1A (a), CYP2B (b), CYP2C (c) and CYP3A (d) activities were measured in primary rat hepatocyte cultures after 24 h, 48 h and 72 h of exposure with compound 8 (A) and nifedipine (B) or control (0.1% DMSO). β-NF (50 μM for CYP1A) and PB (1 mM for CYP2B or 2 mM for CYP2C and 3A) were used for 24 h, 48 h and

72 h of treatment as reference CYP inducers. α-NF (10 µM for CYP1A), Ery (10 µM for CYP2B) and Keto (25 µM for CYP2C and 3A) were added for 2 h (α-NF) or 24 h (Ery and Keto) in a culture as reference CYP inhibitors. Results are expressed as fold-change *vs* control (0.1% DMSO, set at 1). Statistical analysis was done only when the fold change was <1 for CYP inhibition and ≥2 for CYP induction. Values were expressed as means±SEM from a triplicate of 3 independent cultures. $^{*}p<0.05$, $^{**}p<0.01$, $^{***}p<0.001$ *vs* control (0.1% DMSO) for each time of culture.

Discussion of study II

The major findings of this study are that compound **8** (N^2-methyl-N^4-[(thiophen-2-yl)methyl]quinazoline-2,4-diamine) induced a vasorelaxant effect on resistance vessels through endothelium-independent mechanisms, that translated into an *in vivo* acute hypotensive effect in rats. These favorable pharmacological effects were associated with low liver hepatocyte toxicity as well as a low effect on CYP activities.

In the cardiovascular system, vascular function and blood pressure are controlled by the tone of smooth muscle surrounding the small arteries and arterioles (Jackson, 2000). The regulation of the VSMCs is dependent on a complex interplay of vasodilation and vasoconstriction factors by neurotransmitters, circulating hormones, and endothelium-derived factors (Jackson, 2000; Nava & Llorens, 2019). The present study, conducted *ex vivo* on isolated MA, a model of resistance vessels (Li et al., 2005), demonstrated that compound **8** induced a strong vasorelaxant effect as its effect was equivalent to that of nifedipine, a calcium entry-blocking agent that lowers blood pressure by relaxing arterial and arteriolar smooth muscle (Robinson, 1985). Like nifedipine, the vasorelaxant effect of compound **8** was independent of the presence of endothelium. The results obtained *in vivo* demonstrated that compound **8** had a direct effect on arteries without obvious cardiac effects. Indeed, intravenous infusion of compound **8** reduced blood pressure but did not reduce heart rate. On the contrary, a small increase in heart rate was observed likely as a reflection of decreased

baroreflex activation secondary to the hypotensive effect. The acute hypotensive effect of compound **8** on MAP was not different from nifedipine. This result encourages initiating future studies on animal models of hypertension to determine if compound **8** could exert relevant anti-hypertensive properties.

Mechanistically, ion channels (Ca^{2+} and K^+ channels) on plasma membrane of VSMCs play a central role by determining cytosolic Ca^{2+} concentration and the sensitivity of contractile machinery to Ca^{2+} (Ghosh et al., 2017; Jackson, 2000). Ca^{2+} is a critical factor in the excitation-contraction coupling in VSMCs. The influx of extracellular Ca^{2+} through transmembrane Ca^{2+} channels (VOCC and ROCC) and the release of Ca^{2+} from SR by activation of IP_3 and ryanodine receptors results in increased intracellular Ca^{2+}, which causes VSMC contraction (Ghosh et al., 2017). To assess whether compound **8** modified the extracellular Ca^{2+} influx and intracellular Ca^{2+} release, experiments were conducted on endothelium-denuded MA rings incubated with compound **8** at its EC_{50} (0.6 µM). Our data revealed that compound **8** only inhibited ROCC without any significant effect on VOCC or on intracellular Ca^{2+} release. Regarding K^+, four different types of K^+ channels are expressed in VSMCs, including K_v, K_{ATP}, K_{Ca}, and inward-rectifier K^+ channels (Beleznai et al., 2011; Cheng et al., 2019), but K_v and K_{Ca} are extensively expressed in mesenteric arteries (Beleznai et al., 2011; Walker et al., 2001). Direct activation of K^+ channels hyperpolarizes cell membrane leading to inhibition of Ca^{2+} influx through L-type Ca^{2+} channels and resulting in smooth muscle relaxation (Beleznai et al., 2011; Cheng et al., 2019). In our experiments, only iberiotoxin was able to reduce the relaxant effect of compound **8**, thus demonstrating that an activation of K_{Ca} is involved in its effect. Of note, as cGMP, through the activation of protein kinases G (PKG), is capable of activating K_{Ca} (Archer et al., 1994), an unresolved point is if compound **8** has a direct activating effect on the K_{Ca} channel, or an indirect effect through the increase in cGMP production. Compound **8** were originally identified from a series of quinazolines which demonstrated an inhibitory effect on PDE5 (Chatturong et al., 2022; Paracha et al., 2019). Rat resistance arteries express four major types of PDE, including PDE5 and PDE1, which hydrolyze cGMP; PDE4, which hydrolyzes cAMP; and PDE3, which mainly hydrolyzes cAMP but also cGMP (Komas et al., 1991; Sampson et al., 2001). Physiologically, endothelium-derived NO activates sGC in

VSMC, resulting in cGMP production. The increase in intracellular cGMP concentration activates cGMP-dependent protein kinase, which causes vasorelaxation via the modulation of Ca^{2+} channels as well as by decreasing the Ca^{2+} sensitivity of the vascular smooth muscle contractile proteins (Manuel Morgado et al., 2012). Then intracellular cGMP is rapidly inactivated to GMP by the activity of PDEs. Therefore, cGMP concentration in VSMCs is mainly dependent on the balance between its production by sGC and its breakdown by PDE (Francis et al., 2010; Maurice et al., 2014; M. Morgado et al., 2012; Rybalkin et al., 2003). In favor of the contribution of PDE inhibition to the relaxant effect of compound **8**, our results showed that it enhanced SNP (an activator of sGC)-induced vasorelaxation on endothelium-denuded MA rings. However, compound **8** has a dual effect on the sGC-PDE pathway as our data also indicated that it acts as a direct activator of sGC. Finally, as many quinazolines with anti-hypertensive properties act through an α_1-antagonist effect (Eguchi et al., 1991; El-Sabbagh et al., 2010), this mechanism was evaluated. Indeed, compound **8** shares a scaffold with classic α_1-adrenergic receptor binders such as prazosin, an α_1-adrenergic blocker. Both molecules contain a 2,4-diamino quinazoline scaffold, albeit, with prazosin being substituted at only the 2 positions. The results showed that compound **8** slightly but significantly lowered PE-induced contraction with no effect on the E_{max}. This result might reflect either a direct competitive antagonistic effect of compound **8** on α_1-adrenergic receptor and/or might be the consequence of the inhibitory effect of compound **8** on ROCC as PE-induced contraction involves the opening of these channels (Rinaldi et al., 1991). Further studies of radioligand binding assays at the α_1-adrenergic receptor would be required to ascertain that compound **8** has indeed an affinity for this receptor.

Evaluation of toxicity and side effects of new drug candidate must be done in parallel with optimization of their efficacy at early discovery phases. In the present study, both liver toxicity and the potential of drug-drug interactions through CYP activity changes were assessed in isolated rat hepatocytes. This is of particular importance given that many anti-hypertensive drugs or drugs used for reducing cardiovascular risk, such as statins (Vaughan & Gotto, 2004), are strongly metabolized by CYP (Zisaki et al., 2015). Regarding toxicity, a reduction of hepatocytes viability was observed with compound **8** only for concentrations >10 µM.

As IC_{50} on hepatocytes after 72h of exposure was ~19 µM and EC_{50} for the vasorelaxant effect on MA was 0.56 µM, it is unlikely that such hepatotoxicity may occur at pharmacological concentrations. Likewise, compound **8** did not change CYP activities for concentrations ranging from 0.1 to 5 µM. A weak inhibition of CYP1A and CYP3A activities was observed only at 10 µM, so again, it is unlikely that this effect would be observed at pharmacological doses.

Of note, the weak inhibitory activity of compound **8** against CYP1A and CYP3A activities can be rationalized from a consideration of its molecular properties. While CYP3A4 has a substrate preference for neutral, medium to high molecular weight molecules, the CYP1A2 isoform demonstrates a preference for lower molecular weight, neutral molecules from a systematic analysis of 10,000s of drug-like molecules (Gleeson, 2008). The almost 2-fold decreased activity observed for the CYP1A isoform in the presence of compound **8**, due to its inhibitory effect, is not unexpected given its physico-chemical properties (medium sized, neutral, aromatic molecule). Burton et al. (2006) found that the presence of aromaticity features was key to discriminating inhibitors from non-inhibitors of CYP1A2. Moreover, Shimada and Guengerich (2006) demonstrated that even large polycyclic aromatic hydrocarbons can have significant inhibitory activity at CYP1A isoforms.

In conclusion, this study identified a N^2-methyl-N^4-[(thiophen-2-yl) methyl]quinazoline-2,4-diamine**)** with a potent vasodilator effect on the resistance vasculature associated with a hypotensive effect. Its relaxant effect involves the opening of K_{Ca} channels, inhibition of transmembrane calcium influx and α_1-adrenergic receptors, and potentiation of the sGC/cGMP pathway. Whether compound **8** could be a new drug candidate for the treatment of arterial hypertension deserves future studies investigating its antihypertensive effect in animal models of hypertension, after an oral and chronic administration of the drug. Data on liver toxicity and CYP interactions suggest that this compound has potential for further development and indicate that compound **8** may also serve as a pilot molecule for the development of additional analogs with vasodilating properties.

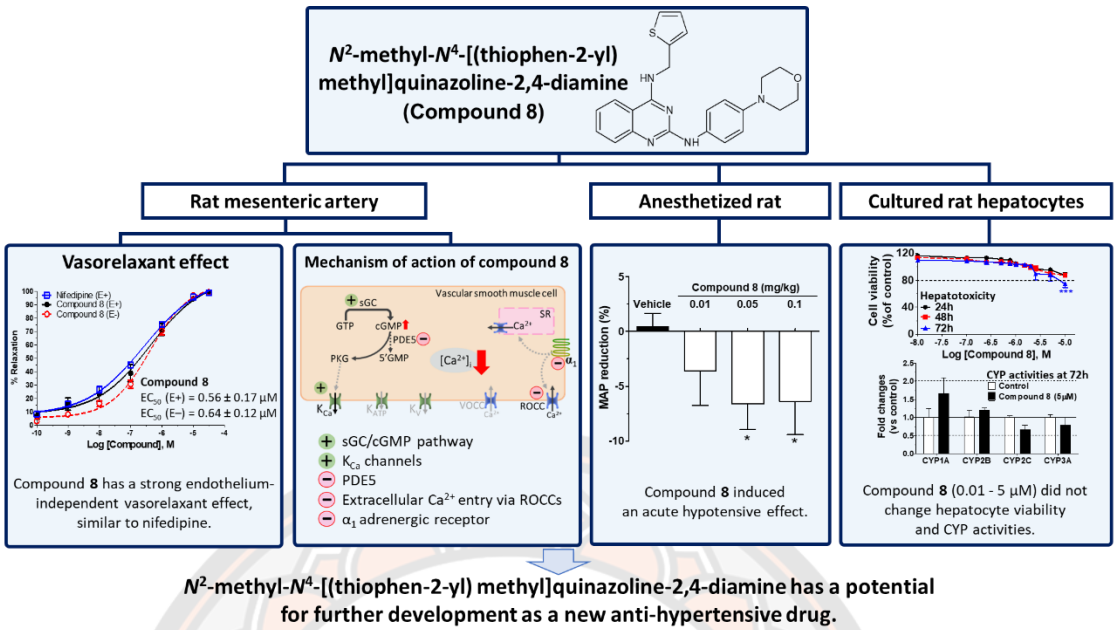

Figure 57 A summary of the mechanisms of action of compound 8

CHAPTER V

CONCLUSIONS AND PERSPECTIVES

PDE5 inhibitors are potent and selective pulmonary vasodilators (Badlam & Bull, 2017; Liu et al., 2007; Michelakis et al., 2002; Schuster et al., 2017). They promote NO/cGMP signaling pathway by inhibiting degradation of cGMP which promotes protein kinase stimulation resulting in the relaxation of vascular smooth muscle (Badlam & Bull, 2017; M. Morgado et al., 2012). Moreover, the PDE5 enzyme is also widely expressed in smooth muscle cells including VSMCs (Komas et al., 1991). Long-term conditions with high PDE5 levels in the VSMC of PA lead to decreased activity of cGMP/PKG, which causes an increase in $[Ca^{2+}]_i$, resulting in vasoconstriction and ultimately leading to diseases such as PAH (Corinaldesi et al., 2016). Recently, quinazoline derivatives (N^2,N^4-disubstituted quinazoline 2,4-diamines) have been designed based on their pharmacophore similarity to sildenafil and found to have PDE5 inhibitory activity (Paracha et al., 2019; Pobsuk et al., 2019). Thus, the potent PDE5 inhibitory activity of the quinazoline derivatives could clinically translate into a vasodilator effect. However, the effects of the quinazoline derivatives have rarely been reported in studies on rat pulmonary circulation and systemic circulation, thus their mechanisms of action are still unclear. Therefore, the objectives of the present study were to investigate the effect of the quinazoline derivatives with PDE5 inhibitory activities on cardiovascular function and its underlying mechanisms both pulmonary circulation and systemic circulation. Their cytotoxicity on isolated rat VSMCs and isolated rat hepatocytes as well as their impact on CYP inhibition and induction were also evaluated. These outcomes demonstrated the pharmacological effects of this series of quinazolines (compounds **5**, **8** and **11**) and gave confidence for their overall use in the development of pharmaceutical products, particularly when related to liver toxicity, CYP inhibition, and induction effects. This has spurred further efforts to develop additional analogs with a view to improving their PDE5 selectivity and maximizing their vasorelaxant

effects. This scientific data demonstrated that the quinazoline derivatives could have the potential to be drugs for PAH or systemic hypertension.

The first part of the study has provided new pharmacological and development information on a series of N^2, N^4-diamino quinazoline analogues (compound **4**, **5**, **8**, **9**, **10** and **11**) by identifying, in an *in vitro* study of human PDE5, that two quinazoline derivatives (compounds **5** and **11**) have high inhibitory properties and potent vasorelaxant effects on isolated rat PA, and do not induce vascular cytotoxicity. Despite a lower activity on PDE5 than shown by sildenafil, compounds **5** and **11** have a greater selectivity for pulmonary *vs* systemic vasculature than sildenafil. Their vasorelaxant effects on PA relied on both endothelium-dependent and endothelium-independent mechanisms. These involved not only PDE5 inhibition but also other relevant mechanisms in the context of PAH: including direct activation of sGC, blockade of Ca^{2+} channels and activation of NO-dependent endothelial function. Compounds **5** and **11** also exhibited weak hepatocyte toxicity as well as a weak inhibitory effect on CYP3A ($>10^{-5}$ M).

The second part of the study identified that compound **8** has a potent vasodilator effect on the resistance vasculature through endothelium-independent mechanisms, this translated into an *in vivo* acute hypotensive effect in rats. Its relaxant effect involves the opening of K_{Ca} channels, inhibition of transmembrane Ca^{2+} influx and α_1-adrenergic receptors, and potentiation of the sGC/cGMP pathway. Compound **8** also exhibited low liver hepatocyte toxicity as well as low effect on CYP1A and 3A activities ($>10^{-5}$ M).

The investigation of the relationships between molecular structure compounds and their biological activity helps in the discovery of new chemical compounds with specific biological properties. Although the quinazoline derivatives share the same core chemical structure, the substitutions in different molecular positions result in them having different target-specific properties. In the structure-activity relationship for quinazoline derivatives, it was found that substitution of benzyl (compound **5**) or 2-thiophenemethyl (compounds **8** and **11**) at R^1 did not demonstrate significantly different PDE5 inhibitory activity and vasorelaxation activity. This result showed that the substitution at R^1 might not play a prominent role in receptor binding, a finding that corresponds with the previous study of Pobsuk et al.

(2019) on the binding of quinazoline derivatives with the PDE5 enzyme. However, complementing substitution at R^2 with various groups was likely to enhance all tested activities (Paracha et al., 2019; Pobsuk et al., 2019). Thus, we can state that the ring at R^1 might not take a direct part in the binding of the compound but may influence a change to the desired conformation of the molecule to interact at target sites. As shown in Figure 58, compounds **5**, **8** and **11** shares structural similarity with prazosin via the 2,4 diamino quinazoline, but only compounds **5** and **11** share structural similarity with sildenafil at the R^2 position of the core structure of quinazoline. The results demonstrated that 3-sulphonamide (–3-SO_2NH_2) at the R^2 position in compounds **5** and **11** is important for their activities, where both compounds have a stronger PDE5 inhibitory effect and are more selective in inducing pulmonary vasculature relaxation than compound **8**. As mentioned previously, compound **8** has a structure similar to prazosin and also has 4-morpholino at the R^2 position, which makes compound **8** more selective in inducing systemic vasculature relaxation. Paracha et al. (2019) reported that compound **8** plays a similar role as prazosin in inhibiting the α_1-adrenergic receptor by reducing PE-induced contraction by around 40% as well as PDE5 inhibition. Thus, compounds **5** and **11** could be potential leads for developing new PDE5 for the treatment of PAH, whereas compound **8** could be a potential lead for developing new anti-hypertensive drugs.

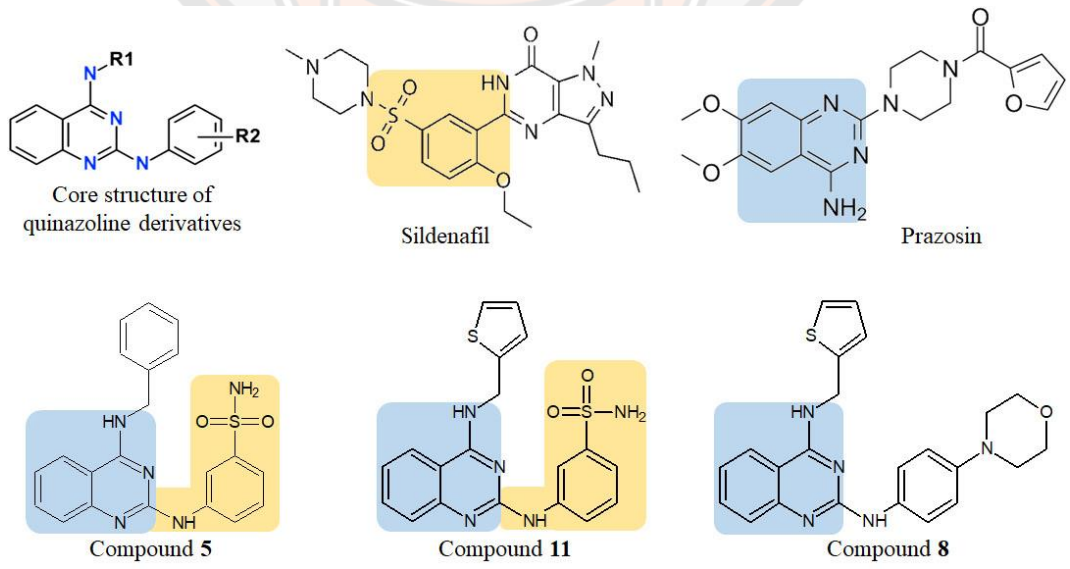

Figure 58 Chemical structure of sildenafil, prazosin and quinazoline derivatives

When comparing compounds **5** and **11** against sildenafil, it was observed that the vasorelaxant effect on PA of compounds **5** and **11** was less than that of sildenafil. However, the compounds had a greater selectivity for pulmonary *vs* systemic vasculature than sildenafil. Also, compounds **5** and **11** did not affect the PA VSMCs, while sildenafil at 100 µM reduced their cell viability. The effects of compounds **5** and **11** on liver toxicity were only evident for concentrations of >10 µM. The half-maximal inhibitory concentration after 72 h of exposure to compound **5** was 18 µM and for compound **11** was 19 µM, whereas the half-maximal effective concentration to induce PA vasorelaxation was approximately 0.9 µM for compound **5** and 1.0 µM for compound **11** indicating that it is unlikely that such hepatotoxicity may occur at pharmacological concentrations. In PAH treatments, PDE5 inhibitors are often used in combination with endothelin-1 antagonists (e.g., bosentan), which are strongly metabolized by CYP3A4 and 2C9 (Srinivas, 2016). The present study showed that the main effect on CYP was a weak CYP3A inhibition for both compounds **5** and **11** (only at 10 µM), while sildenafil showed similar inhibition of CYP34, but at 5 and 10 µM. Compound **5** showed a weak CYP2C inhibition also only at 5 and 10 µM. Additionally, compounds **5** and **11** did not increase CYP1A activity in a concentration-dependent and time-dependent manner, in contrast to sildenafil which did increase CYP1A activity. These findings suggest that both compounds **5** and **11** have the potential for further development for the treatment of PAH.

When comparing compound **8** and nifedipine, it was observed that compound **8** induced a strong vasorelaxant effect equivalent to that of nifedipine. The vasorelaxant effect of both compound **8** and nifedipine was endothelium-independent and the hypotensive effect of compound **8** on MAP was also no different than that of nifedipine. As well, the effects of compound **8** on liver toxicity are only evident for concentrations of >10 µM. The half-maximal inhibitory concentration after 72 h of exposure to compound **8** was 19 µM, whereas the half-maximal effective concentration to induce MA vasorelaxation was approximately 0.6 µM, indicating that it is unlikely that such hepatotoxicity may occur at pharmacological concentrations. Many anti-hypertensive drugs or drugs used for reducing cardiovascular risk, such as statins (Vaughan & Gotto, 2004), are strongly metabolized by CYP (Zisaki et al., 2015). While nifedipine showed a strong inducing

effect on all CYP activities, compound **8** did not change CYP activities for concentrations ranging from 0.1 to 5 µM. A weak inhibition of CYP1A and 3A activities was observed only at 10 µM, so again, it is unlikely that this effect would be observed at pharmacological doses. This study demonstrated that the relaxant effect of compound **8** was not mediated by an activation of endothelial function. In the context of hypertension in which endothelial dysfunction is both a hallmark and a target for reducing the cardiovascular complications of the disease (Xu et al., 2021), it will be necessary to check if the compound might decrease endothelial dysfunction when administered *in vivo* in relevant animal models.

Although all results obtained from this research project were tested in non-clinical situations, our results nonetheless offer scientific evidence or knowledge of the physiological and pharmacological action of quinazoline derivatives. The results from this study provide scientific evidence which will inform the future development of therapies for PAH and hypertension. The *in vitro* and *ex vivo* data suggest that compounds **5** and **11** can inhibit PDE5 and also induce PA relaxation, thus they have the potential to reduce the PAH context. As compound **8** can induce MA relaxation and induce acute hypotension, it might therefore have the potential to reduce the hypertension context. However, there is a need for animal models or clinical studies to confirm these results in a wider context. Further development is needed for quinazoline derivatives to be demonstrated as an alternative drug or supplement for patients with PAH or systemic hypertension.

Further studies

This study leaves important matters unanswered:

1. The effects of compounds **5** and **11** on cardiovascular disease need to be confirmed in *in vivo* studies using animal models of PAH, after an oral and chronic administration of the drug. The compounds have to be tested not only for vascular relaxation but also for their effects on vascular remodeling. The most commonly used animal models of PAH are (*i*) the chronic hypoxic model, where animals are exposed to low O_2 levels for a prolonged period of time, and (*ii*) the monocrotaline injury model, where animals are injected with a chemical called monocrotaline, which results in lung vascular functional and histological changes and leads to PAH

(Stenmark et al., 2009). These models have been used for a long time and have helped researchers better understand PAH and develop new drugs for PAH.

2. Study the therapeutic effects of compounds **5** and **11** on the PAH model and aimed to clarify the possible mechanisms underlying their inhibitory action on vascular remodeling, progressive fibroproliferative remodeling, inflammation of the pulmonary artery, and right ventricular hypertrophy.

3. The effects of compound **8** on cardiovascular disease need further investigation for its anti-hypertensive effects, in animal models of hypertension, such as the model of spontaneously hypertensive rat (SHR) after an oral and chronic administration of the drug.

REFERENCES

REFERENCES

Abou-Seri, S. M., Abouzid, K., & El Ella, D. A. A. (2011). Molecular modeling study and synthesis of quinazolinone-arylpiperazine derivatives as α_1-adrenoreceptor antagonists. *European journal of medicinal chemistry*, *46*(2), 647-658. https://doi.org/10.1016/j.ejmech.2010.11.045

Ahmed, O., Hussein, A., & Ahmed, R. (2012). Antidiabetic and antioxidant effects of newly synthesized pyrimido [1, 6-a] pyrimidine derivatives in neonatal streptozotocin-induced diabetic rats. *Med chem*, *2*, 20-28.

Ahmed, W. S., Geethakumari, A. M., & Biswas, K. H. (2021). Phosphodiesterase 5 (PDE5): Structure-function regulation and therapeutic applications of inhibitors. *Biomedicine & Pharmacotherapy*, *134*, 111128. https://doi.org/10.1016/j.biopha.2020.111128

Ajani, O. O., Aderohunmu, D. V., Umeokoro, E. N., & Olomieja, A. O. (2016). Quinazoline pharmacophore in therapeutic medicine. *Bangladesh Journal of Pharmacology*, *11*(3), 716-733.

Akinaga, J., García-Sáinz, J. A., & A, S. P. (2019). Updates in the function and regulation of α_1 -adrenoceptors. *Br J Pharmacol*, *176*(14), 2343-2357. https://doi.org/10.1111/bph.14617

Al-Azawi, K. (2016). Synthesis, characterization and antioxidant studies of quinazolin derivatives. *Oriental Journal of Chemistry*, *32*(1), 585-590. https://doi.org/10.13005/ojc/320166

Alagarsamy, V., Chitra, K., Saravanan, G., Solomon, V. R., Sulthana, M. T., & Narendhar, B. (2018). An overview of quinazolines: Pharmacological significance and recent developments. *European Journal of Medicinal Chemistry*, *151*, 628-685. https://doi.org/10.1016/j.ejmech.2018.03.076

Alagarsamy, V., Solomon, V. R., & Dhanabal, K. (2007). Synthesis and pharmacological evaluation of some 3-phenyl-2-substituted-3H-quinazolin-4-one as analgesic, anti-inflammatory agents. *Bioorganic & medicinal chemistry*, *15*(1), 235-241. https://doi.org/10.1016/j.bmc.2006.09.065

Alderton, W. K., Cooper, C. E., & Knowles, R. G. (2001). Nitric oxide synthases: structure, function and inhibition. *Biochemical Journal*, *357*(Pt 3), 593-615. http://www.ncbi.nlm.nih.gov/pmc/articles/PMC1221991/

Almehizia, A. A., Abuelizz, H. A., Taie, H. A., ElHassane, A., Marzouk, M., & Al-Salahi, R. (2019). Investigation the antioxidant activity of benzo [g] triazoloquinazolines correlated with a DFT study. *Saudi pharmaceutical journal*, *27*(1), 133-137.

Alsibaee, A. M., Al-Yousef, H. M., & Al-Salem, H. S. (2023). Quinazolinones, the winning horse in drug discovery. *Molecules*, *28*(3), 978. https://doi.org/10.3390/molecules28030978

Alvarado, M., Barceló, M., Carro, L., Masaguer, C. F., & Raviña, E. (2006). Synthesis and biological evaluation of new quinazoline and cinnoline derivatives as potential atypical antipsychotics. *Chemistry & biodiversity*, *3*(1), 106-117. https://doi.org/10.1002/cbdv.200690001

Amberg, G. C., & Navedo, M. F. (2013). Calcium dynamics in vascular smooth muscle. *Microcirculation*, *20*(4), 281-289. https://doi.org/10.1111/micc.12046

Amsallem, E., Kasparian, C., Haddour, G., Boissel, J. P., Nony, P., & Group, C. H. (2005). Phosphodiesterase III inhibitors for heart failure. *Cochrane Database of Systematic Reviews*, *2013*(1). https://doi.org/10.1002/14651858.CD002230

Andersson, K. E. (2018). PDE5 inhibitors–pharmacology and clinical applications 20 years after sildenafil discovery. *British journal of pharmacology*, *175*(13), 2554-2565.

Archer, S. L., Huang, J. M., Hampl, V., Nelson, D. P., Shultz, P. J., & Weir, E. K. (1994). Nitric oxide and cGMP cause vasorelaxation by activation of a charybdotoxin-sensitive K channel by cGMP-dependent protein kinase. *Proc Natl Acad Sci U S A*, *91*(16), 7583-7587. https://doi.org/10.1073/pnas.91.16.7583

Arnett, D. K., & Claas, S. A. (2009). Pharmacogenetics of antihypertensive treatment: detailing disciplinary dissonance. *Pharmacogenomics*, *10*(8), 1295-1307. https://doi.org/10.2217/pgs.09.61

Ausó, E., Gómez-Vicente, V., & Esquiva, G. (2021). Visual side effects linked to sildenafil consumption: An update. *Biomedicines*, *9*(3). https://doi.org/10.3390/ biomedicines9030291

Bachmann, K. (2009). Chapter 8 - Drug metabolism., *Pharmacology*, 131-173. Academic Press. https://doi.org/10.1016/B978-0-12-369521-5.00008-7

Badlam, J. B., & Bull, T. M. (2017). Steps forward in the treatment of pulmonary arterial hypertension: latest developments and clinical opportunities. *Ther Adv Chronic Dis*, *8*(2-3), 47-64. https://doi.org/10.1177/2040622317693218

Baillie, G. S., Tejeda, G. S., & Kelly, M. P. (2019). Therapeutic targeting of 3',5'-cyclic nucleotide phosphodiesterases: inhibition and beyond. *Nat Rev Drug Discov*, *18*(10), 770-796. https://doi.org/10.1038/s41573-019-0033-4

Barnes, P. J., & Liu, S. F. (1995). Regulation of pulmonary vascular tone. *Pharmacological reviews*, *47*(1), 87-131.

Barst, R. J., Ivy, D., Dingemanse, J., Widlitz, A., Schmitt, K., Doran, A., et al. (2003). Pharmacokinetics, safety, and efficacy of bosentan in pediatric patients with pulmonary arterial hypertension. *Clinical Pharmacology & Therapeutics*, *73*(4), 372-382. https://doi.org/10.1016/S0009-9236(03)00005-5

Barst, R. J., Rubin, L. J., Long, W. A., McGoon, M. D., Rich, S., Badesch, D. B., et al. (1996). A comparison of continuous intravenous epoprostenol (prostacyclin) with conventional therapy for primary pulmonary hypertension. *New England Journal of Medicine*, *334*(5), 296-301. https://doi.org/10.1056/ NEJM19960 2013340504

Beleznai, T. Z., Yarova, P. L., Yuill, K. H., & Dora, K. A. (2011). Smooth Muscle Ca^{2+}-Activated and Voltage-Gated K^{+} Channels Modulate Conducted Dilation in Rat Isolated Small Mesenteric Arteries. *Microcirculation*, *18*(6), 487-500. https://doi.org/10.1111/j.1549-8719.2011.00109.x

Bender, A. T., & Beavo, J. A. (2006). Cyclic nucleotide phosphodiesterases: molecular regulation to clinical use. *Pharmacological reviews*, *58*(3), 488-520. https://doi.org/10.1124/pr.58.3.5

Berne, B. R., Koeppen, B., & Stanton, B. B. (2010). Levy physiology. Philadelphia PA: Mosby. In: Elsevier.

Bhandari, S., Nuengchamnong, N., Chaichamnong, N., Seasong, T., Ingkaninan, K., & Temkitthawon, P. (2019). At-line LC-QTOF-MS micro-fractionation of *Derris scandens* (Roxb.) Benth, coupled to radioassay for the early identification of PDE5A1 inhibitors. *Phytochemical Analysis*. https://doi.org/10.1002/pca.2895

Bhatia, S., Frantz, R. P., Severson, C. J., Durst, L. A., & McGoon, M. D. (2003). Immediate and long-term hemodynamic and clinical effects of sildenafil in patients with pulmonary arterial hypertension receiving vasodilator therapy. Mayo Clinic Proceedings,

Bi, Y., Stoy, P., Adam, L., He, B., Krupinski, J., Normandin, D., et al. (2004). Quinolines as extremely potent and selective PDE5 inhibitors as potential agents for treatment of erectile dysfunction. *Bioorganic & medicinal chemistry letters*, *14*(6), 1577-1580. https://doi.org/10.1016/j.bmcl.2003.12.090

Birgegard, G. (2006). Anagrelide treatment in myeloproliferative disorders. *Semin Thromb Hemost*, *32*(3), 260-266. https://doi.org/10.1055/s-2006-939437

Brassard, M., Neraud, B., Trabado, S., Salenave, S., Brailly-Tabard, S., Borget, I., et al. (2011). Endocrine effects of the tyrosine kinase inhibitor vandetanib in patients treated for thyroid cancer. *The Journal of Clinical Endocrinology & Metabolism*, *96*(9), 2741-2749. https://doi.org/10.1210/jc.2010-2771

Budhiraja, R., Tuder, R. M., & Hassoun, P. M. (2004). Endothelial dysfunction in pulmonary hypertension. *Circulation*, *109*(2), 159-165. https://doi.org/10.1161/01.CIR.0000102381.57477.50

Burton, J., Ijjaali, I., Barberan, O., Petitet, F., Vercauteren, D. P., & Michel, A. (2006). Recursive Partitioning for the Prediction of Cytochromes P450 2D6 and 1A2 Inhibition: Importance of the Quality of the Dataset. *Journal of Medicinal Chemistry*, *49*(21), 6231-6240. https://doi.org/10.1021/jm060267u

Bylund, D. B., Eikenberg, D. C., Hieble, J. P., Langer, S. Z., Lefkowitz, R. J., Minneman, K. P., et al. (1994). International Union of Pharmacology nomenclature of adrenoceptors. *Pharmacol Rev*, *46*(2), 121-136.

Cesarini, V., Guida, E., Campolo, F., Crescioli, C., Di Baldassarre, A., Pisano, C., et al. (2020). Type 5 phosphodiesterase (PDE5) and the vascular tree: From embryogenesis to aging and disease. *Mech Ageing Dev, 190*, 111311. https://doi.org/10.1016/j.mad.2020.111311

Chandregowda, V., Kush, A., & Reddy, G. C. (2009). Synthesis and *in vitro* antitumor activities of novel 4-anilinoquinazoline derivatives. *European journal of medicinal chemistry*, *44*(7), 3046-3055. https://doi.org/10.1016/j.ejmech. 2008.07.023

Chatturong, U., Martin, H., Totoson, P., Ingkaninan, K., Temkitthawon, P., Sermsenaphorn, S., et al. (2022). Quinazoline-based human phosphodiesterase 5 inhibitors exhibited a selective vasorelaxant effect on rat isolated pulmonary arteries involving NO-sGC-cGMP pathway and calcium inhibitory effects. *Vascular Pharmacology*, *147*, 107111. https://doi.org/10.1016/j.vph.2022. 107111

Chemla, D., Lau, E. M., Papelier, Y., Attal, P., & Hervé, P. (2015). Pulmonary vascular resistance and compliance relationship in pulmonary hypertension. *European Respiratory Journal*, *46*(4), 1178-1189. https://doi.org/10.1183/13993003.00741-2015

Chen, A. L., & Chen, K. (1933). The constituents of Wu Chü Yü (*Evodia rutæcarpa*). *Journal of the American Pharmaceutical Association*, *22*(8), 716-719. https://doi.org/10.1002/jps.3080220804

Chen, J.-N., Wang, X.-F., Li, T., Wu, D.-W., Fu, X.-B., Zhang, G.-J., et al. (2016). Design, synthesis, and biological evaluation of novel quinazolinyl-diaryl urea derivatives as potential anticancer agents. *European Journal of Medicinal Chemistry*, *107*, 12-25. https://doi.org/https://doi.org/10.1016/j.ejmech.2015.10.045

Cheng, J., Wen, J., Wang, N., Wang, C., Xu, Q., & Yang, Y. (2019). Ion Channels and Vascular Diseases. *Arteriosclerosis, Thrombosis, and Vascular Biology*, *39*(5), e146-e156. https://doi.org/10.1161/ATVBAHA.119.312004

Chiou, W.-F., Liao, J.-F., & Chen, C.-F. (1996). Comparative study on the vasodilatory effects of three quinazoline alkaloids isolated from Evodia rutaecarpa. *Journal of natural products*, *59*(4), 374-378. https://doi.org/10.1021/np960161+

Ciardiello, F. (2000). Epidermal growth factor receptor tyrosine kinase inhibitors as anticancer agents. *Drugs*, *60*(1), 25-32. https://doi.org/10.2165/00003495-200060001-00003

Clapp, L. H., & Gurung, R. (2015). The mechanistic basis of prostacyclin and its stable analogues in pulmonary arterial hypertension: Role of membrane versus nuclear receptors. *Prostaglandins & Other Lipid Mediators*, *120*, 56-71. https://doi.org/10.1016/j.prostaglandins.2015.04.007

Clissold, S. P., & Beresford, R. (1987). Proquazone. *Drugs*, *33*(5), 478-502. https://doi.org/10.2165/00003495-198733050-00004

Cole, W. C., & Welsh, D. G. (2011). Role of myosin light chain kinase and myosin light chain phosphatase in the resistance arterial myogenic response to intravascular pressure. *Archives of Biochemistry and Biophysics*, *510*(2), 160-173. https://doi.org/10.1016/j.abb.2011.02.024

Corinaldesi, C., Di Luigi, L., Lenzi, A., & Crescioli, C. (2015). Phosphodiesterase type 5 inhibitors: back and forward from cardiac indications. *Journal of Endocrinological Investigation*, 1-9. https://doi.org/10.1007/s40618-015-0340-5

Corinaldesi, C., Di Luigi, L., Lenzi, A., & Crescioli, C. (2016). Phosphodiesterase type 5 inhibitors: back and forward from cardiac indications. *Journal of endocrinological investigation*, *39*(2), 143-151. https://doi.org/10.1007/s40618-015-0340-5

Cornu, R., Rougier, N., Pellequer, Y., Lamprecht, A., Hamon, P., Li, R., et al. (2018). Interspecies differences in the cytochrome P450 activity of hepatocytes exposed to PLGA and silica nanoparticles: an in vitro and in vivo investigation. *Nanoscale*, *10*(11), 5171-5181. https://doi.org/10.1039/C8NR00226F

Cruz-Burgos, M., Losada-Garcia, A., Cruz-Hernández, C. D., Cortés-Ramírez, S. A., Camacho-Arroyo, I., Gonzalez-Covarrubias, V., et al. (2021). New Approaches in Oncology for Repositioning Drugs: The Case of PDE5 Inhibitor Sildenafil. *Frontiers in Oncology*, *11*, 208.

Davel, A. P., Victorio, J. A., Delbin, M. A., Fukuda, L. E., & Rossoni, L. V. (2015). Enhanced endothelium-dependent relaxation of rat pulmonary artery following β-adrenergic overstimulation: Involvement of the NO/cGMP/VASP pathway. *Life Sciences*, *125*, 49-56. https://doi.org/10.1016/j.lfs.2015.01.018

De, A. K., Muthiyan, R., Mondal, S., Mahanta, N., Bhattacharya, D., Ponraj, P., et al. (2019). A natural quinazoline derivative from marine sponge *Hyrtios erectus* induces apoptosis of breast cancer cells via ROS production and intrinsic or extrinsic apoptosis pathways. *Marine drugs*, *17*(12), 658. https://doi.org/10.3390/md17120658

DeSaix, P., Betts, G. J., Johnson, E., Johnson, J. E., Oksana, K., Kruse, D. H., et al. (2013). *Anatomy and physiology*. OpenStax.

Devendran, A., Kar, S., Bailey, R., & Trivieri, M. G. (2022). The Role of Bone Morphogenetic Protein Receptor Type 2 (BMPR2) and the Prospects of Utilizing Induced Pluripotent Stem Cells (iPSCs) in Pulmonary Arterial Hypertension Disease Modeling. *Cells*, *11*(23). https://doi.org/10.3390/cells11233823

Eguchi, Y., Sasaki, F., Sugimoto, A., Ebisawa, H., & Ishikawa, M. (1991). Studies on hypotensive agents. Synthesis of 1-substituted 3-(2-chlorophenyl)-6-ethoxycarbonyl-5,7-dimethyl-2,4(1H,3H)-quinazoline diones. *Chem Pharm Bull (Tokyo)*, *39*(7), 1753-1759. https://doi.org/10.1248/cpb.39.1753

El-Sabbagh, O. I., Shabaan, M. A., Kadry, H. H., & Al-Din, E. S. (2010). New octahydroquinazoline derivatives: Synthesis and hypotensive activity. *European Journal of Medicinal Chemistry*, *45*(11), 5390-5396. https://doi.org/10.1016/j.ejmech.2010.08.064

Elliott, W. J., & Ram, C. V. (2011). Calcium channel blockers. *J Clin Hypertens (Greenwich)*, *13*(9), 687-689. https://doi.org/10.1111/j.1751-7176.2011.00513.x

Elton, T. S., Oparil, S., Taylor, G. R., Hicks, P. H., Yang, R. H., Jin, H., et al. (1992a). Normobaric hypoxia stimulates endothelin-1 gene expression in the rat. *American Journal of Physiology-Regulatory, Integrative and Comparative Physiology*, *263*(6), R1260-R1264. https://doi.org/10.1152/ajpregu.1992.263.6.R1260

Elton, T. S., Oparil, S., Taylor, G. R., Hicks, P. H., Yang, R. H., Jin, H., et al. (1992b). Normobaric hypoxia stimulates endothelin-1 gene expression in the rat. *Am J Physiol*, *263*(6 Pt 2), R1260-1264. https://doi.org/10.1152/ajpregu.1992. 263.6.R1260

Faisal, M., & Saeed, A. (2021). Chemical insights into the synthetic chemistry of quinazolines: Recent advances. *Frontiers in Chemistry*, *8*. https://doi.org/10.3389/fchem.2020.594717

Feletou, M., & Vanhoutte, P. M. (2006). Endothelium-derived hyperpolarizing factor: where are we now? *Arterioscler Thromb Vasc Biol*, *26*(6), 1215-1225. https://doi.org/10.1161/01.ATV.0000217611.81085.c5

Feletou, M., & Vanhoutte, P. M. (2009). EDHF: an update. *Clin Sci (Lond)*, *117*(4), 139-155. https://doi.org/10.1042/cs20090096

Félétou, M., & Vanhoutte, P. M. (2006). Endothelium-derived hyperpolarizing factor: where are we now? *Arteriosclerosis, thrombosis, and vascular biology*, *26*(6), 1215-1225. https://doi.org/10.1161/01.ATV.0000217611.81085.c5

Félétou, M., & Vanhoutte, P. M. (2009). EDHF: an update. *Clinical science*, *117*(4), 139-155. https://doi.org/10.1042/CS20090096

Firth, A. L., Mandel, J., & Yuan, J. X.-J. (2010). Idiopathic pulmonary arterial hypertension. *Disease models & mechanisms*, *3*(5-6), 268-273. https://doi.org/10.1242/dmm.003616

Forst, T., Uhlig-Laske, B., Ring, A., Ritzhaupt, A., Graefe-Mody, U., & Dugi, K. A. (2011). The oral DPP-4 inhibitor linagliptin significantly lowers HbA1c after 4 weeks of treatment in patients with type 2 diabetes mellitus. *Diabetes, Obesity and Metabolism*, *13*(6), 542-550. https://doi.org/10.1111/j.1463-1326.2011.01386.x

Francis, S., Morris, G., & Corbin, J. (2008). Molecular mechanisms that could contribute to prolonged effectiveness of PDE5 inhibitors to improve erectile function. *International journal of impotence research*, *20*(4), 333-342. https://doi.org/10.1038/ijir.2008.4

Francis, S. H., Busch, J. L., Corbin, J. D., & Sibley, D. (2010). cGMP-dependent protein kinases and cGMP phosphodiesterases in nitric oxide and cGMP action. *Pharmacol Rev*, *62*(3), 525-563. https://doi.org/10.1124/pr.110.002907

Francis, S. H., Lincoln, T. M., & Corbin, J. D. (1980). Characterization of a novel cGMP binding protein from rat lung. *Journal of Biological Chemistry*, *255*(2), 620-626. https://doi.org/10.1016/S0021-9258(19)86221-X

Fuso, L., Baldi, F., & Di Perna, A. (2011). Therapeutic strategies in pulmonary hypertension. *Front Pharmacol*, *2*, 21. https://doi.org/10.3389/fphar.2011.00021

Galiè, N., Ghofrani, H. A., Torbicki, A., Barst, R. J., Rubin, L. J., Badesch, D., et al. (2005). Sildenafil citrate therapy for pulmonary arterial hypertension. *New England Journal of Medicine*, *353*(20), 2148-2157. https://doi.org/10.1056/NEJMoa050010

Galiè, N., McLaughlin, V. V., Rubin, L. J., & Simonneau, G. (2019). An overview of the 6th World Symposium on Pulmonary Hypertension. In: European Respiratory Journal

Galiè, N., Palazzini, M., Leci, E., & Manes, A. (2010). Current Therapeutic Approaches to Pulmonary Arterial Hypertension. *Revista Española de Cardiología (English Edition)*, *63*(6), 708-724. https://doi.org/10.1016/S1885-5857(10)70145-6

Galiè, N., Torbicki, A., Barst, R., Dartevelle, P., Haworth, S., Higenbottam, T., et al. (2004). Guidelines on diagnosis and treatment of pulmonary arterial hypertension: The Task Force on Diagnosis and Treatment of Pulmonary Arterial Hypertension of the European Society of Cardiology. *European heart journal*, *25*(24), 2243-2278. https://doi.org/10.1016/j.ehj.2004.09.014

Gallo, G., Volpe, M., & Savoia, C. (2022). Endothelial Dysfunction in Hypertension: Current Concepts and Clinical Implications. *Frontiers in Medicine*, *8*. https://doi.org/10.3389/fmed.2021.798958

García-Álvarez, A., Pereda, D., García-Lunar, I., Sanz-Rosa, D., Fernández-Jiménez, R., García-Prieto, J., et al. (2016). Beta-3 adrenergic agonists reduce pulmonary vascular resistance and improve right ventricular performance in a porcine model of chronic pulmonary hypertension. *Basic Res Cardiol*, *111*(4), 49. https://doi.org/10.1007/s00395-016-0567-0

Geldsetzer, P., Manne-Goehler, J., Marcus, M. E., Ebert, C., Zhumadilov, Z., Wesseh, C. S., et al. (2019). The state of hypertension care in 44 low-income and middle-income countries: a cross-sectional study of nationally representative individual-level data from 1·1 million adults. *Lancet*, *394*(10199), 652-662. https://doi.org/10.1016/s0140-6736(19)30955-9

Ghofrani, H. A., Osterloh, I. H., & Grimminger, F. (2006). Sildenafil: from angina to erectile dysfunction to pulmonary hypertension and beyond. *Nature Reviews Drug Discovery*, *5*(8), 689-702.

Ghosh, D., Syed, A. U., Prada, M. P., Nystoriak, M. A., Santana, L. F., Nieves-Cintrón, M., et al. (2017). Calcium Channels in Vascular Smooth Muscle. *Adv Pharmacol*, *78*, 49-87. https://doi.org/10.1016/bs.apha.2016.08.002

Gidwani, S., & Nair, A. (2014). The Burden of Pulmonary Hypertension in Resource-Limited Settings. *Global Heart*, *9*(3), 297-310. http://dx.doi.org/10.1016/j.gheart.2014.08.007

Gleeson, M. P. (2008). Generation of a Set of Simple, Interpretable ADMET Rules of Thumb. *Journal of Medicinal Chemistry*, *51*(4), 817-834. https://doi.org/10.1021/jm701122q

Gopal, V. K., Francis, S. H., & Corbin, J. D. (2001). Allosteric sites of phosphodiesterase-5 (PDE5). *European Journal of Biochemistry*, *268*(11), 3304-3312. https://doi.org/10.1046/j.1432-1327.2001.02233.x

Gordan, R., Gwathmey, J. K., & Xie, L. H. (2015). Autonomic and endocrine control of cardiovascular function. *World J Cardiol*, *7*(4), 204-214. https://doi.org/10.4330/wjc.v7.i4.204

Graziano, S., Montana, A., Zaami, S., Rotolo, M. C., Minutillo, A., Busardò, F. P., et al. (2017). Sildenafil-associated hepatoxicity: a review of the literature. *Eur Rev Med Pharmacol Sci*, *21*(1 Suppl), 17-22.

Gredic, M., Blanco, I., Kovacs, G., Helyes, Z., Ferdinandy, P., Olschewski, H., et al. (2021). Pulmonary hypertension in chronic obstructive pulmonary disease. *British journal of pharmacology*, *178*(1), 132-151.

Grünig, E., Benjamin, N., Krüger, U., Kaemmerer, H., Harutyunova, S., Olsson, K. M., et al. (2018). General measures and supportive therapy for pulmonary arterial hypertension: Updated recommendations from the Cologne Consensus Conference 2018. *Int J Cardiol*, *272s*, 30-36. https://doi.org/10.1016/j.ijcard.2018.08.085

Guazzi, M. (2008). Clinical Use of Phosphodiesterase-5 Inhibitors in Chronic Heart Failure. *Circulation: Heart Failure*, *1*(4), 272-280. https://doi.org/10.1161/circheartfailure.108.802116

Guengerich, F. P. (2011). Mechanisms of drug toxicity and relevance to pharmaceutical development. *Drug Metab Pharmacokinet*, *26*(1), 3-14. https://doi.org/10.2133/ dmpk.dmpk-10-rv-062

Gunasekara, N. S., & Faulds, D. (1998). Raltitrexed. *Drugs*, *55*(3), 423-435. https://doi.org/10.2165/00003495-199855030-00012

Gupta, V., Kashaw, S. K., Jatav, V., & Mishra, P. (2008). Synthesis and antimicrobial activity of some new 3–[5-(4-substituted) phenyl-1, 3, 4-oxadiazole-2yl]-2-styrylquinazoline-4 (3H)-ones. *Medicinal Chemistry Research*, *17*(2-7), 205-211.

Hara, H., Ichikawa, M., Oku, H., Shimazawa, M., & Araie, M. (2005). Bunazosin, a Selective α1 -Adrenoceptor Antagonist, as an Anti-glaucoma Drug: Effects on Ocular Circulation and Retinal Neuronal Damage. *Cardiovascular Drug Reviews*, *23*(1), 43-56. https://doi.org/10.1111/j.1527-3466.2005.tb00156.x

Hassoun, P. M. (2021). Pulmonary Arterial Hypertension. *N Engl J Med*, *385*(25), 2361-2376. https://doi.org/10.1056/NEJMra2000348

Hatzimouratidis, K., Salonia, A., Adaikan, G., Buvat, J., Carrier, S., El-Meliegy, A., et al. (2016). Pharmacotherapy for erectile dysfunction: recommendations from the Fourth International Consultation for Sexual Medicine (ICSM 2015). *The journal of sexual medicine*, *13*(4), 465-488.

Hemnes, A. R., & Champion, H. C. (2006). Sildenafil, a PDE5 inhibitor, in the treatment of pulmonary hypertension. *Expert Review of Cardiovascular Therapy*, *4*(3), 293-300. https://doi.org/10.1586/14779072.4.3.293

Hoeper, M. M., Simonneau, G., Corris, P. A., Ghofrani, H.-A., Klinger, J. R., Langleben, D., et al. (2017). RESPITE: switching to riociguat in pulmonary arterial hypertension patients with inadequate response to phosphodiesterase-5 inhibitors. *European Respiratory Journal*, *50*(3), 1602425. https://doi.org/10.1183/13993003.02425-2016

Horton, D. A., Bourne, G. T., & Smythe, M. L. (2003). The combinatorial synthesis of bicyclic privileged structures or privileged substructures. *Chemical reviews*, *103*(3), 893-930.

Houtchens, J., Martin, D., & Klinger, J. R. (2011a). Diagnosis and management of pulmonary arterial hypertension. *Pulmonary medicine*, *2011*.

Houtchens, J., Martin, D., & Klinger, J. R. (2011b). Diagnosis and Management of Pulmonary Arterial Hypertension. *Pulmonary Medicine*, *2011*, 845864. https://doi.org/10.1155/2011/845864

Huang, S. A., & Lie, J. D. (2013). Phosphodiesterase-5 (PDE5) Inhibitors In the Management of Erectile Dysfunction. *P t*, *38*(7), 407-419.

Humbert, M. (2010). Pulmonary arterial hypertension and chronic thromboembolic pulmonary hypertension: pathophysiology. *European Respiratory Review*, *19*(115), 59-63.

Humbert, M., Guignabert, C., Bonnet, S., Dorfmüller, P., Klinger, J. R., Nicolls, M. R., et al. (2019). Pathology and pathobiology of pulmonary hypertension: state of the art and research perspectives. *European Respiratory Journal*, *53*(1).

Humbert, M., Kovacs, G., Hoeper, M. M., Badagliacca, R., Berger, R. M. F., Brida, M., et al. (2022). 2022 ESC/ERS Guidelines for the diagnosis and treatment of pulmonary hypertension. *European Respiratory Journal*, 2200879. https://doi.org/10.1183/13993003.00879-2022

Humbert, M., Montani, D., Perros, F., Dorfmüller, P., Adnot, S., & Eddahibi, S. (2008). Endothelial cell dysfunction and cross talk between endothelium and smooth muscle cells in pulmonary arterial hypertension. *Vascular Pharmacology*, *49*(4), 113-118. https://doi.org/10.1016/j.vph.2008.06.003

Humbert, M., Sitbon, O., & Simonneau, G. (2004). Treatment of pulmonary arterial hypertension. *New England Journal of Medicine*, *351*(14), 1425-1436.

Jackson, W. F. (2000). Ion channels and vascular tone. *Hypertension*, *35*(1), 173-178. https://doi.org/10.1161/01.HYP.35.1.173

Jadhavar, P. S., Patel, K. I., Dhameliya, T. M., Saha, N., Vaja, M. D., Krishna, V. S., et al. (2020). Benzimidazoquinazolines as new potent anti-TB chemotypes: Design, synthesis, and biological evaluation. *Bioorganic Chemistry*, *99*, 103774. https://doi.org/10.1016/j.bioorg.2020.103774

Jankowich, M., & Choudhary, G. (2020). Endothelin-1 levels and cardiovascular events. *Trends in Cardiovascular Medicine*, *30*(1), 1-8. https://doi.org/10. 1016/j.tcm. 2019.01.007

Jardin, A., Bensadoun, H., Delauche-Cavallier, M. C., Attatli, P., & The, B. P. H. A. L. F. G. (1991). Alfuzosin for treatment of benign prostatic hypertrophy. *The Lancet*, *337*(8755), 1457-1461. https://doi.org/10.1016/0140-6736(91)93140-5

Jiann, B.-P. (2016). Evolution of phosphodiesterase type 5 inhibitors in treatment of erectile dysfunction in Taiwan. *Urological Science*, *27*(2), 66-70. https://doi.org/10.1016/j.urols.2016.04.003

Joyner, M. J., Schrage, W. G., & Eisenach, J. H. (2007). 91 - Control of Blood Pressure—Normal and Abnormal. In S. Gilman (Ed.), *Neurobiology of Disease*, 997-1005. Academic Press. https://doi.org/10.1016/B978-012088 592-3/50093-1

Kamkaew, N., Paracha, T. U., Ingkaninan, K., Waranuch, N., & Chootip, K. (2019). Vasodilatory effects and mechanisms of action of Bacopa monnieri active compounds on rat mesenteric arteries. *Molecules*, *24*(12), 2243.

Kandathil, A., & Chamarthy, M. (2018). Pulmonary vascular anatomy and anatomical variants. *Cardiovascular diagnosis and therapy*, *8*(3), 201.

Karan, R., Agarwal, P., Sinha, M., & Mahato, N. (2021). Recent Advances on Quinazoline Derivatives: A Potential Bioactive Scaffold in Medicinal Chemistry. *ChemEngineering*, *5*(4), 73.

Keravis, T., & Lugnier, C. (2011). Cyclic nucleotide phosphodiesterase (PDE) isozymes as targets of the intracellular signalling network: benefits of PDE inhibitors in various diseases and perspectives for future therapeutic

developments. *British Journal of Pharmacology*, *165*(5), 1288-1305. https://doi.org/10.1111/j.1476-5381.2011.01729.x

Keravis, T., & Lugnier, C. (2012). Cyclic nucleotide phosphodiesterase (PDE) isozymes as targets of the intracellular signalling network: benefits of PDE inhibitors in various diseases and perspectives for future therapeutic developments. *British journal of pharmacology*, *165*(5), 1288-1305.

Kim, Y. H., Choi, H., Lee, J., Hwang, I.-C., Moon, S. K., Kim, S. J., et al. (2008). Quinazolines as potent and highly selective PDE5 inhibitors as potential therapeutics for male erectile dysfunction. *Bioorganic & medicinal chemistry letters*, *18*(23), 6279-6282.

Komas, N., Lugnier, C., Andriantsitohaina, R., & Stoclet, J. C. (1991). Characterisation of cyclic nucleotide phosphodiesterases from rat mesenteric artery. *European Journal of Pharmacology*, *208*(1), 85-87. https://doi.org/10.1016/0922-4106(91)90056-n

Ku, H.-Y., Ahn, H.-J., Seo, K.-A., Kim, H., Oh, M., Bae, S. K., et al. (2008). The Contributions of Cytochromes P450 3A4 and 3A5 to the Metabolism of the Phosphodiesterase Type 5 Inhibitors Sildenafil, Udenafil, and Vardenafil. *Drug Metabolism and Disposition*, *36*(6), 986-990. https://doi.org/10.1124/dmd.107.020099

Kumar, A., Sharma, V., Singh, V. P., Kaundal, M., Gupta, M. K., Bariwal, J., et al. (2015). Herbs to curb cyclic nucleotide phosphodiesterase and their potential role in Alzheimer's disease. *Mechanisms of ageing and development*, *149*, 75-87.

Kummer, W. (2011). Pulmonary Vascular Innervation and Its Role in Responses to Hypoxia. *Proceedings of the American Thoracic Society*, *8*(6), 471-476. https://doi.org/10.1513/pats.201101-013MW

Kurakula, K., Smolders, V., Tura-Ceide, O., Jukema, J. W., Quax, P. H. A., & Goumans, M. J. (2021). Endothelial Dysfunction in Pulmonary Hypertension: Cause or Consequence? *Biomedicines*, *9*(1). https://doi.org/10.3390/biomedicines9010057

Lai, Y.-C., Potoka, K. C., Champion, H. C., Mora, A. L., & Gladwin, M. T. (2014). Pulmonary arterial hypertension: the clinical syndrome. *Circulation research*, *115*(1), 115-130.

Lang, I. M., & Gaine, S. P. (2015). Recent advances in targeting the prostacyclin pathway in pulmonary arterial hypertension. *European Respiratory Review*, *24*(138), 630-641.

Le Ribeuz, H., Capuano, V., Girerd, B., Humbert, M., Montani, D., & Antigny, F. (2020). Implication of Potassium Channels in the Pathophysiology of Pulmonary Arterial Hypertension. *Biomolecules*, *10*(9). https://doi.org/10.3390/biom 10091261

Leal, M. A. S., Aires, R., Pandolfi, T., Marques, V. B., Campagnaro, B. P., Pereira, T. M. C., et al. (2020). Sildenafil reduces aortic endothelial dysfunction and structural damage in spontaneously hypertensive rats: Role of NO, NADPH and COX-1 pathways. *Vascular Pharmacology*, *124*, 106601. https://doi.org/10. 1016/j.vph.2019.106601

Lefebvre, H., Duparc, C., Naccache, A., Lopez, A.-G., Castanet, M., & Louiset, E. (2019). Chapter Thirteen - Paracrine Regulation of Aldosterone Secretion in Physiological and Pathophysiological Conditions. In G. Litwack (Ed.), *Vitamins and Hormones*, *109*, 303-339. Academic Press. https://doi.org/10. 1016/bs.vh.2018.10.001

Li, A. P. (1997). Primary Hepatocyte Cultures as an in Vitro Experimental Model for the Evaluation of Pharmacokinetic Drug–Drug Interactions. In A. P. Li (Ed.), *Advances in Pharmacology* , *43*, 103-130. Academic Press. https://doi.org/10. 1016/S1054-3589(08)60203-3

Li, A. P. (2009). Evaluation of luciferin-isopropyl acetal as a CYP3A4 substrate for human hepatocytes: effects of organic solvents, cytochrome P450 (P450) inhibitors, and P450 inducers. *Drug Metab Dispos*, *37*(8), 1598-1603. https://doi.org/10.1124/dmd.109.027268

Li, Y., Brookes, Z. L., & Kaufman, S. (2005). Acute and chronic effects of relaxin on vasoactivity, myogenic reactivity and compliance of the rat mesenteric arterial and venous vasculature. *Regul Pept*, *132*(1-3), 41-46. https://doi.org/10. 1016/j.regpep.2005.09.009

Liu, H., Liu, Z.-y., & Guan, Q. (2007). Oral sildenafil prevents and reverses the development of pulmonary hypertension in monocrotaline-treated rats. *Interactive CardioVascular and Thoracic Surgery*, *6*(5), 608-613. https://doi.org/10.1510/icvts.2006.147033

Liu, S.-F., Nambiar Veetil, N., Li, Q., Kucherenko, M. M., Knosalla, C., & Kuebler, W. M. (2022). Pulmonary hypertension: Linking inflammation and pulmonary arterial stiffening . *Frontiers in Immunology*, *13*. https://doi.org/10.3389/fimmu.2022.959209

Liu, Z., & Khalil, R. A. (2018). Evolving mechanisms of vascular smooth muscle contraction highlight key targets in vascular disease. *Biochemical Pharmacology*, *153*, 91-122. https://doi.org/10.1016/j.bcp.2018.02.012

Lourenço, A. P., Fontoura, D., Henriques-Coelho, T., & Leite-Moreira, A. F. (2012). Current pathophysiological concepts and management of pulmonary hypertension. *International Journal of Cardiology*, *155*(3), 350-361.

Lynch, T., & Price, A. (2007). The effect of cytochrome P450 metabolism on drug response, interactions, and adverse effects. *Am Fam Physician*, *76*(3), 391-396.

Mahavadi, S., Nalli, A., Al-Shboul, O., & Murthy, K. S. (2014). Inhibition of MLC 20 phosphorylation downstream of Ca 2+ and RhoA: a novel mechanism involving phosphorylation of myosin phosphatase interacting protein (M-RIP) by PKG and stimulation of MLC phosphatase activity. *Cell biochemistry and biophysics*, *68*(1), 1-8.

Mahn, K., Ojo, O. O., Chadwick, G., Aaronson, P. I., Ward, J. P., & Lee, T. H. (2010). Ca^{2+} homeostasis and structural and functional remodelling of airway smooth muscle in asthma. *Thorax*, *65*(6), 547-552.

Malenfant, S., Margaillan, G., Loehr, J. E., Bonnet, S., & Provencher, S. (2013). The emergence of new therapeutic targets in pulmonary arterial hypertension: from now to the near future. *Expert Rev Respir Med*, *7*(1), 43-55. https://doi.org/10.1586/ers.12.83

Mandegar, M., & Yuan, J. X. (2002). Role of K+ channels in pulmonary hypertension. *Vascul Pharmacol*, *38*(1), 25-33. https://doi.org/10.1016/s1537-1891(02)00123-4

Manoury, B., Idres, S., Leblais, V., & Fischmeister, R. (2020). Ion channels as effectors of cyclic nucleotide pathways: Functional relevance for arterial tone regulation. *Pharmacology & therapeutics*, *209*, 107499. https://doi.org/10.1016/j. pharmthera.2020.107499

Maron, B. A., Abman, S. H., Elliott, C. G., Frantz, R. P., Hopper, R. K., Horn, E. M., et al. (2021). Pulmonary Arterial Hypertension: Diagnosis, Treatment, and Novel Advances. *Am J Respir Crit Care Med*, *203*(12), 1472-1487. https://doi.org/10.1164/rccm.202012-4317SO

Martini, F., Ober, W. C., & Nath, J. L. (2011). *Visual anatomy and physiology*. Pearson.

Martyniak, A., & Tomasik, P. J. (2022). A New Perspective on the Renin-Angiotensin System. *Diagnostics*, *13*(1), 16. https://doi.org/10.3390/diagnostics13010016

Maurice, D. H., Ke, H., Ahmad, F., Wang, Y., Chung, J., & Manganiello, V. C. (2014). Advances in targeting cyclic nucleotide phosphodiesterases [Review]. *Nat Rev Drug Discov*, *13*(4), 290-314. https://doi.org/10.1038/nrd4228

McDonnell, A. M., & Dang, C. H. (2013). Basic review of the cytochrome p450 system. *J Adv Pract Oncol*, *4*(4), 263-268. https://doi.org/10.6004/jadpro. 2013.4.4.7

McLaughlin, V. V., & McGoon, M. D. (2006). Pulmonary Arterial Hypertension. *Circulation*, *114*(13), 1417-1431. https://doi.org/10.1161/circulationaha.104. 503540

McLaughlin, V. V., Shah, S. J., Souza, R., & Humbert, M. (2015). Management of pulmonary arterial hypertension. *Journal of the American College of Cardiology*, *65*(18), 1976-1997.

McLaughlin, V. V., Shah, S. J., Souza, R., & Humbert, M. (2015). Management of Pulmonary Arterial Hypertension. *Journal of the American College of Cardiology*, *65*(18), 1976-1997. https://doi.org/10.1016/j.jacc.2015.03.540

Memon, H. A., & Park, M. H. (2017). Pulmonary arterial hypertension in women. *Methodist DeBakey cardiovascular journal*, *13*(4), 224.

Michelakis, E., Tymchak, W., Lien, D., Webster, L., Hashimoto, K., & Archer, S. (2002). Oral sildenafil is an effective and specific pulmonary vasodilator in patients with pulmonary arterial hypertension: comparison with inhaled nitric oxide. *Circulation*, *105*(20), 2398-2403.

Mihalek, A. D., Scott, C. D., & Mazimba, S. (2022). Evaluating Riociguat in the Treatment of Pulmonary Arterial Hypertension: A Real-World Perspective. *Vascular Health and Risk Management*, 823-832.

Miller, M. S. (2015). Phosphodiesterase inhibition in the treatment of autoimmune and inflammatory diseases: Current status and potential. *J. Recept. Ligand Channel Res*, *8*, 19-30.

Mills, K. T., Stefanescu, A., & He, J. (2020). The global epidemiology of hypertension. *Nat Rev Nephrol*, *16*(4), 223-237. https://doi.org/10.1038/s41581-019-0244-2

Misarkova, E., Behuliak, M., Bencze, M., & Zicha, J. (2016). Excitation-contraction coupling and excitation-transcription coupling in blood vessels: their possible interactions in hypertensive vascular remodeling. *Physiol Res*, *65*(2), 173-191.

Misárková, E., Behuliak, M., Bencze, M., & Zicha, J. (2016). Excitation-contraction coupling and excitation-transcription coupling in blood vessels: their possible interactions in hypertensive vascular remodeling. *Physiological research*, *65*(2).

Misra, A., Dwivedi, J., Shukla, S., Kishore, D., & Sharma, S. (2020). Bacterial cell leakage potential of newly synthesized quinazoline derivatives of 1,5-benzodiazepines analogue. *Journal of Heterocyclic Chemistry*, *57*(4), 1545-1558. https://doi.org/10.1002/jhet.3879

Mitchell, J. A., & Kirkby, N. S. (2019). Eicosanoids, prostacyclin and cyclooxygenase in the cardiovascular system. *British journal of pharmacology*, *176*(8), 1038-1050.

Morgado, M., Cairrao, E., Santos-Silva, A. J., & Verde, I. (2012). Cyclic nucleotide-dependent relaxation pathways in vascular smooth muscle. *Cell Mol Life Sci*, *69*(2), 247-266. https://doi.org/10.1007/s00018-011-0815-2

Morrell, N. W. (2014). Pulmonary Circulation. In *Reference Module in Biomedical Sciences*. Elsevier. https://doi.org/10.1016/B978-0-12-801238-3.00216-6

Morrell, N. W., Adnot, S., Archer, S. L., Dupuis, J., Jones, P. L., MacLean, M. R., et al. (2009). Cellular and molecular basis of pulmonary arterial hypertension. *Journal of the American College of Cardiology*, *54*(1 Supplement), S20-S31.

Münzel, T., Sinning, C., Post, F., Warnholtz, A., & Schulz, E. (2008). Pathophysiology, diagnosis and prognostic implications of endothelial dysfunction. *Ann Med*, *40*(3), 180-196. https://doi.org/10.1080/07853890701854702

Murray, F., Insel, P. A., & Yuan, J. X. (2006). Role of O(2)-sensitive K(+) and Ca(2+) channels in the regulation of the pulmonary circulation: potential role of caveolae and implications for high altitude pulmonary edema. *Respir Physiol Neurobiol*, *151*(2-3), 192-208. https://doi.org/10.1016/j.resp.2005.10.003

Nava, E., & Llorens, S. (2019). The Local Regulation of Vascular Function: From an Inside-Outside to an Outside-Inside Model. *Frontiers in Physiology*, *10*. https://doi.org/10.3389/fphys.2019.00729

Nie, X.-q., Chen, H.-h., Zhang, J.-y., Zhang, Y.-j., Yang, J.-w., Pan, H.-j., et al. (2016). Rutaecarpine ameliorates hyperlipidemia and hyperglycemia in fat-fed, streptozotocin-treated rats via regulating the IRS-1/PI3K/Akt and AMPK/ACC2 signaling pathways. *Acta Pharmacologica Sinica*, *37*(4), 483-496. https://doi.org/10.1038/aps.2015.167

Norel, X., Walch, L., Gascard, J. P., deMontpreville, V., & Brink, C. (2004). Prostacyclin release and receptor activation: differential control of human pulmonary venous and arterial tone. *Br J Pharmacol*, *142*(4), 788-796. https://doi.org/10.1038/sj.bjp.0705843

Oguzhan, Y., Melik, S., & Husamettin, G. (2013). Pharmacology of arterial grafts for coronary artery bypass surgery. In S. A. Wilbert (Ed.), *Artery Bypass* (pp. Ch. 15). IntechOpen. https://doi.org/10.5772/54723

Omori, K., & Kotera, J. (2007). Overview of PDEs and their regulation. *Circulation research*, *100*(3), 309-327. https://doi.org/10.1161/01.RES.0000256354.95791.f1

Paracha, T. U., Pobsuk, N., Salaloy, N., Suphakun, P., Pekthong, D., Hannongbua, S., et al. (2019). Elucidation of vasodilation response and structure activity relationships of N^2, N^4-disubstituted quinazoline 2, 4-diamines in a rat pulmonary artery model. *Molecules, 24*(2), 281. https://doi.org/10.3390/molecules24020281

Paul, M., Mehr, A. P., & Kreutz, R. (2006). Physiology of local renin-angiotensin systems. *Physiological reviews, 86*(3), 747-803. https://doi.org/10.1152/physrev.00036.2005

Paulis, L., Líšková, S., Pintérová, M., Dobešová, Z., Kuneš, J., & Zicha, J. (2007). Nifedipine-sensitive noradrenergic vasoconstriction is enhanced in spontaneously hypertensive rats: the influence of chronic captopril treatment. *Acta Physiologica, 191*(4), 255-266. https://doi.org/10.1111/j.1748-1716.2007.01737.x

Peacock, A., Murphy, N., McMurray, J., Caballero, L., & Stewart, S. (2007). An epidemiological study of pulmonary arterial hypertension. *European Respiratory Journal, 30*(1), 104-109. https://doi.org/10.1183/09031936.00092306

Perros, F., Ranchoux, B., Izikki, M., Bentebbal, S., Happé, C., Antigny, F., et al. (2015). Nebivolol for Improving Endothelial Dysfunction, Pulmonary Vascular Remodeling, and Right Heart Function in Pulmonary Hypertension. *Journal of the American College of Cardiology, 65*(7), 668-680. https://doi.org/10.1016/j.jacc.2014.11.050

Pesto, S., Begic, Z., Prevljak, S., Pecar, E., Kukavica, N., & Begic, E. (2016). Pulmonary hypertension–new trends of diagnostic and therapy. *Medical Archives, 70*(4), 303. https://doi.org/10.5455/medarh.2016.70.303-307

Pilewski, R. M., Scheib, E. T., Misage, J. R., Kessler, E., Krifcher, E., & Shapiro, A. P. (1971). Technique of controlled drug assay in hypertension.; V. Comparison of hydrochlorothiazide with a new quinethazone diuretic, metolazone. *Clinical Pharmacology & Therapeutics*, *12*(5), 843-848. https://doi.org/10.1002/ cpt1971125843

Pirahanchi, Y., Marsidi, J. L., & Brown, K. N. (2022). *Physiology, Endothelial Derived Relaxation Factor*. StatPearls Publishing, Treasure Island (FL).

Pluchart, H., Khouri, C., Blaise, S., Roustit, M., & Cracowski, J.-L. (2017). Targeting the prostacyclin pathway: beyond pulmonary arterial hypertension. *Trends in pharmacological sciences*, *38*(6), 512-523. https://doi.org/10.1016/j.tips.2017.03.003

Pobsuk, N., Paracha, T. U., Chaichamnong, N., Salaloy, N., Suphakun, P., Hannongbua, S., et al. (2019). Design, synthesis and evaluation of N^2,N^4-diaminoquinazoline based inhibitors of phosphodiesterase type 5. *Bioorganic & medicinal chemistry letters*, *29*(2), 267-270. https://doi.org/10.1016/j.bmcl.2018.11.043

Poulsen, J. B., Andersen, K. R., Kjær, K. H., Vestergaard, A. L., Justesen, J., & Martensen, P. M. (2012). Characterization of human phosphodiesterase 12 and identification of a novel 2′-5′ oligoadenylate nuclease–The ectonucleotide pyrophosphatase/phosphodiesterase 1. *Biochimie*, *94*(5), 1098-1107. https://doi.org/10.1016/j.biochi.2012.01.012

Priest, R. M., Hucks, D., & Ward, J. P. (1997). Noradrenaline, beta-adrenoceptor mediated vasorelaxation and nitric oxide in large and small pulmonary arteries of the rat. *Br J Pharmacol*, *122*(7), 1375-1384. https://doi.org/10.1038/sj.bjp.0701528

Pugsley, M., & Tabrizchi, R. (2000). The vascular system: An overview of structure and function. *Journal of pharmacological and toxicological methods*, *44*(2), 333-340. https://doi.org/10.1016/S1056-8719(00)00125-8

Rahimi, K., Bidel, Z., Nazarzadeh, M., Copland, E., Canoy, D., Ramakrishnan, R., et al. (2021). Pharmacological blood pressure lowering for primary and secondary prevention of cardiovascular disease across different levels of blood pressure: an individual participant-level data meta-analysis. *The Lancet, 397*(10285), 1625-1636. https://doi.org/10.1016/S0140-6736(21)00590-0

Rahimi, R., Ghiasi, S., Azimi, H., Fakhari, S., & Abdollahi, M. (2010). A review of the herbal phosphodiesterase inhibitors; future perspective of new drugs. *Cytokine, 49*(2), 123-129. https://doi.org/10.1016/j.cyto.2009.11.005

Raja, S. G., Danton, M. D., MacArthur, K. J., & Pollock, J. C. (2006). Treatment of pulmonary arterial hypertension with sildenafil: from pathophysiology to clinical evidence. *J Cardiothorac Vasc Anesth*, *20*(5), 722-735. https://doi.org/10.1053/j.jvca.2005.12.011

Ramani, G. V., & Park, M. H. (2010). Update on the clinical utility of sildenafil in the treatment of pulmonary arterial hypertension. *Drug design, development and therapy*, *4*, 61.

Ramani, G. V., & Park, M. H. (2010). Update on the clinical utility of sildenafil in the treatment of pulmonary arterial hypertension. *Drug design, development and therapy*, *4*, 61-70. http://www.ncbi.nlm.nih.gov/pmc/articles/PMC2880338/

Rich, S., Seidlitz, M., Dodin, E., Osimani, D., Judd, D., Genthner, D., et al. (1998). The short-term effects of digoxin in patients with right ventricular dysfunction from pulmonary hypertension. *Chest*, *114*(3), 787-792. https://doi.org/10. 1378/ chest.114.3.787

Rinaldi, G. J., Grand, C., & Cingolani, H. E. (1991). Characteristics of the fast and slow components of the response to noradrenaline in rat aorta. *Can J Cardiol, 7*(7), 316-322.

Robinson, B. F. (1985). Calcium-entry blocking agents in the treatment of systemic hypertension. *The American Journal of Cardiology*, *55*(3), B102-B106. https://doi.org/10.1016/0002-9149(85)90618-6

Rohini, R., Reddy, P. M., Shanker, K., Hu, A., & Ravinder, V. (2010). Antimicrobial study of newly synthesized 6-substituted indolo [1, 2-c] quinazolines. *European journal of medicinal chemistry*, *45*(3), 1200-1205. https://doi.org/ 10.1016/ j.ejmech.2009.11.038

Rorbach, J., Nicholls, T. J., & Minczuk, M. (2011). PDE12 removes mitochondrial RNA poly (A) tails and controls translation in human mitochondria. *Nucleic Acids Research*, *39*(17), 7750-7763.

Rotella, D. P., Sun, Z., Zhu, Y., Krupinski, J., Pongrac, R., Seliger, L., et al. (2000). N-3-substituted imidazoquinazolinones: Potent and selective PDE5 inhibitors as potential agents for treatment of erectile dysfunction. *Journal of medicinal chemistry*, *43*(7), 1257-1263. https://doi.org/10.1021/jm000081+

Rubin, L. J., Badesch, D. B., Barst, R. J., Galie, N., Black, C. M., Keogh, A., et al. (2002). Bosentan therapy for pulmonary arterial hypertension. *New England Journal of Medicine*, *346*(12), 896-903. https://doi.org/10.1056/NEJMoa012212

Rubin, L. J., Mendoza, J., Hood, M., McGoon, M., Barst, R., Williams, W. B., et al. (1990). Treatment of primary pulmonary hypertension with continuous intravenous prostacyclin (Epoprostenol). *Annals of Internal Medicine*, *112*(7), 485-491. https://doi.org/10.7326/0003-4819-112-7-485

Rudinsky, B., Bell, A., Hipps, R., & Meadow, W. (1993). Relative contribution of endothelium-derived relaxation factor to vascular tone in the systemic, pulmonary, and cerebral circulations of piglets. *Dev Pharmacol Ther*, *20*(3-4), 152-161. https://doi.org/10.1159/000457556

Rybalkin, S. D., Yan, C., Bornfeldt, K. E., & Beavo, J. A. (2003). Cyclic GMP Phosphodiesterases and Regulation of Smooth Muscle Function. *Circulation research*, *93*(4), 280.

Salvi, S. S. (1999). Alpha 1-adrenergic hypothesis for pulmonary hypertension. *Chest*, *115*(6), 1708-1719. https://doi.org/10.1378/chest.115.6.1708

Sampson, L. J., Hinton, J. M., & Garland, C. J. (2001). Evidence for expression and function of phosphodiesterase type 5 (PDE-V) in rat resistance arteries. *British Journal of Pharmacology*, *132*(1), 13-17. https://doi.org/10.1038/sj.bjp.0703831

Santos-Gomes, J., Gandra, I., Adão, R., Perros, F., & Brás-Silva, C. (2022). An overview of circulating pulmonary arterial hypertension biomarkers. *Frontiers in Cardiovascular Medicine*, *9*, 924873. https://doi.org/10.3389/fcvm.2022.924873

Santos-Ribeiro, D., Mendes-Ferreira, P., Maia-Rocha, C., Adão, R., Leite-Moreira, A. F., & Brás-Silva, C. (2016). Pulmonary arterial hypertension: Basic knowledge for clinicians. *Archives of cardiovascular diseases*, *109*(10), 550-561. https://doi.org/10.1016/j.acvd.2016.03.004

Satoh, K., Shimokawa, H., & Berk, B. C. (2010). Cyclophilin A: promising new target in cardiovascular therapy. *Circulation journal : official journal of the Japanese Circulation Society*, *74*(11), 2249-2256. https://doi.org/10.1253/circj.cj-10-0904

Schermuly, R. T., Stasch, J. P., Pullamsetti, S. S., Middendorff, R., Müller, D., Schlüter, K. D., et al. (2008). Expression and Function of Soluble Guanylate Cyclase in Pulmonary Arterial Hypertension. *European Respiratory Journal*. https://doi.org/10.1183/09031936.00114407

Schuster, R., Zeindl, L., Holzer, W., Khumpirapang, N., Okonogi, S., Viernstein, H., et al. (2017). Eulophia macrobulbon – an orchid with significant anti-inflammatory and antioxidant effect and anticancerogenic potential exerted by its root extract. *Phytomedicine*, *24*, 157-165. https://doi.org/10.1016/j.phymed.2016.11.018

Secomb, T. W. (2016). Hemodynamics. *Compr Physiol*, *6*(2), 975-1003. https://doi.org/10.1002/cphy.c150038

Selvam, T. P., & Kumar, P. V. (2015). Quinazoline marketed drugs. *Research in Pharmacy*, *1*(1).

Shao, D., Park, J. E. S., & Wort, S. J. (2011). The role of endothelin-1 in the pathogenesis of pulmonary arterial hypertension. *Pharmacological Research*, *63*(6), 504-511. https://doi.org/10.1016/j.phrs.2011.03.003

Shaul, P. W., Magness, R. R., Muntz, K. H., DeBeltz, D., & Buja, L. M. (1990). Alpha 1-adrenergic receptors in pulmonary and systemic vascular smooth muscle. Alterations with development and pregnancy. *Circulation research*, *67*(5), 1193-1200. https://doi.org/10.1161/01.RES.67.5.1193

Sheng, Y., & Zhu, L. (2018). The crosstalk between autonomic nervous system and blood vessels. *Int J Physiol Pathophysiol Pharmacol*, *10*(1), 17-28.

Sheweita, S. A., Wally, M., & Hassan, M. (2016). Erectile dysfunction drugs changed the protein expressions and activities of drug-metabolising enzymes in the liver of male rats. *Oxid Med Cell Longev*, *2016*, 4970906. https://doi.org/10.1155/2016/4970906

Shi, L., Tang, J., Tong, L., & Liu, Z. (2014). Risk of interstitial lung disease with gefitinib and erlotinib in advanced non-small cell lung cancer: A systematic review and meta-analysis of clinical trials. *Lung Cancer*, *83*(2), 231-239. https://doi.org/10.1016/j.lungcan.2013.11.016

Shimada, T., & Guengerich, F. P. (2006). Inhibition of Human Cytochrome P450 1A1-, 1A2-, and 1B1-Mediated Activation of Procarcinogens to Genotoxic Metabolites by Polycyclic Aromatic Hydrocarbons. *Chemical Research in Toxicology*, *19*(2), 288-294. https://doi.org/10.1021/tx050291v

Shimoda, L. A. (2006). Pulmonary circulation. In G. J. Laurent & S. D. Shapiro (Eds.), *Encyclopedia of Respiratory Medicine* (pp. 537-544). Academic Press. https://doi.org/10.1016/B0-12-370879-6/00332-X

Silverthorn, D. U. (2004). *Human physiology : an integrated approach*. Pearson/Benjamin Cummings.

Simon, M. A., & Pinsky, M. R. (2011). Right ventricular dysfunction and failure in chronic pressure overload. *Cardiol Res Pract*, *2011*, 568095. https://doi.org/10.4061/2011/568095

Simonneau, G., Montani, D., Celermajer, D. S., Denton, C. P., Gatzoulis, M. A., Krowka, M., et al. (2019). Haemodynamic definitions and updated clinical classification of pulmonary hypertension. *European Respiratory Journal*, *53*(1), 1801913. https://doi.org/10.1183/13993003.01913-2018

Siques, P., Brito, J., & Pena, E. (2018). Reactive oxygen species and pulmonary vasculature during hypobaric hypoxia. *Frontiers in physiology*, *9*, 865. https://doi.org/10.3389/fphys.2018.00865

Soldatow, V. Y., Lecluyse, E. L., Griffith, L. G., & Rusyn, I. (2013). *In vitro* models for liver toxicity testing. *Toxicol Res (Camb)*, *2*(1), 23-39. https://doi.org/10.1039/c2tx20051a

Soma, S., Takahashi, H., Muramatsu, M., Oka, M., & Fukuchi, Y. (1999). Localization and distribution of endothelin receptor subtypes in pulmonary vasculature of normal and hypoxia-exposed rats. *Am J Respir Cell Mol Biol*, *20*(4), 620-630. https://doi.org/10.1165/ajrcmb.20.4.3356

Sommer, N., Ghofrani, H. A., Pak, O., Bonnet, S., Provencher, S., Sitbon, O., et al. (2021). Current and future treatments of pulmonary arterial hypertension. *British journal of pharmacology*, *178*(1), 6-30.

Srinivas, N. R. (2016). Clinical drug-drug interactions of bosentan, a potent endothelial receptor antagonist, with various drugs: Physiological role of enzymes and transporters. *Gen Physiol Biophys*, *35*(3), 243-258. https://doi.org/10.4149/gpb_2015050

Stanaszek, W. F., Kellerman, D., Brogden, R. N., & Romankiewicz, J. A. (1983). Prazosin update. *Drugs*, *25*(4), 339-384. https://doi.org/10.2165/00003495-198325040-00002

Stenmark, K. R., Fagan, K. A., & Frid, M. G. (2006). Hypoxia-induced pulmonary vascular remodeling: cellular and molecular mechanisms. *Circulation research*, *99*(7), 675-691. https://doi.org/10.1161/01.RES.0000243584.45145.3f

Stenmark, K. R., Meyrick, B., Galie, N., Mooi, W. J., & McMurtry, I. F. (2009). Animal models of pulmonary arterial hypertension: the hope for etiological discovery and pharmacological cure. *Am J Physiol Lung Cell Mol Physiol*, *297*(6), L1013-1032. https://doi.org/10.1152/ajplung.00217.2009

Stewart DJ, Levy RD, Cernacek P, & LanglebenD. (1991). Increased plasma endothelin-1 in pulmonary hypertension: Marker or mediator of disease? *Annals of Internal Medicine*, *114*(6), 464-469. https://doi.org/10.7326/0003-4819-114-6-464

Suresh, K., & Shimoda, L. A. (2016). Lung Circulation. *Compr Physiol*, *6*(2), 897-943. https://doi.org/10.1002/cphy.c140049

Sysol, J., & Machado, R. (2018). Classification and pathophysiology of pulmonary hypertension. *Continuing Cardiology Education*, *4*(1), 2-12. https://doi.org/10.1002/cce2.71

Tettey, A., Jiang, Y., Li, X., & Li, Y. (2021). Therapy for pulmonary arterial hypertension: glance on nitric oxide pathway. *Frontiers in pharmacology, 12*. https://doi.org/10.3389/fphar.2021.767002

Thenappan, T., Ryan, J. J., & Archer, S. L. (2012). Evolving epidemiology of pulmonary arterial hypertension. *American Thoracic Society*.

Thomas, G. D. (2011). Neural control of the circulation. *Advances in Physiology Education*, *35*(1), 28-32. https://doi.org/10.1152/advan.00114.2010

Tiberi, F., & Corinaldesi, G. (1981). Clinical trial of the activity and therapeutic effectiveness of 3 drugs with diuretic and antihypertensive action. *Minerva Medica*, *72*(2), 95-100.

To-on, K., Chatturong, U., Panklai, T., Palang, I., Inchan, A., Wisutthathum, S., et al. (2022). Isolation of intrapulmonary artery and smooth muscle cells to investigate vascular responses. *JoVE*(184), e63686. https://doi.org/10.3791/63686

Toque, H. A., Teixeira, C. E., Priviero, F. B., Morganti, R. P., Antunes, E., & De Nucci, G. (2008). Vardenafil, but not sildenafil or tadalafil, has calcium-channel blocking activity in rabbit isolated pulmonary artery and human washed platelets. *Br J Pharmacol*, *154*(4), 787-796. https://doi.org/10.1038/bjp. 2008.141

Touyz, R. M., Alves-Lopes, R., Rios, F. J., Camargo, L. L., Anagnostopoulou, A., Arner, A., et al. (2018). Vascular smooth muscle contraction in hypertension. *Cardiovascular Research*, *114*(4), 529-539. https://doi.org/10.1093/cvr/cvy023

Triggle, C. R., Samuel, S. M., Ravishankar, S., Marei, I., Arunachalam, G., & Ding, H. (2012). The endothelium: influencing vascular smooth muscle in many ways. *Canadian journal of physiology and pharmacology*, *90*(6), 713-738. https://doi.org/10.1139/y2012-073

Truog, W. E., & Kinsella, J. P. (2017). Pulmonary gas exchange in the developing lung. In R. A. Polin, S. H. Abman, D. H. Rowitch, W. E. Benitz, & W. W. Fox (Eds.), *Fetal and Neonatal Physiology (Fifth Edition)* (pp. 714-724). Elsevier. https://doi.org/10.1016/B978-0-323-35214-7.00070-6

Tuder, R. M. (2017). Pulmonary vascular remodeling in pulmonary hypertension. *Cell Tissue Res*, *367*(3), 643-649. https://doi.org/10.1007/s00441-016-2539-y

Tykocki, N. R., Boerman, E. M., & Jackson, W. F. (2017). Smooth muscle ion channels and regulation of vascular tone in resistance arteries and arterioles. *Compr Physiol*, *7*(2), 485-581. https://doi.org/10.1002/cphy.c160011

Unger, T., Borghi, C., Charchar, F., Khan, N. A., Poulter, N. R., Prabhakaran, D., et al. (2020). 2020 International Society of Hypertension Global Hypertension Practice Guidelines. *Hypertension*, *75*(6), 1334-1357. https://doi.org/10.1161/HYPERTENSIONAHA.120.15026

Vaidya, B., & Gupta, V. (2015). Novel therapeutic approaches for pulmonary arterial hypertension: Unique molecular targets to site-specific drug delivery. *Journal of Controlled Release*, *211*, 118-133. http://doi.org/10.1016/j.jconrel.2015.05.287

Vaillancourt, M., Chia, P., Sarji, S., Nguyen, J., Hoftman, N., Ruffenach, G., et al. (2017). Autonomic nervous system involvement in pulmonary arterial hypertension. *Respir Res*, *18*(1), 201. https://doi.org/10.1186/s12931-017-0679-6

Vaja, R., & Rana, M. (2020). Drugs and the liver. *Anaesthesia & Intensive Care Medicine*, *21*(10), 517-523. https://doi.org/10.1016/j.mpaic.2020.07.001

Vaughan, C. J., & Gotto, A. M. (2004). Update on Statins: 2003. *Circulation*, *110*(7), 886-892. https://doi.org/10.1161/01.CIR.0000139312.10076.BA

Verdecchia, P., Cavallini, C., & Angeli, F. (2022). Advances in the treatment strategies in hypertension: Present and future. *Journal of Cardiovascular Development and Disease*, *9*(3), 72. https://doi.org/10.3390/jcdd9030072

Verhoeven, F., Totoson, P., Marie, C., Prigent-Tessier, A., Wendling, D., Tournier-Nappey, M., et al. (2017). Diclofenac but not celecoxib improves endothelial function in rheumatoid arthritis: A study in adjuvant-induced arthritis. *Atherosclerosis*, *266*, 136-144. https://doi.org/10.1016/j.atherosclerosis.2017.09.033

Veyssier-Belot, C., & Cacoub, P. (1999). Role of endothelial and smooth muscle cells in the physiopathology and treatment management of pulmonary hypertension. *Cardiovascular research*, *44*(2), 274-282. https://doi.org/10.1016/s0008-6363(99)00230-8

Walker, S. D., Dora, K. A., Ings, N. T., Crane, G. J., & Garland, C. J. (2001). Activation of endothelial cell IK_{Ca} with 1-ethyl-2-benzimidazolinone evokes smooth muscle hyperpolarization in rat isolated mesenteric artery. *Br J Pharmacol*, *134*(7), 1548-1554. https://doi.org/10.1038/sj.bjp.0704415

Wallis, R. M. (1999). The pharmacology of sildenafil, a novel and selective inhibitor of phosphodiesterase (PDE) type 5. *Nihon Yakurigaku Zasshi*, *114 Suppl 1*, 22p-26p. https://doi.org/10.1254/fpj.114.supplement_22

Ward, J. P., & Linden, R. W. (2017). *Physiology at a Glance*. John Wiley & Sons.

Waypa, G. B., & Schumacker, P. T. (2010). Hypoxia-induced changes in pulmonary and systemic vascular resistance: Where is the O2 sensor? *Respiratory Physiology & Neurobiology*, *174*(3), 201-211. https://doi.org/10.1016/j.resp.2010.08.007

Wilkens, H., Guth, A., König, J., Forestier, N., Cremers, B., Hennen, B., et al. (2001). Effect of inhaled iloprost plus oral sildenafil in patients with primary pulmonary hypertension. *Circulation*, *104*(11), 1218-1222. https://doi.org/10.1161/hc3601. 096826

Wisutthathum, S., Chootip, K., Martin, H., Ingkaninan, K., Temkitthawon, P., Totoson, P., et al. (2018a). Vasorelaxant and Hypotensive Effects of an Ethanolic Extract of Eulophia macrobulbon and Its Main Compound 1-(4′-Hydroxybenzyl)-4,8-Dimethoxyphenanthrene-2,7-Diol. *Frontiers in pharmacology*, *9*. https://doi.org/10.3389/fphar.2018.00484

Wisutthathum, S., Chootip, K., Martin, H., Ingkaninan, K., Temkitthawon, P., Totoson, P., et al. (2018b). Vasorelaxant and hypotensive effects of an ethanolic extract of *Eulophia macrobulbon* and its main compound 1-(4′-hydroxybenzyl)-4, 8-dimethoxyphenanthrene-2, 7-diol. *Frontiers in pharmacology*, *9*, 484. https://doi.org/10.3389/fphar.2018.00484

Wisutthathum, S., Demougeot, C., Totoson, P., Adthapanyawanich, K., Ingkaninan, K., Temkitthawon, P., et al. (2018). *Eulophia macrobulbon* extract relaxes rat isolated pulmonary artery and protects against monocrotaline-induced pulmonary arterial hypertension. *Phytomedicine*, *50*, 157-165. https://doi.org/10.1016/j.phymed.2018.05.014

Wood, E. R., Bledsoe, R., Chai, J., Daka, P., Deng, H., Ding, Y., et al. (2015). The role of phosphodiesterase 12 (PDE12) as a negative regulator of the innate immune response and the discovery of antiviral inhibitors. *Journal of Biological Chemistry*, *290*(32), 19681-19696.

Xu, S., Ilyas, I., Little, P. J., Li, H., Kamato, D., Zheng, X., et al. (2021). Endothelial Dysfunction in Atherosclerotic Cardiovascular Diseases and Beyond: From Mechanism to Pharmacotherapies. *Pharmacol Rev*, *73*(3), 924-967. https://doi.org/10.1124/pharmrev.120.000096

Xu, Y., Liu, H., Chen, J., & Zhou, Q. (2010). Acquired resistance of lung adenocarcinoma to EGFR-tyrosine kinase inhibitors gefitinib and erlotinib. *Cancer Biology & Therapy*, *9*(8), 572-582. https://doi.org/10.4161/cbt.9.8.11881

Yanagisawa, M., Kurihara, H., Kimura, S., Tomobe, Y., Kobayashi, M., Mitsui, Y., et al. (1988). A novel potent vasoconstrictor peptide produced by vascular endothelial cells. *Nature*, *332*(6163), 411-415. https://doi.org/10.1038/332411a0

Yoon, J. S., Jeong, E. J., Yang, H., Kim, S. H., Sung, S. H., & Kim, Y. C. (2012). Inhibitory alkaloids from Dictamnus dasycarpus root barks on lipopolysaccharide-induced nitric oxide production in BV2 cells. *Journal of Enzyme Inhibition and Medicinal Chemistry*, *27*(4), 490-494. https://doi.org/10.3109/14756366.2011.598151

Zhao, M., Ma, J., Li, M., Zhang, Y., Jiang, B., Zhao, X., et al. (2021). Cytochrome P450 enzymes and drug metabolism in humans. *International journal of molecular sciences*, *22*(23).

Zhao, Y., Vanhoutte, P. M., & Leung, S. W. (2015). Vascular nitric oxide: Beyond eNOS. *Journal of pharmacological sciences*, *129*(2), 83-94. https://doi.org/10.1016/j.jphs.2015.09.002

Zirak, M. R., Rahimian, R., Mousavizadeh, K., & Dehpour, A. R. (2021). Mechanisms underlie the proconvulsant effects of sildenafil. *Biomedicine and Pharmacotherapy*, *134*.

Zisaki, A., Miskovic, L., & Hatzimanikatis, V. (2015). Antihypertensive drugs metabolism: An update to pharmacokinetic profiles and computational approaches. *Curr Pharm Des*, *21*(6), 806-822. https://doi.org/10.2174/1381612820666141024151119

Zuo, S.-J., Li, S., Yu, R.-H., Zheng, G.-X., Cao, Y.-X., & Zhang, S.-Q. (2014a). Discovery of novel 3-benzylquinazolin-4 (3*H*)-ones as potent vasodilative agents. *Bioorganic & medicinal chemistry letters*, *24*(24), 5597-5601. https://doi.org/10.1016/j.bmcl.2014.10.092

Zuo, S.-J., Li, S., Yu, R.-H., Zheng, G.-X., Cao, Y.-X., & Zhang, S.-Q. (2014b). Discovery of novel 3-benzylquinazolin-4(3H)-ones as potent vasodilative agents. *Bioorganic & Medicinal Chemistry Letters*, *24*(24), 5597-5601. https://doi.org/10.1016/j.bmcl.2014.10.092

APPENDIXES

APPENDIX A ANIMAL ETHIC

1. Experimental protocols approved by the local committees for ethics in animal experimentation of Naresuan University Animal Care and Use Committee (NUACUC), Naresuan University, Thailand (Animal Ethics Approval Number: NU-AE620304)

เอกสารรับรองโครงการ
คณะกรรมการกำกับดูแลการดำเนินการต่อสัตว์เพื่องานทางวิทยาศาสตร์
มหาวิทยาลัยนเรศวร (คกส.)

ชื่อโครงการ	ฤทธิ์การคลายตัวของหลอดเลือดแดงปอดที่แยกจากหนูและกลไกการออกฤทธิ์ของอนุพันธ์ควินาโซลีน Vasorelaxant effect on rat isolated pulmonary artery and mechanism of action of quinazoline derivatives
เลขที่โครงการ	NU-AE620304
เลขที่เอกสารรับรอง	62 01 006
ประเภทการรับรอง	เต็มรูปแบบ
ชื่อหัวหน้าโครงการ/ผู้ยื่นขอฯ	รศ.ดร.กรองกาญจน์ ชูทิพย์
สังกัดหน่วยงาน /คณะ	วิทยาศาสตร์การแพทย์
วันที่รับรอง	16 พฤษภาคม 2562
วันสิ้นสุดการรับรอง	16 พฤษภาคม 2565

ขอรับรองว่าโครงการวิจัยนี้ ได้รับการรับรองด้านจรรยาบรรณการใช้สัตว์
จากคณะกรรมการกำกับดูแลการดำเนินการต่อสัตว์เพื่องานทางวิทยาศาสตร์ มหาวิทยาลัยนเรศวร (คกส.)

(รองศาสตราจารย์ ดร.รัตติมา จีนาพงษา)
ประธานคณะกรรมการกำกับดูแลการดำเนินการต่อสัตว์เพื่องานทางวิทยาศาสตร์ (คกส.)
มหาวิทยาลัยนเรศวร

หมายเหตุ เอกสารรับรองฉบับนี้ใช้ควบคู่กับหนังสือราชการ
เลขที่ อว 0603.01.16/0195 ลงวันที่ 23 พ.ค. 2562

2. Experimental protocols approved by the local committees for ethics in animal experimentation of Franche-Comté University, Besançon, France (No. 2019-003-PT-5PR).

Liberté • Égalité • Fraternité
RÉPUBLIQUE FRANÇAISE

MINISTERE DE L'ENSEIGNEMENT SUPERIEUR,
DE LA RECHERCHE ET DE L'INNOVATION

Paris, le 16 décembre 2019

Objet : Notification de décision relative à l'autorisation de projet utilisant des animaux à des fins scientifiques

Direction générale de la recherche et de l'innovation

Service de la performance, du financement et de la contractualisation avec les organismes de recherche

Département des pratiques de recherche réglementées

Cellule Animaux utilisés à des Fins Scientifiques - AFiS -

Affaire suivie par
Véronique Delassault
Responsable administrative de la cellule AFiS

Tél : 01 55 55 97 27
veronique.delassault
@recherche.gouv.fr

autorisation-projet
@recherche.gouv.fr

1 rue Descartes
75231 Paris Cedex 05

En application des dispositions du code rural et de la pêche maritime, notamment ses articles R.214-87 à R.214-126, le projet :

- référencé sous le numéro APAFIS#8699-2017010210088460 v6
- ayant pour titre : Mécanismes et traitements de la dysfonction endothéliale : application à la polyarthrite rhumatoïde et à la santé cérébrale.
- déposé par l'établissement utilisateur : Animalerie centrale Université de Franche-Comté (UFC)/UFR "Sciences Médicales & Pharmaceutiques (SMP)" - SFR "IBCT" FED4234, numéro d'agrément A2505610, dont le responsable est Monsieur Emmanuel SAMAIN,
- et dont la responsabilité de la mise en œuvre générale du projet et de sa conformité à l'autorisation est assurée par : Madame Céline PR DEMOUGEOT, Madame Perle DR TOTOSON, Madame Sylvie DR DEVAUX,

est autorisé.

L'autorisation de projet est accordée, sous réserve de la validité de l'agrément de l'établissement utilisateur, pour une durée de 5 ans à compter de la présente notification.

Le projet précité a été évalué sur le plan éthique par le comité d'éthique en expérimentation animale n°058 et a reçu un avis favorable.

Ce projet fera l'objet, à l'issue de sa réalisation, d'une appréciation rétrospective. Il vous appartiendra de prendre contact directement avec le comité d'éthique.

Pour la ministre et par délégation
le chef du département
des pratiques de recherche réglementées

Laurent PINON

Monsieur Emmanuel SAMAIN
Animalerie centrale Université de Franche-Comté (UFC)/UFR "Sciences Médicales & Pharmaceutiques (SMP)" - SFR "IBCT" FED4234

AVIS DU COMITÉ D'ÉTHIQUE
(à transmettre au secrétariat autorisation de projet :
autorisation-projet@recherche.gouv.fr)

Date : 08.12.2019

Référence du dossier : APAFiS #8699 (Fichier téléchargé « Mécanismesettraiteme_2017010210088460_v6 P. Totoson 11.10.2019.apafis »

Titre du Projet : Mécanismes et traitements de la dysfonction endothéliale : application à la polyarthrite rhumatoïde et à la santé cérébrale - Dr Perle TOTOSON & Pr Céline DEMOUGEOT

1- Avis éthique sur le projet : ☒ Favorable
☐ Défavorable

Motif(s) en cas d'avis défavorable :

2- Proposition de reclassement des procédures expérimentales selon le degré de gravité indiqué par le responsable de projet : ☐ **oui** ☒ **non**

Procédure(s) reclassée(s) et proposition de reclassement :
- procédure n° :
  reclassement :

(le bloc Procédure(s) reclassée(s) et proposition de reclassement est à reproduire le cas échéant)

3- En application de l'article R.214-120 du décret n°2013-118 du 1er février 2013, le projet devra t'il bénéficier d'une appréciation rétrospective à l'issue de sa réalisation : ☒ **oui** ☐ **non**

4- Le cas échéant (cf point 4.3 du dossier), avis sur la réutilisation d'un animal pour autant que l'animal n'ait pas été utilisé, préalablement à ce projet, plus d'une fois dans une procédure expérimentale entraînant une douleur intense, de l'angoisse ou une souffrance équivalente (article R.214-113 du décret n°2013-118 du 1er février 2013) :

☐ Favorable ☐ Défavorable **NA**

Motif(s) en cas d'avis défavorable :

Nom du Comité d'éthique/**Comité d'Ethique Bisontin en Expérimentation Animale (CEBEA) #58**

et signature du Président

Pr Dominique MEILLET, PU-PH

APPENDIX B PUBLICATIONS

First publication

Vascular Pharmacology 147 (2022) 107111

Contents lists available at ScienceDirect

Vascular Pharmacology

journal homepage: www.elsevier.com/locate/vph

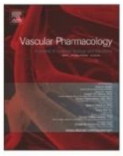

Quinazoline-based human phosphodiesterase 5 inhibitors exhibited a selective vasorelaxant effect on rat isolated pulmonary arteries involving NO-sGC-cGMP pathway and calcium inhibitory effects

Usana Chatturong [a,b], Hélène Martin [b], Perle Totoson [b], Kornkanok Ingkaninan [c], Prapapan Temkitthawon [c], Saharat Sermsenaphorn [d], Thanachon Somarin [d], Adchatawut Konsue [d], M. Paul Gleeson [d], Céline Demougeot [b,1], Krongkarn Chootip [a,*,1]

[a] Department of Physiology, Faculty of Medical Science and Center of Excellence for Innovation in Chemistry, Naresuan University, Phitsanulok 65000, Thailand
[b] PEPITE EA4267, Université Bourgogne Franche-Comté, Besançon 25030, France
[c] Department of Pharmaceutical Chemistry and Pharmacognosy, Faculty of Pharmaceutical Sciences and Center of Excellence for Innovation in Chemistry, Naresuan University, Phitsanulok 65000, Thailand
[d] Department of Biomedical Engineering, Faculty of Engineering, King Mongkut's Institute of Technology, Ladkrabang, Bangkok 10520, Thailand

ARTICLE INFO

Keywords:
Quinazoline derivatives
PDE5
Vasorelaxation
Rat pulmonary artery
Cytotoxicity
CYP activities

ABSTRACT

Phosphodiesterase 5 (PDE5) inhibitors are an attractive option among the currently available therapies in the management of pulmonary arterial hypertension (PAH). Good selectivity for PDE5 is associated with reduced side effects and greater vasorelaxant effect on pulmonary arteries (PA). This study investigated the vasorelaxant effects of a series of quinazoline-based PDE5 inhibitors and their precise mechanisms action using rat isolated PA and aorta, as compared to sildenafil. Their effects on rat hepatocytes (viability and CYP activities) were also evaluated. Compounds **5** and **11** displayed lower human PDE5 IC_{50} of the analogs studied here and induced a greater relaxant effect on PA (EC_{50} 0.94 ± 0.30 and 1.03 ± 0.23 μM, respectively). As compared to sildenafil (EC_{50} = 0.05 ± 0.02 μM on PA), the relaxant effect of **5** and **11** on PA was lower but their selectivity for PA compared to aorta was higher. The effects of **5** and **11** were reduced by N^G-nitro-L-arginine methyl ester, 1H-[1,2,4]oxadiazolo[4,3-*a*]quinoxaline-1-one, but not by indomethacin or potassium channels blockers. They also enhanced the relaxant effect of sodium nitroprusside, and inhibited extracellular Ca^{2+} influx and intracellular Ca^{2+}release. Compounds **5** and **11** did not reduce hepatocyte viability except at concentration > 10 μM, inhibited CYP3A at 10 μM, like sildenafil, but did not induce CYP1A. In conclusion, this study identified 2 quinazoline analogues with good PDE5 inhibitory activity and good selectivity for the pulmonary vasculature. Their relaxant effect involves both the potentiation of nitric oxide-sGC-cGMP pathway and calcium inhibition. These compounds are potential leads for developing new drugs for PAH.

1. Introduction

Pulmonary arterial hypertension (PAH) is associated with pulmonary vascular remodeling and a continuous increase in pulmonary vascular resistance. This results in elevated pulmonary arterial pressure leading to right ventricular hypertrophy, right heart failure, and ultimately death if the condition remains untreated [1]. PAH pathogenesis begins with structural changes of the small pulmonary artery (PA) from the narrowing or obstruction, caused by several factors including hypoxia, genetic susceptibility, enhanced inflammation, vasoconstriction, vascular smooth muscle cell (VSMC) proliferation, and endothelial dysfunction [2]. Phosphodiesterase 5 (PDE5) inhibitors are an important option in treating PAH [3]. PDE5, a major PDE isoform upregulated in PAH, specifically hydrolyses cyclic guanosine monophosphate (cGMP) in VSMCs into 5′GMP, thus a high expression of PDE5 could reduce cGMP and cause vasoconstriction. Therefore, PDE5 inhibitors are powerful vasorelaxant drugs [4,5]. Among them, sildenafil is a first-line drug for the treatment of PAH, in monotherapy or in association with

* Corresponding author.
E-mail address: krongkarnc@nu.ac.th (K. Chootip).
[1] Contributed equally to the work

https://doi.org/10.1016/j.vph.2022.107111
Received 26 July 2022; Received in revised form 16 September 2022; Accepted 20 September 2022
Available online 24 September 2022

endothelin receptor antagonists [4]. Most of the side effects of sildenafil are secondary to a loss of selectivity for PDE5 (*e.g.*, visual disturbances) and/or for the pulmonary circulation (*e.g.*, systemic hypotension, headache, flushing, nasal congestion) [6–8]. In addition, although the hepatic toxicity of sildenafil is rare, some cases of sildenafil-associated hepatotoxicity have been reported in the last decade [9]. Moreover, sildenafil is suspected to be a weak inhibitor of cytochrome P450 (CYP) 1A2, 2C9, 2C19, 2D6, 2E1 and 3A4 ($IC_{50} > 150$ μM) [10]. Altogether, these data encourage the identification of new PDE5 inhibitors to improve the management of PAH.

Several quinazoline derivatives have been reported to treat hypertension [11] and erectile dysfunction [12,13]. Twenty N^2,N^4-disubstituted quinazoline 2,4-diamines, with a pharmacophore similar to sildenafil, were developed as PDE5 inhibitor [14]. Among these compounds, six (compounds **4**, **5**, **8**, **9**, **10** and **11)** presented promising inhibitory effects on rat PDE5 and induced PA vasorelaxation [15]. To determine their R&D potential as novel PAH drug treatments, the present study investigated (*i*) their inhibitory effect on human PDE5, (*ii*) their selectivity on rat PA and mechanisms involved in their vasorelaxant effect, (*iii*) their toxicity on rat isolated hepatocytes and (*iv*) their impact on CYP inhibition and induction. Sildenafil was used as a reference comparator.

2. Materials and methods

2.1. Compounds preparation

Six N^2,N^4-disubstituted quinazoline 2,4-diamines **4**, **5**, **8**, **9**, **10** and **11** (Table 1) were synthesized and purified to >95% as previously reported [14]. All samples were dissolved in 100% dimethyl sulfoxide (DMSO) and diluted serially with distilled water or culture medium to obtain the final test concentrations.

2.2. Human PDE5 inhibitory activity

PDE5 enzyme was extracted from human embryonic kidney 293 (HEK293) cells transfected with human PDE5A1 plasmids and PDE5 inhibition of 6 quinazoline derivatives and sildenafil (10^{-12}–10^{-4} M) was determined by a two-step enzymatic reaction modified from previous report [16], as described in detail in **Supplemental methods**.

2.3. Animals

Adult male Wistar rats (200–250 g) were purchased from Nomura Siam International Co, Ltd. (Bangkok, Thailand) for vascular reactivity experiments in PA and aorta, or from Janvier (Le Genest Saint Isle, France) for hepatotoxicity and CYP activities. All animal experimentation protocols were approved by the respective local ethics committees (NU–AE620304 of Naresuan University Animal Care and Use Committee, Phitsanulok, Thailand and No. 2019–003-PT-5PR of Franche-Comté University, Besançon, France).

2.4. Vasorelaxant effects on isolated intrapulmonary artery and thoracic aorta

The vasorelaxant effects of the 6 compounds were assessed in terms of their selectivity on pulmonary *vs* systemic circulation, using isolated PA and aorta. After anesthesia with sodium thiopental (60 mg/kg, *i.p.*), thoracic aorta and PA were isolated, placed in cold Krebs solution composed of (mM): NaCl 122, KCl 5, N-[2-Hydroxyethyl] piperazine-N′-[2-ethane-sulfonic acid] (HEPES) 10, KH_2PO_4 0.5, NaH_2PO_4 0.5, $MgCl_2$ 1, $CaCl_2$ 1.8 and glucose 11, adjusted to pH 7.4 with 1 M NaOH, cleaned and cut into ~2-mm-length. Rings were suspended in Krebs solution at 37 °C and aerated for isometric tension recording in organ chambers, as previously described [17,18]. The presence of functional endothelium was confirmed by a relaxation to 10^{-5} M acetylcholine (ACh) ≥80% in vessels preconstricted with phenylephrine (10^{-5} M, PE). In some rings, the endothelium was mechanically removed. Rings were constricted with 10^{-5} M PE and quinazoline derivatives (10^{-10}–3×10^{-5} M) or sildenafil (10^{-11}–10^{-5} M) were added cumulatively to endothelium-intact or endothelium-denuded rings to obtain concentration-response curves (CRCs). DMSO (0.13% at maximum) was used as the vehicle. Then, the contribution of endothelium-dependent pathways, soluble guanylyl cyclase (sGC)/cGMP pathway, vascular smooth muscle potassium (K^+) channels, as well as their effect on intracellular and extracellular Ca^{2+} fluxes was determined as described in detail in **Supplemental methods**.

2.5. Hepatocytes viability and CYP induction/inhibition assays

After anesthesia with sodium pentobarbital (60 mg/kg, *i.p.*), hepatocytes were isolated by a two-step collagenase perfusion, as previously described [19]. Hepatocytes were seeded in collagen I coated 96-well plates in a fresh William's E culture medium. Compounds or vehicle (0.1% DMSO) were added to the cultures ($0.01–100 \times 10^{-6}$ M) and daily renewed. After 24 h, 48 h and 72 h of exposure, cellular viability was determined by using MTT (0.5 mg/mL) and incubated at 37 °C for 3 h. Results are expressed as a percentage of cell viability as compared to the

Table 1
Quinazoline compounds and sildenafil: Chemical features and pharmacological parameters.

Compound ID	Core Structure	R^1	R^2	MW	PDE5 activity IC_{50} ($\times 10^{-6}$ M)	Vasorelaxation EC_{50} ($\times 10^{-6}$ M)		SI of vasorelaxation
						PA	Aorta	
4	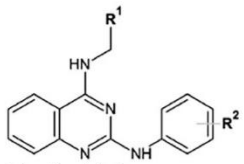 Quinazoline derivatives	−phenyl	−4-SO_2NH_2	405.5	0.015 ± 0.002***	3.92 ± 1.15***	3.73 ± 0.81**	1.0
5		−phenyl	−3-SO_2NH_2	405.5	0.005 ± 0.001*	0.94 ± 0.30**	7.36 ± 1.44***,##	7.8
8		−2-thiophene	−4-morpholino	417.5	0.062 ± 0.007***	6.16 ± 1.30***	1.26 ± 0.33*,##	0.2
9		−2-thiophene	−4-SO_2NH_2	411.5	0.019 ± 0.008***	3.72 ± 0.62***	3.84 ± 1.68**	1.0
10		−2-thiophene	−4-$CONH_2$	375.5	0.045 ± 0.021***	3.55 ± 1.10***	2.41 ± 0.55**	0.7
11		−2-thiophene	−3-SO_2NH_2	411.5	0.005 ± 0.001*	1.03 ± 0.23**	6.49 ± 1.18***,##	6.3
Sildenafil				474.6	0.002 ± 0.0004	0.05 ± 0.02	0.11 ± 0.07	2.1

IC_{50} values were calculated from an *in vitro* assay on PDE5 enzyme extracted from human embryonic kidney 293 (HEK293) cells transfected with human PDE5A1 plasmids. EC_{50} was calculated from concentration-response curves of vasorelaxation on endothelium-intact isolated pulmonary artery (PA) and aorta. Selectivity index (SI) is the ratio of (EC_{50} aorta)/(EC_{50} PA) that reflects the selectivity of each compound for PA *vs* aorta. Values are means ± SEM ($n = 3$ for IC_{50} and $n = 5$–6 for EC_{50}). $^*p \leq 0.05$, $^{**}p \leq 0.01$, $^{***}p \leq 0.001$ *vs* sildenafil; $^{\#\#}p \leq 0.01$ *vs* PA.

vehicle.

Measurement of CYP-dependent activities was determined as previously described [19]. Culture medium containing 0.1–10 × 10^{-6} M of compounds or vehicle (0.1% DMSO) was added to the cultures and daily renewed. Specific CYP inducers and inhibitors were also used in parallel. CYP1A and CYP2B-dependent activities were evaluated by measuring the ethoxyresorufin-O-deethylase (EROD) and the benzyloxyresorufin-O-dealkylase (BROD) activity, respectively. CYP2C and CYP3A activities were measured by using the P450-Glo™ CYP2C9 and CYP3A4 assay kit (Promega, Charbonnières-les-bains, France). CYP activities were expressed as fold change *vs* control (0.1% DMSO), which was set at 1. According to the OECD Guideline for the testing of chemicals [20], statistical analysis was processed only when fold change was < 1 for CYP inhibition and ≥ 2 for CYP induction.

2.6. Statistical analysis

All data were expressed as mean ± standard error of mean (SEM). Values were analyzed using GraphPad Prism (version 5.0, San Diego, USA). Vasorelaxant responses were expressed as the percentage of relaxation of the contractile response to 10^{-5} M PE. EC_{50} (half maximal effective concentration) and IC_{50} (half maximal inhibitory concentration) were calculated by fitting the original dose–response curves using GraphPad Prism software. CRCs were compared by two-way analysis of variance (ANOVA) for repeated measures. Comparison between two values was assessed by the unpaired Student's *t*-test. $p \leq 0.05$ was considered statistically significant.

3. Results

3.1. Quinazoline derivatives inhibited human PDE5 activity

As shown in Table 1, all quinazoline derivatives inhibited human PDE5 activity, ranging from 5 nM for **5** and **11** to 62 nM for **8**. The order of inhibitory activity was compounds **5** = **11** > **4** > **9** > **10** > **8**. For comparison, sildenafil displayed at IC_{50} of 2 nM, only 2.5-fold more potent than the most potent quinazoline derivatives ($p < 0.05$).

3.2. Compounds *5* and *11* induced a stronger vasorelaxant effect on PA as compared to aorta

The ability of quinazoline derivatives to selectively vasodilate PA was assessed using both PA and aorta (Fig. 1). While all compounds vasodilated both vessels, only two compounds (**5** and **11**) induced a greater relaxation in PA compared to aorta (Fig. 1B and F). Conversely, sildenafil induced a similar vasorelaxant effect in PA and aorta (Fig. 1G). Even though compounds **5** and **11** had a lower relaxant effect on PA than sildenafil (Table 1), the calculated selectivity index (SI) (EC_{50} (aorta)/EC_{50} (PA)) was greater for compounds **5** (7.8) and **11** (6.3) than sildenafil (2.1).

3.3. The vasorelaxant effect of compounds *5* and *11* was endothelium- and NO-dependent

More detailed investigation of the pharmacological mechanisms involved in the vasorelaxant effect of compounds (**5**, **11**) were subsequently studied in PA (**Supplemental Table 1**). The removal of endothelium significantly decreased the relaxation effect of all compounds (Fig. 2A–C). Inhibition of nitric oxide synthase (NOS) by L-NAME reduced the relaxation induced by compounds **5**, **11** and sildenafil, whereas blockade of cyclooxygenase or inhibition of endothelium-derived hyperpolarizing factors did not change their effect (Fig. 2D–F).

3.4. Potentiation of sGC/cGMP pathway was involved in relaxation to quinazoline derivatives

To confirm if the PDE5 inhibitory effects of the quinazoline derivatives may be involved in their relaxant effect, we investigated their capacity to potentiate the relaxant effect of a NO-donor, sodium nitro prusside (SNP) that activates sGC and increases cGMP synthesis. Consistent with a contribution of PDE5 inhibition, compounds **5**, **11** and sildenafil increased SNP-induced relaxation in endothelium-denuded PA compared to vehicle (Fig. 2J–L). To determine if a direct activation of sGC might be also involved, the effect of the sGC inhibitor, ODQ was studied. Fig. 2G–I shows that the relaxation induced by compounds **5**, **11** and sildenafil was reduced by ODQ.

3.5. The vasorelaxant effect of compounds *5* and *11* relied on receptor-operated Ca^{2+} channels (ROCC) inhibition but not activation of K^+ channels

Potassium channels blockers (4-AP, glibenclamide, and iberiotoxin) did not change vasorelaxation of compounds **5**, **11** and sildenafil in endothelium-denuded vessels (Fig. 3A-C Then, the impact of compounds on Ca^{2+} fluxes was studied. Compounds **5**, **11** and sildenafil reduced the contraction elicited by extracellular Ca^{2+} influx in PE-exposed rings (opening of ROCC) (Fig. 3D) whereas no change was observed after high K^+ exposure (opening of voltage-operated Ca^{2+} channels, VOCC) (Fig. 3E). Regarding intracellular Ca^{2+} fluxes, compounds **5** and **11** and sildenafil lowered PE-induced Ca^{2+} release from sarcoplasmic reticulum (SR) (Fig. 3F).

3.6. Effect of compounds *5*, *11* and sildenafil on rat hepatocyte viability

Rat hepatocytes in primary cultures were exposed to compounds **5**, **11**, sildenafil and vehicle (0.1% DMSO) for 24 h, 48 h and 72 h before MTT assay. As shown in Fig. 4A–C, viability remained >80% with all compounds at concentrations up to 10^{-5} M. At higher concentrations (10^{-5} to 10^{-4} M), compounds **5** and **11** led to a time- and concentration-dependent decrease in cell viability. IC_{50} values for compound **5** at 24 h, 48 h, 72 h were (×10^{-6} M) 73 ± 12, 43 ± 6 and 18 ± 0.1, respectively and for compound **11**: 61 ± 10, 23 ± 1 and 19 ± 0.3, respectively. Sildenafil was less toxic with viability ≥80% whatever the time or concentration.

3.7. Effect of compounds *5*, *11* and sildenafil on CYP-dependent activities

CYP1A, 2B, 2C and 3A activities were measured in rat hepatocytes after 24 h, 48 h and 72 h exposure with non-cytotoxic concentrations of the compounds (Fig. 4A-C). Compound **5** did not change CYP1A and 2B activities but inhibited CYP2C and 3A (Fig. 4J, M), only at the highest concentrations. Compound **11** increased CYP1A activity in a concentration independent-manner (Fig. 4E) and inhibited CYP3A activity at the highest concentration (10^{-5} M, Fig. 4N). Sildenafil led to a concentration-dependent increase in CYP1A activity, up to 6-fold (Fig. 4F) and inhibited CYP3A, only at the two highest concentrations (Fig. 4O).

4. Discussion

The present study has provided us with new pharmacological and developability information on a series of quinazoline-based PDE5 inhibitors. It is found that (*i*) two quinazolines compounds, **5** and **11**, had *in vitro* inhibitory properties on human PDE5 and potent vasorelaxant effect on rat isolated pulmonary arteries, (*ii*) their effect relied on both endothelium-dependent and endothelium-independent mechanisms, (*iii*) they had greater selectivity for pulmonary *vs* systemic circulation than sildenafil, (*iv*) they exhibited a weak hepatocyte toxicity as well as a weak inhibitory effect on CYP3A (>10^{-5} M).

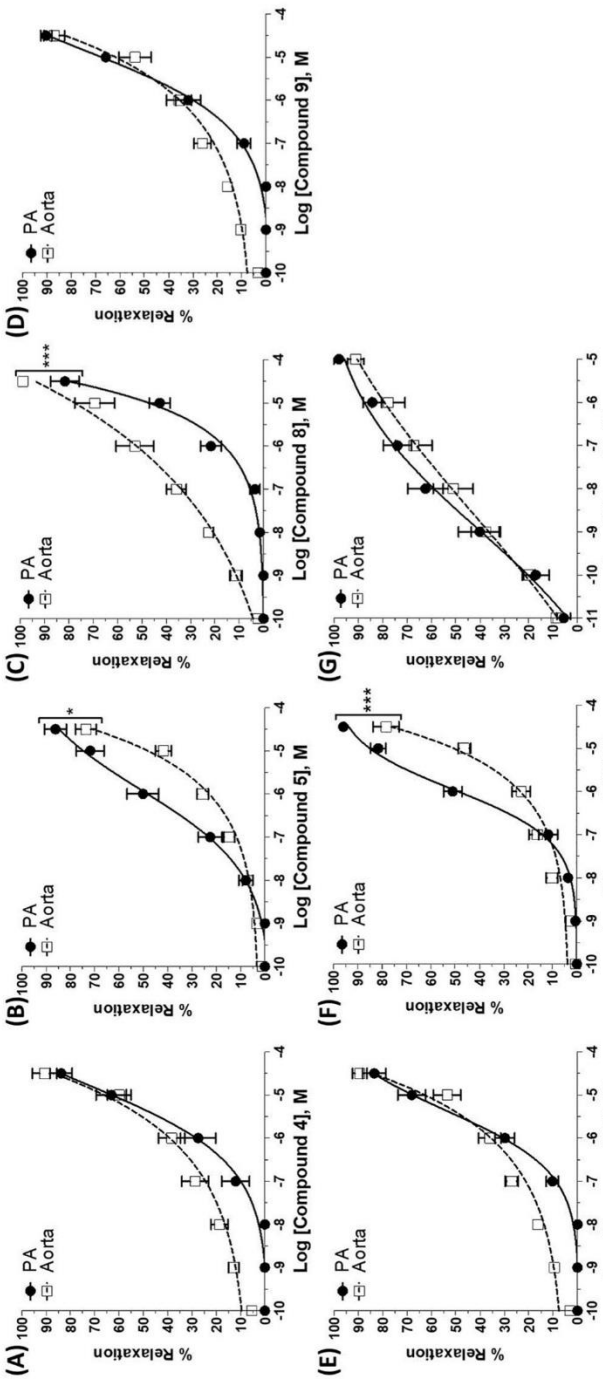

Fig. 1. Comparison of the vasorelaxant effect on pulmonary artery (PA) *vs* aorta of quinazoline compounds and sildenafil.
The vasorelaxant effect of six quinazoline derivatives and sildenafil was studied in endothelium-intact PA and aortic rings preconstricted with 10^{-5} M PE. Values are means ± SEM ($n = 5$–6). $^{*}p \leq 0.05$, $^{***}p \leq 0.001$ *vs* PA.

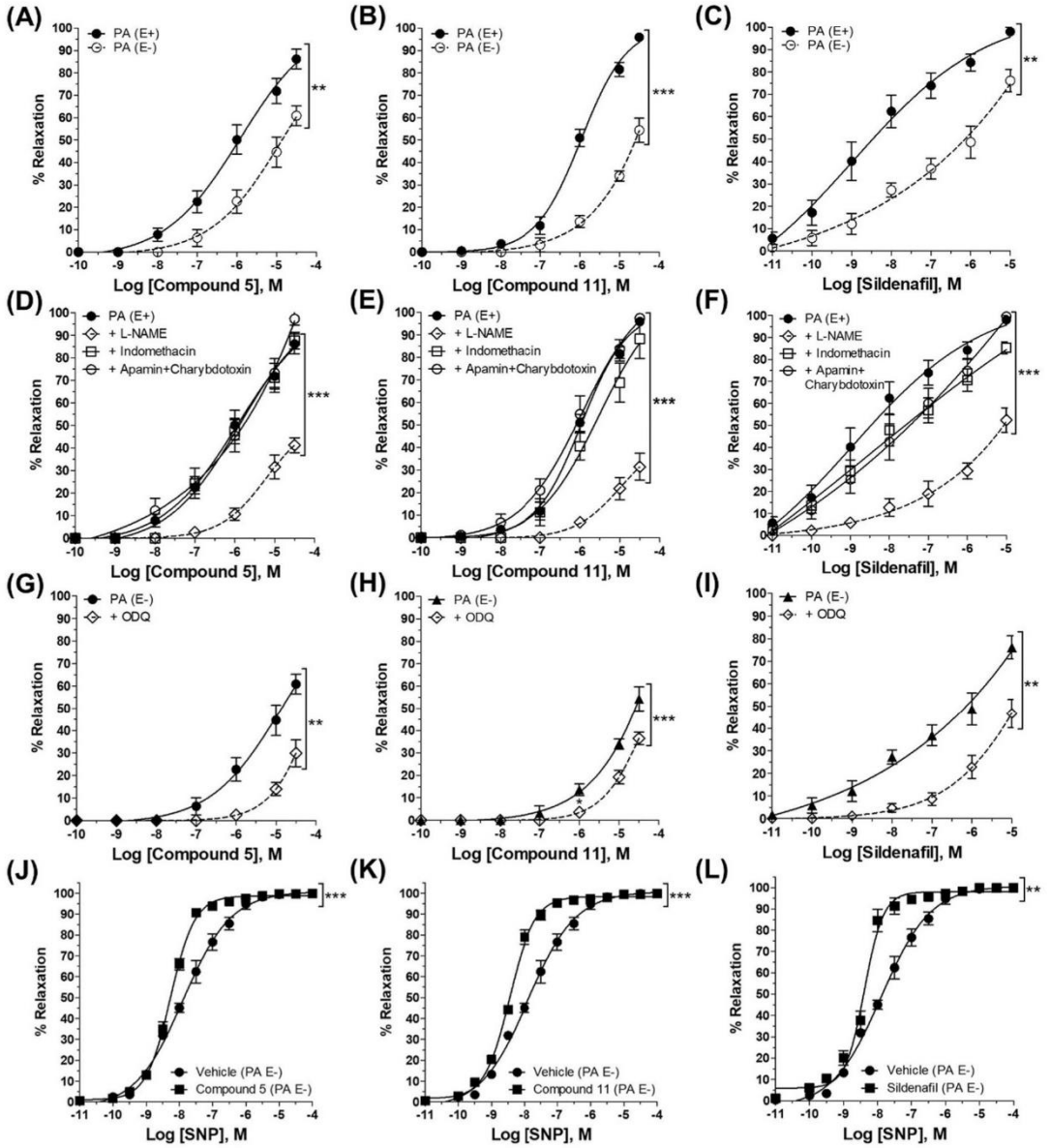

Fig. 2. Contribution of the endothelium and NO-sGC-cGMP pathway to the vasorelaxant effects of compounds **5**, **11** and sildenafil in pulmonary artery (PA). (**A-C**) Concentration-response curves of the compounds in PA with (E+) and without (E–) endothelium. (**D-F**) Vasorelaxant effect of the compounds after incubation with L-NAME, indomethacin or apamin+charybdotoxin in PA (E+) or (**G–I**) with ODQ in PA (E–). (**J–L**) Vasorelaxant effect of SNP after incubation with the compounds at its EC_{50}. Values are means ± SEM ($n = 5$–6). $^{**}p \leq 0.01$, $^{***}p \leq 0.001$ *vs* PA or vehicle.

Pulmonary vasculature regulation via the sGC/cGMP pathway is a critical target for PAH treatment. Degradation of cGMP in pulmonary VSMCs is primarily regulated by PDE5, and the inhibition of this enzyme leads to increase in cGMP and vasorelaxation, thus alleviating the PAH. The present study evaluated 6 quinazoline derivatives (N^2,N^4-disubstituted quinazoline 2,4-diamines) which exhibited PDE5 inhibitory activity in HEK293 cells transfected with human PDE5A1 plasmids. Among them, compounds **5** and **11** had the greatest *in vitro* potency, comparable to that of the drug, sildenafil. The results indicated that 3-sulphonamide ($-3\text{-}SO_2NH_2$) of compounds **5** and **11** is important for this activity, while the effect of thiophene substitution by a phenyl ring at the R^1 has a smaller, but favorable, impact on the activity. This

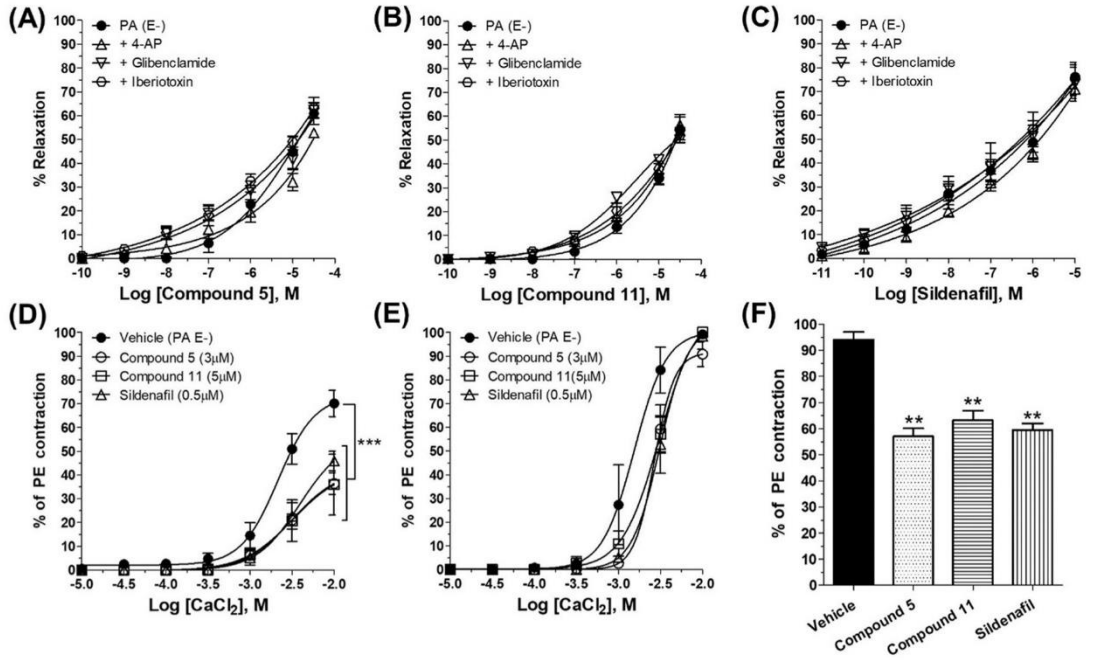

Fig. 3. Contribution of potassium and calcium channels to the vasorelaxant effects of compounds 5, 11 and sildenafil in pulmonary artery (PA) without endothelium (E-).

(**A-C**) Concentration-response curves (CRCs) of compounds after incubation PA rings with/without various K^+ channel inhibitors: 4-AP (K_V blocker), glibenclamide (K_{ATP} blocker) and iberiotoxin (K_{Ca} blocker). (**D**) Effect of compounds on receptor-operated calcium channels: CRCs of $CaCl_2$ after incubation PA rings with each compound plus 10^{-5} M PE in Ca^{2+}-free Krebs solution. (**E**) Effect of compounds on voltage-operated calcium channels: CRCs of $CaCl_2$ after incubation PA rings with each compound plus 8×10^{-2} M K^+ in Ca^{2+}-free Krebs solution. (**F**) Effect of compounds on Ca^{2+} release from sarcoplasmic reticulum: Responses to 10^{-5} M PE after incubation of PA rings with each compound in Ca^{2+}-free Krebs solution. Values are means ± SEM (n = 5–6). $^{**}p \leq 0.01$, $^{***}p \leq 0.001$ *vs* vehicle.

configuration appears to maximize the H-bond interactions as well as pi-stacking interactions within the PDE5 active site, as observed for other quinazolines derivatives [14].

Consistent with their effects on PDE5 and the role of PDE5 in pulmonary vasculature, compounds **5** and **11** were also the most efficient to induce vasodilation in isolated pulmonary artery. As a confirmation that their vasorelaxant effects were indeed secondary to PDE5 inhibition, our data showed that they enhanced the vasorelaxant effect of a NO-donor on endothelium-denuded PA rings, indicating that cGMP levels in VSMCs have been increased by the 2 quinazolines. Of interest, the selective sGC inhibitor ODQ was able to reduce the vasorelaxant effect of compounds **5** and **11** in endothelium-denuded arteries, thus indicating that a direct activation of sGC is also involved. The present study did not identify whether the compounds act as GC stimulators (as riociguat) requiring heme-containing sGC or as sGC activators (as cinaciguat) activating heme-free sGC. However, this dual action on the sGC/cGMP pathway is of particular interest as both expressions of PDE5 and sGC are upregulated in PAH [21]. Growing evidence indicates that endothelial dysfunction of PA is a pivotal mechanism involved in the pathogenesis of PAH. Endothelial dysfunction results in the increased vascular resistance through an imbalance between the production of contracting and relaxing factors but also in the uncontrolled proliferation of endothelial cells and smooth muscle cells, fibroblasts, thus leading to the vascular remodeling in PAH [22]. The present study demonstrated that removal of the endothelium significantly impaired the relaxant effect of compounds **5** and **11**. By using selective inhibitors of the main endothelium pathways, we showed that these quinazolines can activate eNOS. Combined with their effect on the sGC/cGMP pathway in VSMCs, this indicates that these compounds can enhance the entire NO/sGC/cGMP pathway in pulmonary artery, similar to sildenafil.

Hypoxia was reported to selectively inhibit the function and expression of voltage-gated K^+ (K_V) channels in PA VSMCs, thus contributing to the development of PAH [23,24]. Here, none of the compounds **5** or **11** had an effect on K_V, K_{ATP} or K_{Ca} channels in endothelium-denuded PA rings. Thus, we investigated whether the 2 quinazolines may hamper intracellular or extracellular Ca^{2+} fluxes in VSMC. Indeed in PAH, hypoxia upregulates transient receptor potential channels leading to enhanced Ca^{2+} entry through receptor- and store-operated Ca^{2+} channels thereby inducing pulmonary vasoconstriction [25]. Our data indicated that compounds **5**, **11** inhibited intracellular Ca^{2+} release from the SR as well as extracellular Ca^{2+} influx via ROCC.

We found the same result with sildenafil effect on K^+ channels and Ca^{2+} homeostasis. Although the lack of VOCC inhibitory effect of sildenafil was previously reported in rabbit isolated PA [26], the present study provided the new information that it inhibited ROCC and Ca^{2+} release.

The developability of a series is dependent on having negligible on or off-target toxicity. Side effects, rather than unsatisfactory pharmacological efficacy, have been estimated to be responsible for the attrition of approximately one-third of drug candidates and is a major contributor to the high cost of drug development, particularly when not recognized until late in clinical trials or post-marketing [27]. This has led to the concept that evaluation of toxicity and side effects of new drug candidates must be done in parallel with optimization of their efficacy at early

here the drug-drug interaction potential of compounds **5** and **11**. Our results showed that the main effect on CYP was a weak CYP3A inhibition for both compounds, and a weak CYP2C inhibition for compound **5** only. As mentioned for liver toxicity, these effects are only evident for concentrations ~10^{-5} M, so it is unlikely that they would be observed at pharmacological doses. Our study revealed that both quinazoline compounds exhibited greater inhibitory effect on CYP3A than sildenafil, which was previously shown to have a weak inhibitory effect [10]. Additionally, **5** and **11** did not increase in a concentration- and time-dependent manner CYP1A activity, in contrast to sildenafil. These findings suggest that the quinazoline compounds have potential for further development.

The most common adverse drug reactions of marketed PDE5 inhibitors include headache, flushing, nasal congestion, nasopharyngitis (linked to a systemic vasodilatory effect), and dyspepsia. Visual disturbances have been reported with PDE5 inhibitors, due to their lack of PDE5 selectivity and their capacity to inhibit retinal PDE6 [29]. Previous data obtained in rat PDE5 and PDE6 showed that compounds **5** and **11** were ~4.6 times more selective for PDE5, which is similar to sildenafil (~6.5 times) [14]. However, the results obtained here show that the selectivity of compounds **5** and **11** for PA *vs* aorta was greater (around 3-fold) than sildenafil suggesting that these compounds are more selective for pulmonary circulation than for systemic circulation than sildenafil.

5. Conclusion

The present study identified 2 quinazoline derivatives with potent human PDE5 inhibitory activity and vasorelaxant effects on the rat pulmonary artery. Despite a lower activity on PDE5 than sildenafil, they have a greater selectivity for pulmonary artery *vs* systemic vasculature. Their vasorelaxant effects involved not only PDE5 inhibition but also other relevant mechanisms in the context of PAH: including direct activation of sGC, blockade of Ca^{2+} channels and activation of NO-dependent endothelial function. Further studies are needed to confirm these positive effects *in vivo*, in animal model of PAH. This work demonstrates the pharmacological effects of this series of quinazolines and give us confidence in their overall developability, particularly when related to liver toxicity, CYP inhibition, and induction effects. This has spurred further efforts to develop additional analogs with a view to improving their PDE5 selectivity and maximizing their vasorelaxant effects.

CRediT author statement

Usana Chatturong: Methodology, Investigation, Formal analysis, Writing – original draft, Writing – review & editing, Visualization. **Hélène Martin:** Methodology, Formal analysis, Resources, Writing–review & editing, Visualization. **Perle Totoson:** Methodology, Writing–review & editing. **Kornkanok Ingkaninan:** Methodology, Resources, Writing–review & editing. **Prapapan Temkitthawon:** Methodology, Resources, Writing–review & editing. **Saharat Sermsenaphorn:** Compound preparation. **Thanachon Somarin**: Compound preparation. **Adchatawut Konsue:** Compound preparation. **M. Paul Gleeson:** Compound preparation, Formal analysis, Writing – review & editing. **Céline Demougeot:** Conceptualization, Methodology, Resources, Formal analysis, Writing – review & editing, Visualization, Supervision, Funding acquisition. **Krongkarn Chootip:** Conceptualization, Methodology, Resources, Formal analysis, Writing – review & editing, Visualization, Supervision, Project administration, Funding acquisition.

Financial support

This work was supported by the Royal Golden Jubilee (Ph.D. grant PHD/0228/2561, National Research Council of Thailand), the Franco-Thai Scholarship Program, King Mongkut's Institute of Technology Ladkrabang (KREF046401) and the French Ministry for Higher Education and Research. We also thank the Center of Excellence for Innovation in Chemistry (PERCH-CIC) for facility support.

Declaration of Competing Interest

The authors declare that they have no conflict of interest.

Data availability

Data will be made available on request.

Appendix A. Supplementary data

Supplementary data to this article can be found online at https://doi.org/10.1016/j.vph.2022.107111.

References

[1] K. Tello, W. Seeger, R. Naeije, R. Vanderpool, H.A. Ghofrani, M. Richter, R. J. Tedford, H.J. Bogaard, Right heart failure in pulmonary hypertension: diagnosis and new perspectives on vascular and direct right ventricular treatment, Br. J. Pharmacol. 178 (1) (2021) 90–107.
[2] A. Huertas, C. Guignabert, J.A. Barberà, P. Bärtsch, J. Bhattacharya, S. Bhattacharya, M.R. Bonsignore, L. Dewachter, A.T. Dinh-Xuan, P. Dorfmüller, Pulmonary vascular endothelium: the orchestra conductor in respiratory diseases: highlights from basic research to therapy, Eur. Respir. J. 51 (4) (2018).
[3] N. Sommer, H.A. Ghofrani, O. Pak, S. Bonnet, S. Provencher, O. Sitbon, S. Rosenkranz, M.M. Hoeper, D.G. Kiely, Current and future treatments of pulmonary arterial hypertension, Br. J. Pharmacol. 178 (1) (2021) 6–30.
[4] K.E. Andersson, PDE5 inhibitors–pharmacology and clinical applications 20 years after sildenafil discovery, Br. J. Pharmacol. 175 (13) (2018) 2554–2565.
[5] M. Gredic, I. Blanco, G. Kovacs, Z. Helyes, P. Ferdinandy, H. Olschewski, J. A. Barberà, N. Weissmann, Pulmonary hypertension in chronic obstructive pulmonary disease, Br. J. Pharmacol. 178 (1) (2021) 132–151.
[6] S. Bhatia, R.P. Frantz, C.J. Severson, L.A. Durst, M.D. McGoon, Immediate and long-term hemodynamic and clinical effects of sildenafil in patients with pulmonary arterial hypertension receiving vasodilator therapy, Mayo Clin. Proc. (2003) 1207–1213. Elsevier.
[7] N. Galiè, H.A. Ghofrani, A. Torbicki, R.J. Barst, L.J. Rubin, D. Badesch, T. Fleming, T. Parpia, G. Burgess, A. Branzi, Sildenafil citrate therapy for pulmonary arterial hypertension, N. Engl. J. Med. 353 (20) (2005) 2148–2157.
[8] M.A.S. Leal, R. Aires, T. Pandolfi, V.B. Marques, B.P. Campagnaro, T.M.C. Pereira, S.S. Meyrelles, M. Campos-Toimil, E.C. Vasquez, Sildenafil reduces aortic endothelial dysfunction and structural damage in spontaneously hypertensive rats: role of NO, NADPH and COX-1 pathways, Vasc. Pharmacol. 124 (2020), 106601.
[9] S. Graziano, A. Montana, S. Zaami, M.C. Rotolo, A. Minutillo, F.P. Busardò, E. Marinelli, Sildenafil-associated hepatoxicity: a review of the literature, Eur. Rev. Med. Pharmacol. Sci. 21 (1 Suppl) (2017) 17–22.
[10] S.A. Sheweita, M. Wally, M. Hassan, Erectile dysfunction drugs changed the protein expressions and activities of drug-metabolising enzymes in the liver of male rats, Oxidative Med. Cell. Longev. (2016) 4970906.
[11] S.-J. Zuo, S. Li, R.-H. Yu, G.-X. Zheng, Y.-X. Cao, S.-Q. Zhang, Discovery of novel 3-benzylquinazolin−4 (3H)-ones as potent vasodilative agents, Bioorg. Med. Chem. Lett. 24 (24) (2014) 5597–5601.
[12] Y. Bi, P. Stoy, L. Adam, B. He, J. Krupinski, D. Normandin, R. Pongrac, L. Seliger, A. Watson, J.E. Macor, Quinolines as extremely potent and selective PDE5 inhibitors as potential agents for treatment of erectile dysfunction, Bioorg. Med. Chem. Lett. 14 (6) (2004) 1577–1580.
[13] Y.H. Kim, H. Choi, J. Lee, I.-C. Hwang, S.K. Moon, S.J. Kim, H.W. Lee, S.S. Lee, S. K. Ahn, S.W. Kim, Quinazolines as potent and highly selective PDE5 inhibitors as potential therapeutics for male erectile dysfunction, Bioorg. Med. Chem. Lett. 18 (23) (2008) 6279–6282.
[14] N. Pobsuk, T.U. Paracha, N. Chaichamnong, N. Salaloy, P. Suphakun, S. Hannongbua, K. Choowongkomon, D. Pekthong, K. Chootip, K. Ingkaninan, Design, synthesis and evaluation of N^2, N^4-diaminoquinazoline based inhibitors of phosphodiesterase type 5, Bioorg. Med. Chem. Lett. 29 (2) (2019) 267–270.
[15] T.U. Paracha, N. Pobsuk, N. Salaloy, P. Suphakun, D. Pekthong, S. Hannongbua, K. Choowongkomon, N. Khorana, P. Temkitthawon, K. Ingkaninan, Elucidation of vasodilation response and structure activity relationships of N^2, N^4-disubstituted quinazoline 2, 4-diamines in a rat pulmonary artery model, Molecules 24 (2) (2019) 281.
[16] S. Bhandari, N. Nuengchamnong, N. Chaichamnong, T. Seasong, K. Ingkaninan, P. Temkitthawon, At-line LC-QTOF-MS micro-fractionation of Derris scandens (Roxb.) Benth, coupled to radioassay for the early identification of PDE5A1 inhibitors, Phytochem. Anal. 31 (3) (2020) 297–305.
[17] J. Chaisakul, M.R.A. Rusmili, W.C. Hodgson, P. Hatthachote, K. Suwan, A. Inchan, L. Chanhome, I. Othman, K. Chootip, A pharmacological examination of the

cardiovascular effects of Malayan Krait (Bungarus candidus) venoms, Toxins 9 (4) (2017) 122.
[18] S. Wisutthathum, C. Demougeot, P. Totoson, K. Adthapanyawanich, K. Ingkaninan, P. Temkitthawon, K. Chootip, Eulophia macrobulbon extract relaxes rat isolated pulmonary artery and protects against monocrotaline-induced pulmonary arterial hypertension, Phytomedicine 50 (2018) 157–165.
[19] R. Cornu, N. Rougier, Y. Pellequer, A. Lamprecht, P. Hamon, R. Li, A. Beduneau, H. Martin, Interspecies differences in the cytochrome P450 activity of hepatocytes exposed to PLGA and silica nanoparticles: an in vitro and in vivo investigation, Nanoscale 10 (11) (2018) 5171–5181.
[20] Guideline, OECD GUIDELINE FOR THE TESTING OF CHEMICALS, Human cytochrome P450 (CYP) n-fold induction in vitro test method, 2014.
[21] A. Dasgupta, L. Bowman, C.L. D'Arsigny, S.L. Archer, Soluble guanylate cyclase: a new therapeutic target for pulmonary arterial hypertension and chronic thromboembolic pulmonary hypertension, Clin. Pharmacol. Ther. 97 (1) (2015) 88–102.
[22] K. Kurakula, V. Smolders, O. Tura-Ceide, J.W. Jukema, P.H.A. Quax, M. J. Goumans, Endothelial dysfunction in pulmonary hypertension: cause or consequence? Biomedicines 9 (1) (2021).
[23] M. Mandegar, J.X. Yuan, Role of K^+ channels in pulmonary hypertension, Vasc. Pharmacol. 38 (1) (2002) 25–33.
[24] H. Le Ribeuz, V. Capuano, B. Girerd, M. Humbert, D. Montani, F. Antigny, Implication of potassium channels in the pathophysiology of pulmonary arterial hypertension, Biomolecules 10 (9) (2020).
[25] F. Murray, P.A. Insel, J.X. Yuan, Role of O_2-sensitive K^+ and Ca^{2+} channels in the regulation of the pulmonary circulation: potential role of caveolae and implications for high altitude pulmonary edema, Respir. Physiol. Neurobiol. 151 (2–3) (2006) 192–208.
[26] H.A. Toque, C.E. Teixeira, F.B. Priviero, R.P. Morganti, E. Antunes, G. De Nucci, Vardenafil, but not sildenafil or tadalafil, has calcium-channel blocking activity in rabbit isolated pulmonary artery and human washed platelets, Br. J. Pharmacol. 154 (4) (2008) 787–796.
[27] F.P. Guengerich, Mechanisms of drug toxicity and relevance to pharmaceutical development, Drug Metab Pharmacokinet 26 (1) (2011) 3–14.
[28] N.R. Srinivas, Clinical drug-drug interactions of bosentan, a potent endothelial receptor antagonist, with various drugs: physiological role of enzymes and transporters, Gen. Physiol. Biophys. 35 (3) (2016) 243–258.
[29] S.A. Huang, J.D. Lie, Phosphodiesterase-5 (PDE5) inhibitors in the Management of Erectile Dysfunction, P T 38 (7) (2013) 407–419.

Supplemental material

Quinazoline-based human phosphodiesterase 5 inhibitors exhibited a selective vasorelaxant effect on rat isolated pulmonary arteries involving NO-sGC-cGMP pathway and calcium inhibitory effects

Usana Chatturong[a,b], Hélène Martin[b], Perle Totoson[b], Kornkanok Ingkaninan[c], Prapapan Temkitthawon[c], Saharat Sermsenaphorn[d], Thanachon Somarin[d], Adchatawut Konsue[d], M. Paul Gleeson[d], Céline Demougeot[b,1] Krongkarn Chootip[a,1,*]

[a] Department of Physiology, Faculty of Medical Science and Center of Excellence for Innovation in Chemistry, Naresuan University, Phitsanulok 65000, Thailand

[b] PEPITE EA4267, Université Bourgogne Franche-Comté, Besançon 25030, France

[c] Department of Pharmaceutical Chemistry and Pharmacognosy, Faculty of Pharmaceutical Sciences and Center of Excellence for Innovation in Chemistry, Naresuan University, Phitsanulok 65000, Thailand

[d] Department of Biomedical Engineering, Faculty of Engineering, King Mongkut's Institute of Technology, Ladkrabang, Bangkok 10520, Thailand

[*] Corresponding authors

E-mail address: krongkarnc@nu.ac.th (K. Chootip).

[1] Contributed equally to the work

Supplemental methods

1. Human PDE5 inhibitory activity

PDE5 enzyme preparation and inhibition assay were modified from Bhandari et al [1]. PDE5 enzyme was extracted from human embryonic kidney 293 (HEK293) cells transfected with human PDE5A1 plasmids. These transfected cells were lysed by sonication in Tris buffer (50 mM Tris-HCl pH 7.5), 2 mM ethylenediaminetetraacetic acid (EDTA), 1 mM dithiothreitol (DTT), and 1:100 of 100 mM phenylmethylsulfonyl fluoride (PMSF)). The homogenate was then centrifuged at 14,000 rpm for 20 min at 4 °C and the supernatant was collected as a source of PDE5 enzyme. To measure PDE5 inhibition assay, in first step the reaction mixture comprised 25 µL of Buffer C (100 mM Tris-HCl pH 7.5, 100 mM imidazole, 15 mM $MgCl_2$ and 1.0 mg mL^{-1} bovine serum albumin (BSA)), 25 µL of 10 mM ethylene glycol-bis (β-aminoethyl ether)-N,N,N′,N′-tetra acetic acid (EGTA), 25 µL of PDE5 solution, and 25 µL of test sample (quinazoline derivatives), sildenafil (positive control), or only solvent (5% DMSO) as a blank. The reaction was started by adding 25 µL of 5 µM [^{3}H] cGMP and incubated at 30 °C for 10 min. Then, the reaction was terminated by placing the sample tubes in hot boiling water (100 °C) for 1 min and simultaneously placed in ice-cold water. Second step was initiated by adding 25 µL of 2.5 mg/mL snake venom (5′-nucleotidase) and incubated at 30 °C for 5 min. The assay was diluted with 250 µL 20 mM Tris-HCl (low salt buffer pH 6.8) and transferred to a diethylaminoethyl sephadex (DEAE-Sephadex) ion exchange resin column, the reaction mixture sample was passed through the resin column. Uncharged [^{3}H] guanosine eluted from the resin with 1 mL of low salt buffer by 2 times, and the eluates were collected in a scintillation vial. Finally, 4 mL Ultima Gold (scintillating cocktail) were added to the vial and mixed completely, and the radioactivity was measured using the β-counter (Tri-Crab ® 2910 TR, Perkin Elmer). The higher count of uncharged guanosine represented lower PDE5 inhibitory activity, and vice versa. The PDE5 activity in the study were standardized to possess hydrolysis activity around 20–30% of the total substrate count. The calculation of hydrolysis of sample and control is shown in equation (1) and (2), and the PDE inhibitory activity is calculated from equation (3).

$$\%\ hydrolysis\ of\ sample = \left[\frac{(CPM_{sample} - CPM_{blank})}{(CPM_{total\ count} - CPM_{blank})}\right] \times 100 \qquad (1)$$

$$\%\ hydrolysis\ of\ control = \left[\frac{(CPM_{control} - CPM_{blank})}{(CPM_{total\ count} - CPM_{blank})}\right] \times 100 \qquad (2)$$

$$\%\ PDE5\ inhibition = \left[1 - \frac{(\%\ Hydrolysis_{sample})}{(\%\ Hydrolysis_{control})}\right] \times 100 \qquad (3)$$

Where, CPM_{sample} is the radioactive count rate of the assay with the enzyme, CPM_{blank} is the same but without the enzyme, $CPM_{total\ count}$ is the count rate of 25 µL of substrate plus 2 mL of low salt buffer, and $CPM_{control}$ is the radioactive count rate of the assay with enzyme but without any sample. All experiments were performed in triplicate.

2 Mechanisms involved in vasorelaxation in pulmonary artery (PA): Experimental protocols

2.1 Role of endothelium-dependent pathways

The contribution of the endothelium was studied by comparing the vasodilator effects of the compounds in endothelium-intact and endothelium-denuded rings. To investigate the role of endothelium nitric oxide synthase (eNOS), cyclooxygenase (COX) and endothelium-derived hyperpolarizing factors (EDHFs), endothelium-intact rings were pretreated with N^G-nitro-L-arginine methyl ester (L–NAME, a NOS inhibitor, 10^{-4} M), indomethacin (a COX inhibitor, 10^{-5} M), or apamin plus charybdotoxin (small– and large–conductance Ca^{2+}–activated K^+ channel blockers, 10^{-7} M/10^{-7} M), respectively, for 30 min before contraction with 10^{-5} M PE and exposed to cumulative concentrations of quinazoline compounds or sildenafil [2].

2.2 Role of vascular smooth muscle potassium (K^+) channels

Endothelium–denuded rings were incubated with 4–aminopyridine (4–AP, voltage–gated K^+ channel (K_V) blocker, 10^{-3} M), glibenclamide (ATP–sensitive K^+ channel (K_{ATP}) blocker, 10^{-5} M), and iberiotoxin (large conductance Ca^{2+}–activated K^+ channels (K_{Ca}) blocker, 10^{-7} M) for 30 min before contraction with 10^{-5} M PE and exposed to cumulative concentrations of quinazoline compounds or sildenafil [2].

2.3 Role of soluble guanylyl cyclase (sGC)/cGMP pathway

To evaluate whether the vasorelaxant effect may be dependent on PDE5 inhibition, we determined if compounds might increase the relaxant effect of a NO donor that activates sGC in VSMC and increase the cGMP–induced vasorelaxation. Endothelium–denuded rings were incubated with vehicle (0.02% DMSO) or compounds at their EC_{50} (3×10^{-6} M for compound **5**, 5×10^{-6} M for compound **11** or 5×10^{-7} M for sildenafil) for 10 min. Then rings were precontracted with 10^{-5} M PE and exposed to cumulative concentrations of sodium nitroprusside (SNP, 10^{-11} – 10^{-4} M), a NO donor. To discard the possibility that compounds directly activate sGC, the effect of ODQ (1H–[1,2,4]oxadiazolo[4,3-a]quinoxaline-1-one, a selective sGC inhibitor, 10^{-5} M for 30 min) was also studied [2].

2.4 Effect on extracellular Ca^{2+} influx

To study the role of receptor-operated Ca^{2+} channel (ROCC) or voltage–operated Ca^{2+} channel (VOCC) in the vasorelaxant effect, endothelium-denuded rings were incubated in Ca^{2+}–free Krebs solution containing 2×10^{-3} M EGTA for 40 min. Then 10^{-5} M PE was added to deplete intracellular Ca^{2+} store from sarcoplasmic reticulum (SR). After 4 washes with Ca^{2+}–free Krebs solution every 10 min, rings were incubated with vehicle or compounds at their EC_{50} for 10 min in Ca^{2+}–free Krebs solution with 10^{-5} M PE to open ROCC or with 8×10^{-2} M K^+ solution to open VOCC. Then, cumulative concentrations of $CaCl_2$ ($10^{-5} – 10^{-2}$ M) were added to evoke a contractile response [2]. The %contraction of $CaCl_2$ was normalized with maximum contraction of 10^{-5} M PE in the normal Krebs solution condition.

2.5 Effect on intracellular Ca^{2+} release from sarcoplasmic reticulum (SR)

Endothelium-denuded rings were precontracted with 8×10^{-2} M K^+ solution for 5 min to stimulate the initial Ca^{2+} loading into the SR Ca^{2+} stores. Then, baths were replaced with Ca^{2+}–free Krebs solution for 15 min and 10^{-5} M PE was added to release Ca^{2+} from SR, thereby eliciting a transient contraction. Then the same protocol was repeated after incubation for 15 min with vehicle or compounds at their EC_{50} before adding 10^{-5} M PE [3].

Supplemental references

[1] S. Bhandari, N. Nuengchamnong, N. Chaichamnong, T. Seasong, K. Ingkaninan, P. Temkitthawon, At-line LC-QTOF-MS micro-fractionation of Derris scandens (Roxb.) Benth, coupled to radioassay for the early identification of PDE5A1 inhibitors, Phytochem. Anal. 31 (3) (2020) 297-305.

[2] S. Wisutthathum, C. Demougeot, P. Totoson, K. Adthapanyawanich, K. Ingkaninan, P. Temkitthawon, K. Chootip, Eulophia macrobulbon extract relaxes rat isolated pulmonary artery and protects against monocrotaline-induced pulmonary arterial hypertension, Phytomedicine 50 (2018) 157-165.

[3] K. To-on, U. Chatturong, T. Panklai, I. Palang, A. Inchan, S. Wisutthathum, T.U. Paracha, P. Apaikawee, K. Chootip, Isolation of Intrapulmonary Artery and Smooth Muscle Cells to Investigate Vascular Responses, JoVE (184) (2022) e63686.

Supplemental results

Supplemental Table 1. EC_{50} and E_{max} values for the vasorelaxant response of compounds 5, 11 and sildenafil

Compounds	5	11	Sildenafil
Endothelium-intact (E+)			
Compound (E+)			
EC_{50} (10^{-6} M)	$0.94 \pm 0.30^{*}$	$1.03 \pm 0.23^{**}$	0.05 ± 0.02
E_{max} (%)	87.9 ± 5.03	96.1 ± 1.30	98.0 ± 1.63
+ L-NAME			
EC_{50} (10^{-6} M)	$5.17 \pm 1.41^{\#}$	$5.81 \pm 1.18^{\#\#}$	$4.26 \pm 0.69^{\#\#\#}$
E_{max} (%)	$41.3 \pm 3.3^{\#\#\#}$	$31.48 \pm 5.93^{*,\#\#\#}$	$52.42 \pm 5.54^{\#\#\#}$
+ Indomethacin			
EC_{50} (10^{-6} M)	0.82 ± 0.41	$4.09 \pm 1.15^{***}$	$0.48 \pm 0.08^{\#\#\#}$
E_{max} (%)	87.67 ± 3.66	91.85 ± 7.26	81.25 ± 2.72
+ Apamin + Charybdotoxin			
EC_{50} (10^{-6} M)	0.79 ± 0.31	$1.86 \pm 0.21^{*}$	$0.40 \pm 0.11^{\#}$
E_{max} (%)	97.3 ± 2.73	97.5 ± 1.63	99.5 ± 0.49
Endothelium-denuded (E-)			
Compound (E–)			
EC_{50} (10^{-6} M)	$3.17 \pm 0.51^{*,\#\#}$	$5.32 \pm 0.87^{**,\#\#}$	$0.53 \pm 0.11^{\#\#}$
E_{max} (%)	$60.9 \pm 4.43^{*,\#\#}$	$54.4 \pm 5.39^{*,\#\#\#}$	$79.3 \pm 5.06^{\#}$
+ ODQ			
EC_{50} (10^{-6} M)	$10.54 \pm 1.15^{\#\#}$	$12.34 \pm 1.77^{\#\#}$	$9.06 \pm 0.69^{\#\#\#}$
E_{max} (%)	$30.0 \pm 5.94^{\#\#}$	$33.0 \pm 4.17^{\#}$	$46.7 \pm 6.32^{\#\#\#}$
+ 4-AP			
EC_{50} (10^{-6} M)	$5.91 \pm 1.56^{**}$	$7.80 \pm 2.14^{**}$	2.55 ± 0.36
E_{max} (%)	$52.8 \pm 1.73^{*}$	55.1 ± 5.15	70.9 ± 4.90
+ Glibenclamide			
EC_{50} (10^{-6} M)	$3.15 \pm 0.86^{*}$	$5.76 \pm 0.86^{**}$	1.87 ± 0.62
E_{max} (%)	62.3 ± 3.24	$52.2 \pm 2.09^{*}$	73.6 ± 6.59
+ Iberiotoxin			
EC_{50} (10^{-6} M)	2.89 ± 1.42	$5.83 \pm 1.52^{**}$	2.01 ± 0.69
E_{max} (%)	63.2 ± 4.34	$52.0 \pm 3.18^{*}$	75.2 ± 6.97

Experiments were made on endothelium–intact (E+) and endothelium–denuded (E–) PA with and without inhibitors. Data are means ± SEM (n = 5–6). $^{*}p \leq 0.05$, $^{**}p \leq 0.01$, $^{***}p \leq 0.001$ *vs* sildenafil in the same condition; $^{\#}p \leq 0.05$, $^{\#\#}p \leq 0.01$, $^{\#\#\#}p \leq 0.001$ *vs* endothelium –intact (E+) or endothelium–denuded (E–) without inhibitors.

Second publication

European Journal of Pharmacology 953 (2023) 175829

Contents lists available at ScienceDirect

European Journal of Pharmacology

journal homepage: www.elsevier.com/locate/ejphar

The new quinazoline derivative (N^2-methyl-N^4-[(thiophen-2-yl)methyl] quinazoline-2,4-diamine) vasodilates isolated mesenteric arteries through endothelium-independent mechanisms and has acute hypotensive effects in Wistar rats

Usana Chatturong [a,b], Krongkarn Chootip [a,*], Hélène Martin [b], Maude Tournier-Nappey [b], Kornkanok Ingkaninan [c], Prapapan Temkitthawon [c], Saharat Sermsenaphorn [d], Thanachon Somarin [d], Adchatawut Konsue [d], M. Paul Gleeson [d], Perle Totoson [b], Céline Demougeot [b]

[a] Department of Physiology, Faculty of Medical Science and Center of Excellence for Innovation in Chemistry, Naresuan University, Phitsanulok, 65000, Thailand
[b] Université de Franche-Comté, PEPITE, Besançon, 25030, France
[c] Department of Pharmaceutical Chemistry and Pharmacognosy, Faculty of Pharmaceutical Sciences and Center of Excellence for Innovation in Chemistry, Naresuan University, Phitsanulok, 65000, Thailand
[d] Department of Biomedical Engineering, Faculty of Engineering, King Mongkut's Institute of Technology, Ladkrabang, Bangkok, 10520, Thailand

ARTICLE INFO

Keywords:
Quinazoline derivatives
Vasorelaxation
Mesenteric artery
Hypotensive effect
CYP activities

ABSTRACT

During the screening of new N^2,N^4-disubstituted quinazoline 2,4-diamines as phosphodiesterase-5 inhibitors and pulmonary artery vasodilators, one N^2-methyl-N^4-[(thiophen-2-yl)methyl]quinazoline-2,4-diamine (compound **8**) presented a greater selectivity for systemic than pulmonary vasculature. The present study aimed to characterize its vasorelaxant and hypotensive effects in Wistar rats. Vasorelaxant effects of compound **8** and underlying mechanisms were evaluated on isolated mesenteric arteries. Acute hypotensive effect was evaluated in anesthetized rats. Additionally, cell viability and cytochrome P450 (CYP) activities were studied in rat isolated hepatocytes. Nifedipine was used as a comparator. Compound **8** induced a strong vasorelaxant effect, similar to nifedipine. This was unaffected by endothelium removal but was decreased by inhibitors of guanylate cyclase (ODQ) and K_{Ca} channel (iberiotoxin). Compound **8** enhanced sodium nitroprusside-induced relaxation, but inhibited vasoconstriction evoked by α_1-adrenergic receptor activation and extracellular Ca^{2+} influx via receptor-operated Ca^{2+} channels. Acute intravenous infusion of compound **8** (0.05 and 0.1 mg/kg) produced hypotension. It showed similar potency to nifedipine for lowering diastolic and mean arterial blood pressure, but less so for the effect on systolic blood pressure. Compound **8** had no effect on hepatocyte viability and CYP activities except at high concentration (10 μM) at which a weak inhibitory effect on CYP1A and 3A was observed. In conclusion, this study identified a N^2-methyl-N^4-[(thiophen-2-yl)methyl]quinazoline-2,4-diamine with a potent vasodilator effect on resistance vessels, leading to an acute hypotensive effect and a low risk of liver toxicity or drug-drug interactions. These vascular effects were mediated mainly through sGC/cGMP pathway, opening of K_{Ca} channels, and inhibition of calcium entry.

1. Introduction

Quinazoline is an aromatic heterocyclic chemical compound with the formula $C_8H_6N_2$ and is also known as benzo-1,3-diazine or 1,3-diazanaphthalene. It is a bicyclic structure comprising of two fused six-member simple aromatic rings, one benzene ring and one pyrimidine ring (Alagarsamy et al., 2018). These motifs make quinazolines good templates for the development of molecules of biological and pharmaceutical interest (Horton et al., 2003). Many medicines, agrochemicals, and veterinary treatments use quinazoline frameworks as building blocks to develop various compounds, which were used as marketed drugs for the treatment of arterial hypertension (Prazosin, Alfuzosin,

* Corresponding author.
E-mail address: krongkarnc@nu.ac.th (K. Chootip).

https://doi.org/10.1016/j.ejphar.2023.175829
Received 16 March 2023; Received in revised form 6 May 2023; Accepted 31 May 2023
Available online 10 June 2023

Bunazosin, Quinethazone), yeast infection (Trimetrexate), cancer (Gefitinib, Erlotinib), or used as a sodium channel blocker for pharmacological studies (Tetrodotoxin) (Selvam & Kumar, 2015). Consistently, pharmacological studies also demonstrated that quinazoline derivatives exhibited anti-inflammation (Yoon et al., 2012), anti-cancer (Chen et al., 2016), anti-hyperlipidemia and anti-hyperglycemia (Nie et al., 2016), anti-erectile dysfunction (Kim et al., 2008), anti-hypertension (Zuo et al., 2014) and phosphodiesterase-5 (PDE5) inhibitory properties (Chatturong et al., 2022; Paracha et al., 2019; Pobsuk et al., 2019; Somnarin et al., 2022).

Recently, twenty N^2,N^4-disubstituted quinazoline 2,4-diamines were designed based on their pharmacophore's similarity to sildenafil, with the aim to develop new PDE5 inhibitors for the treatment of pulmonary hypertension (Paracha et al., 2019; Pobsuk et al., 2019). Among them, six compounds (compounds **4**, **5**, **8**, **9**, **10** and **11**) presented promising inhibitory effects on rat PDE5 (Paracha et al., 2019). During the screening of their vasorelaxant effect on rat pulmonary artery as compared to aorta, one compound (compound **8**, N^2-methyl--N^4-[(thiophen-2-yl)methyl]quinazoline-2,4-diamine) showed a 5-fold greater selectivity for aorta than pulmonary artery (Chatturong et al., 2022), pointing out its potential value as a vasodilator of the systemic vasculature. With the aim to determine the capacity of compound **8** to vasodilate resistance arteries of the systemic vasculature, and to unravel its mechanisms, the present study investigated (*i*) *ex vivo*, the vasorelaxant effect of compound **8** and the mechanisms involved in rat isolated mesenteric artery, (*ii*) *in vivo*, its acute hypotensive effect in normotensive rats, and for the early evaluation of its drugability, (*iii*) its toxicity on isolated hepatocytes and (*iv*) its effect on liver cytochrome P450 (CYP) activities. Nifedipine was used as a reference comparator.

2. Materials and methods

2.1. Compound preparation

Compound **8** (Fig. 1A) was synthetized and purified to >95% as reported elsewhere (Pobsuk et al., 2019). Compound **8** and nifedipine were dissolved in 100% dimethyl sulfoxide (DMSO) and diluted serially with distilled water or saline solution or culture medium to obtain the final test concentrations.

2.2. Animals

Male Wistar rats (8-week-old) were purchased from Janvier (Le Genest Saint Isle, France). Experimental protocols were approved by the local committee for ethics in animal experimentation No. 2019-003-PT-5PR of Franche-Comté University (Besançon, France), and complied with the Animal research: reporting *in vivo* experiments (ARRIVE) guidelines.

2.3. Vasorelaxant effects on isolated mesenteric arteries (MA)

The vasorelaxant effects of compound **8** *vs* nifedipine were assessed using isolated MA. After anesthesia with sodium pentobarbital (60 mg/kg, *i.p.*), rat small intestine was collected and placed in cold Krebs solution composed of (mM): NaCl 118, KCl 4.7, KH_2PO_4 1.2, $MgSO_4$ 1.2, $CaCl_2$ 2.5, $NaHCO_3$ 25, and glucose 12, maintained at pH 7.4. The second-order branches of MA were isolated, cleaned, cut into rings (2-mm-length), and mounted in organ chambers (containing 6 mL of Krebs solution bubbled with 95%O_2, 5%CO_2 and maintained at pH 7.4, 37°C) via two 40–μm diameter stainless steel wires in Multi Myograph System (Model 610M v.2.2, DMT A/S, Denmark) for isometric tension recording in organ chambers, as previously described (Wisutthathum et al., 2018). The presence of functional endothelium was confirmed by verifying the relaxation to 10 μM acetylcholine (ACh) ≥70% in vessels precontracted with 10 μM phenylephrine (PE). In some rings, endothelium was mechanically removed. Rings were precontracted with 10 μM PE and compound **8** or nifedipine (0.0001–30 μM) were added cumulatively to endothelium-intact rings to obtain concentration-relaxation curves. DMSO (0.13% at maximum) was used as the vehicle. Then, the contribution of endothelium-dependent pathways, vascular smooth muscle potassium (K^+) channels, intracellular and extracellular Ca^{2+} fluxes, soluble guanylyl cyclase (sGC)/cyclic guanosine monophosphate (cGMP) pathway, as well as its effect on alpha-1 (α_1) adrenergic receptors was determined as described in detail in Supplemental methods.

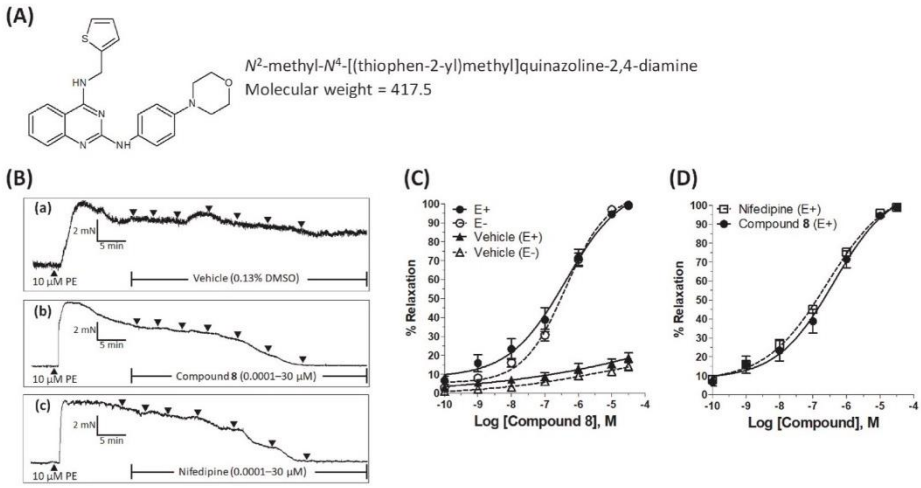

Fig. 1. Chemical structure and vasorelaxant effect of compound **8** on rat mesenteric artery (MA).
(**A**) Chemical structure and molecular weight of compound **8**. (**B**) Representative traces of the vasorelaxant effect of vehicle (0.13% DMSO) **(a)**, compound **8 (b)**, and nifedipine **(c)** on MA with endothelium (E+) precontracted with phenylephrine (PE, 10 μM). (**C**) Concentration-response curves of compound **8** or vehicle in MA with (E+) or without (E–) endothelium precontracted with PE. (**D**) Comparison of the vasorelaxant effect of compound **8** and nifedipine in (E+) MA. Values are means ± SEM (n = 6–12 rats).

2.4. Acute hypotensive effect of compound 8

To investigate the hypotensive effect of compound **8** as compared to nifedipine, rats were anesthetized (sodium pentobarbital, 60 mg/kg, *i.p.*) and systolic blood pressure (SBP), diastolic blood pressure (DBP), and heart rate (HR) were measured after cannulation of the left carotid artery and connection of the catheter to a pressure recorder system (Gould-EasyGraf chart-recorder, USA) under rectal temperature control (Verhoeven et al., 2017), as described in detail in Supplemental methods and Fig. S1. After 15-min stabilization period, all parameters were recorded before and during intravenous infusion of vehicle (saline solution containing 5% DMSO), compound **8** or nifedipine (0.01, 0.05, or 0.1 mg/kg) (Paulis et al., 2007). Successive infusions were separated for sufficient time (15 min) to allow fully recovery of the cardiovascular parameters.

2.5. Hepatocyte viability and CYP induction/inhibition assays

After anesthesia (sodium pentobarbital, 60 mg/kg, *i.p.*), rat hepatocytes were isolated by two-step collagenase perfusion and were seeded in collagen I coated 96-well plates, as previously described (Chatturong et al., 2022).

For hepatocyte viability assay, fresh William's E culture medium containing 0.01–100 μM of compound **8** was added to the cultures and daily renewed. Evaluation of cell viability after 24h, 48h and 72h of exposure was determined by using 3-(4,5-dimethylthiazol-2-yl)-2,5-diphenyltetrazolium bromide (MTT, 0.5 mg/mL) incubated for 3h at 37°C. Then, the formazan crystals produced were dissolved in DMSO and the absorbance was measured at 570 nm using a microplate reader. Cell viability was calculated as the percentage of cell viability in comparison to 0.1% DMSO.

For CYP induction/inhibition evaluation, rat hepatocytes were treated with compound **8** (0.1–10 μM) or 0.1% DMSO for 24h, 48h and 72h, as previously described (Chatturong et al., 2022). Specific CYP inducers and inhibitors were also used in parallel. CYP1A and CYP2B activities were evaluated by measuring ethoxyresorufin-O-deethylase (EROD) and benzyloxyresorufin-O-dealkylase (BROD) activity, respectively, as previously described (Chatturong et al., 2022). CYP2C and CYP3A activities were measured by using the P450-Glo™ CYP2C9 and CYP3A4 assay kit (Promega, Charbonnières-les-bains, France) according to the manufacturer's instructions. CYP activities were expressed as fold-change *vs* 0.1% DMSO, which was set at 1.

2.6. Statistical analysis

Data were expressed as mean ± standard error of mean (SEM). Vasorelaxant responses were expressed as the percentage of inhibition of the contractile response to PE. Values were analyzed using GraphPad Prism software (version 5.0). EC_{50} (half maximal effective concentration) and IC_{50} (half maximal inhibitory concentration) were calculated by fitting the original concentration-response curves. Concentration-response curves were compared using two-way analysis of variance (ANOVA) for repeated measures followed by the Bonferroni's test. According to the OECD Guideline for the testing of chemicals (Guideline, 2014), statistical analysis was processed only when fold-change was <1 for CYP inhibition and ≥ 2 for CYP induction. Comparison between two values was assessed by unpaired Student's *t*-test. $p<0.05$ was considered statistically significant.

3. Results

3.1. Compound 8 induced a robust endothelium-independent vasorelaxant effect

As presented in Fig. 1 and Table 1, compound **8** induced a potent vasodilator effect on MA ($EC_{50} = 0.56 \pm 0.17$ μM, $E_{max} = 98.8 \pm 0.5\%$). This effect was endothelium-independent (Fig. 1C), and equivalent to that of nifedipine (Fig. 1D).

Table 1
EC_{50} and E_{max} values of the relaxant effect of vehicle, compound **8**, and nifedipine on rat mesenteric arteries.

	Contractile force induced by 10 μM PE (mN)	EC_{50} (μM)	E_{max} (%)	*n*
Endothelium-intact arteries (E+)				
Vehicle (E+)	4.14 ± 0.51	–	18.9 ± 2.4	6
Compound **8** (E+)	4.80 ± 0.71	0.56 ± 0.17	98.8 ± 0.5	8
Nifedipine (E+)	4.84 ± 0.55	0.41 ± 0.09	98.7 ± 0.4	6
Endothelium-denuded arteries (E-)				
Vehicle (E–)	9.85 ± 1.36	–	14.1 ± 2.2	7
Compound **8** (E–)	9.73 ± 1.02	0.64 ± 0.12	99.2 ± 0.2	12
+4–AP	8.54 ± 1.65	0.35 ± 0.19	99.3 ± 0.4	7
+ Glibenclamide	8.84 ± 1.18	1.30 ± 0.42	99.1 ± 0.4	7
+ Iberiotoxin	9.65 ± 1.14	6.05 ± 2.27**	99.1 ± 0.2	7
+ ODQ	8.10 ± 0.94	4.79 ± 1.48**	97.4 ± 1.1*	6

Values are means ± SEM of the number *n* of animals. *$p<0.05$, **$p<0.01$ *vs* compound **8** (E–). The values of the contractile force (mN) are the constriction responses of mesenteric artery rings to phenylephrine (PE, 10 μM) before adding the cumulative concentrations of the test compound.

3.2. The relaxant effect of compound 8 relied on activation of K_{Ca} channels, ROCC inhibition, potentiation of sGC/cGMP pathway and inhibition of α_1-adrenergic receptors

To study the mechanisms involved, endothelium-denuded MA were first incubated with various K^+ channels blockers (Fig. 2A–D, Table 1). Among them, only iberiotoxin significantly reduced the vasorelaxant effect (Fig. 2D) as a reflection of an activation of K_{Ca} channels by compound **8**. Then, the contribution of extracellular or intracellular Ca^{2+} fluxes was evaluated. As compared to vehicle, compound **8** reduced the contraction elicited by extracellular Ca^{2+} influx in PE-exposed rings (opening of ROCC, Fig. 2E) whereas it did not change neither the extracellular Ca^{2+} influx in high K^+ (80 mM)-exposed rings (opening of VOCC, Fig. 2F) nor the intracellular Ca^{2+} release from SR (Fig. 2G).

As its chemical structure was inspired from that of the PDE5 inhibitor, sildenafil, the possible role of compound **8** as a potentiator of the sGC/cGMP pathway was studied. As shown in Fig. 2H, consistent with a PDE5 inhibitory effect, compound **8** slightly but significantly enhanced the relaxant effect of SNP, a NO donor that activates sGC and increases cGMP synthesis. Consistently, EC_{50} of SNP was reduced by compound **8** incubation (0.008 ± 0.001 μM (compound **8**, $n = 7$) *vs* $EC_{50} = 0.017 \pm 0.005$ μM (vehicle, $n = 9$), $p<0.05$). To determine if a direct activation of sGC might be also involved, the effect of ODQ, a sGC inhibitor was studied. Fig. 2I and Table 1 shows that ODQ markedly decreased the relaxation induced by compound **8**.

Finally, to determine the contribution of α_1-adrenergic receptors blockade, the effect of compound **8** on PE-induced contraction was studied. As compared to vehicle, compound **8** slightly but significantly decreased PE-induced contraction (Fig. 2J–K). Compound **8** enhanced the EC_{50} of PE (4.3 ± 1.0 μM (compound **8**, $n = 6$) *vs* 1.9 ± 0.3 μM (vehicle, $n = 6$), $p<0.05$) but did not change the E_{max} value ($106.6 \pm 1.7\%$ (compound **8**) *vs* $107.5 \pm 2.7\%$ (vehicle)).

3.3. In vivo, compound 8 induced an acute hypotensive effect

Fig. 3 presented the effects of intravenous injection of vehicle,

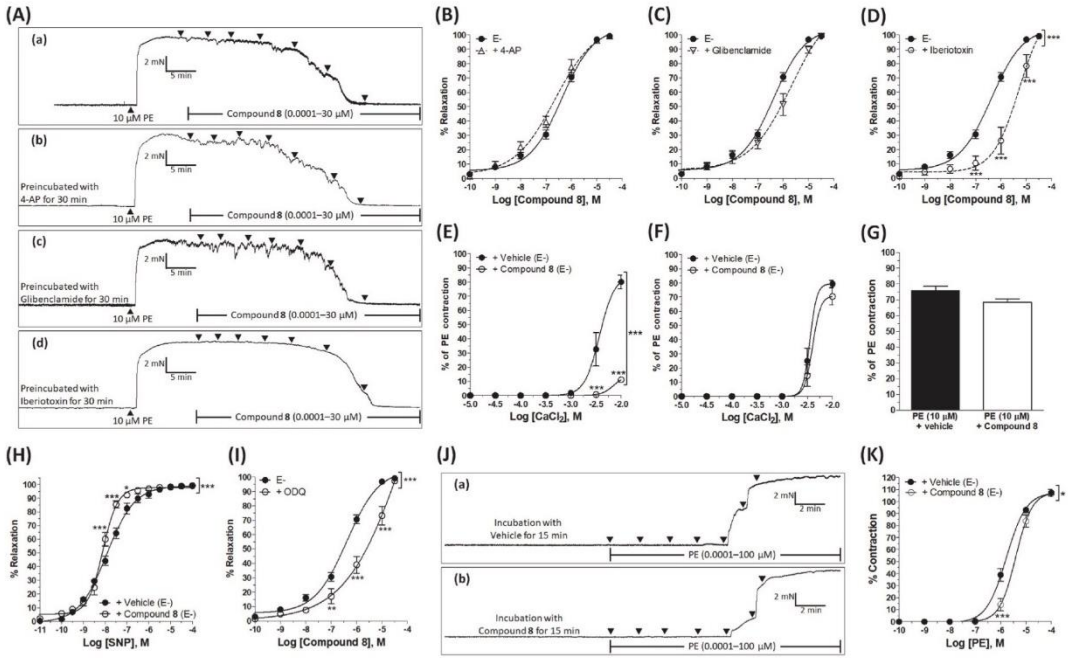

Fig. 2. Effects of compound **8** on potassium channels, calcium channels, sGC/cGMP pathway, and α_1-adrenergic receptors on rat mesenteric artery (MA).
Experiments were performed on endothelium-denuded (E–) MA. (**A**) Representative traces of the vasorelaxant effect of compound **8** in phenylephrine (PE)-pre-contracted MA rings in the absence or presence of K^+ channel inhibitors. (**B–D**) Concentration-response curves (CRCs) of compound **8** in the presence or absence of various K^+ channel inhibitors: **4**–AP (K_V blocker, **B**), glibenclamide (K_{ATP} blocker, **C**) or iberiotoxin (K_{Ca} blocker, **D**). (**E–F**) Effect of compound on receptor-operated Ca^{2+} channels (ROCC) or voltage-operated Ca^{2+} channels (VOCC): CRCs of $CaCl_2$ after incubation of MA rings with compound **8** or vehicle and exposure to PE (**E**, ROCC opening) or high K^+ (80 mM) (**F**, VOCC opening) in a Ca^{2+}-free Krebs solution. (**G**) Effect of compound **8** on Ca^{2+} release from sarcoplasmic reticulum (SR): after incubation with verapamil (VOCC inhibitor), rings were exposed to PE to open Ca^{2+} receptors of SR, in a Ca^{2+}-free Krebs solution containing compound **8** or vehicle. (**H**) CRCs of SNP (NO donor) after incubation with compound **8** or vehicle. (**I**) CRCs of compound **8** after incubation with ODQ. (**J**) Representative traces of the vasoconstriction induced by PE after incubation with vehicle (**a**) or compound **8** (**b**). (**K**) CRCs for PE-induced contraction after incubation with compound **8** or vehicle. The response curve of control (E–) in (**B–D**) and (**I**) was replicated for comparison. Values are means ± SEM (n = 6–12 rats). $^*p<0.05$ $^{***}p<0.001$ *vs* E– or vehicle.

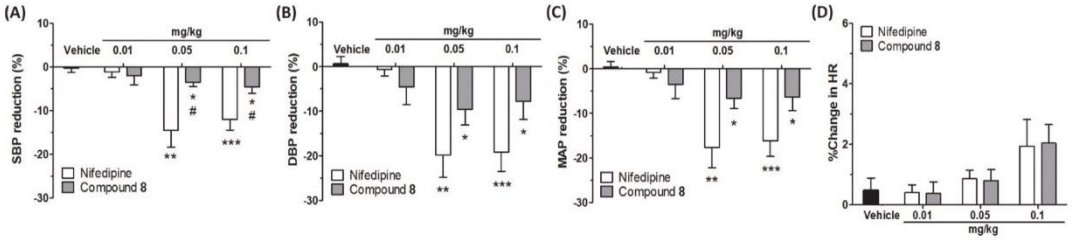

Fig. 3. Acute hypotensive effect of compound **8** on blood pressure in rats.
Experiments were conducted in anesthetized rats. The bars show the percentage reduction in (**A**) systolic (SBP), (**B**) diastolic (DBP), (**C**) mean (MAP) arterial blood pressure and (**D**) the percentage change in heart rate (HR), calculated from the values measured at the peak effect after intravenous infusion of vehicle (5% DMSO), compound **8** or nifedipine (0.01, 0.05 and 0.1 mg/kg BW), as compared to the baseline value before each infusion. Values are means ± SEM (n = 5 rats per group). $^*p<0.05$, $^{**}p<0.01$, $^{***}p<0.001$*vs* vehicle. $^{\#}p<0.05$ *vs* nifedipine at the same dose.

compound **8** and nifedipine on blood pressure and HR. Baseline values for SBP, DBP, and MAP (mmHg) were 139 ± 9, 103 ± 8, 115 ± 9, respectively, and 439 ± 18 beats per minute (bpm) for HR. As compared to vehicle, infusion of compound **8** or nifedipine at the doses of 0.05 and 0.1 mg/kg lowered SBP, DBP and MAP without significant changes in HR (Fig. 3A–D). The effect of compound **8** was lower than that of nifedipine for the effect on SBP (Fig. 3A) but not different for the effect on DBP, MAP and HR (Fig. 3B–D).

3.4. Compound **8** reduced hepatocyte viability in a concentration- and time-dependent effect

Rat hepatocytes in primary cultures were exposed to compound **8** or vehicle (0.1% DMSO) for 24h, 48h and 72h. As shown in Fig. 4A, viability remained >80% with compound **8** at concentrations up to 10 μM. At higher concentrations, compound **8** led to a concentration- and time-dependent decrease in cell viability. IC_{50} values for compound **8** after 24h, 48h and 72h-exposure were 56 ± 2, 28 ± 4 and 19 ± 2 μM, respectively.

3.5. Compound **8** had negligeable effects on CYP-dependent activities

CYP1A, 2B, 2C and 3A activities were measured in rat hepatocytes exposed to non-cytotoxic concentrations of compound **8** for 24h, 48h and 72h (Fig. 4). Compound **8** did not change any CYP activities at concentrations ranging from 0.1 to 5 μM, whatever the time of exposure (Fig. 4B, C, D, E). Only at the highest concentration tested (10 μM), a small but significant inhibition of CYP1A (Fig. 4B) and CYP3A (Fig. 4E) was observed.

4. Discussion

The major findings of this study are that compound **8** (N^2-methyl-N^4-[(thiophen-2-yl)methyl]quinazoline-2,4-diamine) induced a vaso-relaxant effect on resistance vessels through endothelium-independent mechanisms, that translated into an *in vivo* acute hypotensive effect in rats. These favorable pharmacological effects were associated with a low hepatocyte toxicity as well as a low effect on CYP activities.

In the cardiovascular system, vascular function and blood pressure are controlled by the tone of smooth muscle surrounding the small arteries and arterioles (Jackson, 2000). The regulation of vascular smooth muscle cells (VSMCs) is dependent on a complex interplay of vasodilation and vasoconstriction factors by neurotransmitters, circulating hormones, and endothelium-derived factors (Jackson, 2000; Nava and Llorens, 2019). The present study, conducted *ex vivo* on isolated MA, a model of resistance vessels (Li et al., 2005), demonstrated that compound **8** induced a strong vasorelaxant effect as its effect was equivalent to that of nifedipine, a calcium entry-blocking agent that lowers blood pressure by relaxing arterial and arteriolar smooth muscle (Robinson, 1985). Like nifedipine, the vasorelaxant effect of compound **8** was independent of the presence of endothelium. Our results obtained *in vivo* demonstrated that compound **8** had a direct effect on arteries without obvious cardiac effect. Indeed, intravenous infusion of compound **8** reduced blood pressure but did not reduce HR. On the contrary, a small increase in heart rate was observed likely as a reflection of decreased baroreflex activation secondary to the hypotensive effect. The acute hypotensive effect of compound **8** on MAP was not different from nifedipine. This result encourages initiating future studies on animal models of hypertension to determine if compound **8** could exert relevant anti-hypertensive properties.

Mechanistically, ion channels (Ca^{2+} and K^+ channels) on plasma membrane of VSMCs play a central role by determining cytosolic Ca^{2+} concentration and the sensitivity of contractile machinery to Ca^{2+} (Ghosh et al., 2017; Jackson, 2000). Ca^{2+} is a critical factor in the excitation-contraction coupling in VSMCs. The influx of extracellular Ca^{2+} through transmembrane Ca^{2+} channels (VOCC and ROCC) and the release of Ca^{2+} from SR by activation of IP_3 and ryanodine receptors results in increased intracellular Ca^{2+}, which causes VSMC contraction (Ghosh et al., 2017). To assess whether compound **8** modified the extracellular Ca^{2+} influx and intracellular Ca^{2+} release, experiments were conducted on endothelium-denuded MA rings incubated with compound **8** at its EC_{50} (0.6 μM). Our data revealed that compound **8** only inhibited ROCC without any significant effect on VOCC or on intracellular Ca^{2+} release. Regarding K^+, four different types of K^+ channels are expressed in VSMCs, including K_v, K_{ATP}, K_{Ca}, and inward-rectifier K^+ channels (Beleznai et al., 2011; Cheng et al., 2019), but K_v and K_{Ca} are extensively expressed in mesenteric arteries (Beleznai et al., 2011; Walker et al., 2001). Direct activation of K^+ channels hyperpolarizes cell membrane leading to inhibition of Ca^{2+} influx through L-type Ca^{2+} channels and resulting in smooth muscle relaxation (Beleznai et al., 2011; Cheng et al., 2019). In our experiments, only

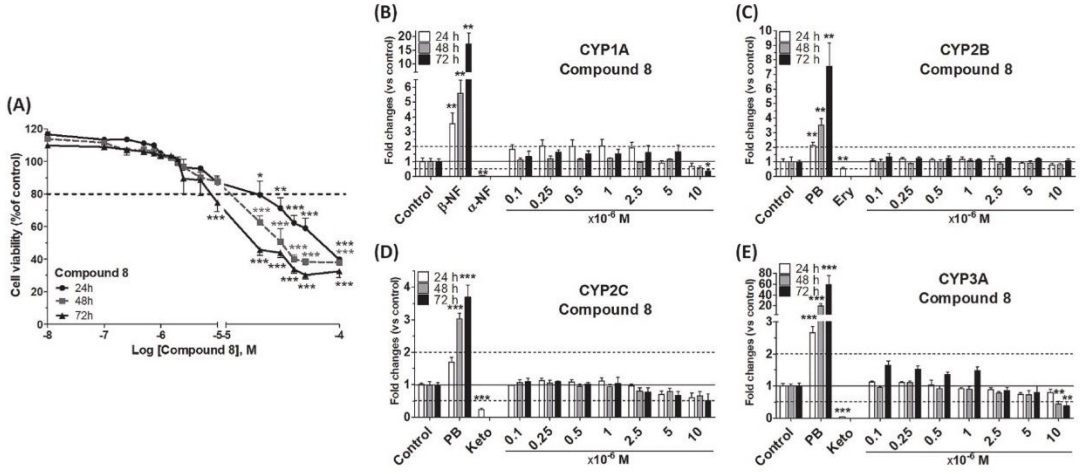

Fig. 4. Effects of compound **8** on rat hepatocytes viability and CYP activities.
Experiments were performed on primary rat hepatocyte cultures after 24h, 48h or 72h exposure with compound **8** or vehicle (0.1% DMSO). (**A**) Effect of compound **8** on cell viability and (**B-E**) on CYP activities. Phenobarbital (PB, 10^{-3} M for CYP2B or 2×10^{-3} M for CYP2C and 3A) and β–naphthoflavone (β–NF, 5×10^{-5} M for CYP1A) were used as reference CYP inducers. Erythromycin (Ery, 10^{-5} M for CYP2B), ketoconazole (Keto, 2.5×10^{-5} M for CYP2C and 3A) and α–naphthoflavone (α–NF, 10^{-5} M for CYP1A) were used as reference CYP inhibitors. Values are means ± SEM from triplicate of 3 independent cultures. *$p<0.05$, **$p<0.01$, ***$p<0.001$ *vs* control (0.1% DMSO).

iberiotoxin was able to reduce the relaxant effect of compound **8**, thus demonstrating that an activation of K_{Ca} is involved in its effect. Of note, as cGMP, through the activation of protein kinases G (PKG), is capable of activating K_{Ca} (Archer et al., 1994), an unresolved point is if compound **8** has a direct activating effect on the K_{Ca} channel, or an indirect effect through the increase in cGMP production. Compound **8** were originally identified from a series of quinazolines which demonstrated an inhibitory effect on PDE5 (Chatturong et al., 2022; Paracha et al., 2019). Rat resistance arteries express four major types of PDE, including PDE5 and PDE1, which hydrolyze cGMP; PDE4, which hydrolyzes cAMP; and PDE3, which mainly hydrolyzes cAMP but also cGMP (Komas et al., 1991; Sampson et al., 2001). Physiologically, endothelium-derived NO activates sGC in VSMC, resulting in cGMP production. The increase in intracellular cGMP concentration activates cGMP-dependent protein kinase, which causes vasorelaxation via the modulation of Ca^{2+} channels as well as by decreasing the Ca^{2+} sensitivity of the vascular smooth muscle contractile proteins (Manuel Morgado et al., 2012). Then intracellular cGMP is rapidly inactivated to GMP by the activity of PDEs. Therefore, cGMP concentration in VSMCs is mainly dependent on the balance between its production by sGC and its breakdown by PDE (Francis et al., 2010; Maurice et al., 2014; M. Morgado et al., 2012; Rybalkin et al., 2003). In favor of the contribution of PDE inhibition to the relaxant effect of compound **8**, our results showed that it enhanced SNP (an activator of sGC)-induced vasorelaxation on endothelium-denuded MA rings. However, compound **8** has a dual effect on the sGC-PDE pathway as our data also indicated that it acts as a direct activator of sGC. Finally, as many quinazolines with anti-hypertensive properties act through an α_1-antagonist effect (Eguchi et al., 1991; El-Sabbagh et al., 2010), this mechanism was evaluated. Indeed, compound **8** shares a scaffold with classic α_1-adrenergic receptor binders such as prazosin, an α_1-adrenergic blocker. Both molecules contain a 2, 4-diamino quinazoline scaffold, albeit, with prazosin being substituted at only the 2 positions. The results showed that compound **8** slightly but significantly lowered PE-induced contraction with no effect on the E_{max}. This result might reflect either a direct competitive antagonistic effect of compound **8** on α_1-adrenergic receptor and/or might be the consequence of the inhibitory effect of compound **8** on ROCC as PE-induced contraction involves the opening of these channels (Rinaldi et al., 1991). Further studies of radioligand binding assays at the α_1-adrenergic receptor would be required to ascertain that compound **8** has indeed an affinity for this receptor.

Evaluation of toxicity and side effects of new drug candidate must be done in parallel with optimization of their efficacy at early discovery phases. In the present study, both liver toxicity and the potential of drug-drug interactions through CYP activity changes were assessed in isolated rat hepatocytes. This is of particular importance given that many anti-hypertensive drugs or drugs used for reducing cardiovascular risk, such as statins (Vaughan and Gotto, 2004), are strongly metabolized by CYP (Zisaki et al., 2015). Regarding toxicity, a reduction of hepatocytes viability was observed with compound **8** only for concentrations >10 μM. As IC_{50} on hepatocytes after 72h of exposure was ~19 μM and EC_{50} for the vasorelaxant effect on MA was 0.56 μM, it is unlikely that such hepatotoxicity may occur at pharmacological concentrations. Likewise, compound **8** did not change CYP activities at concentrations ranging from 0.1 to 5 μM. A weak inhibition of CYP1A and CYP3A activities was observed only at 10 μM, so again, it is unlikely that this effect would be observed at pharmacological doses.

Of note, the weak inhibitory activity of compound **8** against CYP1A and CYP3A activities can be rationalized from a consideration of its molecular properties. While CYP3A4 has a substrate preference for neutral, medium to high molecular weight molecules, the CYP1A2 isoform demonstrates a preference for lower molecular weight, neutral molecules from a systematic analysis of 10,000s of drug-like molecules (Gleeson, 2008). The almost 2-fold decreased activity observed for the CYP1A isoform in the presence of compound **8**, due to its inhibitory effect, is not unexpected given its physico-chemical properties (medium sized, neutral, aromatic molecule). Burton et al. (2006) found that the presence of aromaticity features was key to discriminating inhibitors from non-inhibitors of CYP1A2. Moreover, Shimada and Guengerich (2006) demonstrated that even large polycyclic aromatic hydrocarbons can have significant inhibitory activity at CYP1A isoforms.

5. Conclusions

In conclusion, the present study identified a N^2-methyl-N^4-[(thiophen-2-yl)methyl]quinazoline-2,4-diamine) with a potent vasodilator effect on the resistance vasculature associated with a hypotensive effect. Its relaxant effect involves the opening of K_{Ca} channels, inhibition of transmembrane calcium influx and α_1-adrenergic receptors, and potentiation of the sGC/cGMP pathway. Whether compound **8** could be a new drug candidate for the treatment of arterial hypertension deserves future studies investigating its antihypertensive effect in animal models of hypertension, after an oral and chronic administration of the drug. Data on liver toxicity and CYP interactions suggest that this compound has potential for further development and indicate that compound **8** may also serve as a pilot molecule for the development of additional analogs with vasodilating properties.

CRediT authorship contribution statement

Usana Chatturong: Conceptualization, Methodology, Investigation, Project administration, Formal analysis, Writing – original draft, Writing – review & editing, Visualization. **Krongkarn Chootip:** Conceptualization, Methodology, Resources, Formal analysis, Writing – review & editing, Visualization, Supervision, Project administration, Funding acquisition. **Hélène Martin:** Methodology, Formal analysis, Resources, Writing – review & editing, Visualization. **Maude Tournier-Nappey:** Methodology. **Kornkanok Ingkaninan:** Writing – review & editing. **Prapapan Temkitthawon:** Writing – review & editing. **Saharat Sermsenaphorn:** Methodology. **Thanachon Somarin:** Methodology. **Adchatawut Konsue:** Methodology. **M. Paul Gleeson:** Methodology, Formal analysis, Writing – review & editing. **Perle Totoson:** Methodology, Formal analysis, Resources, Writing – review & editing. **Céline Demougeot:** Conceptualization, Methodology, Resources, Formal analysis, Writing – review & editing, Visualization, Supervision, Funding acquisition.

Declaration of competing interest

The authors declare that they have no known competing financial interests or personal relationships that could have appeared to influence the work reported in this paper.

Data availability

Data will be made available on request.

Acknowledgments

This work was supported by the Royal Golden Jubilee (Ph.D. grant PHD/0228/2561, National Research Council of Thailand), the Franco-Thai Scholarship Program, King Mongkut's Institute of Technology Ladkrabang (RE-KRIS-FF66-03), the French Ministry for Higher Education and Research, and partially supported by Global and Frontier Research University Fund, Naresuan University (R2566C053). We also thank the Center of Excellence for Innovation in Chemistry (PERCH-CIC), Ministry of Higher Education, Science, Research and Innovation on research facility support.

Appendix A. Supplementary data

Supplementary data to this article can be found online at https://doi.

org/10.1016/j.ejphar.2023.175829.

References

Alagarsamy, V., Chitra, K., Saravanan, G., Solomon, V.R., Sulthana, M.T., Narendhar, B., 2018. An overview of quinazolines: pharmacological significance and recent developments. Eur. J. Med. Chem. 151, 628–685. https://doi.org/10.1016/j.ejmech.2018.03.076.

Archer, S.L., Huang, J.M., Hampl, V., Nelson, D.P., Shultz, P.J., Weir, E.K., 1994. Nitric oxide and cGMP cause vasorelaxation by activation of a charybdotoxin-sensitive K channel by cGMP-dependent protein kinase. Proc. Natl. Acad. Sci. U. S. A. 91 (16), 7583–7587. https://doi.org/10.1073/pnas.91.16.7583.

Beleznai, T.Z., Yarova, P.L., Yuill, K.H., Dora, K.A., 2011. Smooth muscle Ca^{2+}-activated and voltage-gated K^+ channels modulate conducted dilation in rat isolated small mesenteric arteries. Microcirculation 18 (6), 487–500. https://doi.org/10.1111/j.1549-8719.2011.00109.x.

Burton, J., Ijjaali, I., Barberan, O., Petitet, F., Vercauteren, D.P., Michel, A., 2006. Recursive partitioning for the prediction of cytochromes P450 2D6 and 1A2 inhibition: importance of the quality of the dataset. J. Med. Chem. 49 (21), 6231–6240. https://doi.org/10.1021/jm060267u.

Chatturong, U., Martin, H., Totoson, P., Ingkaninan, K., Temkitthawon, P., Sermsenaphorn, S., et al., 2022. Quinazoline-based human phosphodiesterase 5 inhibitors exhibited a selective vasorelaxant effect on rat isolated pulmonary arteries involving NO-sGC-cGMP pathway and calcium inhibitory effects. Vasc. Pharmacol. 147, 107111 https://doi.org/10.1016/j.vph.2022.107111.

Chen, J.-N., Wang, X.-F., Li, T., Wu, D.-W., Fu, X.-B., Zhang, G.-J., et al., 2016. Design, synthesis, and biological evaluation of novel quinazolinyl-diaryl urea derivatives as potential anticancer agents. Eur. J. Med. Chem. 107, 12–25. https://doi.org/10.1016/j.ejmech.2015.10.045.

Cheng, J., Wen, J., Wang, N., Wang, C., Xu, Q., Yang, Y., 2019. Ion channels and vascular diseases. Arterioscler. Thromb. Vasc. Biol. 39 (5), e146–e156. https://doi.org/10.1161/ATVBAHA.119.312004.

Eguchi, Y., Sasaki, F., Sugimoto, A., Ebisawa, H., Ishikawa, M., 1991. Studies on hypotensive agents. Synthesis of 1-substituted 3-(2-chlorophenyl)-6-ethoxycarbonyl-5,7-dimethyl-2,4(1H,3H)-quinazoline diones. Chem. Pharm. Bull. (Tokyo) 39 (7), 1753–1759. https://doi.org/10.1248/cpb.39.1753.

El-Sabbagh, O.I., Shabaan, M.A., Kadry, H.H., Al-Din, E.S., 2010. New octahydroquinazoline derivatives: synthesis and hypotensive activity. Eur. J. Med. Chem. 45 (11), 5390–5396. https://doi.org/10.1016/j.ejmech.2010.08.064.

Francis, S.H., Busch, J.L., Corbin, J.D., Sibley, D., 2010. cGMP-dependent protein kinases and cGMP phosphodiesterases in nitric oxide and cGMP action. Pharmacol. Rev. 62 (3), 525–563. https://doi.org/10.1124/pr.110.002907.

Ghosh, D., Syed, A.U., Prada, M.P., Nystoriak, M.A., Santana, L.F., Nieves-Cintrón, M., et al., 2017. Calcium channels in vascular smooth muscle. Adv. Pharmacol. 78, 49–87. https://doi.org/10.1016/bs.apha.2016.08.002.

Gleeson, M.P., 2008. Generation of a set of simple, interpretable ADMET rules of thumb. J. Med. Chem. 51 (4), 817–834. https://doi.org/10.1021/jm701122q.

Guideline, 2014. OECD Guideline for the Testing of Chemicals, Human Cytochrome P450 (CYP) *n*-fold Induction *in vitro* Test Method.

Horton, D.A., Bourne, G.T., Smythe, M.L., 2003. The combinatorial synthesis of bicyclic privileged structures or privileged substructures. Chem. Rev. 103 (3), 893–930. https://doi.org/10.1021/cr020033s.

Jackson, W.F., 2000. Ion channels and vascular tone. Hypertension 35 (1), 173–178. https://doi.org/10.1161/01.HYP.35.1.173.

Kim, Y.H., Choi, H., Lee, J., Hwang, I.-C., Moon, S.K., Kim, S.J., et al., 2008. Quinazolines as potent and highly selective PDE5 inhibitors as potential therapeutics for male erectile dysfunction. Bioorg. Med. Chem. Lett 18 (23), 6279–6282. https://doi.org/10.1016/j.bmcl.2008.09.108.

Komas, N., Lugnier, C., Andriantsitohaina, R., Stoclet, J.C., 1991. Characterisation of cyclic nucleotide phosphodiesterases from rat mesenteric artery. Eur. J. Pharmacol. 208 (1), 85–87. https://doi.org/10.1016/0922-4106(91)90056-n.

Li, Y., Brookes, Z.L., Kaufman, S., 2005. Acute and chronic effects of relaxin on vasoactivity, myogenic reactivity and compliance of the rat mesenteric arterial and venous vasculature. Regul. Pept. 132 (1–3), 41–46. https://doi.org/10.1016/j.regpep.2005.09.009.

Maurice, D.H., Ke, H., Ahmad, F., Wang, Y., Chung, J., Manganiello, V.C., 2014. Advances in targeting cyclic nucleotide phosphodiesterases. Nat. Rev. Drug Discov. 13 (4), 290–314. https://doi.org/10.1038/nrd4228 [Review].

Morgado, M., Cairrao, E., Santos-Silva, A.J., Verde, I., 2012. Cyclic nucleotide-dependent relaxation pathways in vascular smooth muscle. Cell. Mol. Life Sci. 69 (2), 247–266. https://doi.org/10.1007/s00018-011-0815-2.

Nava, E., Llorens, S., 2019. The local regulation of vascular function: from an inside-outside to an outside-inside model. Front. Physiol. 10 https://doi.org/10.3389/fphys.2019.00729 [review].

Nie, X.-q., Chen, H.-h., Zhang, J.-y., Zhang, Y.-j., Yang, J.-w., Pan, H.-j., et al., 2016. Rutaecarpine ameliorates hyperlipidemia and hyperglycemia in fat-fed, streptozotocin-treated rats via regulating the IRS-1/PI3K/Akt and AMPK/ACC2 signaling pathways. Acta Pharmacol. Sin. 37 (4), 483–496. https://doi.org/10.1038/aps.2015.167.

Paracha, T.U., Pobsuk, N., Salaloy, N., Suphakun, P., Pekthong, D., Hannongbua, S., et al., 2019. Elucidation of vasodilation response and structure activity relationships of N^2,N^4-disubstituted quinazoline 2,4-diamines in a rat pulmonary artery model. Molecules 24 (2), 281. https://doi.org/10.3390/molecules24020281.

Paulis, L., Líšková, S., Pintérová, M., Dobešová, Z., Kuneš, J., Zicha, J., 2007. Nifedipine-sensitive noradrenergic vasoconstriction is enhanced in spontaneously hypertensive rats: the influence of chronic captopril treatment. Acta Physiol. 191 (4), 255–266. https://doi.org/10.1111/j.1748-1716.2007.01737.x.

Pobsuk, N., Paracha, T.U., Chaichamnong, N., Salaloy, N., Suphakun, P., Hannongbua, S., et al., 2019. Design, synthesis and evaluation of N^2,N^4-diaminoquinazoline based inhibitors of phosphodiesterase type 5. Bioorg. Med. Chem. Lett 29 (2), 267–270. https://doi.org/10.1016/j.bmcl.2018.11.043.

Rinaldi, G.J., Grand, C., Cingolani, H.E., 1991. Characteristics of the fast and slow components of the response to noradrenaline in rat aorta. Can. J. Cardiol. 7 (7), 316–322.

Robinson, B.F., 1985. Calcium-entry blocking agents in the treatment of systemic hypertension. Am. J. Cardiol. 55 (3), B102–B106. https://doi.org/10.1016/0002-9149(85)90618-6.

Rybalkin, S.D., Yan, C., Bornfeldt, K.E., Beavo, J.A., 2003. Cyclic GMP phosphodiesterases and regulation of smooth muscle function. Circ. Res. 93 (4), 280. https://doi.org/10.1161/01.RES.0000087541.15600.2B.

Sampson, L.J., Hinton, J.M., Garland, C.J., 2001. Evidence for expression and function of phosphodiesterase type 5 (PDE-V) in rat resistance arteries. Br. J. Pharmacol. 132 (1), 13–17. https://doi.org/10.1038/sj.bjp.0703831.

Selvam, T.P., Kumar, P.V., 2015. Quinazoline marketed drugs. Res. Pharm. 1 (1).

Shimada, T., Guengerich, F.P., 2006. Inhibition of human cytochrome P450 1A1-, 1A2-, and 1B1-mediated activation of procarcinogens to genotoxic metabolites by polycyclic aromatic hydrocarbons. Chem. Res. Toxicol. 19 (2), 288–294. https://doi.org/10.1021/tx050291v.

Somnarin, T., Pobsuk, N., Chantakul, R., Panklai, T., Temkitthawon, P., Hannongbua, S., et al., 2022. Computational design, synthesis and biological evaluation of PDE5 inhibitors based on *N2,N4*-diaminoquinazoline and *N2,N6*-diaminopurine scaffolds. Bioorg. Med. Chem. 76, 117092 https://doi.org/10.1016/j.bmc.2022.117092.

Vaughan, C.J., Gotto, A.M., 2004. Update on statins: 2003. Circulation 110 (7), 886–892. https://doi.org/10.1161/01.CIR.0000139312.10076.BA.

Verhoeven, F., Totoson, P., Marie, C., Prigent-Tessier, A., Wendling, D., Tournier-Nappey, M., et al., 2017. Diclofenac but not celecoxib improves endothelial function in rheumatoid arthritis: a study in adjuvant-induced arthritis. Atherosclerosis 266, 136–144. https://doi.org/10.1016/j.atherosclerosis.2017.09.033.

Walker, S.D., Dora, K.A., Ings, N.T., Crane, G.J., Garland, C.J., 2001. Activation of endothelial cell IK_{Ca} with 1-ethyl-2-benzimidazolinone evokes smooth muscle hyperpolarization in rat isolated mesenteric artery. Br. J. Pharmacol. 134 (7), 1548–1554. https://doi.org/10.1038/sj.bjp.0704415.

Wisutthathum, S., Chootip, K., Martin, H., Ingkaninan, K., Temkitthawon, P., Totoson, P., et al., 2018. Vasorelaxant and hypotensive effects of an ethanolic extract of *Eulophia macrobulbon* and its main compound 1-(4′-Hydroxybenzyl)-4,8-Dimethoxyphenanthrene-2,7-Diol. Front. Pharmacol. 9 https://doi.org/10.3389/fphar.2018.00484 [original research].

Yoon, J.S., Jeong, E.J., Yang, H., Kim, S.H., Sung, S.H., Kim, Y.C., 2012. Inhibitory alkaloids from Dictamnus dasycarpus root barks on lipopolysaccharide-induced nitric oxide production in BV2 cells. J. Enzym. Inhib. Med. Chem. 27 (4), 490–494. https://doi.org/10.3109/14756366.2011.598151.

Zisaki, A., Miskovic, L., Hatzimanikatis, V., 2015. Antihypertensive drugs metabolism: an update to pharmacokinetic profiles and computational approaches. Curr. Pharmaceut. Des. 21 (6), 806–822. https://doi.org/10.2174/1381612820666141024151119.

Zuo, S.-J., Li, S., Yu, R.-H., Zheng, G.-X., Cao, Y.-X., Zhang, S.-Q., 2014. Discovery of novel 3-benzylquinazolin-4(3H)-ones as potent vasodilative agents. Bioorg. Med. Chem. Lett 24 (24), 5597–5601. https://doi.org/10.1016/j.bmcl.2014.10.092.

Supplemental material

The new quinazoline derivative (N^2-methyl-N^4-[(thiophen-2-yl)methyl]quinazoline-2,4-diamine) vasodilates isolated mesenteric arteries through endothelium-independent mechanisms and has acute hypotensive effects in Wistar rats.

Usana Chatturong[a,b], Krongkarn Chootip[a,*], Hélène Martin[b], Maude Tournier-Nappey[b], Kornkanok Ingkaninan[c], Prapapan Temkitthawon[c], Saharat Sermsenaphorn[d], Thanachon Somarin[d], Adchatawut Konsue[d], M. Paul Gleeson[d], Perle Totoson[b] and Céline Demougeot[b]

[a] Department of Physiology, Faculty of Medical Science and Center of Excellence for Innovation in Chemistry, Naresuan University, Phitsanulok 65000, Thailand

[b] Université de Franche-Comté, PEPITE EA4267, Besançon 25030, France

[c] Department of Pharmaceutical Chemistry and Pharmacognosy, Faculty of Pharmaceutical Sciences and Center of Excellence for Innovation in Chemistry, Naresuan University, Phitsanulok 65000, Thailand

[d] Department of Biomedical Engineering, Faculty of Engineering, King Mongkut's Institute of Technology, Ladkrabang, Bangkok 10520, Thailand

[*] **Corresponding author**

Krongkarn Chootip

Address: Department of Physiology, Faculty of Medical Science and Center of Excellence for Innovation in Chemistry, Naresuan University, Phitsanulok 65000, Thailand

E-mail: krongkarnc@nu.ac.th

Supplemental methods

1. Mesenteric arteries preparation

After anesthesia with sodium pentobarbital (60 mg/kg, *i.p.*), the rat small intestine was collected and placed in cold Krebs solution composed of (mM): NaCl 118, KCl 4.7, KH_2PO_4 1.2, $MgSO_4$ 1.2, $CaCl_2$ 2.5, $NaHCO_3$ 25, and glucose 12, maintained at pH of 7.4. The second-order branches of mesenteric arteries (MA) were isolated, cleaned, cut into rings (2–mm in length) and mounted in organ chambers (containing 6 mL of Krebs solution bubbled with 95% O_2, 5% CO_2 and maintained at pH of 7.4, 37ºC) via two 40–mm diameter stainless steel wires in myograph. To measure isometric force, a wire was connected to a Multi Myograph System (Model 610M v.2.2, DMT A/S, Denmark). Data were recorded using Chart^{TM} Ver.7 (ADInstruments, France). For active tension development, the mesenteric rings were stretched to their optimal lumen diameter. The internal circumference/wall tension ratio of the segments was adjusted to 90% of what the vessels would have if they were exposed to a passive tension equivalent to that produced by a transmural pressure of 100 mmHg to find the optimal lumen diameter. The optimal lumen diameter was determined using specific software for normalization of resistance arteries (DMT Normalization Module; ADInstruments). After an initial equilibration period of 30 min, viability of the rings was checked with a 10^{-2} M high K^+ solution for 10 min and then returning to normal Krebs solution (Wisutthathum et al., 2018). The presence of functional endothelium was confirmed verifying the relaxation to 10^{-5}M acetylcholine (ACh) ≥70% in vessels precontracted with 10^{-5}M phenylephrine (PE). In some rings, endothelium was mechanically removed by gently rubbing inside the lumen of the vessel with a small wire. Relaxation ≤10% to 10^{-5} M ACh considered a successfully endothelium removal. Arteries were again allowed to equilibrate 30 min before the start of the experiments.

2. Vascular reactivity study

*2.1. Vasorelaxant effect of compound **8** and nifedipine*

Endothelium-intact or endothelium-denuded rings were first contracted with 10^{-5} M PE, then, compound **8** or nifedipine (10^{-10}–3×10^{-5} M) were added cumulatively to obtain concentration-relaxation curves. DMSO (0.133% at maximum) was used as the negative control (vehicle).

2.2. Role of potassium (K^+) channels

Endothelium-denuded rings were incubated with various blockers of K^+ channels for 30 min: voltage-gated K^+ channel (K_V) (4–aminopyridine, 4–AP, 10^{-3} M), ATP–sensitive K^+ channel (K_{ATP}) (glibenclamide, 10^{-5} M) or large conductance Ca^{2+}–activated K^+ channels (K_{Ca}) (Iberiotoxin, 10^{-7} M). Then rings were contracted with 10^{-5} M PE and cumulating concentrations of compound **8** were added.

2.3. Role of soluble guanylyl cyclase (sGC)/cyclic guanosine monophosphate (cGMP) pathway

As compound **8** pertains to a series of quinazolines developed for their potential as PDE5 inhibitors (Chatturong et al., 2022), the role of sGC/cGMP pathway was investigated. First, to determine if compound **8** might modulate cGMP levels, endothelium-denuded rings were incubated with compound **8** at its EC_{50} (6×10^{-7} M) or with vehicle (0.02%DMSO) for 10 min before precontraction with 10^{-5} M PE. Then, cumulative concentrations of sodium nitroprusside (SNP, a nitric oxide (NO) donor, 10^{-11}–10^{-4} M) were added to activate the sGC and to enhance cGMP production in vascular smooth muscle. Second, to determine if compound **8** directly activated sGC, endothelium-denuded arteries were preincubated with 1H-[1,2,4]oxadiazolo[4,3-

a]quinoxaline-1-one (ODQ, a selective sGC inhibitor, 10^{-5}M) for 30 min before adding 10^{-5}M PE and subsequent cumulative concentrations of compound **8**.

2.4. Role of extracellular Ca^{2+} influx

Endothelium-denuded arteries were incubated in a Ca^{2+}-free Krebs solution containing methylene glycol-bis (2-aminoethylether)-N,N,N',N'-tetraacetic acid (EGTA, 10^{-3} M) for 40 min. Then 10^{-5} M PE was added to eliminate intracellular Ca^{2+} store from sarcoplasmic reticulum (SR) and then rings were washed 4 times every 10 min with a Ca^{2+}–free Krebs solution. Arteries were incubated with compound **8** at its EC_{50} or with vehicle for 10 min before adding 10^{-5} M PE (to open Receptor-Operated Ca^{2+} Channels, ROCC) or 8×10^{-2} M high K^+ solution (to open Voltage-Operated Ca^{2+} Channels, VOCC). Then cumulative concentrations of $CaCl_2$ (10^{-5}–10^{-2} M) were added to evoke a contractile response (Wisutthathum et al., 2018). The %contraction of $CaCl_2$ was normalized with maximum contraction of 10^{-5} M PE in the normal Krebs solution condition.

2.5. Role of intracellular Ca^{2+} release

Endothelium-denuded arteries were incubated with 10^{-7} M verapamil (L-type voltage dependent Ca^{2+} channel inhibitor) for 30 min. Then, compound **8** at its EC_{50} (6×10^{-7} M) or vehicle were incubated for 10 min before adding 10^{-5} M PE to stimulate intracellular Ca^{2+} release through the opening of inositol 1,4,5 trisphosphate (IP_3) receptors from SR (Wisutthathum et al., 2018).

2.6. Effect on α_1-adrenergic receptors

Endothelium-denuded arteries were incubated with compound **8** at its EC_{50} (6×10^{-7} M) or vehicle for 15 min. Then accumulating concentrations of the α_1-adrenergic receptor agonist, PE (10^{-10}–10^{-4} M) were added (Paracha et al., 2019).

3. Acute hypotensive effect of compound 8

To investigate whether the direct *ex vivo* vascular effect of compound **8** on resistance vessels translates into an *in vivo* effect, the acute hypotensive effect of compound **8** was compared with nifedipine in anesthetized rats. Male Wistar rats were anesthetized with sodium pentobarbital (60 mg/kg, *i.p.*) and supplemented as needed to maintain deep anesthesia. The left carotid artery and penile vein were cannulated with a polyethylene tube (PE50, 0.58 mm i.d. x 0.96 mm o.d.) filled with heparinized saline solution (heparin 50 units/mL of 0.9% sodium chloride solution). The arterial catheter was connected to a pressure recorder system (Gould-EasyGraf chart-recorder, USA) under rectal temperature control (Verhoeven et al., 2017). After a 15-min stabilization period, systolic arterial blood pressure (SBP), diastolic blood pressure (DBP), and heart rate (HR) were recorded before and during intravenous infusion (at 1 mL/min) of a vehicle (0.9% sodium chloride solution containing 5% DMSO), compound **8** or nifedipine (0.01, 0.05, or 0.1 mg/kg BW) (Paulis et al., 2007). The tested compounds were dissolved in 100% DMSO and diluted with 0.9% sodium chloride solution to obtain the final test dose. Successive infusions were separated for sufficient time (15 min) to allow full recovery of the cardiovascular parameters. Blood pressure was read off manually from the channel recording paper and HR was calculated by counting systolic pressure peaks.

Supplemental table

Table S1 Acute effect of compound **8** and nifedipine on blood pressure in anesthetized rats.

Groups	SBP (mmHg)	DBP (mmHg)	MAP (mmHg)	HR (bpm)	% change from baseline at each dose				
					SBP (%)	DBP (%)	MAP (%)	HR (%)	*n*
Baseline (first)	139±9	103±8	115±9	439±18					8
Vehicle (5% DMSO)	132±10	97±9	108±9	430±20	-0.6±0.9	0.7±1.5	0.3±1.1	0.3±0.5	8
Nifedipine									
Baseline	112±11	80±11	90±11	415±17					5
0.01 mg/kg	110±11	79±10	89±10	415±16	-1.4±1.06	-0.7±1.31	-0.8±1.1	0.4±0.2	5
Baseline	119±10	87±10	97±10	432±14					5
0.05 mg/kg	102±9	69±8	80±8	434±15	-14.5±3.4**	-19.9±4.4**	-17.7±4.0**	0.9±0.3	5
Baseline	111±9	81±9	91±9	434±14					5
0.1 mg/kg	97±6	64±5	75±5	442±14	-12.0±2.2***	-19.2±3.9***	-16.2±3.1***	1.9±0.8	5
Compound **8**									
Baseline	145±10	100±10	115±10	454±24					5
0.01 mg/kg	141±9	94±7	110±7	456±26	-2.0±1.86	-4.7±3.5	-3.6±2.83	0.4±0.3	5
Baseline	145±8	95±7	112±7	437±23					5
0.05 mg/kg	141±7	85±6	104±6	441±24	-2.6±1.2$^{*,\#}$	-9.6±3.2*	-6.6±2.09*	0.8±0.3	5
Baseline	146±7	94±7	112±7	412±25					5
0.1 mg/kg	140±5	87±7	104±6	420±24	-4.5±1.6$^{*,\#}$	-7.9±3.6*	-6.4±2.73*	2.0±0.6	5

The systolic blood pressure (SBP), diastolic blood pressure (DBP), mean arterial blood pressure (MAP), and heart rate (HR) were measured during the peak effect of single intravenous injections of vehicle, nifedipine, and compound **8** at the doses indicated. bpm: beats per minute, i.v.: intravenous infusion. All data are expressed as means±SEM of *n* animals. $^{*}p<0.05$, $^{**}p<0.01$, $^{***}p<0.001$ *vs* vehicle. $^{\#}p<0.05$ *vs* nifedipine at the same dose.

Supplemental figure

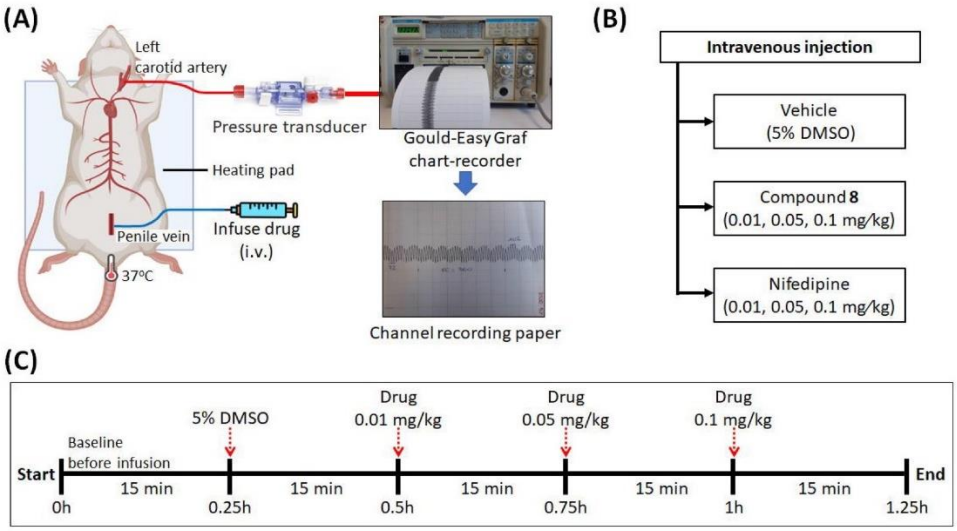

Fig. S1 Flow chart and schematic diagram of the acute hypotensive effect study.

(**A**) Schematic diagram illustrating rat cannulation for testing the acute hypotensive effect of the test compound. The rats were anesthetized, and blood pressure was measured after cannulation of the left carotid artery and connection of the catheter to a pressure recorder system (Gould-EasyGraf chart-recorder, USA) under rectal temperature control. The intravenous infusion (i.v.) of vehicle, nifedipine, or compound **8** were made into the penile vein. (**B**) The experimental group of the vehicle, nifedipine, and compound **8** infusion. (**C**) Graphical visualization of the time course of the experiments.

Supplemental references

Chatturong, U., Martin, H., Totoson, P., Ingkaninan, K., Temkitthawon, P., Sermsenaphorn, S., et al. (2022). Quinazoline-based human phosphodiesterase 5 inhibitors exhibited a selective vasorelaxant effect on rat isolated pulmonary arteries involving NO-sGC-cGMP pathway and calcium inhibitory effects. *Vascular Pharmacology*, *147*, 107111. https://doi.org/10.1016/j.vph.2022.107111

Paracha, T. U., Pobsuk, N., Salaloy, N., Suphakun, P., Pekthong, D., Hannongbua, S., et al. (2019). Elucidation of Vasodilation Response and Structure Activity Relationships of N^2,N^4-Disubstituted Quinazoline 2,4-Diamines in a Rat Pulmonary Artery Model. *Molecules*, *24*(2), 281. https://doi.org/10.3390/molecules24020281

Paulis, L., Líšková, S., Pintérová, M., Dobešová, Z., Kuneš, J., & Zicha, J. (2007). Nifedipine-sensitive noradrenergic vasoconstriction is enhanced in spontaneously hypertensive rats: the influence of chronic captopril treatment. *Acta Physiologica*, *191*(4), 255-266. https://doi.org/10.1111/j.1748-1716.2007.01737.x

Verhoeven, F., Totoson, P., Marie, C., Prigent-Tessier, A., Wendling, D., Tournier-Nappey, M., et al. (2017). Diclofenac but not celecoxib improves endothelial function in rheumatoid arthritis: A study in adjuvant-induced arthritis. *Atherosclerosis*, *266*, 136-144. https://doi.org/10.1016/j.atherosclerosis.2017.09.033

Wisutthathum, S., Chootip, K., Martin, H., Ingkaninan, K., Temkitthawon, P., Totoson, P., et al. (2018). Vasorelaxant and Hypotensive Effects of an Ethanolic Extract of *Eulophia macrobulbon* and Its Main Compound 1-(4′-Hydroxybenzyl)-4,8-Dimethoxyphenanthrene-2,7-Diol. *Frontiers in Pharmacology*, *9*. https://doi.org/10.3389/fphar.2018.00484

APPENDIX C COMMUNICATIONS

1. Poster presentation at the congress of the Joint Physiological Pharmacological Society Conference (JPPSC), Department of Physiology, Faculty of Medical Science, Naresuan University, Thailand, 8-10 June 2022.

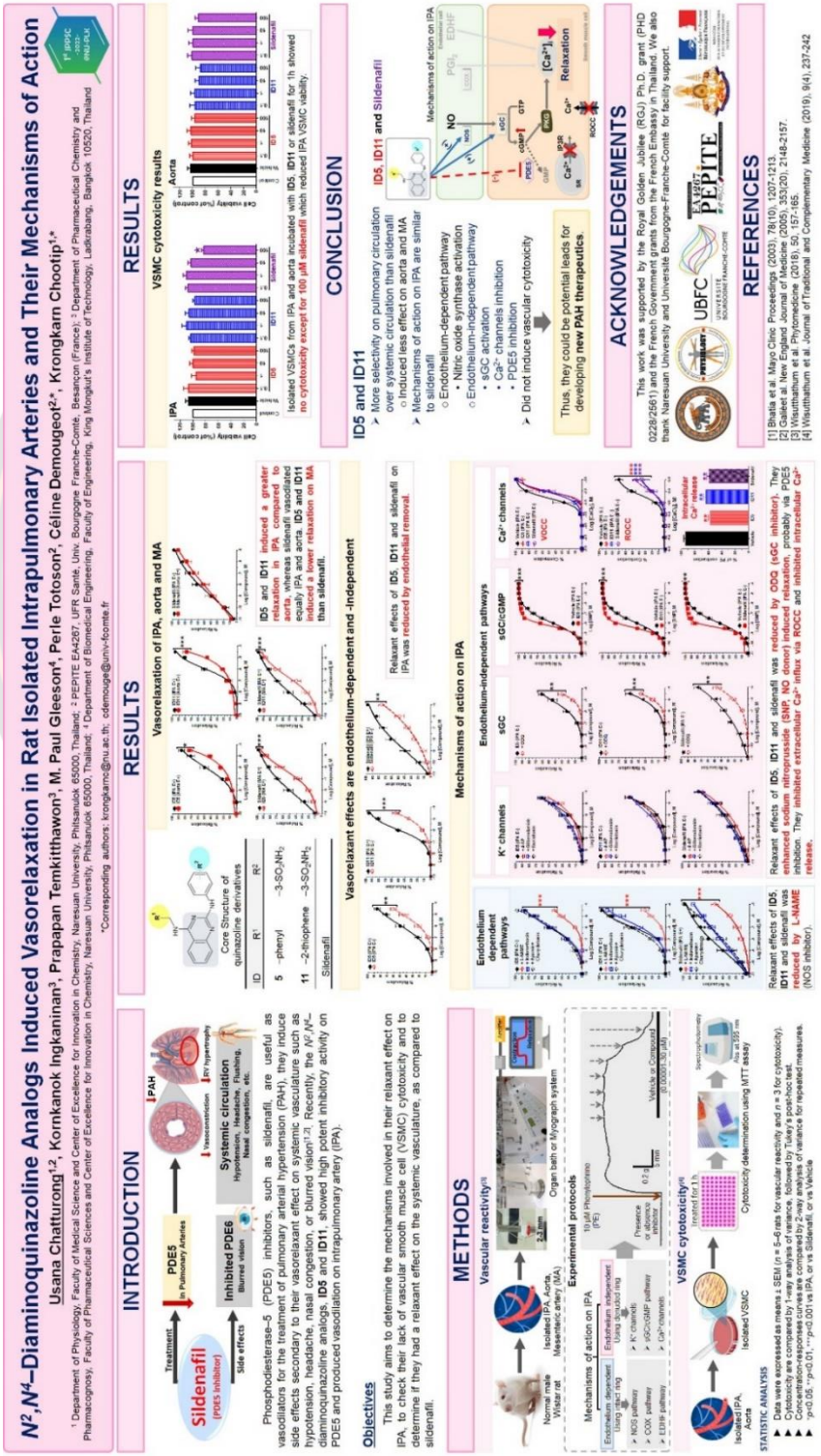

Received a “Best presentation award” for this poster.

2. Poster presentation at the congress of the Société Française de Pharmacologie et de Thérapeutique (SFPT), at Faculté de Médecine-Pôle Recherche, Lille, France,14-16 June 2022.

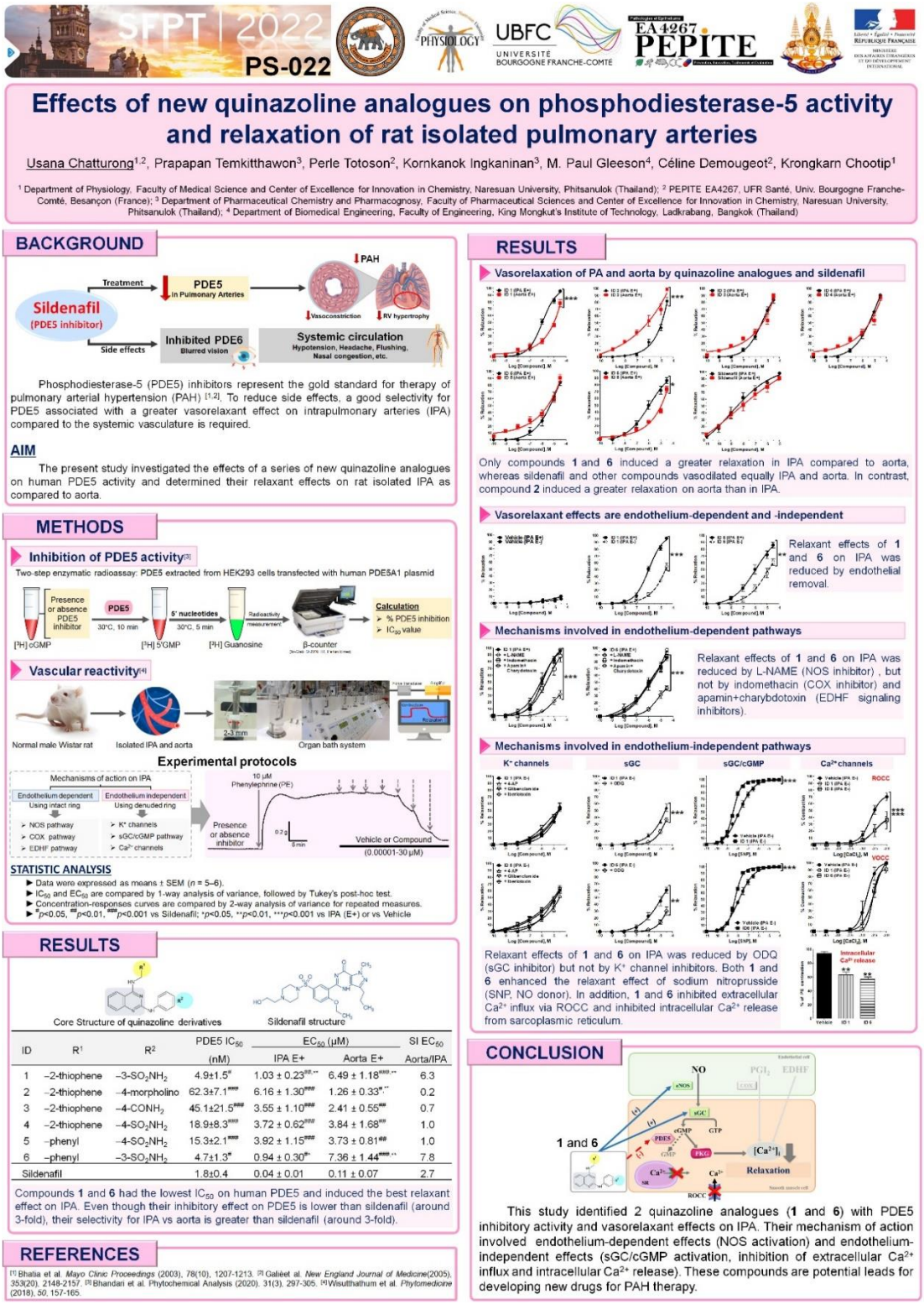

Fundamental & Clinical Pharmacology. 2022;36 (Suppl. S1):92-169 , PS-022.

Keywords: potentially inappropriate medication, older adults, frailty.

PS-021 | Renal disease associated with injectable amoxicillin with or without clavulanic acid

C. Bordet[1]; L. Letinier[1]; J. Périno[2]; G. Miremont[1]; A. Pariente[2]

[1]Centre Régional de PharmacoVigilance -, CRPV –, Bordeaux, France; [2]Inserm -, Université de Bordeaux, Bordeaux, France

Introduction: Since 2010, French pharmacovigilance spontaneous reports of crystalluria associated amoxicillin have increased [1]. This case-control study was conducted to assess the risk of crystalluria or altered renal function with amoxicillin overdosage and associated risk factors in a hospital setting.
Material and methods: Patients over 18 years old hospitalized in one teaching Hospital from 2017 to 2019 and treated with injectable amoxicillin were included. Cases were defined as the patients with a diagnosis of crystalluria or alteration of renal function. The exposure was defined as an overdosage of amoxicillin (doses >3 grams per injection, or 12 grams daily). Characteristics of the population were described then variables with number over 2 were included in a multivariate regression model (OR, CI 95%). Cases were matched to the controls on gender, period of antibiotic administrations and hospital service.
Results: Among the 498 patients included, 54 were cases and 83 were exposed. Multivariate analysis included the following variables: amoxicillin overdosage, age, gender, concurrent administration of furosemide or another diuretic, administration of amoxicillin in an emergency, internal medicine or infectious disease department. Amoxicillin overdosage [OR = 3.36, CI 95% (1.68; 6.75)] regardless the age was significantly associated with crystalluria or alteration of renal function; added furosemide [OR = 2.43, IC95% (1.29; 4.60), $p = 0.0062$)] or other diuretics [OR = 2.13, IC95% (1.01; 4.50), $p = 0.0475$)] increased this risk. Administration of amoxicillin in emergency, internal medicine, or infectious disease services was protective regarding this risk.
Discussion/Conclusion: Injectable amoxicillin overdosage significantly increased the risk of renal disease and crystalluria as described in pharmacovigilance studies [1,2]. Concurrent administration of furosemide or another diuretic increased this risk.

References:
[1] Vodovar D, et al. Dramatic increase of amoxicillin-induced crystal nephropathy found in a cohort study of French pharmacovigilance centers. Antimicrob Agents Chemother.2018; 62:e01630-17.
[2] Thomas L, et al. Amoxicillin-induced crystal nephropathy: A nationwide French pharmacovigilance databases study. Br J Clin Pharmacol.2020;86: 2256-65.

Keywords: pharmacoepidemiology, amoxicillin, crystalluria, pharmacovigilance, drug safety.

PS-022 | Effects of new quinazoline analogues on phosphodiesterase-5 activity and relaxation of rat isolated pulmonary arteries

U. Chatturong[1]; P. Temkitthawon[2]; P. Totoson[1]; K. Ingkaninan[2]; M. P. Gleeson[3]; C. Demougeot[1]; K. Chootip[4]

[1]Pepite EA4267, UFR Santé, Univ. Bourgogne Franche-Comté -, Besançon, France; [2]Department of Pharmaceutical Chemistry and Pharmacognosy, Faculty of Pharmaceutical Sciences and Center of Excellence for Innovation in Chemistry, Naresuan University -, Phitsanulok, (Thailand); [3]Department of Biomedical Engineering, Faculty of Engineering, King Mongkut's Institute of Technology, Ladkrabang -, Bangkok, (Thailand); [4]Department of Physiology, Faculty of Medical Science and Center of Excellence for Innovation in Chemistry, Naresuan University -, Phitsanulok, (Thailand)

Introduction: Phosphodiesterase-5 (PDE5) inhibitors represent the gold standard for therapy of pulmonary arterial hypertension (PAH). To reduce side effects, a good selectivity for PDE5 associated with a greater vasorelaxant effect on intrapulmonary arteries (IPA) compared to the systemic vasculature is required. The present study investigated the effects of a series of new quinazoline analogues on PDE5 activity and determined their relaxing effects on rat isolated IPA and aorta.
Material and methods: PDE5 inhibitory activity of 6 quinazoline analogs (1–6) was evaluated using enzymatic radioassay. The vasorelaxation to quinazoline analogues (10–10 to 3.10–5 M) was assessed in 10–5 M phenylephrine precontracted IPA and aortic rings isolated from male Wistar rats using the organ bath technique. Various inhibitors involving endothelium-dependent and endothelium-independent pathways were employed to characterize the mechanism of vasorelaxant action of quinazoline analogues.
Results: Compounds 1 and 6 had lower IC50 on PDE5 (4.7 ± 1.3 and 4.9 ± 1.5 nM, respectively), compared to others and induced a greater relaxing effect on IPA (EC50 = 1.0 ± 0.2 and 0.9 ± 0.3 μM, respectively) compared to the aorta (EC50 = 6.5 ± 1.2 and

7.4 ± 1.4 μM, respectively). The effects were less pronounced than sildenafil (IC50 = 1.8 ± 0.4 nM, $p < 0.05$) whom selectivity for the pulmonary vasculature is low (IPA EC50 = 0.04 ± 0.01 and aorta EC50 = 0.11 ± 0.07 μM). Relaxing effects of 1 and 6 on IPA was reduced by endothelial removal, NG-nitro-L-arginine methyl ester and 1H-[1,2,4]oxadiazolo [4,3-a]quinoxaline-1-one, but not by indomethacin, apamin/charybdotoxin, 4-aminopyridine, iberiotoxin, glibenclamide or barium chloride. Both 1, 6 inhibited extracellular Ca2+ influx and intracellular Ca2+ release. In addition, 1 and 6 enhanced the relaxant effect of sodium nitroprusside.

Discussion/Conclusion: This study identified 2 quinazoline analogues with PDE5 inhibitory activity and vasorelaxant effects on IPA. Their mechanism of action involved endothelium-dependent effects (nitric oxide synthase activation) and endothelium-independent effects (inhibition of extracellular Ca2+ influx and intracellular Ca2+ release). These compounds are potential leads for developing new drugs for PAH therapy [1–3].

References:
[1] Paracha TU, et al. Molecules. 2019; 24 (2): 281.
[2] Pobsuk N, et al. Bioorganic & medicinal chemistry letters. 2019; 29 (2): 267-270.
[3] Wisutthathum S, et al. Phytomedicine. 2018; 50: 157-165.

Keywords: quinazoline analogues, PDE5, vasorelaxation, pulmonary artery.

PS-023 | Baclofen misuse: Analysis of 46 patients with non-medical use

J. M. Pelerin[1]; L. Fristot[1]; V. Gibaja[1]; B. Revol[2]; P. Gillet[3]; J. Lima-Tournebize[3]

[1]CEIP-Addictovigilance, French Addictovigilance Network (FAN), CHRU -, Nancy, France; [2]CEIP-Addictovigilance, French Addictovigilance Network (FAN), CHU -, Grenoble, France; [3]CEIP-Addictovigilance, French Addictovigilance Network (FAN), CHRU Nancy, France; Université de Lorraine, CNRS, Imopa, F-54 000 -, Nancy, France

Introduction: Baclofen is commonly used to treat spasticity and, most recently, addictive disorders, particularly alcohol use disorders. Various countries have seen an increase in baclofen misuse cases over the last decade [1–2]. This study aimed to describe 46 clinical cases of non-medical use of baclofen reported to the east France addictovigilance center and the literature.

Material and methods: We examined spontaneous reports of baclofen abuse to the East France addictovigilance center. A literature search was conducted simultaneously using the databases PubMed®, Web of Sciences®, and Google Scholar®. We performed both investigations in February 2021, with no time constraints.

Results: Forty-six cases were analysed (33 from the literature review and 13 from addictovigilance base). For some parameters, the literature cases differed significantly from the east France cases (p-values < 0.05). No cases of adolescents or young adults misusing baclofen were reported to the east France addictovigilance center, and the dose in literature was higher. In addition, we observed that respiratory and cardiovascular effects were significantly different in the literature cases than in the east France cases. Baclofen's non-medical use mainly affected male subjects with addictive history. Euphoria search was the most common reason for misuse. Route of administration included oral, snorting, and sublingual use. Most patients misusing baclofen presented severe complications, mainly represented by neurological and respiratory disturbances. Physical and psychological dependence on baclofen was observed in three persons.

Discussion/Conclusion: Although baclofen abuse is still relatively uncommon or (most likely) underestimated, this study helped to confirm the intrinsic abuse potential of baclofen and highlight the baclofen-abuse-related health harms. When prescribing baclofen, careful consideration and benefit-risk analysis should be used, and emergency departments should be aware of the dangers in abuse situations [3–5]. The literature and addiction surveillance networks do not detect the same populations and have a complementary role.

References:
[1] Jamshidi N, et al. Alcohol Alcohol. 2019;54:73–78.
[2] Romito JW, et al. SAGE Open Med. 2010;9:1-19.
[3] Léger M, et al. Alcohol Alcohol. 2017;52: 665–670.
[4] Pelissier F, et al. Clin Toxicol. 2017;55:275–284.
[5] Reynolds K, et al. Clin Toxicol. 2020;58:763–772.

Keywords: baclofen, non-medical use, recreational, abuse, case series.

3. Poster presentation at the congress of the Forum des Jeunes Chercheurs 2022, École Doctorale Environnement & Santé, Bâtiment Gabriel, Université de Bourgogne, Dijon, France, 16-17 June 2022.

Vasorelaxant effect of 2 new N^2,N^4–diaminoquinazoline analogs on rat isolated intrapulmonary arteries and mechanisms involved

Usana Chatturong[1,2], Perle Totoson[1], Kornkanok Ingkaninan[3], Prapapan Temkitthawon[3], M. Paul Gleeson[4], Céline Demougeot[1] and Krongkarn Chootip[2]

[1] PEPITE EA4267, UFR Santé, Univ. Bourgogne Franche-Comté, Besançon (France). [2] Department of Physiology, Faculty of Medical Science and Center of Excellence for Innovation in Chemistry, Naresuan University, Phitsanulok (Thailand). [3] Department of Pharmaceutical Chemistry and Pharmacognosy, Faculty of Pharmaceutical Sciences and Center of Excellence for Innovation in Chemistry, Naresuan University, Phitsanulok (Thailand). [4] Department of Biomedical Engineering, Faculty of Engineering, King Mongkut's Institute of Technology, Ladkrabang, Bangkok (Thailand)

INTRODUCTION

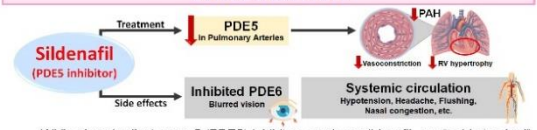

While phosphodiesterase–5 (PDE5) inhibitors, such as sildenafil, are "gold standard" for treatment of pulmonary arterial hypertension (PAH), they induce side effects secondary to their vasorelaxant effect on systemic vasculature such as hypotension, headache or nasal congestion. We developed new N^2,N^4–diaminoquinazoline analogs as PDE5 inhibitors and identified 2 compounds (**ID5** and **ID11**) with a high PDE5 inhibitory activity and vasorelaxant effects on pulmonary artery.

AIM

The present study aimed to determine the mechanisms involved in their relaxant effect on IPA, to check their lack of vascular smooth muscle cell (VSMC) cytotoxicity and to determine if they had a relaxant effect on the systemic vasculature, as compared to sildenafil.

METHODS

Vascular reactivity[3]

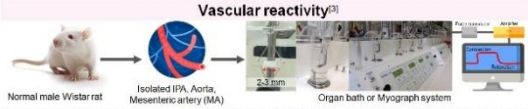

Experimental protocols

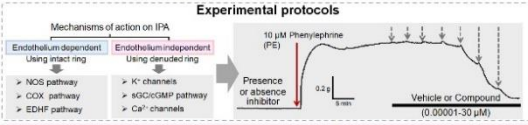

VSMC cytotoxicity[4]

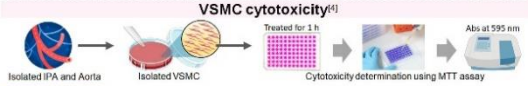

STATISTIC ANALYSIS

- Data were expressed as means ± SEM (n = 5–6 rats for vascular reactivity and n = 3 for cytotoxicity).
- Cytotoxicity are compared by 1-way analysis of variance, followed by Tukey's post-hoc test.
- Concentration-responses curves are compared by 2-way analysis of variance for repeated measures.
- *p<0.05, **p<0.01, ***p<0.001 vs IPA, or vs Sildenafil, or vs Vehicle

RESULTS

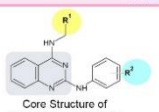

Core Structure of quinazoline derivatives

ID	R^1	R^2
5	-phenyl	$-3\text{-}SO_2NH_2$
11	-2-thiophene	$-3\text{-}SO_2NH_2$
Sildenafil		

Vasorelaxation of pulmonary artery (IPA), aorta and mesenteric artery (MA)

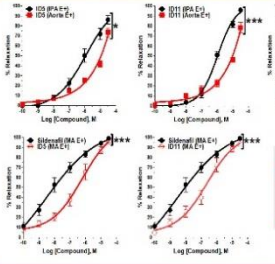

ID5 and **ID11** induced a greater relaxation of IPA compared to aorta, whereas sildenafil vasodilated equally IPA and aorta. **ID5 and ID11 induced a lower relaxation on MA than sildenafil.**

REFERENCES

[1] Bhatia et al. Mayo Clinic Proceedings (2003), 78(10), 1207-1213.
[2] Galiè et al. New England Journal of Medicine (2005), 353(20), 2148-2157.
[3] Wisutthathum et al. Phytomedicine (2018), 50, 157-165.
[4] Wisutthathum et al. Journal of Traditional and Complementary Medicine (2019), 9(4), 237-242

RESULTS

Vasorelaxant effects are endothelium-dependent and -independent

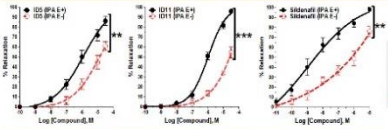

Relaxant effects of **ID5**, **ID11** and sildenafil on IPA was **reduced by endothelial removal**.

Endothelium-dependent mechanisms

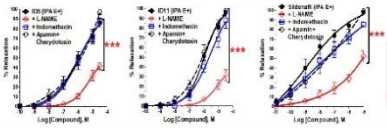

Relaxant effects of **ID5**, **ID11** and sildenafil was **reduced by L-NAME** (NOS inhibitor).

Endothelium-independent mechanisms

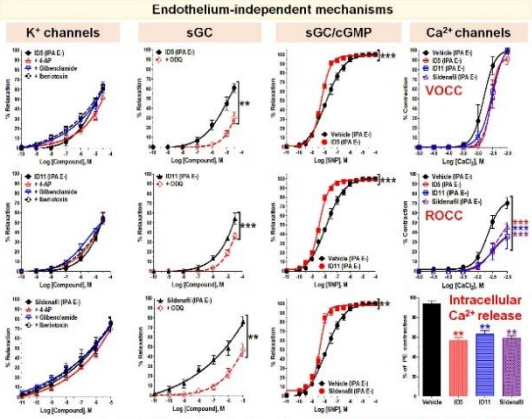

Relaxant effects of **ID5**, **ID11** and sildenafil was **reduced by ODQ (sGC inhibitor).** They **enhanced sodium nitroprusside (SNP, NO donor) induced relaxation**, probably via PDE5 inhibition. They **inhibited extracellular Ca^{2+} influx via ROCC** (receptor-operated calcium channels) and **inhibited intracellular Ca^{2+} release.**

VSMC cytotoxicity results

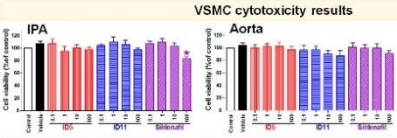

ID5, **ID11** showed **no cytotoxicity on VSMC. By contrasts, sildenafil** at high concentration reduced viability of VSMC from IPA.

CONCLUSION

ID5 and ID11

- More selective for pulmonary circulation over systemic circulation than sildenafil
- Similar mode of action on IPA than sildenafil
  - Endothelium-dependent pathway
    - Nitric oxide synthase activation
  - Endothelium-independent pathway
    - sGC activation
    - Ca^{2+} channels inhibition
    - PDE5 inhibition
- Did not induce vascular cytotoxicity

Thus, they could be potential leads for developing **new PAH therapeutics.**

ID5, ID11 and Sildenafil

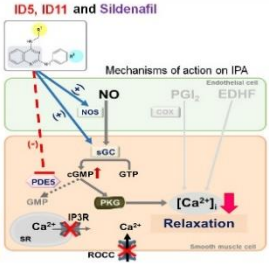

4. Poster presentation at the congress of the National RGJ and RRI Conference, Thailand Research Expo 2022, Bangkok, Thailand, 4-5 August 2022.